Hydrogen Bonding in the Recovery of Phenols and Methyl-*t*-butyl Ether

Molecular Modeling and Calorimetry

Hydrogen Bonding in the Recovery of Phenols and Methyl-*t*-butyl Ether

Molecular Modeling and Calorimetry

RUUD CUYPERS

Thesis

Submitted in fulfillment of the requirements for the degree of doctor

at Wageningen University

by the authority of the Rector Magnificus

Prof. dr. M.J. Kropff,

in the presence of the

Thesis Committee appointed by the Academic Board

to be defended in public

on Wednesday 13 October 2010

at 4 p.m. in the Aula.

"…want tussen droom en daad staan wetten in de weg en praktische bezwaren…"

Willem Elsschot

TABLE OF CONTENTS

CHAPTER 1

1

General Introduction.

Abstract

This chapter clarifies the goals of the presented research on phenol and methyl-*t*-butyl ether (MTBE) extraction, and the ways in which this research was performed. The principles related to the separation of complex mixtures are briefly discussed, and some background is given on extraction, in particular using Solvent-Impregnated Resins (SIRs). The reasons for choosing hydrogen-bond interactions are clarified, and the threefold approach to the research questions – molecular modeling, synthesis and physical measurements – is discussed. The thesis outline is presented at the end of this chapter.

Introduction

The purification of waste water is not a process that many people are usually concerned with, but without it the whole of the western society would collapse. Clean potable water has become a common good, a necessity, but it is actually a privilege, and it has been so for quite a long time already. Surface water purification is nowadays carried out on a massive industrial scale, and with excellent results; in the western world, clean water is at our disposal virtually everywhere and always. However, cleaning industrial waste water can be a tedious task. Apolar and slightly polar compounds can be relatively easily removed from water e.g. by extraction to an apolar phase, amongst others, but the more polar pollutants will preferentially remain solubilized in the water phase. Phenol and Methyl-*tert*-butyl ether (MTBE), the two main compounds that this thesis deals with, each possess a relatively polar group (–O–H and –O–, respectively). Because of these polar groups and because of the fact that these molecules both have a relatively low molecular weight, their water solubility at room temperature is relatively high (87 g/L and 42 g/L for phenol[1] and MTBE,[2] respectively). Current methods of MTBE or phenol removal are dependent on their concentration and include distillation, extraction, biological degradation (using bacteria), oxidation, membrane separation, air stripping, activated carbon adsorption, and others.[3] Downsides to all these methods exist; for example, distillation of phenol-containing solutions requires a lot of energy, which makes it only profitable for comparatively high concentrations of phenol, and activated carbon adsorption of MTBE suffers from competing adsorption of other substances that are in the water, thereby diminishing MTBE adsorption efficiency. A more effective extraction method is therefore needed to clean water that is contaminated with either phenol or MTBE.

Phenol

Phenol (C_6H_5OH; M = 94.11 g/mol, Figure 1A) is used as a base compound in many industrial chemical processes. It is used for the production of bisphenol A, an important compound in the production of polymers.[4] In addition, it finds industrial use as the starting compound in the production of aspirin from salicylic acid made by the Kolbe synthesis,[5] in the production of phenolic resins (like Bakelite, which is a polymer from phenol and formaldehyde)[6] and herbicides,[7] and in the production of cyclohexanone, which can be converted to caprolactam, the main ingredient for the production of nylon 6.[8] Furthermore, it is used in many other synthetic compounds used worldwide today.

Production of large quantities of waste material as a result of the production of these synthetic

compounds is currently still inevitable, although a trend is seen towards a more atom-efficient chemistry. Phenol dissolved in surface water can be harmful for aquatic life already at low concentrations.[1] Because of a low taste threshold, water containing low quantities of phenol cannot be used as drinking water. Furthermore, phenol is a systemic poison, it is readily taken up by the skin and acute poisoning by ingestion or inhalation might occur.[1] It is highly toxic and severely irritant. Therefore, it has a listing in the Dutch chemicals library of the SER (Social and Economic Council of the Netherlands), that was issued by the Health Council of the Netherlands and by the European Union, where its 8 hour time-averaged limit is set at 8 mg/m^3, effective from 2007 onwards.[9]
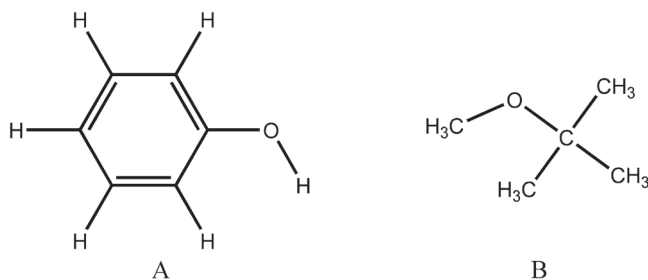

Figure 1. Structural formula of (A) phenol and (B) MTBE.

MTBE

MTBE ($CH_3OC(CH_3)_3$; M = 88.14 g/mol, Figure 1B) is used as an additive to oxygenate fuels in order to raise the octane number to prevent engine knocking, thereby actually replacing other highly toxic and currently banned compounds, like tetraethyl lead.[10] It is also used as a relatively inexpensive solvent in organic chemistry practice (its properties are similar to diethyl ether only with a higher boiling point), and is also used medically to dissolve gallstones.[11] Because of the widespread use of fuels, MTBE has entered the environment on a large scale, largely via exhausts of incomplete combustion. Due to its relatively high water solubility, ground water pollution by MTBE is widespread, especially around fuel stations. Combined with the low soil adsorption coefficient of MTBE this causes immediate groundwater contamination from leakages of storage facilities.[12] In the United States, more than 80% of 1000 tested groundwater sites were shown to be contaminated with MTBE and concentrations as high as 23 mg/L have been measured.[13] Although it is not highly toxic, its very low odor threshold (15 µg/L,[14] vaguely reminiscent of ether) and taste threshold (40 µg/L[14]) prevent water containing even small quantities of MTBE to be used as drinking water. Currently, MTBE is no longer used in gasoline fuels, as it is replaced by the analog

ethyl-*tert*-butyl ether (ETBE), which is more easy to remove because of its lower water solubility. The high current concentrations of MTBE in the environment nevertheless require efficient methods to diminish a long-term problem in water purification.

Extraction

Many ways of purification of a complex mixture of compounds exist, including adsorption, centrifugation, chromatography, distillation, evaporation, extraction, filtration, recrystallization, and others. Extraction (or liquid-liquid extraction, solvent extraction or partitioning) of a liquid mixture of compounds is based on the relatively high solubility of the compound of interest in one liquid phase and a low solubility in another liquid phase, while all the other compounds display an inverse preference. Furthermore, the extraction liquid must be insoluble in and immiscible with the liquid that contains the compound to be extracted. By repeating the extraction procedure several times in a batch process (separation funnel) or by having an apparent excess of extractant for the desired compound in a continuous process (continuous extraction / Soxhlet extraction) one can obtain the desired compound in a pure form in the extraction liquid. This compound can then be used in a further procedure by evaporating the solvent to concentrate it, or, such as in the case of purification of a liquid, the solution from which this compound was obtained can be further utilized, free of the extracted compound.

Solvent-Impregnated Resin (SIR) extraction

Due to limitations of currently used approaches and ever-increasing demands on the reduction of environmental pollution, new separation methods are gaining interest. Porous polymers enter the arena of separation technology slowly but steadily. Solvent-Impregnated Resins[15] (SIRs, Figure 2) are porous polymer beads containing apolar organic extractant liquids. SIRs are used as three-phase separation systems. A solute is present in an aqueous phase; the SIR contains the stationary, water-immiscible organic liquid phase impregnated in the pores of the otherwise inert resin particle. When brought into contact with a SIR, the solute will preferentially partition from the aqueous phase into the impregnated solvent phase (with physical distribution coefficient K_{phys}). Ion-exchange SIRs are already widely used[16-19] to separate heavy metal ions from aqueous phases in a fast and simple way, making use of the solubility of the solute in the liquid organic phase, in exchange for protons. Only recently, investigations on other applications have been performed, e.g. the recovery of apolar organics as described in this thesis and that of Burghoff.[20] Bench-scale or pilot-scale recovery of polar organics like organic acids,[21, 22] amino acids[23] and flavonoids have
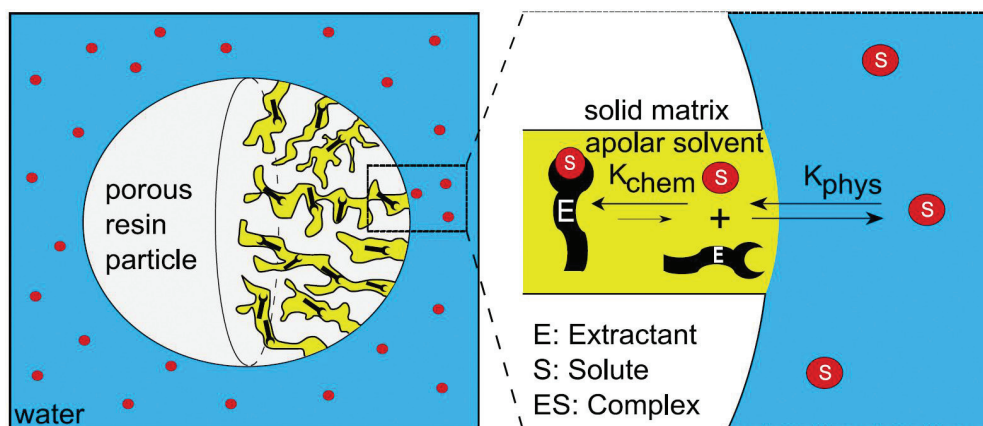
Figure 2. Working principle of Solvent-Impregnated Resins (SIRs) with an active extractant in the pores.

also been realized.[24]

SIRs are not yet fully integrated in the field of polar organics extraction from aqueous systems. A drawback to the use of solely the organic extraction liquid in SIRs is the limited solubility of more polar compounds like phenols and ethers in such a medium. In order for solutes to be effectively taken up by the SIR particle, the distribution coefficient K_{phys} from the water to the organic phase has to be as large as possible (highly variable, but typically > 100). Because of the relatively high solubility of phenols and ethers in water, the distribution coefficient K_{phys} will not be very large and separation will only partially take place. This phenomenon also exists in other separations involving polar organic compounds.

In order to enhance extraction, complex-forming extractants can be added to the organic solvent. By means of complex formation inside the organic solvent (with equilibrium binding constant K_{chem}), the overall equilibrium distribution can be further shifted towards the SIR, with a concomitant enhancement of the extraction efficiency.

A tight binding of the pollutant molecules to the extractant will eventually ensure high distribution coefficients. However, a moderate binding strength would enable a relatively easy regeneration of the complexing agent after a binding event, enabling multiple uses of the same compound. This way, the same particles, impregnated with a particular extraction liquid and complexing agent, can be used for many extraction cycles. Moreover, because of the use of this extractant inside the SIR particles, the SIR particles themselves would be suitable for an even broader spectrum of purification, because the impregnated organic liquid along with the extractant can

be both replaced by other species, facilitating other extraction needs. This would ensure a versatile and relatively cheap system.

In principle, molecular recognition and complexation of the solute inside the SIR particles, as indicated in Figure 2, can provide a new and fast way to separate more polar organic solutes from aqueous streams, possibly at a large, industrial scale. For the effective removal of polar organic solutes like phenols and ethers, as e.g. desired in water-cleaning processes, the additional complexation step of the solute in the solvent phase is crucial for large-scale application, due to the solute's relatively high solubility in water.

SIRs usually consist of a porous polymer material, e.g. polypropylene. An organic extraction liquid is impregnated into the pores of the resins, and complexing agents that are chosen for the extraction process will be dissolved in it. The main impregnation method is the so-called wet method of impregnation (Figure 3). A solution of extractant in the appropriate extraction liquid is absorbed by the polymer resin, and the impregnated resin obtained after filtration is a three-component system: polymer, organic solvent and extractant. The SIR obtained from this method combines the beneficial properties of extraction and chemical complexation.
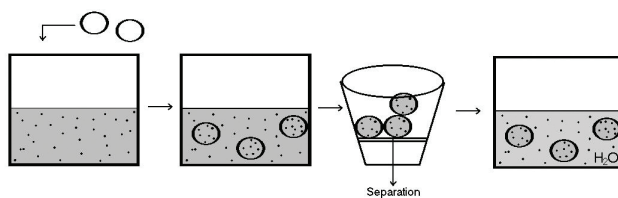
Figure 3. The wet method of impregnation.[15]

Other impregnation methods include dry impregnation, where a two-component system is obtained containing the polymer bead and extractant, and the modified method, where a modifier is added to enhance water permeability in the polymer resin during the extraction procedure, yielding a three-component system with polymer, extractant and modifier. The dry and modified methods yield SIRs without organic solvent in the pores, which therefore lack the extraction properties of the organic solvent. A fourth way to insert extractants into a polymer resin involves polymerization of the resin bead in the presence of the extractant molecule. Resins of this kind are called Levextrel resins (see e.g. ref [25]).

In addition to the type of extractant and the way in which it is present inside the SIR, the organic

solvent also plays an important role in binding affinity of the solute of interest: it influences the solubility of the extractant, of the solute, and of the formed complex. This solvent can be varied as well, and this provides yet another handle for fine-tuning the anticipated interactions.

Hydrogen bonds

The systems at hand ask for selective, reversible, and sufficiently strong complexation of phenols and ethers. Van der Waals interactions and hydrophobic interactions, however reversible, are non-specific and relatively weak for these compounds. Therefore, as the mentioned compounds exhibit electropositive and electronegative moieties, respectively, the obvious choice for an extractant is one that is able to form hydrogen bonds (H-bonds; also: association) to the substrates.

In his book *The Nature of the Chemical Bond*, Linus Pauling credits T.S. Moore and T.F. Winmill with the first use of the term 'hydrogen bond' in 1912.[26, 27] Moore and Winmill used the H-bond to account for the fact that trimethylammonium hydroxide is a weaker base than tetramethylammonium hydroxide. The description of H-bonding in its more well-known setting, water, came some years later, in 1920, from Latimer and Rodebush, mentioning that "a hydrogen nucleus held by two octets constitutes a weak bond".[28] However, Huggins, who worked in the same labs as Moore and Winmill, later claimed that he was the first to recognize the H-bond.[29]
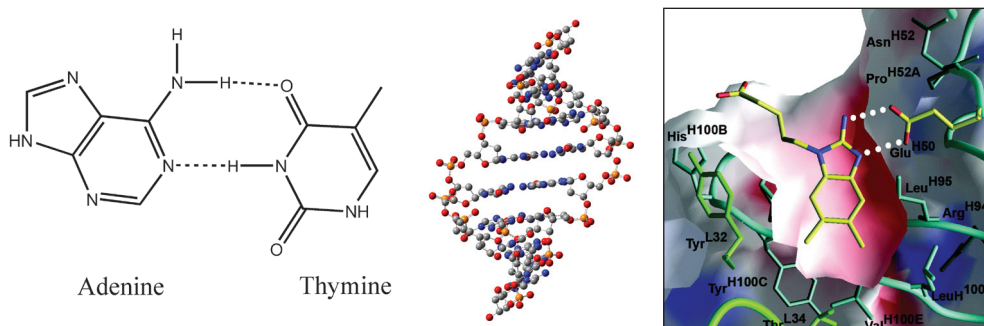
Figure 4. H-bonding interactions in biology. Left: Schematic representation of DNA base-pairs Adenine – Thymine, held together by H-bonds; middle: helix structure of DNA consisting of such base pairs; right: H-bonds in antibody-antigen recognition.

H-bonds can be found in many different forms and strengths and they are present in many natural systems. H-bonds form the key interactions in the DNA double helix (Figure 4; left, middle), antibody/antigen interactions (Figure 4, right),[30] the secondary structure of proteins and nucleic

acids, and even in modern self-healing synthetic rubbers and plastics. They are also responsible for the high boiling point of water (with four possibilities for H-bonding in a small molecule), and the fact that ice is less dense than liquid water is due to a crystal structure that is stabilized by H-bonds.

A H-bond is a donor-acceptor interaction specifically involving hydrogen atoms.[31, 32] An attractive force develops between an electronegative entity (atom or group of atoms with a lone pair of electrons or π-electrons, Figure 5) and a hydrogen atom covalently bound to another electronegative atom. It largely results from a dipole-dipole interaction with a hydrogen atom bound to nitrogen, oxygen, sulphur or fluorine, and is generally weaker than an ionic bond or single covalent bond (which is typically an order of magnitude stronger,[31, 33] although at the extreme ends the binding strengths overlap).[31] H-bonds can be formed in between two identical electronegative atoms (homonuclear H-bond, e.g. $-O-H\cdots O$) and in between two different electronegative atoms (heteronuclear H-bond, e.g. $-O-H\cdots N$), and between separate molecules (intermolecular H-bond) or within a single molecule (intramolecular H-bond, Figure 5).

The H-bond is often described as an electrostatic dipole - dipole interaction.[31] The electronegative atom attracts the electron cloud from around the hydrogen nucleus and leaves it with a positive partial charge. Because of the small size of hydrogen the resulting partial charge represents a large charge density, which is subsequently attracted by another electronegative atom. The directional property of H-bonds occurs because the dipole – dipole interactions are maximum when the dipoles are colinear.[31] Hence, H-bonds will always tend to be linear. However, they also have some features of covalent bonding:[34, 35] they are strong, produce interatomic distances shorter than the sum of the Van der Waals radii of the individual atoms (i.e. the distance between the electron donor atom and hydrogen atom, or H-bond length, is restricted), and usually involve a limited number of interaction partners, which can be interpreted as a kind of valence.[31]
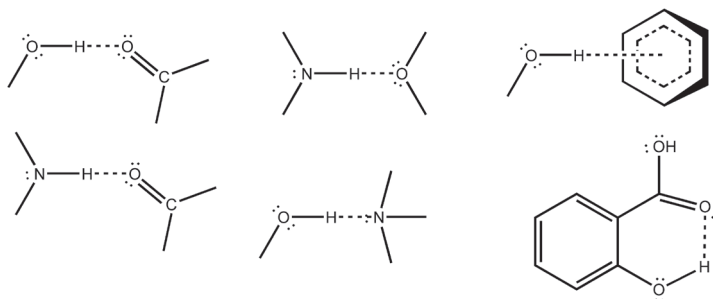

Figure 5. Different forms of H-bonds (clockwise: O–H•••O, N–H•••O, O–H•••π, O–H•••O (intramolecular, resonance assisted), O–H•••N, and N–H•••O H–bond).

Weak H-bonds, lower than approximately 4 kcal/mol binding strength and with H-bond lengths much longer than the covalent bond between the hydrogen atom and the donor electronegative atom, can be formed between weak donor and acceptor groups like C–H as donor and C≡C or π-electrons as acceptor. This can occur when carbon is bound to several electronegative atoms like e.g. in $CHCl_3$ (see e.g. ref [36]). Much stronger H-bonds, between 4 and 15 kcal/mol binding strength and with H-bond lengths only slightly shorter than the covalent bond X–H, can be formed between compounds like acids, alcohols, phenols, hydrates and all biological compounds. Even stronger H-bonds, of over 15 kcal/mol binding strength, are present between charged species like N^+–H and $–O^-$, as well as in proton sponges and HF complexes, amongst others. As can clearly be seen from the examples above, the nature of the H-bond depends on the nature of the donor and acceptor groups.

H-bond lengths and geometries are dependent on many factors, including bond strength, temperature, and chemical environment (possible steric hindrance). The H-bond strength itself is dependent on temperature, bond angle, and polarity of the environment. Consequently, molecules bound by H-bonds can be released upon addition of a certain stimulus, for example a change in chemical environment or by increasing the temperature.[37] Because of the reversible nature of the H-bond and its tunable strength, H-bonds do have great potential to be used as driving force to accomplish the selective, reversible, and sufficiently strong complexation of phenols and ethers for use in SIR separation systems at room temperature. In addition, they would allow the subsequent removal of the bound molecules from the organic phase for re-generation of the binding agents, e.g. by applying higher temperatures.

Research approach

The research described in this thesis is targeted towards the rational design of complexing agents for polar organics (phenols and ethers) from water, for use inside the apolar liquid impregnated in a SIR. The approach that was chosen to obtain possibly interesting and applicable compounds for use in SIRs was threefold:

- molecular modeling of potentially interesting compounds,
- synthesis of selected compounds,
- experimental determination of the binding strength towards phenols and MTBE.

Molecular modeling

Via modeling experiments, potentially interesting compounds were investigated for their binding affinities towards the compounds of interest, phenol and MTBE. The primary reason for optimizing an extractant via molecular design is to improve our understanding of the complexation at the molecular level. Molecular modeling can facilitate this understanding by providing useful data about the complex (e.g. binding strength, complex geometry, charges and bond orders, geometrical and electronically bond-strength limiting and enhancing factors) that can be compared with experiments.

Nowadays, many accurate modeling algorithms are available.[38] Molecular Mechanics (MM) uses sets of known parameter values for a certain molecule (such as the molecular structure, conformational energies and vibrational spectra) to model this molecule or large systems containing many of these molecules interacting with each other, with the primary objective to predict the geometry. At 0 K, when there is no influence of motion and of temperature, the systems behavior is treated classically (atomic interactions and vibrations are treated as springs) and usually an equilibrium geometry can be found. If motion and temperature do influence the system, a reasonably accurate prediction of the behavior in time can be made if Molecular Dynamics (MD) is applied, solving the classical equations of motion for the given atoms and molecules. Quantum mechanics (QM) tries to solve the Schrödinger Equation ($H\Psi = E\Psi$) to model the system at hand. Three kinds of QM methods are most frequently used: semi-empirical methods, density functional theory (DFT), and *ab initio* calculations. Semi-empirical methods solve a simplified Schrödinger Equation using measured parameters. DFT uses the electron density, which is optimized to a self-consistent field optimum value by the process of iteration, to solve the approximate Schrödinger equation, taking electron exchange and correlation energy terms into account. *Ab initio* (Latin for "from first principles") QM tries to minimize the approximations in solving the complete Schrödinger equation, thereby also taking electron exchange and correlation energy terms into account.

MM and MD are mainly used for modeling very large systems (up to 100,000 atoms and more) with many molecules interacting all at the same time. Examples are micellar systems, protein – protein interactions, DNA – protein interaction modeling, and lipid bilayer modeling in cells. *Ab initio* QM methods are mainly used for very accurate energy calculations in relatively small systems (up to ~100 atoms), such as single-molecule geometry investigations, reaction intermediate geometry calculations or otherwise small but specific systems. Semi-empirical and DFT QM methods can treat systems of sizes in between the mentioned values, e.g. a piece of double stranded DNA, up

to approximately 1000 atoms, while for smaller systems it is also used as a fast approach to gain approximate insight in the molecular structure and properties.

Both *ab initio* and DFT were used in the work described in this thesis to gain information about the molecular H-bond system at hand. Geometry information was mainly obtained using DFT, as this is known to combine accuracy for this feature and speed. H-bond length, binding angle, and other steric interactions were easily accessible via the optimized geometries of the model complexes. Electronic properties, like charges and bond orders on the relevant atoms, were obtained using both DFT and *ab initio* methods. H-bond energies were obtained using both these methods, as well as via other methods to be able to make comparisons between the various methods and to benchmark the obtained results. Especially the recently developed spin component-scaled MP2 (SCS-MP2)[39-42] and M06-2X methods,[43, 44] and the composite CBS-Q model[45] were evaluated for their use in the investigated systems. In addition, a complete basis set extrapolation at the MP2 level (MP2/CBS)[46] was used. Solvent effects were investigated theoretically by using the polarized continuum model (PCM) solvent model,[47-49] as well as by using the solute electron density-based (SMD) model.[50]

Molecular modeling is an ideal method for studying complex molecular interactions like complex formation. Computer speed and memory capacity have come to the point where it is now possible to model certain systems in the same time as it would have cost to perform synthesis in the laboratory. This theoretical treatment is, of course, much less expensive and less elaborate. Often, small molecular model systems are used to describe a particular region of a molecule, e.g. a reaction center. To gain more knowledge on larger molecular systems, even partitioning of the system can be used. The program Gaussian (Gaussian 09 (G09) and its predecessor G03) was used throughout this work.[51]

Synthesis

Organic synthesis enables one to design and obtain compounds that were previously not available. A careful design provides the chemist with a material having physical properties that resemble those of the ideally desired compound. For the current work, a suitable molecular structure was chosen based on its ability to, in principle, form stable complexes with phenols and ethers. For phenols, molecules with a relatively strong H-bond acceptor moiety were chosen, while for ethers strong H-bond donors were picked. Next, the H-bond strength can be fine-tuned by changing the H-bond forming moiety, by adding electron-donating or electron-withdrawing groups or by tuning the steric hindrance around the binding atoms. Solubility, in either organic

solvent or water, can be optimized by adding or removing relevant apolar or polar moieties to an interesting molecule. In this thesis, the synthesis of some of the used compounds has been described where necessary.

Isothermal Titration Calorimetry.

Physical measurements of the properties exhibited by the compounds of interest are crucial. After purification and characterization, the synthesized compounds (and several commercially obtained compounds) were investigated for their complex-forming abilities. Characteristics like binding affinity (K_{chem}), stoichiometry (N) and reaction enthalpy of binding (ΔH^0) can be measured using Isothermal Titration Calorimetry (ITC).[52, 53] Since the Gibbs free energy is related to the equilibrium constant and the other thermodynamic parameters via

$$\Delta G^0 =- RT\ln K_{chem} = \Delta H^0 - T\Delta S^0 \qquad (1)$$

with R the gas constant and T the absolute temperature, the overall change in Gibbs free energy (ΔG^0) and in entropy (ΔS^0) can be calculated from those values.

ITC is a sensitive technique that measures the heat of reaction of two components after mixing. It has been used for measurements of reactions between metals and polymers,[54] protein - ligand binding,[55] kinetics of enzymes,[56] and more. ITC measurements presented in this thesis are performed on an isothermal titration calorimeter, as depicted in Figure 6. The calorimeter consists of two identical cells in an adiabatic jacket. The jacket is kept at a constant temperature by the cooling system that surrounds it. Very sensitive thermopile/thermocouple electronics detect heat changes between the cells (cell feedback network) and between the cells and the surroundings.
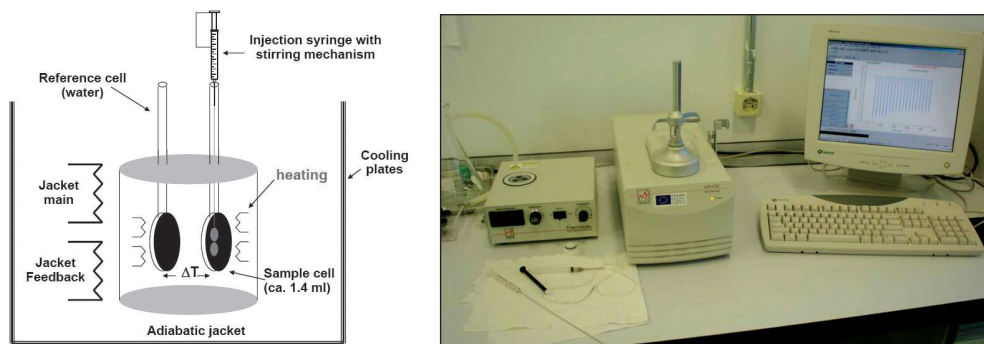

Figure 6. Schematic diagram of an isothermal titration calorimeter[52] and photograph of the one that was used for the binding experiments.

Heaters on the cells and on the surroundings are activated when temperature differences arise. In this way, the temperature of the cells is kept constant.

During an experiment the reference cell is heated by a small constant power, the reference offset. The temperature difference between the two cells is constantly measured. During an ITC experiment, upon addition of the reactant heat is evolved (exothermic reaction) or taken up (endothermic reaction) by the reaction mixture, and in order to maintain a constant temperature for all components in both cells, the power applied by the cell feedback is adjusted and the heaters will be either switched off or switched on, respectively. Since the cell feedback has units of power (μcal/s), integration of this signal over time yields the overall change in thermal energy (ΔH^0), while the equilibrium constant (K_{chem}) and the stoichiometry (N) can be obtained from fitting the data. Subsequently ΔG^0 and ΔS^0 can thus be derived. Results are depicted in a plot of the heat change per mole of titrant as a function of molar ratio of the titrant versus the substrate, see Figure 7A (see also Chapter 4).

The binding isotherm can be characterized by the dimensionless parameter c, defined as

$$c = K_{chem} \cdot [\,M\,] \cdot N \tag{2}$$

with [M] the concentration of free substrate. In order to measure the binding constant accurately, values of c between 1 and 1000 are recommended.[57] Large values of c prohibit the calculation of K_{chem}, since the transition is very sharp. Low values of c result in binding isotherms lacking the typical sigmoid shape, in which the point of equivalence can not be determined. Values of c between 10 and 50 are best to produce the most accurate data (see Figure 7B). In practice it is not possible to measure K_{chem} values larger than approximately 10^7 M^{-1} and lower than approximately 10^1 M^{-1}. If binding affinities are outside this range, other types of measurements are more suitable.

Research goals

H-bonds have been investigated in great detail, and many features about especially O–H•••O, N–H•••N and N–H•••O H-bonds are well-understood. However, much is still to be improved regarding the level of knowledge on less ordinary H-bonds. The investigations on the compounds and complexes that are described in this thesis, P=O•••H–O, N^+–O^-•••H–O and O–H•••O< H-bonds, conducted with the help of modeling studies and ITC, will shed light on the demands and restrictions that arise when the goal is to reversibly complex specific solutes from an aqueous environment by H-bonds.
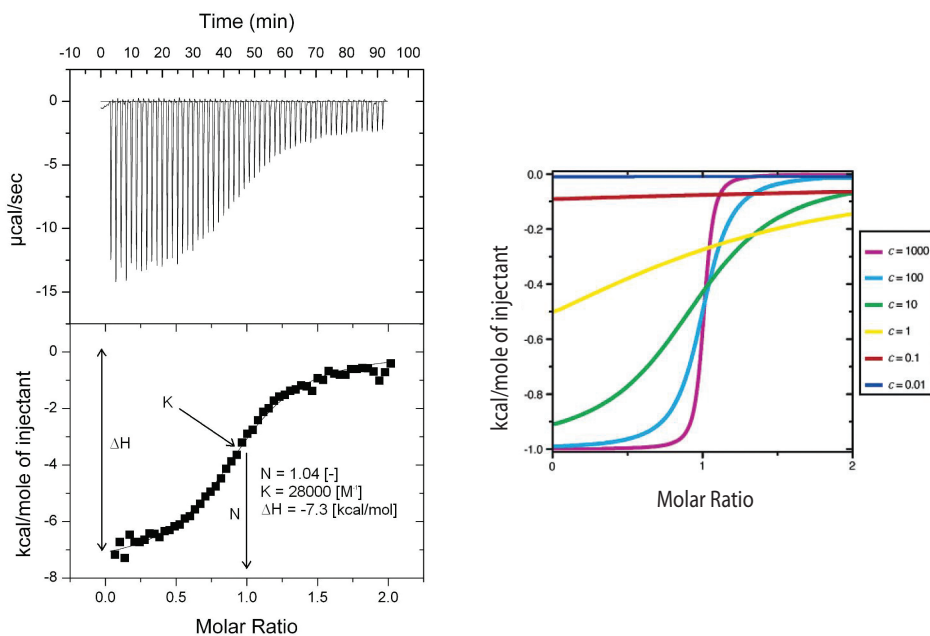
Figure 7. Left: Typical ITC measurement for the determination of the binding affinity for dimethyldodecyl-amine-N-oxide to phenol (see also chapter 4) and the data after processing; right: Binding isotherms at different values for c.[57]

Outline of this thesis

In this thesis, investigations that are relevant for the use of SIRs for phenol recovery and MTBE recovery are described. The approach to develop a working SIR for phenol and, separately, for MTBE recovery consists of two distinct working areas. The first area, described in this thesis, involves the organic complexing agents that are used inside the SIRs. Modeling of possibly interesting compounds and, subsequently, synthesis and characterization of these compounds is carried out. For interesting compounds that are identified in the modeling studies, detailed studies of complexation strengths and behavior are also conducted. The second area deals with the design of the SIR particles and with process properties like complex-forming kinetics inside the resin particles, when used in separating columns for the purification of an aqueous phase. That part of the research was described in a separate thesis by Burghoff.[20]

Chapters 2 and 3 deal with the binding of phenol and thiophenol by phosphine oxides, phosphates,

and their thio-analogs. In Chapter 2 the complexation of phosphine oxides and phosphates with phenol and thiophenol is described, elucidated by modeling experiments, ITC measurements, and liquid-liquid extraction experiments. In particular, the binding behavior of one of the phosphine oxides (tri-n-octylphosphine oxide) towards several phenols substituted with electron-withdrawing groups (EWG) was studied, both in the presence and absence of water. Chapter 3 extends these investigations to the modeling of the full homologous series of mono-, di- and tri-substituted phosphine oxides and phosphates and their thio-analogs, to establish a basis for future binding of phenols by strong H-bond acceptors in SIR-based separations. By application of several different modeling methods, these systems are described in great detail, including solvent effects. Valuable information was gained, not only about the systems under investigation, but also about the methods of describing them in the models that were used.

Chapter 4 treats the complexation of phenols by a group of even stronger H-bond acceptors, amine-N-oxides. The binding properties for phenol and thiophenol of three different amine-N-oxides were investigated using ITC measurements, and a larger group was subject to several different methods of modeling.

In Chapter 5 the binding properties of EWG-phenols towards MTBE are investigated. It gives modeling results of a large number of different EWG-substituted phenols for MTBE binding, as well as the synthesis and measurement results for four selected, apolar EWG-phenols.

In Chapter 6, the main results described in this thesis about the search for suitable extractant molecules for use in SIRs for the recovery of low-concentration polar organics (like phenol and MTBE) from water are briefly discussed, and the targets achieved are compared with the desired goals that were set initially. In addition, future perspectives to further develop the research into this area are discussed, and a critical evaluation of the main scientific challenges relevant for the potential of this highly exciting field is given.

References

(1)   INEOS Phenol, Phenol EC safety data sheet, **2007**.

(2)   European Fuel Oxygenates Association, **2010**.

(3)   J. S. Watson, *Separation methods for waste and environmental applications*, Marcel Dekker, Inc, Basel, 1999.

(4)   R. A. Reinicke, B. C. Gates, *Aiche Journal* **1974**, *20,* 933.

(5)   A. S. Lindsey, H. Jeskey, *Chem. Rev.* **1957**, 57, 583.

(6)   L. H. Baekeland, *Chemtech* **1976**, *6,* 40.

(7)   W. Oettmeier, C. Kude, H. J. Soll, *Pest. Biochem.and Physiol.* **1987**, *27,* 50.

(8)   H. Z. Liu, T. Jiang, B. X. Han, S. G. Liang, Y. X. Zhou, *Science* **2009**, *326,* 1250.

(9)   SER, **2009**, http://www.ser.nl/nl/grenswaarden/fenol.aspx.

(10)   http://www.epa.gov/mtbe/gas.htm, **2010**.

(11)   N. Uchida, T. Nakatsu, S. Hirabayashi, A. Minami, H. Fukuma, T. Ezaki, S. A. Morshed, C. Fuke, K. Ameno, I. Ijiri, M. Nishioka, *J. Gastroenter.* **1994**, *29,* 486.

(12)   A. A. M. Langenhoff, Netherlands Centre for Soil Quality Management and Knowledge Transfer (SKB SV-018), 2000.

(13)   A. A. Keller, *"Health and Environment Assessment of MTBE, Report to Legislature of the State of California, Volume III"* 1998.

(14)   U. Peters, F. Nierlich, E. Schulte-Körne, M. Sakuth, R. Deeb, M. Laugier, M. Suominen, M. Kavanaugh, in *Encyclopedia of Industrial Chemistry, Methyl-tert-Butyl Ether*, 7 ed., John Wiley & Sons, 2003.

(15)   J. L. Cortina, A. Warshawsky, in *Ion Exch. Solvent Extr., Vol. 13* (Eds.: J. A. Marinsky, Y. Marcus), Dekker, New York, 1997, pp. 195.

(16)   S. S. El-Dessouky, E. H. Borai, *J. Radioanal. Nucl. Chem.* **2006**, *268,* 247.

(17)   B. B. Gupta, Z. B. Ismail, *Comp. Interf.* **2006**, *13,* 487.

(18)   J. S. Liu, H. Chen, Z. L. Guo, Y. C. Hu, *J. Appl. Pol. Sc.* **2006**, *100,* 253.

(19)   K. Ohnaka, A. Yuchi, *Chem. Lett.* **2005**, *34,* 868.

(20)   B. Burghoff, *PhD thesis*, Eindhoven Technical University (Eindhoven), **2009**.

(21)   R.-S. Juang, H.-L. Chang, *Ind. Eng. Chem. Res.* **1995**, *34*, 1294.

(22)   M. Traving, H.-J. Bart, *Chem. Eng. Technol.* **2002**, *25*, 997.

(23)   A. Kostova, H.-J. Bart, *Chemie Ingenieur Technik* **2004**, *76,* 1743.

(24)   H. Kitazaki, M. Ishimaru, K. Inone, K. Yoshida, S. Nakamura, in *Proceedings of the International Solvent Extraction Conference,* ISEC'96 ed., Melbourne, Australia, 1996, pp. 1667.

(25)   V. Korovin, Y. Shestak, *Hydrometallurgy* **2009**, *95,* 346.

(26)   L. Pauling, *The Nature of the Chemical Bond and the Structure of Molecules and Crystals: an Introduction to Modern Structural Chemistry,* Cornell University Press, Ithaca, NY, 1939.

(27)   T. S. Moore, T. F. Winmill, *J. Chem. Soc.* **1912**, *101,* 1635.

(28) W. M. Latimer, W. H. Rodebush, *J. Am. Chem. Soc.* **1920**, *42,* 1419.

(29) M. L. Huggins, *Angew. Chem. Int. Ed.* **1971**, *10*, 147.

(30) E. W. Debler, S. Ito, F. P. Seebeck, A. Heine, D. Hilvert, I. A. Wilson, *Proc. Nat. Ac. Sc.* **2005**, *102,* 4984.

(31) G. A. Jeffrey, *An Introduction to Hydrogen Bonding*, Oxford University Press, New York, Oxford, 1997.

(32) G. R. Desiraju, T. Steiner, *The Weak Hydrogen Bond*, 1 ed., Oxford University Press, New York, 1999.

(33) Y. Maréchal, *The Hydrogen bond and the water molecule*, Elsevier, Amsterdam, 2007.

(34) E. D. Isaacs, A. Shukla, P. M. Platzman, D. R. Hamann, B. Barbiellini, C. A. Tulk, *Phys. Rev. Lett.* **1999**, 82, 600.

(35) F. Cordier, M. Rogowski, S. Grzesiek, A. Bax, *J. Magn. Res.* **1999**, *140*, 510.

(36) D. C. Daniel, J. E. McHale, *J. Phys. Chem. A* **1997**, *101*, 3070.

(37) R. P. Sijbesma, F. H. Beijer, L. Brunsveld, B. J. B. Folmer, J. Hirschberg, R. F. M. Lange, J. K. L. Lowe, E. W. Meijer, *Science* **1997**, *278,* 1601.

(38) A. Hinchcliffe, *Chemical Modeling From Atoms To Liquids,* John Wiley and Sons, Ltd, Chichester, 1999.

(39) J. Antony, S. Grimme, *J. Phys. Chem. A* **2007**, *111*, 4862.

(40) R. A. Bachorz, F. A. Bischoff, S. Hofener, W. Klopper, P. Ottiger, R. Leist, J. A. Frey, S. Leutwyler, *Phys. Chem. Chem. Phys.* **2008**, *10,* 2758.

(41) S. Grimme, *J. Chem. Phys.* **2003**, *118*, 9095.

(42) T. Schwabe, S. Grimme, *Acc. Chem. Res.* **2008**, *41*, 569.

(43) Y. Zhao, D. G. Truhlar, *Acc. Chem. Res.* **2008**, *41*, 157.

(44) Y. Zhao, D. G. Truhlar, *Theor. Chem. Acc.* **2008**, *120*, 215.

(45) J. W. Ochterski, G. A. Petersson, J. A. Montgomery, *J. Chem. Phys.* **1996**, *104,* 2598.

(46) M. R. Nyden, G. A. Petersson, *J. Chem. Phys.* **1981**, *75,* 1843.

(47) J. Tomasi, R. Bonaccorsi, *Croat. Chem. Acta* **1992**, *65,* 29.

(48) J. Tomasi, R. Bonaccorsi, R. Cammi, F. J. O. Delvalle, *J. Mol. Struct. - THEOCHEM* **1991,** *80*, 401.

(49) S. Miertus, E. Scrocco, J. Tomasi, *Chem. Phys.* **1981**, *55*, 117.

(50) A. V. Marenich, C. J. Cramer, D. G. Truhlar, *J. Phys. Chem. B* **2009**, *113*, 6378.

(51) M. J. Frisch, G. W. Trucks, H. B. Schlegel, G. E. Scuseria, M. A. Robb, J. R. Cheeseman, G. Scalmani, V. Barone, B. Mennucci, G. A. Petersson, H. Nakatsuji, M. Caricato, X. Li, H. P. Hratchian, A. F. Izmaylov, J. Bloino, G. Zheng, J. L. Sonnenberg, M. Hada, M. Ehara, K. Toyota, R. Fukuda, J. Hasegawa, M. Ishida, T. Nakajima, Y. Honda, O. Kitao, H. Nakai, T. Vreven, J. Montgomery, J. A., J. E. Peralta, F. Ogliaro, M. Bearpark, J. J. Heyd, E. Brothers, K. N. Kudin, V. N. Staroverov, R. Kobayashi, J. Normand, K. Raghavachari, A. Rendell, J. C. Burant, S. S. Iyengar, J. Tomasi, M. Cossi, N. J. Rega Millam, M. Klene, J. E. Knox, J. B. Cross, V. Bakken, C. Adamo, J. Jaramillo, R. E. Gomperts, O. Stratmann, A. J. Yazyev, R. Austin,

C. Cammi, J. W. Pomelli, R. Ochterski, R. L. Martin, K. Morokuma, V. G. Zakrzewski, G. A. Voth, P. Salvador, J. J. Dannenberg, S. Dapprich, A. D. Daniels, O. Farkas, J. B. Foresman, J. V. Ortiz, J. Cioslowski, D. J. Fox, A.1, Gaussian, Inc., Wallingford CT, 2009.

(52)   M. Chellani, *Am. Biotechnol. Lab*. **1999**, *17*, 14.

(53)   J. E. Ladbury, M. L. Doyle, *Biocalorimetry 2,* John Wiley & Sons, Ltd, New York, 2004.

(54)   G. Camci-Unal, N. L. B. Pohl, *Carbohydrate Polym*. **2010**, *81*, 8.

(55)   B. Baum, L. Muley, M. Smolinski, A. Heine, D. Hangauer, G. Klebe, *J. Mol. Biol*. **2010**, *397,* 1042.

(56)   J. Cheleski, H. J. Wiggers, A. P. Citadini, A. J. da Costa, M. C. Nonato, C. A. Montanari, *Anal. Biochem*. **2010**, *399,* 13.

(57)   ITC Data Analysis in Origin; Tutorial Guide ed., Origin, **2004**.

1

CHAPTER 2

Complexation of Phenols and Thiophenol by Phosphine Oxides and Phosphates. Extraction, Isothermal Titration Calorimetry and *Ab Initio* Calculations.

2

Abstract

In order to develop a new solvent-impregnated resin system for the removal of phenols from water the complex formation of triisobutylphosphine sulfide (TIBPS), tributylphosphate (TBP), and tri-n-octylphosphine oxide (TOPO) with a series of phenols (phenol, thiophenol, 3-chlorophenol, 3,5-dichlorophenol, 4-cyanophenol and pentachlorophenol) was studied. The investigation of complex formation between the extractants and the phenols in the solvent toluene was carried out using liquid – liquid extraction, isothermal titration calorimetry (ITC) and quantum chemical modeling (B3LYP/6-311+G(d,p)//B3LYP/6-311G(d,p) and MP2/6-311++G(2d,2p)//B3LYP/6-311G(d,p)). The equilibrium constant (binding affinity, K_{chem}), enthalpy of complex formation (ΔH^0) and stoichiometry (N) were directly measured with ITC, and the entropy of complexation (ΔS^0) was derived from these results. A first screening of K_{chem} towards phenol revealed a very high binding affinity for TOPO, and very low binding affinities for both other extractants. Modeling results showed that although 1 : 1 complexes were formed, the TIBPS and TBP do not form strong hydrogen bonds. Therefore, in the remainder of the research only TOPO was considered. K_{chem} of TOPO for the phenols in toluene increased from 1,000 to 10,000 M^{-1} in the order phenol < pentachlorophenol < 3-chlorophenol < 4-cyanophenol ≈ 3,5-dichlorophenol (in line with their pK_a values, except for pentachlorophenol) in the absence of water, while the stoichiometric ratio remained 1 : 1. In water-saturated toluene, the binding affinities are lower due to co-complexation of water with the active site of the extractant. The increase in binding affinity for TOPO in the phenol series was confirmed by a detailed *ab initio* study, in which ΔH was calculated to range from -10.7 kcal/mol for phenol to -13.4 kcal/mol for 4-cyanophenol. Pentachlorophenol was found to behave quite differently, showing a ΔH value of -10.5 kcal/mol. In addition, these calculations confirm the formation of 1 : 1 H-bonded complexes.

Introduction

Solvent-impregnated resins[1] (SIRs, Figure 1) are used as three-phase separation systems. A solute is present in an aqueous phase; the SIR contains the stationary, diluent phase, an organic liquid impregnated in the pores of the inert resin particle. When brought in contact with a SIR, the solute will diffuse from the aqueous phase into the diluent phase, with equilibrium constant K_{phys}. Ion-exchange SIRs are already widely used to separate heavy metal ions[2-11] from aqueous phases in a fast and simple way, making use of the solubility of the solute in the liquid organic phase, in exchange for protons. Only recently, other applications have been investigated, e.g. the large-scale recovery of apolar organics[12] and bench-scale or pilot-scale recovery of polar organics like organic acids,[13,14] amino acids[15] and flavonoids.[16] However, large-scale applications for the separation of polar solutes, like ethers and phenols, do not yet exist.

SIRs display general advantages when compared to other separation techniques. While during conventional extraction (liquid – liquid extraction) the solvent and the extractant have to be dispersed, in a SIR setup the dispersion is already achieved by the impregnated particles. This also removes the requirement of an additional phase-separation step. In addition, the impregnation step decreases solvent loss.[17] Furthermore, SIRs have a crucial advantage over e.g. ion-exchange resins with chemically bound extractants, as they can be reused for different separation tasks by simply rinsing one extractant out and re-impregnating them with another one, thereby saving expensive resin design and production. A SIR system works well for highly apolar solutes,[1] but to adequately separate more polar organic compounds from aqueous streams, improved extraction is required.

In order to enhance extraction, complex-forming extractants can be added to the diluent. By means of complex formation, with equilibrium constant K_{chem}, the overall equilibrium concentration of solute in the diluent phase can, in principle, be increased, in which case the overall extraction would be significantly enhanced. An optimization of the complex-forming ability of the extractant (high K_{chem}) can thus improve the SIRs performance.[18]

In principle, molecular recognition and complexation of the solute inside the SIR particles, as indicated in Figure 1, can provide a new and fast way to separate more polar organic solutes from aqueous streams. Ultimately, the extractant itself should possess a low melting point and be a liquid at room temperature, so that a diluent would no longer be necessary. A high boiling point would also be beneficial, because it facilitates regeneration at elevated temperatures. For the effective removal of polar and protic organic solutes like ethers and phenols, as e.g. desired in
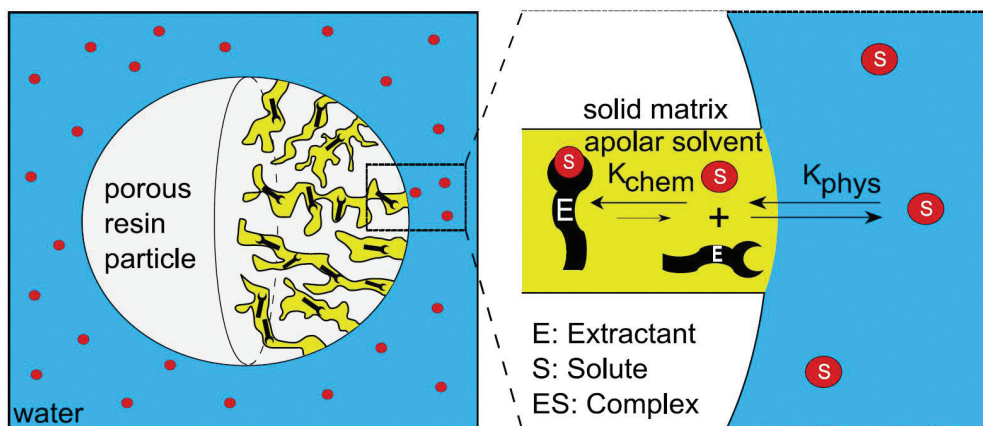
Figure 1. Operational principle of solvent-impregnated resins with an active extracting agent in the pores.

water-cleaning processes, the additional complexation step of the solute in the diluent phase turns out to be crucial for large-scale application, due to the relatively high solute solubility in water. The current techniques of phenol extraction include common liquid-liquid extraction, membrane-based solvent extraction in coupled ultrafiltration modules[19] and hollow fiber modules.[20] Also, dual-solvent extraction processes are used to recover organic pollutants from water, but these are very energy-consuming and can lead to contamination of the waste water with the polar extractant.[21] Therefore, an extractant-impregnated resin approach is currently under development in our labs.

The basis for optimizing an extractant via molecular design is a deeper understanding at the molecular level. Molecular modeling can facilitate this understanding by providing useful data about the complexation processes. The results of the modeling experiments can then be compared with experimental data. In this paper we investigate a set of extractants for the extraction of phenol, thiophenol and substituted phenols from an aqueous environment, to establish the basis for a future industrial design. Strong hydrogen-bonds are desired for SIR-based processes, which prompted this study with phosphates and phosphine oxides that can form hydrogen-bonding complexes with phenols[22] (Table 1). Alkylated phosphates and phosphine oxides combine a low solubility in water with a partial negative charge on the oxygen atom that was expected to be favorable for hydrogen bonding. The most important hydrogen bond characteristics to be explored in this paper are the hydrogen bond strength and the geometry of the resulting complexes. From literature, neutral O–H•••O hydrogen bonds are expected to have a strength

of ca. 4-15 kcal/mol,[22,23] covering a range of H-bond lengths and O–H•••O angles,[24,25] as these parameters depend strongly on the molecular geometry of the system at hand.

Table 1. Compounds under investigation in the calculations, and angular and radial parameters describing H-bond geometry in phosphine oxides and phosphates; H-bond length, d (Å), H-bond angle, α (°), O–H bond length, r (Å), and dihedral angle between C2, C1, and r, ϕ (°).

Compound	Molecular formula
phenol	C_6H_5OH (**1**)
thiophenol	C_6H_5SH (**2**)
3-chlorophenol	$3\text{-}Cl\text{-}C_6H_4OH$ (**3**)
3,5-dichlorophenol	$3,5\text{-}Cl_2\text{-}C_6H_3OH$ (**4**)
4-cyanophenol	$4\text{-}CN\text{-}C_6H_4OH$ (**5**)
pentachlorophenol	$Cl_5\text{-}PhOH$ (**6**)
phosphates	$O{=}PR_3$ ($R = {-}O{-}CH_3$) (**7**)
thiophosphates	$S{=}PR_3$ ($R = {-}O{-}CH_3$) (**8**)
phosphine oxides	$O{=}PR_3$ ($R = {-}CH_2{-}CH_3$) (**9**)
phosphine sulfides	$S{=}PR_3$ ($R = {-}CH_2{-}CH_3$) (**10**)

The interaction between the phenols and the extractants is investigated in detail experimentally with liquid-liquid extraction experiments and isothermal titration calorimetry (ITC). Although a great deal of information about hydrogen bonding of phenols by phosphates and phosphine oxides is already available from literature,[22,26-33] this information was obtained from measurements in CCl_4. Most of the results obtained in these literature reports are based on IR measurements and subsequent derivation of the thermodynamic parameters. Due to the experimental complexity and the assumptions that have to be made, no consistency in the results exists in the literature, as has also been pointed out elegantly by Jeffrey.[22] In addition, we report for the first time

complexation constants obtained in water-saturated toluene to quantify the effect of water on complexation constants when measured in an environment that contains water. These literature reports are therefore different and unsuitable for our purposes, i.e. for understanding the factors essential to the development of a solvent-impregnated resin extraction system for removal of phenols from an aqueous system. Results obtained on different systems cannot be compared directly, as is clear from our results for pentachlorophenol complexation by phosphine oxide (*vide infra*). Where some investigators[26,32] find lower complexation constants for pentachlorophenol compared to phenol, we now report higher complexation constants for the former, based on both ITC measurements and on molecular modeling *in vacuo*.

Liquid-liquid extraction experiments are used to test phosphate, phosphine sulfide and phosphine oxide extractants in two-phase systems for their potential in phenol extraction. With these experiments, the overall distribution coefficients K_D are obtained. In addition, ITC measurements were performed to get insight into the binding affinity K_{chem}, and to obtain the thermodynamic data involved in complex formation. ITC[34-38] can be used to directly measure the binding affinity (equilibrium constant, K_{chem}) and thermodynamic parameters (enthalpy of complex formation ΔH^0, and stoichiometry N) in complexation reactions, and the values of change in entropy, ΔS^0, and free energy, ΔG^0, can be derived from this. Although by far the most of the ITC measurements reported in literature are carried out in aqueous solutions, its use is also unproblematic with co-solvents like methanol or DMSO,[39] or with organic solvents like chloroform,[40,41] toluene[41-43] or others.[44] The reasons to use toluene in our experiments include first of all its utility as a model system for the industrial application of SIRs that we are aiming for (in contrast to CCl_4, which is a probable carcinogen). In addition, toluene presents only a minor influence on hydrogen bonding interactions, and it is a good solvent for the compounds that are under investigation. Many investigations on hydrogen bonding describe experimental work that is carried out in toluene, and clearly indicate that this solvent does not affect hydrogen bond formation much.[45-47]

Hydrogen bonds in all kinds of systems have been extensively studied by density functional theory.[23,24,48-53] In this work, molecular modeling experiments have been applied to investigate the complex formation. The geometries of the monomers and complexes have all been optimized at the B3LYP/6-311G(d,p) level of theory, which generally describes the geometries of these systems well. Two different high-level methods (B3LYP/6-311+G(d,p)//B3LYP/6-311G(d,p) and MP2/6-311++G(2d,2p)//B3LYP/6-311G(d,p), including counterpoise correction for MP2), in combination with an SCRF approach to mimic the solvent effects of toluene were used

to obtain energy data and other properties that are not too dependent on the method used. Although analysis of a small data set of hydrogen-bonded complexes suggests that other density functionals might perform somewhat better in describing hydrogen-bonding interactions,[54] no analysis has been presented in literature that includes a series of compounds with sulfur or phosphor atoms, and therefore the widely used B3LYP functional was used here. In the resulting analysis the theoretical predictions and the experimentally obtained results have been combined in order to provide a detailed picture and insight into the complexing behavior of phenols towards several phosphates and phosphine oxides.

Experimental Section

General. The following materials were used as received without further purification: tri-n-octylphosphine oxide (TOPO) ($\geq$ 99%, Sigma Aldrich), Cyanex 923 (a mixture of four trialkylphosphine oxides R_3PO, $R_2R'PO$, RR'_2PO, and R'_3PO where R = n-C_6H_{13} and R' = n-C_8H_{17}; 93%, Cytec Industries), tri-n-butylphosphate (TBP) (> 99%, Merck), triisobutylphosphine sulfide (TIBPS) (98%, Cytec Industries), phenol (> 99%, Merck), 3-chlorophenol (99%, Janssen Chimica), 3,5-dichlorophenol (99%, Sigma Aldrich), 4-cyanophenol (95%, Sigma Aldrich), pentachlorophenol (99%, Sigma Aldrich) and thiophenol (97%, Janssen Chimica).

All ITC measurements were performed with p.a.-quality toluene dried on molecular sieves (3 Å).

Liquid – liquid extraction. In a SIR system, in equilibrium the overall distribution coefficient K_D is defined as described in equation (1). The concentration of solute in the organic phase (extractant and diluent) based on partitioning is c_S^{org}, the concentration of the complex in the organic phase is c_{ES}^{org} and the concentration of the solute in the aqueous phase is c_S^{aq}.

$$K_D = \frac{c_S^{org} + c_{ES}^{org}}{c_S^{aq}} \qquad (1)$$

The amount of solute in the pores of the SIR particle consists of dissolved solute and complexed solute. The extraction is mainly based on the binding affinity K_{chem} *(vide infra)*, in this case resulting from the hydrogen bond formation between the extractant and the solute. This chemical equilibrium inside the pores of the SIR particle can be described via

$$\text{Solute (S) + Extractant (E)} \quad \xrightleftharpoons{K_{chem}} \quad \text{Complex (ES)} \qquad (2)$$
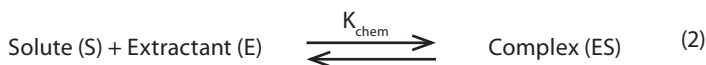
Thus, K_{chem} is derived as in equation (3). The equilibrium concentration of the extractant in the organic phase is represented by c_E^{org}.

$$K_{chem} = \frac{c_{ES}^{org}}{c_S^{org} \cdot c_E^{org}} \qquad (3)$$

The partitioning of phenol between the aqueous phase and the organic phase inside the resin particle is given in equation (4).

$$K_{phys} = \frac{c_S^{org}}{c_S^{aq}} \qquad (4)$$

Inserting equations (3) and (4) into equation (1) gives equation (5), an expression of the overall distribution coefficient K_D, depending on the physical and chemical equilibrium constants.

$$K_D = K_{phys} + K_{phys} \cdot K_{chem} \cdot c_E^{org} \qquad (5)$$

This correlation can also be represented in a graph (Figure 2), which can be used to conveniently determine the influence of both physical and chemical extraction.
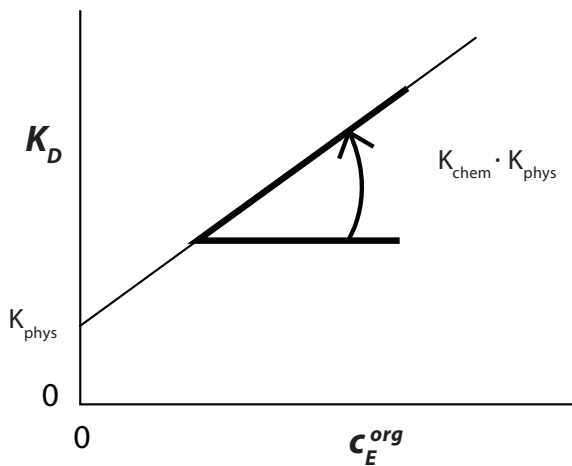

Figure 2. Graphical representation of the overall distribution coefficient K_D with the physical and chemical equilibrium constants, K_{phys} and K_{chem}, respectively.

In the extraction experiments aqueous solutions (presaturated with toluene) of 40 g demineralized water containing 1000 ppm w/w phenol (a typical concentration in large-scale extractions) were mixed with 4 g of extractant solution. The extractant solutions (0.1, 0.5, 1.0 and 1.5 M) were prepared by dissolving either TOPO, Cyanex 923, TBP, or TIBPS in toluene (presaturated with water; the mole fraction solubility of water in toluene at 30 °C is around 0.003,[55-57] i.e. $[H_2O] \sim 28$ mM). Toluene itself has only a very low capacity for phenol *(vide infra)*, which is the reason why it was chosen as a diluent. Toluene, with no extractant dissolved, was also used to extract phenol, in order to determine the physical partitioning of phenol in the extractant solution (K_{phys}). The extraction vessels were stirred at 500 rpm for ≥ 16 h at a constant ambient temperature of 30 °C. Afterwards, the two phases were separated. Samples of the aqueous phase were filtered with two 0.2 μm filter units (Whatman Spartan 30/0.2 RC). Samples of 1 - 10 mL of the aqueous phase were diluted with demineralized water to give a volume of 100 mL. After this, successively 5 mL buffer solution pH 10 (ammonia 25%, ammonium chloride, potassium sodiumtartrate-tetrahydrate, water) 3 mL potassium hexacyanoferrate solution and 3 mL 4-aminoantipyrine solution (4-amino-2,3-dimethyl-1-phenyl-3-pyrazolin-5-one, water) (all according to DEV H 16) were added. According to the Emerson reaction[58,59] the phenol was complexed by 4-aminoantipyrine and this complex was detected with a Varian Cary 300 UV/VIS Spectrophotometer at 510 nm. The equilibrium concentration of phenol in the aqueous phase was calculated using a calibration line; the equilibrium concentration of phenol in the organic phase was calculated from the mass balance. From these concentrations the overall distribution coefficient (K_D) was calculated.

Isothermal Titration Calorimetry (ITC). ITC was performed on a MicroCal VP-ITC microcalorimeter; the setup is described elsewhere.[60] Results were processed using Origin® 7SR2 V7.0383 (B383) by Origin Lab Corporation. The measuring cell (1.46 mL) was flushed and filled with a freshly prepared and degassed solution of the phenolic compound in either carefully dried toluene (usually concentrations between 1 and 10 mM were used) or in toluene that was saturated with water. The 280 μL automatic syringe was flushed and filled with a freshly prepared and degassed solution of the complexing agent in dry toluene at a concentration of roughly 10 times the molarity of the cell solution. Depending on the concentration of the compounds in solution and the magnitude of the heat effect per second, the number of injections and the injected volume per injection were chosen. Between subsequent injections a sufficient amount of time was chosen to allow for the cell feedback to return to the baseline, usually 180 to 300 seconds. Stirring speed for all ITC measurements was 502 rpm (default value). A reference measurement was performed using the same procedure,

only having the solvent, not the solute, in the measuring cell. By subtracting the reference measurement from the actual measurement the net results were obtained and they were fitted using the one-set-of-sites model present in the Origin software.

Modeling. Computational data were all obtained using the Gaussian03 suite of programs.[61] All B3LYP/6-311G(d,p)-optimized stationary points were confirmed as true minima via vibrational frequency calculations. This was followed by single-point calculations of the optimized geometries at the B3LYP/6-311+G(d,p) and MP2/6-311++G(2d,2p) levels of theory. These two methods were chosen to ensure that results are not influenced by method-dependent phenomena, and basis sets were chosen big enough to ensure sufficient accuracy.[53,62] It is known that at this level B3LYP yields accurate energy data in many cases, specifically for minimum energy structures, although hydrogen bond lengths are generally a little underestimated.[63] MP2 performs at this level typically well both in geometry optimization as well as in estimation of interaction energies for hydrogen bonding.[49,52,63] In an effort to reproduce the experimental results as accurately as possible, the effect of the medium (toluene) was also simulated, using the self-consistent reaction field (SCRF) method in the polarizable continuum model (PCM) at the B3LYP/6-311+G(d,p) level.[64] For these calculations the solvent 'toluene' was specified in the input section. Finally, since electrostatic interactions are crucial for the strength of hydrogen bonds,[65-69] natural population analysis (NPA)[70,71] charges were obtained, as these display a relatively small method and basis set dependence and have proven to be reliable charge indicators for related theoretical studies of hydrogen bonds. In addition, atom-atom overlap-weighted natural atomic orbital (NAO) bond orders were obtained.

Specifically MP2 calculations of hydrogen bonding interactions are subject to a basis set superposition error (BSSE) because of over-stabilization due to the supermolecular approach.[72] An *a posteriori* counterpoise (CP)[73,74] BSSE correction has therefore been used (MP2 only), and a zero-point correction to the energy was applied. Complexes that were investigated in this way each consisted of a phenol or thiophenol, and one of the phosphates/phosphine oxides (Table 1). The model compounds resemble the compounds used in liquid-liquid extraction experiments and ITC, but for computational speed the long alkyl tails were replaced by methyl or ethyl groups. In Table 1 the different relevant geometrical parameters are defined for hydrogen bonds in the investigated complexes.

Results and discussion

Liquid – liquid extraction. The physical equilibrium constant (K_{phys}) is determined by the partitioning of phenol in the inert diluent toluene, and amounts to 1.5 at 30 °C. The chemical equilibrium constant (K_{chem}) is dependent on the extractant dissolved in the toluene. As can be seen in Table 2, K_{phys} is very low compared to $K_{chem} \cdot c_E$. Therefore, the extraction is dominated by the chemical interaction of phenol with the respective extractant dissolved in the toluene phase. Table 2 also shows that the trialkylphosphine oxides TOPO and Cyanex 923 have the highest overall distribution coefficients K_D in the liquid – liquid extraction experiments, compared to the other substances, which is also graphically shown in Figure 3.

Table 2. Chemical equilibrium constants, K_{chem} (M^{-1}), calculated from overall distribution coefficients, K_D, determined by liquid – liquid extraction of phenol.

Extractant	c_E^{org} [M]	K_D [-]	K_{chem} [M^{-1}]
Toluene	0.00	1.5*	0
Cyanex 923	0.10	25	551
	0.51	397	
	1.00	677	
	1.56	883	
TOPO	0.10	29	579
	0.50	374	
	1.00	689	
	1.50	791	
TBP	0.10	11	77
	0.47	56	
	0.94	101	
	1.44	148	
TIBPS	0.51	6	5
	1.01	7	
	1.50	11	

*equals K_{phys}

Based on the higher polarity of the phosphate group as compared to the phosphine oxide group, one might have expected a higher phenol distribution coefficient K_D for tributylphosphate (TBP) than for Cyanex 923 or TOPO. However, the K_D of TBP is found to significantly lower. A likely reason for this is the co-extraction of water by TBP from the aqueous phase. This plays a bigger role for TBP than for e.g. TOPO, due to the significantly longer alkyl chains of TOPO, which makes the overall local medium for the complexed water much less polar. It is also seen that the tested tri-isobutylphosphine sulfide (TIBPS) is a less effective phenol extractant than the trialkylphosphine oxides and the trialkylphosphate. The lower electron density at the sulfur in the phosphine sulfide group (see Natural Population Analysis data, *vide infra*) makes it a weaker hydrogen bond acceptor, and therefore a weaker extractant.
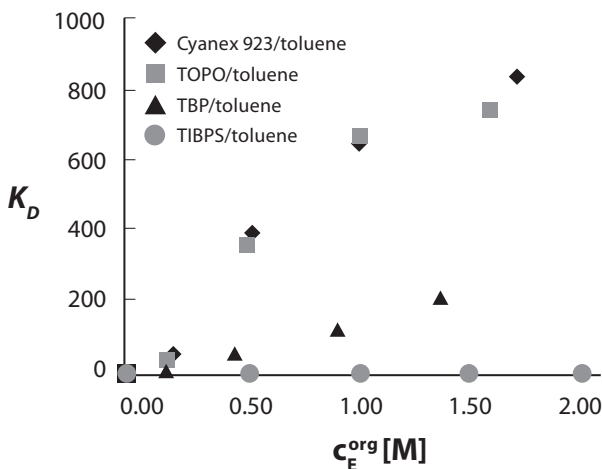
Figure 3. Overall distribution coefficients, K_D, determined by liquid – liquid extraction of phenol.

For the application in SIRs it would be desirable to work without diluents like toluene to avoid a contamination of the aqueous phase with the diluent, and to achieve a higher concentration of extractant inside the SIR. Cyanex 923 would therefore be the preferred extractant, because it is a liquid at room temperature, while TOPO is a solid with a melting point of 52 °C, and would have to be dissolved in a suitable diluent or derivatized (e.g. as iso-octyl compound) to become a liquid.

ITC. Figure 4A shows a result of a calorimetric titration of phenol with TOPO in dry toluene. The binding of phenol to TOPO is exothermic, with ΔH^0 = -6.8 kcal/mol and K_{chem} = $1.0 \cdot 10^3$ M^{-1}. The molar ratio of TOPO / phenol was 0.95 at saturation, indicating that there are no other effects that interfere with direct binding of phenol to TOPO, a fact that was also shown to be true for the other combinations. The entropy factor $T\Delta S^0$ is negative, indicating an overall increased order upon binding. Apparently, the complexing agents do either not have strong interactions with the surrounding medium, or those interactions do not significantly change upon complexation. The values of all thermodynamic parameters obtained for the different complexes are listed in Table 3.
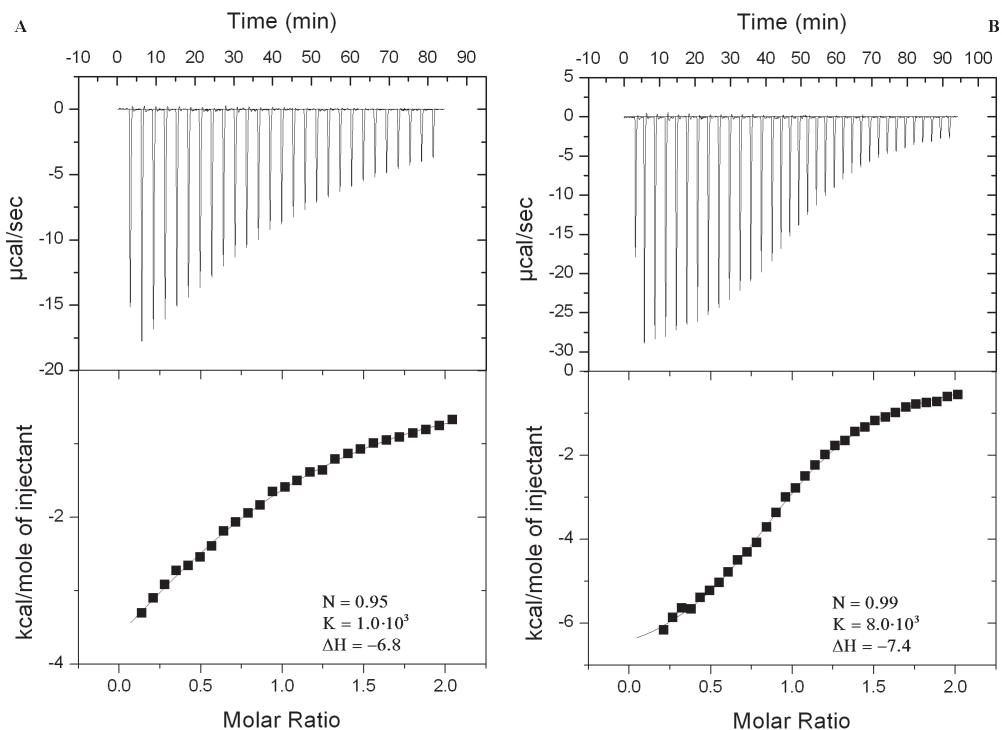

Figure 4. Binding isotherms for TOPO – phenol complexes at 30 °C. Top pane: raw data. Lower pane: processed binding isotherm. Syringe: TOPO in dry toluene (10.8 mM). Cell: A: Phenol (1.08 mM in dry toluene); B: 4-Cyanophenol (1.09 mM in dry toluene). Note the different scale in A and B.

Figure 4B depicts the calorimetric titration of 4-cyanophenol with TOPO in dry toluene. In this case, a clearly sigmoid curve can be observed, which is indicative for strong binding of the solute to the complexing agent, as confirmed by the much higher binding affinity ($K_{chem} = 8.0 \cdot 10^3$ M^{-1}). The higher value is in line with the electron-withdrawing capacity of the 4-CN moiety, which makes this phenol more acidic and therefore a better hydrogen-bond donor.

Table 3. ITC results listing all thermodynamic parameters for TOPO – phenol complexes and the TBP – phenol complex: Stoichiometry N (-), binding affinity K (M^{-1}), enthalpy of complexation ΔH^0 (kcal/mol), change in Gibbs free energy ΔG^0 (kcal/mol), and the entropy TΔS^0 (kcal/mol).

Complex	N	K	ΔH^0	ΔG^0	TΔS^0
TOPO – phenol[a]	0.95 ± 0.01	$(1.0 \pm 0.1) \cdot 10^3$	-6.8 ± 0.2	-4.2 ± 0.1	-2.6 ± 0.1
TOPO – phenol[b]	1.07 ± 0.02	$(5.8 \pm 1.2) \cdot 10^2$	-6.9 ± 0.5	-3.8 ± 0.1	-3.0 ± 0.6
TOPO – 3-chlorophenol[a]	0.97 ± 0.07	$(3.5 \pm 0.5) \cdot 10^3$	-7.1 ± 0.3	-4.9 ± 0.1	-2.2 ± 0.2
TOPO – 3-chlorophenol[b]	1.11 ± 0.01	$(1.6 \pm 0.5) \cdot 10^3$	-9.2 ± 1.2	-4.4 ± 0.2	-4.8 ± 1.4
TOPO– 3,5-dichlorophenol[a]	1.01 ± 0.05	$(9.8 \pm 0.4) \cdot 10^3$	-7.1 ± 0.1	-5.5 ± 0.0	-1.6 ± 0.1
TOPO–3,5-dichlorophenol[b]	1.16 ± 0.01	$(4.0 \pm 1.0) \cdot 10^3$	-8.6 ± 0.8	-5.0 ± 0.2	-3.6 ± 1.0
TOPO – 4-cyanophenol[a]	0.99 ± 0.08	$(8.0 \pm 0.6) \cdot 10^3$	-7.4 ± 0.3	-5.4 ± 0.1	-2.0 ± 0.3
TOPO – 4-cyanophenol[b]	1.09 ± 0.11	$(5.4 \pm 2.5) \cdot 10^3$	-8.1 ± 1.0	-5.1 ± 0.3	-3.0 ± 1.2
TOPO - pentachlorophenol[a]	0.88 ± 0.03	$(1.1 \pm 0.1) \cdot 10^3$	-8.7 ± 0.7	-4.2 ± 0.1	-4.5 ± 0.6
TOPO - pentachlorophenol[b]	0.94 ± 0.04	$(7.7 \pm 0.8) \cdot 10^2$	-8.6 ± 0.6	-4.0 ± 0.1	-4.6 ± 0.6
TBP – phenol[a]	0.98 ± 0.10	$(9.2 \pm 0.9) \cdot 10^1$	-5.8 ± 0.8	-2.7 ± 0.1	-3.0 ± 0.9
TBP – phenol[b]	1.01 ± 0.20	$(5.9 \pm 0.5) \cdot 10^1$	-8.1 ± 0.7	-2.5 ± 0.1	-5.7 ± 0.8

[a]solvent: dry toluene; [b]solvent: water-saturated toluene.

The changes in ΔG^0 upon binding of the phenols with electron-withdrawing substituents (3-chlorophenol, 3,5-dichlorophenol and 4-cyanophenol with pK$_a$ values of 9.02,[75] 8.04[76] and 7.95,[75] respectively) are significantly higher than for phenol itself, accordingly leading to much higher binding affinities for the former phenols. Again, the influence of TΔS^0 to complex formation is negative, so that complexation is enthalpy driven. For pentachlorophenol (pK$_a$ = 4.68[76]) the change in ΔG^0 is also higher than for phenol itself (as expected from the very low pK$_a$) but judging from the very large inhibiting effect of TΔS^0, solvent interactions prevent the formation of a very strong hydrogen bond. As a result, K$_{chem}$ was found to be only marginally higher than for phenol

(K_{chem} = 1.1•10^3 M^{-1} *vs.* 1.0•10^3 M^{-1} for phenol), in contrast to results in literature,[26,32] where penta-chlorophenol was found to have a lower binding affinity towards complexing agents with the P=O moiety (obtained from IR measurements in CCl_4).

In the presence of water, the affinity of phenols towards TOPO is significantly lower. Binding affinities in the presence of water range from 5.8•10^2 M^{-1} for phenol, which was in excellent agreement with the liquid – liquid experiments (579 M^{-1}; *vide supra,* Table 2), to 5.4•10^3 M^{-1} for 4-cyanophenol. This amounts to a water-induced decrease in K_D of 30 - 60 %. The main reason for this decrease is the unfavorable change in entropy. For the TOPO – phenol complex, the differences are the smallest; ΔH^0 is in the presence of water only 1.5 % more negative, whereas ΔS^0 is over 15 % more negative. For the phenols with electron-withdrawing groups these differences are much larger; ΔH^0 is 9 - 30 % more negative in the presence of water, whereas ΔS^0 is 50 - 125 % more negative. Thus, hydrogen bond formation is found to be more favorable (ΔH^0 is more negative), as additional hydrogen bonds can be formed with the water molecules. However, complex formation is severely hindered by the large negative change in entropy (ΔS^0 is more negative), so that ΔG^0 is found to be less negative than in the water-free case. This indicates co-complexation of water by the extractants, where the water molecules are bound tightly to the extractant – phenol complex, losing much of their entropic freedom. Water binding by TOPO in the absence of phenol has been subject of investigation, but because of the very low heat effect this could not be quantified.

For TOPO - pentachlorophenol complexes, the influence of the water is different. In line with previous results, the binding affinity in the presence of water is significantly lower (by 32 %). However, ΔH^0 is less negative in the presence of water and ΔS^0 is hardly affected by the water, in contrast to the other TOPO - phenol complexes. Presumably, the five chlorine atoms show some favorable interaction with the water environment. This means that although in principle much stronger hydrogen bonds could be formed between TOPO and pentachlorophenol in comparison to phenol, this effect is nearly eliminated by the large unfavorable change in entropy, due to the loss of entropic freedom of the water molecules in the vicinity of the complex. The 'energetic signatures', in which the thermodynamic parameters of the investigated interactions are compared graphically, are given in Figure 5. In general, there are three different types of energetic signatures:[38] one for favorable interaction due to hydrogen bond formation, one for Van der Waals interactions and one for a combined process. In hydrogen bond formation, the signature is characterized by a high negative value of ΔH^0, and a relatively small negative value for $T\Delta S^0$. This

is completely in line with the results obtained here. All TOPO – phenol interactions discussed here show the same signature, which is thus indicative for hydrogen bond formation accompanied by a loss of entropic freedom.[38] This effect is more pronounced in the cases where there is water present, as has just been discussed.
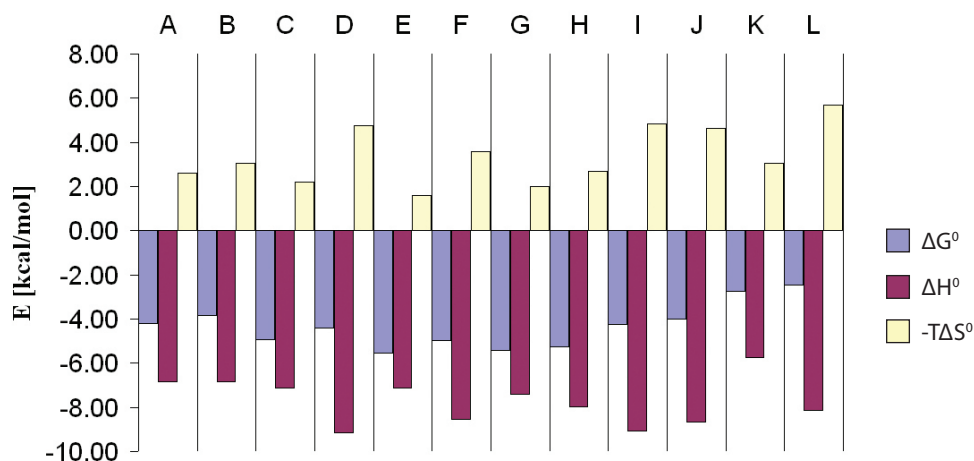

Figure 5. Energetic fingerprints of extractant - phenol complexes. A: TOPO – phenol; B: TOPO – phenol, water present; C: TOPO – 3-chlorophenol; D: TOPO 3-chlorophenol, water present; E: TOPO- 3,5-dichlorophenol; F: TOPO – 3,5-dichlorophenol, water present; G: TOPO – 4-cyanophenol; H: TOPO – 4-cyanophenol, water present; I: TOPO – pentachlorophenol; J: TOPO – pentachlorophenol, water present; K: TBP – phenol; L: TBP – phenol, water present.

In addition to these experiments, ITC measurements have also been performed on the tri-butyl-phosphate (TBP) – phenol, triisobutylphosphine sulfide (TIBPS) – phenol and TOPO – thiophenol complexes. The thermodynamic parameters for the TBP – phenol interactions are given in Table 3. The heat effects measured upon TIBPS – phenol and TOPO – thiophenol interaction were both very low, even at high concentrations. Since the experimental errors in those measurements were therefore relatively large, it was not possible to calculate accurate quantitative thermodynamic parameters from these measurements, both in the absence and in the presence of water. The binding affinities K_{chem} for the TIBPS – phenol and TOPO – thiophenol interactions in absence of water were found to be approximately 8 and 85 M^{-1}, respectively, indicating that hydrogen bonds via sulfur atoms are indeed much weaker than the corresponding O–H•••O hydrogen bonds present in e.g. the TOPO-phenol complex (K_{chem} = 1.0•10^3 M^{-1}). The TBP binding to phenol (K_{chem} =

92 M^{-1}) indicates that phosphate – phenol binding is indeed much weaker than phosphine oxide – phenol binding, as was also found with liquid – liquid extraction experiments. The phosphate – phenol complexes were formed in a 1 : 1 ratio, as was also found for the phosphine oxides. While ΔG^0 is negative, there is clearly less driving force available than for the formation of the phosphine oxide – phenol complex, largely caused by a reduced enthalpy change. However, in the presence of water, a much larger change of ΔH^0 was found, which is indicative for co-complexation of water molecules to the TBP. This was again accompanied by a much larger negative entropy change upon complexation, due to the loss of entropy for the water molecules upon binding to TBP.

DFT and MP2 computations. In the following section, first phosphine oxide – phenol complexes will be discussed, subsequently the phosphate – phenol complexes, and finally substituent effects on the phosphine oxide – substituted phenol complexes.

Phosphine oxides – phenol complexes. As can be seen from the optimized geometries of the selected phosphine oxide – phenol and phosphate – phenol complexes (Figure 6A and 6B, Supp.
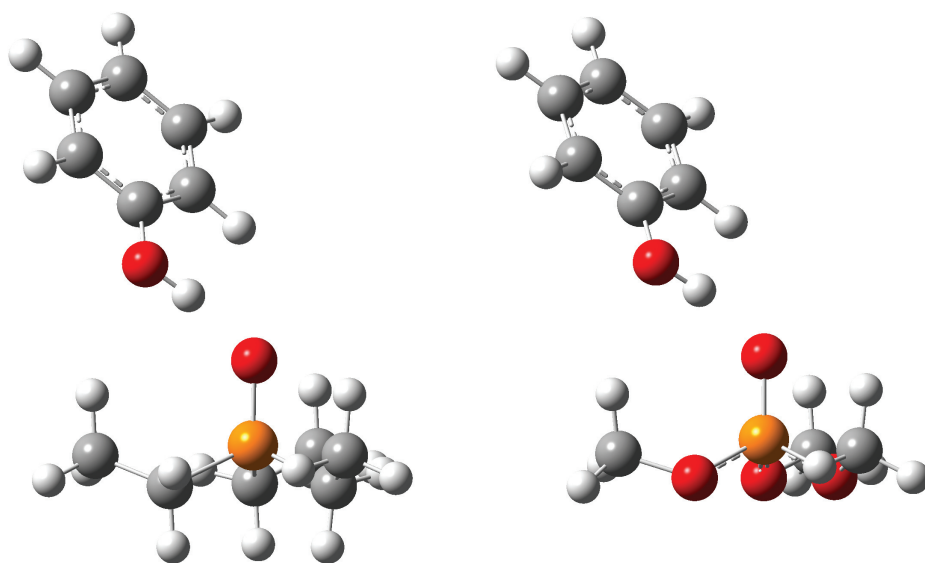
A: triethylphosphine oxide – phenol (**C1**)   *B*: trimethylphosphate – phenol (**C5**)

Figure 6. Optimized structures (B3LYP/6-311G(d,p) (vacuum)) of representative phosphine oxide – phenol and phosphate – phenol complexes. Orange: phosphorus; red: oxygen; black: carbon; white: hydrogen.

Info. Figure S-1 and S-2), phenols form a hydrogen bond to the P=O moiety, showing a geometry with a near-ideal linear hydrogen bond. In the triethylphosphine oxide (TEPO) – phenol complex (complex **C1**, Figure 6A), the hydrogen bond length is short (d = 1.72 Å) and the hydrogen bond angle is almost perfectly linear (α = 171°, Table 4). In addition, the bond lengthening of the hydrogen bond donor is substantial (Δr = 0.021 Å) and the dihedral angle of the phenol is close to zero (ϕ = -2.2°). The enthalpy of complexation ΔH (in vacuum) in complex **C1** is found to be -12.0 kcal/mol both at the B3LYP and MP2 levels of theory, whereas ΔH in toluene (B3LYP) was -10.7 kcal/mol.

With respect to the B3LYP values, the calculated MP2 values for the enthalpy of complex formation for phosphine oxide – phenol complexes are typically equal or slightly more negative, in line with trends from the literature.[51] Results show that complex formation in toluene is slightly less favorable than in vacuum, by ~ 1.3 kcal/mol. This indicates a minor solvent effect, as was also clear from the solvation energies of the solutes and complexes. The natural population analysis (NPA) charges on the oxygen of the phosphine oxide and the hydrogen of the phenol alcohol moiety were found to be -1.11 and +0.51 (see Table 4), respectively, which points to a strong electrostatic tendency for hydrogen bonding. Some covalent character is also apparent, as can be deduced from the atom-atom overlap-weighted NAO bond orders. For example, the bond order between the TEPO oxygen and the phenol hydrogen amounts to 0.076, while the bond order in the phenol O–H bond was found to be 0.600, i.e. 0.061 smaller than that in the isolated phenol molecule (cf. Supporting Information).

Table 4. Selected geometric parameters (see Table 1), enthalpy of complexation ΔH (kcal/mol), and charges on hydrogen bond forming atoms of the triethylphosphine oxide (TEPO) and triethylphosphine sulfide (TEPS) complexes with phenol and thiophenol.[a]

Complex		geometric parameters				ΔH			NPA charge(B3LYP)	
						B3LYP		MP2	phosphine	phenol
		d	α	Δr[b]	ϕ	vacuum	toluene	vacuum	O or S	H
C1	TEPO - phenol	1.72	171	0.021	-2.2	-12.0	-10.7	-12.0	-1.11	+0.51
C2	TEPO- thiophenol	2.00	172	0.011	-5.3	-6.5	-5.4	-7.6	-1.09	+0.19
C3	TEPS - phenol	2.36	171	0.012	+3.4	-6.3	-5.1	-9.4	-0.66	+0.49
C4	TEPS - thiophenol	2.63	170	0.010	-9.4	-3.7	-2.9	-6.5	-0.64	+0.16

[a] d, α, Δr and ϕ, as shown in Table 1.
[b] $\Delta r = d$(O–H) in the complex – d(O–H) of non-complexed phenol; analogous for S; (d(O–H)$_{phenol}$ = 0.963 Å; d(S– H)$_{thiophenol}$ = 1.347 Å).

These theoretical findings suggest that a strong hydrogen bond is formed in a 1 : 1 ratio of phosphine oxide and phenol. This is supported by the liquid – liquid extraction (high distribution coefficients K_D) and ITC results (high K_{chem} high negative ΔH^0 and ΔG^0, and N = 0.95 – 0.99). The modeling data predict a more negative ΔH than obtained with the ITC, i.e. for the TOPO – phenol complex ΔH_{ITC} = -6.8 kcal/mol (Table 3), while $\Delta H_{model}^{toluene}$ = -10.7 kcal/mol (Table 4). Since B3LYP and MP2 yield highly similar data, two factors may seem to attribute this quantitative gap: an incomplete description of the solvent effects by the PCM model, and a contribution of less-than-optimal geometries in the experimental situation, caused by the dynamic nature of hydrogen bond formation. As the theoretical description of solvent effects will likely continue to improve, a more detailed dissection can be expected in the future.

By comparing the overall distribution coefficient K_D and the physical and chemical distribution coefficients K_{phys} and K_{chem} of phenol for a TOPO solution in toluene, it can be seen that the main source for the overall distribution coefficient of ~580 is the binding of phenol to phosphine oxide with a high binding affinity K_{chem}. This clearly shows that reactive extraction can indeed increase the effective partitioning of phenols into the extraction liquid by several orders of magnitude! The TEPO – thiophenol complex (complex **C2**) shows much lower binding enthalpy values, as was also observed in the ITC measurements. The charge on the thiophenol hydrogen is much smaller than for the phenol hydrogen in the corresponding TEPO – phenol complex discussed before, which is the main source for the negative influence of the sulfur atom on the hydrogen bonding. Also the bond order of the hydrogen bond is found to be much lower than for the TEPO – phenol complex (0.038 *vs.* 0.076 for TEPO – phenol, *vide supra*).

The phosphine sulfide complexes to phenol and thiophenol (complexes **C3** and **C4**) both show even less negative enthalpies of complexation; the least negative were found for the triethyl-phosphine sulfide (TEPS) – thiophenol complex. The clearest geometrical differences come from the lengthening of the involved O–H and S–H bonds, which were clearly smaller when sulfur was involved (Δr = 0.010 – 0.012 Å for complexes with sulfur; Δr = 0.021 Å for TEPO – phenol). In line with this, the NPA charges on the sulfur atom of the phosphine sulfide are found to be much less negative than on the corresponding oxygen atom of the phosphine oxide. Again, the sulfur atom is the cause for the reduced tendency to form complexes. Also the lower bond orders of the atoms in the hydrogen bond reflect this weaker binding; the NAO O•••H bond order amounts to 0.047 and 0.045 for TEPS – phenol and TEPS – thiophenol, respectively.

The dihedral angles of the O–H or S–H bonds of the phenols with respect to their benzene ring are found to be close to the ideal value of 0°. However, some small differences between phenols

and thiophenols can be seen. Hydrogen-bound thiophenols tend to show a somewhat larger dihedral angle than phenols. These differences can be understood from the energy barriers of the rotation around the C–O/C–S bond. For phenol, the energy barriers ($E_{O-H\ at\ 90°}$ - $E_{O-H\ at\ 0°}$, angle with respect to the plane of the benzene ring) are calculated to be 3.5 and 3.0 kcal/mol (B3LYP and MP2, respectively), while for thiophenol, the corresponding values are calculated to be only 0.7 and 0.4 kcal/mol, respectively.

Phosphate – phenol complexes. As can be seen from Figure 6B, phenol forms a similar hydrogen bond to trimethylphosphate (TMP), as to triethylphosphine oxide (TEPO). As expected, within the class of phosphates and thiophosphates the TMP - phenol complexes show the highest complexing enthalpies (Table 5). These results are supported by the fact that hydrogen bond lengths are found to be shortest for TMP – phenol complexes and much longer for the complexes involving sulfur atoms, and they reflect the much higher tendency of oxygen over sulfur to form strong hydrogen bonds. With respect to the dihedral angle ϕ of phenol and thiophenol it was found that especially the thiophenol complexes again show a tendency to twist the thiol group out of plane of the benzene ring.

Table 5. Selected geometric parameters (see Table 1), enthalpy of complexation ΔH (kcal/mol), and charges on hydrogen bond forming atoms of the trimethylphosphate (TMP) and trimethyl-thiophosphate (TMTP) complexes with phenol and thiophenol.[a]

Complex		geometric parameters				ΔH			NPA charge(B3LYP)	
						B3LYP		MP2	phosphine	phenol
		d	α	Δr[b]	ϕ	vacuum	toluene	vacuum	O or S	H
C5	TMP - phenol	1.76	168	0.016	-1.4	-9.8	-8.3	-9.8	-1.11	+0.52
C6	TMP - thiophenol	2.06	169	0.008	-7.3	-5.0	-4.0	-6.3	-1.10	+0.18
C7	TMTP - phenol	2.43	167	0.009	+4.5	-4.8	-3.5	-6.0	-0.66	+0.49
C8	TMTP- thiophenol	2.78	171	0.004	-16.6	-2.4	-1.6	-4.6	-0.63	+0.15

[a] $d, \alpha, \Delta r$ and ϕ, as shown in Table 1.
[b] $\Delta r = d(O–H)$ in the complex – $d(O–H)$ of non-complexed phenol; analogous for S; ($d(O–H)_{phenol}$ = 0.963 Å; $d(S–H)_{thiophenol}$ = 1.347 Å).

From Table 5 it can be seen that for thiophenol, charges on the relevant atoms are much smaller in absolute numbers than for phenol. The charge on the phenolic hydrogen atom is ca. +0.5, whereas the charge on the corresponding thiophenol hydrogen atom is ca. +0.2, in line with the observation that hydrogen bonds by thiophenol are intrinsically much weaker than those formed by phenol. The difference between phosphate and thiophosphate can also be clearly observed. The charges on the phosphate oxygen atom and sulfur atom are around -1.1 and -0.6, respectively. This means that the thiophosphate compounds will form weaker hydrogen bonds, in line with both our experimental and theoretical results for the tendency for complexation. The bond order of the TMP – phenol hydrogen bond was found to be 0.063, a somewhat lower value than what was found for TEPO – phenol (0.076). The bond orders of the hydrogen bonds that involve one or two sulfur atoms were found to be significantly smaller: 0.034 (TMP – thiophenol), 0.032 (TMTP – phenol) and 0.021 (TMTP – thiophenol). No significant differences in the charges of the directly involved atoms have been found between phophine oxides and phosphates. However, the fact that phosphates and thiophosphates form weaker complexes than their respective phosphine oxides and sulfides is consistently reflected in differences in orbital overlap, as indicated above. An additional calculation result is that the hydrogen bond length d for the complexes of phosphine oxides and sulfides is consistently smaller than for the corresponding complexes of the phosphates and thiophosphates (cf. values of d in Table 4 versus Table 5). Based on the calculated enthalpies of complex formation, the most suitable extractant for both phenol and thiophenol extraction in the series investigated here is triethylphosphine oxide, as it yields the most negative ΔH upon complex formation. In addition, the liquid – liquid extraction experiments also point to the phosphine oxides as optimal extractants.

Triethylphosphine oxide (TEPO) – substituted phenol complexes. From Table 6 it can be seen that binding enthalpies of as much as 14.4 kcal/mol (for 4-cyanophenol, MP2, vacuum) are found for TEPO - substituted phenol complexes with electron-withdrawing substituents on the phenol. These values are more negative than the value of -12.0 kcal/mol found for the TEPO – phenol complex (complex **C1**, *vide supra*). This points to a positive influence of electron-withdrawing moieties attached to the phenolic compounds on the acidity of the O–H group, and therefore on the binding affinity K_{chem}. For the TEPO – pentachlorophenol complex a ΔH value of -11.5 kcal/mol was found, slightly less negative than for the TEPO – phenol complex. Apparently, the penta-chlorophenol does not yield additional hydrogen-bonding energy, but loses some. This effect might be due to the chlorine atoms, which force the TEPO - pentachlorophenol complex into a

slightly different geometry thereby diverting it from the hydrogen bond optimal geometry. This effect can also be seen in the slightly deviating bond angle ($\alpha = 155°$).

Table 6. Selected geometric parameters (see Table 1) and enthalpy of complexation ΔH (kcal/mol) of the TEPO complexes with substituted phenols.[a]

Complex	geometric parameters				ΔH		
					B3LYP		**MP2**
	d	*α*	*Δr[b]*	*ϕ*	**vacuum**	**toluene**	**vacuum**
C9 TEPO – 3-Cl-PhOH	1.69	173	0.024	-2.0	-13.5	-12.1	-13.3
C10 TEPO – 3,5-Cl$_2$-PhOH	1.66	174	0.026	-2.8	-14.7	-13.2	-14.4
C11 TEPO – 4-CN-PhOH	1.67	173	0.027	-3.2	-14.9	-13.4	-14.3
C12 TEPO – Cl$_5$-PhOH	1.66	155	0.031	+4.2	-11.8	-10.5	-11.5

[a] *d*, *α*, *Δr* and *ϕ*, as shown in Table 1.
[b] $\Delta r = d$(O – H) in the complex – d(O – H) of the phenol molecule (d(O – H)$_{phenol}$ = 0.963 Å in all cases).

Also in the geometric parameters the superior strength of these substituted phenol complexes can be seen. Relatively short hydrogen bonds (*d* ranges from 1.66 to 1.69 Å) and a significant lengthening of the O–H bond length (*Δr* ranges from 0.024 – 0.031 Å) are found, indicative for strong hydrogen bonds. The hydrogen bond angles are very close to the ideal value of 180°, except for the pentachlorophenol complex for reasons just discussed. Charges on all four complexes were found to be very similar. On the TEPO oxygen atom, the charge was -1.14, slightly higher than for the TEPO - phenol complex (-1.10). The charge on the phenol hydrogen was found to be +0.52 for the substituted phenols, near-identical to the value found for phenol itself. Atom-atom overlap-weighted NAO bond orders for the hydrogen bond in these TEPO – substituted phenol complexes range from 0.088 to 0.097. These are significantly higher than for the TEPO – phenol complex (0.076), which suggests that orbital overlap plays a significant role in determining the substituent effects on the stability of the hydrogen-bonded complexes. An interesting feature of the TEPO – penta-chlorophenol complex is the much lower NAO bond order between the phenol oxygen and phenol hydrogen, in comparison to the other substituted phenol complexes (see Supporting Information). This indicates that in this case, although governed by O•••H orbital overlap, the complex formation is also influenced by a decrease of O–H orbital overlap in the pentachlorophenol itself, thereby weakening the complex substantially. Presumably, the abundance of electronegative chlorine atoms stabilizes the partly-bound phenolate species. This can also be an explanation for the deviating hydrogen bond angle that was found for the TEPO – pentachlorophenol complex.
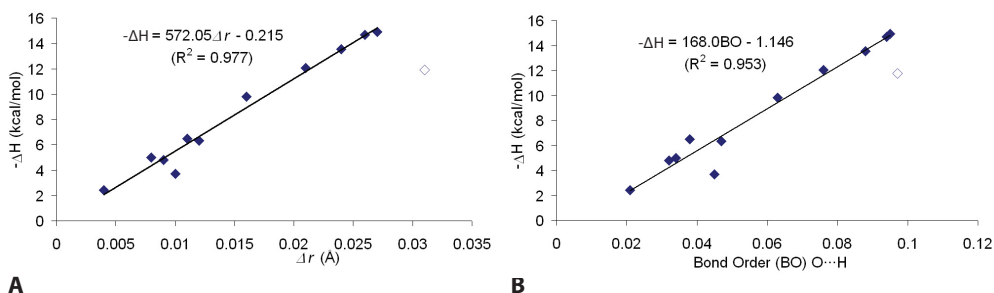
Figure 7. Dependence of binding enthalpy -ΔH on O–H bond lengthening Δr (A) and on the O–H•••O NAO bond order (B). The TEPO – pentachlorophenol data (open symbols) are indicated but not included in the trend lines (B3LYP data, in vacuo).

An interesting phenomenon can be observed if the enthalpy data ΔH are plotted against the bond lengthening Δr for the calculated complexes (Figure 7A). The lengthening of the O–H bond (Δr) increases proportionally with increasing complexation enthalpy (except for pentachlorophenol, for reasons discussed above). Also the NPA bond order is linearly correlated to the complexation enthalpy (Figure 7B; except for pentachlorophenol, for reasons discussed above). This indicates that the amount of orbital overlap between the hydrogen bond donor and acceptor is directly linked to the energy gain on complex formation. These results of strong hydrogen bonds of TEPO to substituted phenols are supported by the findings in the ITC experiments, where it was shown that all four phenols with electron-withdrawing groups (i.e. higher acidities) yield higher binding affinities towards TOPO than phenol.

Conclusions

The combination of liquid – liquid extraction and isothermal calorimetry experiments together with *ab initio* molecular modeling provides a detailed view of the interaction between phenols and phosphates and between phenols and phosphine oxides. The obtained data indicate that the binding of the extractants increases in the order trialkylphosphine sulfide << phosphate < phosphine oxide. Distribution coefficients K_D for phenol, ranging from 6 for triisobutylphosphine sulfide to ~880 for the phosphine oxides, are largely the effect of hydrogen bond formation with equilibrium constant K_{chem}.

The ITC experiments showed that the phenol – phosphine oxide interaction is primarily due to hydrogen bonding. The interaction of substituted phenols with trioctylphosphine oxide clearly

increases in the order phenol < pentachlorophenol < 3-chlorophenol < 4-cyanophenol ≈ 3,5-dichlorophenol (in line with their pK_a values, except for pentachlorophenol), with binding constants from $1.0 \cdot 10^3$ for phenol to $9.8 \cdot 10^3$ M^{-1} for 3,5-dichlorophenol in the absence of water. In the presence of water, binding affinities are lowered by 30 – 60 %, due to co-complexation of water.

Modeling results indeed confirm that the interaction takes place via hydrogen bond formation. The binding strength is found to be high for the phosphine oxide – phenol / phosphate – phenol complexes, and much lower if thio-compounds are involved. This negative influence of sulfur is clearly related to the much smaller negative charges on S (in comparison to O), which yields smaller electrostatic interactions, smaller atom-atom overlap-weighted NAO bond orders and correspondingly weaker hydrogen bonds. NAO bond orders are found to directly influence the hydrogen bond strength. The binding affinity K_{chem} is found to increase substantially by the introduction of electron-withdrawing substituents on the phenols, in line with their respective pK_a values.

A deviation is found for the complexes with pentachlorophenol. Although complexing of pentachlorophenol is stronger than that of phenol, the $T\Delta S^0$ factor shows that the presence of water affects complexation in an inhibiting way. Computations show that complexation is still governed by hydrogen bond formation, but the bound complex is destabilized by the presence of the electronegative chlorine atoms, leading to lower binding enthalpies.

Finally, the choice of the optimum extractant is crucial for future SIR applications. The combination of extraction, ITC and modeling experiments show that phosphine oxides are good candidates for the extraction of phenols from aqueous media. In combination with industrially relevant properties such as a low melting point (removes need for additional diluent) and a high boiling point (for regeneration of the SIR at high temperatures), it becomes clear that the phosphine oxide blend Cyanex 923 combines many of these desired characteristics.

References

(1) J. L. Cortina, A. Warshawsky, "Developments in Solid-Liquid Extraction by Solvent-Impregnated Resins." In *Ion Exch. Solvent Extr.*; J. A. Marinsky, Y. Marcus, Eds.; Dekker: New York, 1997; Vol. 13; pp 195.

(2) K. Ohnaka, A. Yuchi, *Chem. Lett.* **2005**, *34*, 868.

(3) B. Saha, R.J. Gill, D.G. Bailey, N. Kabay, M. Arda, *React. Funct. Polym.* **2004**, *60*, 223.

(4) M. T. Draa, T. Belaid, M. Benamor, *Sep. Purif. Technol.* **2004**, *40*, 77.

(5) S. D. Alexandratos, S. D. Smith, *Solvent Extr. Ion Exch.* **2004**, *22*, 713.

(6) Y. Wang, C. Wang, A. Warshawsky, B. Berkowitz, *Sep. Sci. Technol.* **2003**, *38*, 149.

(7) B.B. Gupta, Z.B. Ismail, *Comp. Interf.* **2006**, *13*, 487.

(8) S.S. El-Dessouky, E.H.J. Borai, *J. Radioanal. Nucl. Chem.* **2006**, *268*, 247.

(9) J.S. Liu, H. Chen, Z.L. Guo, Y.C. Hu, *J. Appl. Polym. Sc.* **2006**, *100*, 253.

(10) J. Serarols, J. Poch, I. Villaescusa, *React. & Funct. Pol.* **2001**, *48*, 37.

(11) A. Warshawsky, J.L. Cortina, M. Aguilar, K. Jerabek, "New Developments in Solvent Impregnated Resins. An Overview"; International Solvent Extraction Conference 1999, 1999, Barcelona, Spain.

(12) *Mem. Techn.* **2007**, *9*, 4.

(13) R.-S. Juang, H.-L. Chang, *Ind. Eng. Chem. Res.* **1995**, *34*, 1294.

(14) M. Traving, H.-J. Bart, *Chem. Eng. Technol.* **2002**, *25*, 997.

(15) A. Kostova, H.-J. Bart, H.-J. *Chemie Ingenieur Technik* **2004**, *76*, 1743.

(16) H. Kitazaki, M. Ishimaru, K. Inoue, K. Yoshida, S. Nakamura, "Separation and Recovery of Flavonoids by means of Solvent Extraction and Adsorption on Solvent-Impregnated Resin"; International Solvent Extraction Conference 1996, 1996, Melbourne, Australia.

(17) K. Babic, G.H.M. Driessen, A.G.J. van der Ham, A.B. de Haan, *J. Chrom. A* **2007**, *1142*, 84.

(18) Other important factors are the total extractant concentration in the resin (low concentration, high concentration or possibly pure), and the nature of the solvent (good or bad solvent for solute and extractant, low solvent leakage). Optimization of these factors is desirable to make the process material- and cost-effective.

(19) Z. Lazarova, S. Boyadzhieva, *Chem. Eng. J.* **2004**, *100*, 129.

(20) W.W. Cichy, J. Szymanowski, *J. Envir. Sc. Techn.* **2002**, *36*, 2088.

(21) J.P. Earhart, K.W. Won, H.Y. Wong, J.M. Prausnitz, C.J. King, *Chem. Eng. Prog.* **1977**, *73*, 67.

(22) G.A. Jeffrey, *An Introduction to Hydrogen Bonding*, Oxford University Press: New York, Oxford, 1997. (and references therein)

(23) E.R. Johnson, D.J.J. McKay, G.A. DiLabio, *Chem. Phys. Lett.* **2007**, *435*, 201.

(24) J.P.M. Lommerse, S.J. Price, R. Taylor, *Comp. Chem.* **1997**, *18*, 757.

(25) S.K. Panigrahi, G.R. Desiraju, *Proteins: Structure, Function, and Bioinformatics* **2007**, *67*, 128.

(26) M.H. Abraham, P.L. Grellier, D.V. Prior, P.P. Duce, J.J. Morris, P.J. Taylor, *J. Chem. Soc., Perkin Trans. 2* **1989**, 699.

(27) M.H. Abraham, P.L. Grellier, D.V. Prior, J.J. Morris, P.J. Taylor, *J. Chem. Soc., Perkin Trans. 2* **1990**, 521.

(28) G. Aksnes, P. Albriktsen, *Acta Chem. Scand.* **1968**, *22*, 1866.

(29) R.M. Badger, S.H. Bauer, *J. Chem. Phys.* **1937**, *5*, 839.

(30) A. Fletcher, *J. Phys. Chem.* **1967**, *71*, 3742.

(31) A. Fletcher, *J. Phys. Chem.* **1968**, *72*, 1839.

(32) T. Gramstad, *Acta Chem. Scand.* **1961**, *15*, 1337.

(33) M. D. Joesten, L.J. Schaad, *Hydrogen bonding*, Marcel Dekker: New York, 1974.

(34) S. Leavitt, E. Freire, *Curr. Op. Struct. Biol.* **2001**, *11*, 560.

(35) T. Wiseman, S. Williston, J.F. Brandts, L.-N. Lin, *Anal. Biochem.* **1989**, *179*, 131.

(36) P.C. Weber, F.R. Salemme, *Curr. Op. Struct. Biol.* **2003**, *13*, 115.

(37) J.E. Ladbury, *Biotechniques* **2004**, *37*, 885.

(38) J.E. Ladbury, M.L. Doyle, *Biocalorimetry 2*, John Wiley & Sons, Ltd, 2004.

(39) H.J. Wiggers, J. Cheleski, A. Zottis, G. Oliva, A.D. Andricopulo, C.A. Montanari, *Anal. Biochem.* **2007**, *370*, 107.

(40) P. Ballester, M. Capo, A. Costa, P.M. Deya, R. Gomila, A. Decken, G. Deslongchamps, *J. Org. Chem.* **2002**, *67,* 8832.

(41) A. Arnaud, L. Bouteiller, *Langmuir* **2004**, *20*, 6858.

(42) D. Merino-Garcia, S.I. Andersen, *Langmuir* **2004**, *20*, 4559.

(43) D. Merino-Garcia, S.I. Andersen, *Petr. Sc. Technol.* **2003**, *21*, 507.

(44) J.L. Sessler, D.E. Gross, W.S. Cho, V.M. Lynch, F.P. Schmidtchen, G.W. Bates, M.E. Light, P.A. Gale, *J. Am. Chem. Soc.* **2006**, *128*, 12281.

(45) A. Arnaud, L. Bouteiller, *Langmuir* **2004**, *20*, 6858.

(46) M. Xiang, M. Jiang, Y. Zhang, C. Wu, L. Feng, *Macromol.* **1997**, *30*, 2313.

(47) T. Mizutani, H. Takagi, Y. Ueno, T. Horiguchi, K. Yamamura, H. Ogoshi, *J. Phys. Org. Chem.* **1998**, *11*, 737.

(48) E.R. Johnson, O.J. Clarkin, G.A. DiLabio, *J. Phys. Chem. A* **2003**, *107,* 9953.

(49) P. Jurečka, J. Šponer, J. Černy, P. Hobza, *Phys. Chem. Chem. Phys.* **2006**, *8,* 1985.

(50) E.S. Kryachko, M.T. Nguyen, *J. Phys. Chem. A* **2002**, *106*, 4267.

(51) A.J. Bienko, Z. Latajka, *Chem. Phys. Lett.* **2003**, *374,* 577.

(52) M. Kone, B. Illien, J. Graton, C. Laurence, *J. Phys. Chem. A* **2005**, *109*, 11907.

(53) K.C. Lopes, R.C.M.U. Araujo, V.H. Rusu, M.N. Ramos, *J. Mol. Struct.* **2007**, *834-836*, 258.

(54) Y. Zhao, D.G. Truhlar, *J. Chem. Theory Comput.* **2007**, *3*, 289.

(55) B.A. Énglin, A.F. Platé, V.M. Tugolukov, M.A. Pryanishnikova, *Chem. Techn. Fuels Oils* **1965**, *1*, 722.

(56) H. Chen, J. Wagner, *J. Chem. Eng. Data* **1994**, *39*, 475.

(57) C. Marche, C. Ferronato, J.C. DeHemptinne, J. Jose, *J. Chem. Eng. Data* **2006**, *51*, 355.

(58) E. Emerson, *J. Org. Chem.* **1943**, *8*, 417.

(59) M. Ettinger, C. Ruchhoft, R. Lishka, *Anal. Chem.* **1951**, *23,* 1783.

(60) M. Chellani, *Am. Biotechnol. Lab.* **1999**, *17,* 14.

(61) M. J. Frisch, G. W. Trucks, H. B. Schlegel, G. E. Scuseria, M. A. Robb, J. R. Cheeseman, J. A. M. Jr., T. Vreven, K. N. Kudin, J. C. Burant, J. M. Millam, S. S. Iyengar, J. Tomasi, V. Barone, B. Mennucci, M. Cossi, G. Scalmani, N. Rega, G. A. Petersson, H. Nakatsuji, M. Hada, M. Ehara, K. Toyota, R. Fukuda, J. Hasegawa,

M. Ishida, T. Nakajima, Y. Honda, O. Kitao, H. Nakai, M. Klene, X. Li, J. E. Knox, H. P. Hratchian, J. B. Cross, C. Adamo, J. Jaramillo, R. Gomperts, R. E. Stratmann, O. Yazyev, A. J. Austin, R. Cammi, C. Pomelli, J. W. Ochterski, P. Y. Ayala, K. Morokuma, G. A. Voth, P. Salvador, J. J. Dannenberg, V. G. Zakrzewski, S. Dapprich, A. D. Daniels, M. C. Strain, O. Farkas, D. K. Malick, A. D. Rabuck, K. Raghavachari, J. B. Foresman, J. V. Ortiz, Q. Cui, A. G. Baboul, S. Clifford, J. Cioslowski, B. B. Stefanov, G. Liu, A. Liashenko, P. Piskorz, I. Komaromi, R. L. Martin, D. J. Fox, T. Keith, M. A. Al-Laham, C. Y. Peng, A. Nanayakkara, M. Challacombe, P. M. W. Gill, B. Johnson, W. Chen, M. W. Wong, C. Gonzalez, J. A. Pople, Gaussian 03, Revision C.02, Gaussian Inc., Wallingford CT, 2004.

(62) A.Y. Li, S.W. Wang, *J. Mol. Struct.: THEOCHEM* **2007**, *807,* 191.

(63) C.J. Cramer, *Essentials Of Computational Chemistry: Theories And Models*, 2nd ed.; John Wiley & Sons, Ltd, 2004.

(64) A.E. Shchavlev, A.N. Pankratov, A.V. Shalabay, *Int. J. Quant. Chem.* **2006**, *106,* 876.

(65) G.B.W.L. Ligthart, D. Guo, A.L. Spek, H. Kooijman, H. Zuilhof, R.P. Sijbesma, *J. Org. Chem.* **2008**, *73*, 111.

(66) D. Hadži, *Theoretical treatments of hydrogen bonding,* John Wiley & Sons, Ltd, 1997.

(67) H. Umeyama, K. Morokuma, *J. Am. Chem. Soc.* **1977**, *99*, 1316.

(68) S. Cybulski, S. Scheiner, *J. Phys. Chem.* **1990**, *94,* 6106.

(69) G. Alagona, *Int. J. Quant. Chem.* **1987**, *32*, 227.

(70) A.E. Reed, R.B. Weinstock, F. Weinhold, *J. Chem. Phys.* **1985**, *83*, 735.

(71) E.D. Glendening, A.E. Reed, J.E. Carpenter, F. Weinhold., NBO Version 3.1.

(72) B. Liu, A.D. McLean, *J. Chem. Phys.* **1973**, *59,* 4557.

(73) S.F. Boys, F. Bernardi, F. *Mol. Phys.* **1970**, *19*, 553.

(74) F.B. van Duijneveldt, J.G.C.M. van Duijneveldt - van de Rijdt, J.H. van Lenthe, *Chem. Rev.* **1994**, *94,* 1873.

(75) K.C. Gross, *Int. J. Quant. Chem.* **2001**, *85,* 569.

(76) V. Pino, F. Conde, J. Ayala, V. González, A. Afonso, *Chromatographia* **2006**, *63,* 167.
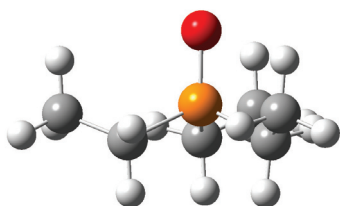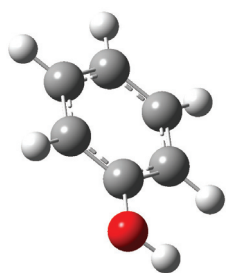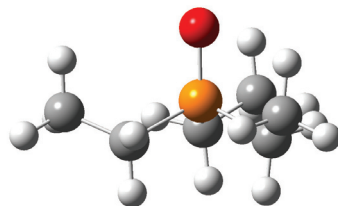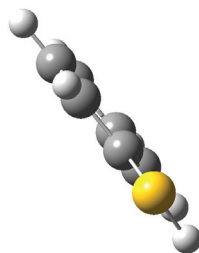
TEPO – PhOH (**C1**)

TEPO – PhSH (**C2**)
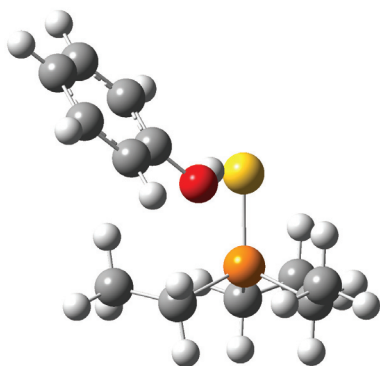
TEPS – PhOH (**C3**)
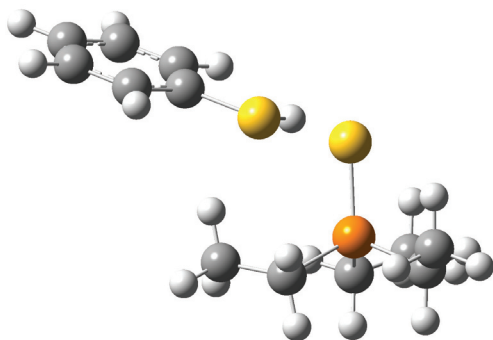
TEPS – PhSH (**C4**)

Figure S-1. Geometry of calculated phosphoryl - phenol complexes (B3LYP/6-311G(d,p)).

TMP – PhOH (**C5**)
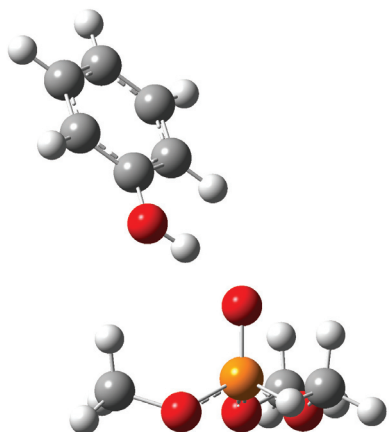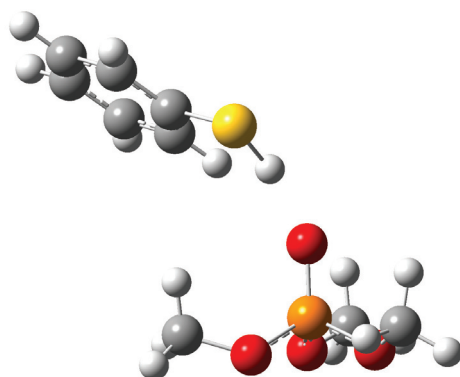
TMP – PhSH (**C6**)
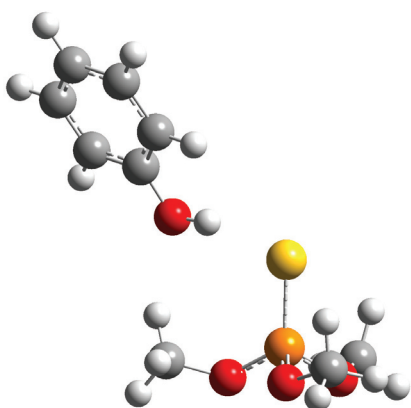
TMTP – PhOH (**C7**)
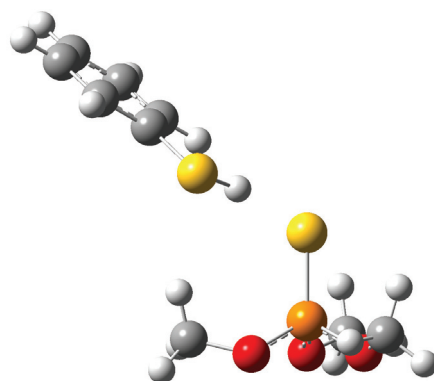
TMTP – PhSH (**C8**)

Figure S-2. Geometry of calculated trimethylphosphate - phenol complexes (B3LYP/6-311G(d,p)).
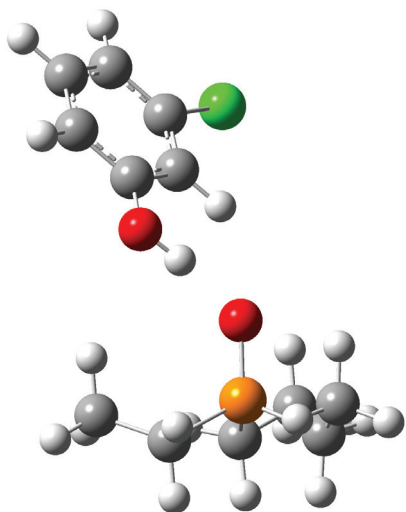
TEPO – 3-Cl-PhOH (**C9**)
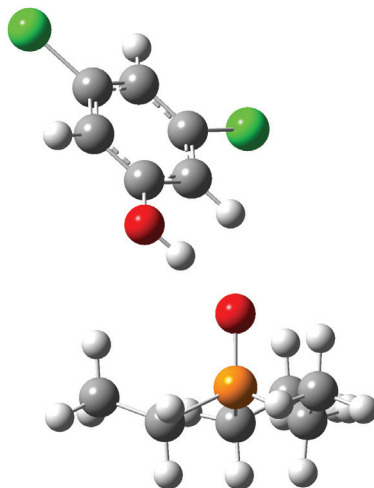
TEPO – 3,5-Cl$_2$-PhOH (**C10**)
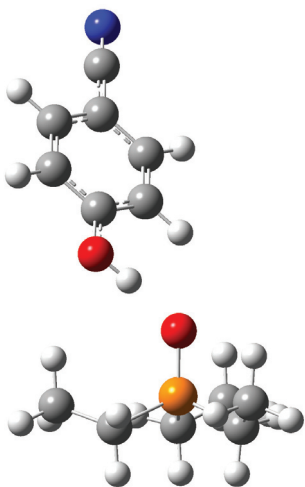
TEPO – 4-CN-PhOH (**C11**)
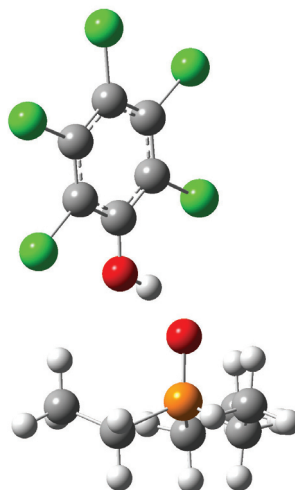
TEPO – Cl$_5$-PhOH (**C12**)

Figure S-3. Geometry of calculated triethylphosphine oxide - substituted phenol complexes (B3LYP/6-311G(d,p)).

Table S-2. Bond orders of the phenol O–H or thiophenol S–H bond of individual species and complexes and of the H•••O hydrogen bond in complexes (B3LYP/6-311+G(d,p)).

species	NAO Bond Order	
	O-H / S-H	H•••O
PhOH	0.661	-
PhSH	0.724	-
3-Cl-PhOH	0.659	-
3,5-Cl$_2$-PhOH	0.655	-
4-CN-PhOH	0.659	-
Cl$_5$-PhOH	0.644	-
TEPO - PhOH	0.600	0.076
TEPO - PhSH	0.708	0.038
TEPS - PhOH	0.611	0.047
TEPS - PhSH	0.708	0.045
TMP - PhOH	0.611	0.063
TMP - PhSH	0.712	0.034
TMTP - PhOH	0.629	0.032
TMTP - PhSH	0.711	0.021
TEPO - 3-Cl-PhOH	0.594	0.088
TEPO - 3,5-Cl$_2$-PhOH	0.589	0.094
TEPO - 4-CN-PhOH	0.588	0.095
TEPO - Cl$_5$-PhOH	0.578	0.097

2

CHAPTER 3

Hydrogen Bonding in Phosphine Oxide / Phosphate – Phenol Complexes.

Abstract

In order to develop a new solvent-impregnated resin (SIR) system for the removal of phenols and thiophenols from water, the complex formation by hydrogen bonding of phosphine oxides and phosphates was studied using isothermal titration calorimetry (ITC) and quantum chemical modeling. Six different computational methods were used: B3LYP, M06-2X, MP2, spin component-scaled (SCS) MP2 (all four with 6-311+G(d,p) basis set), a complete basis set extrapolation at the MP2 level (MP2/CBS), and the composite CBS-Q model. This revealed a range of binding enthalpies (ΔH) for phenol – phosphine oxide and phenol – phosphate complexes and their thio-analogs. Both structural (bond lengths/angles) and electronic elements (charges, bond orders) were studied. Furthermore, solvent effects were investigated theoretically by the PCM solvent model and experimentally via ITC. From our calculations, a trialkylphosphine oxide was found to be the most promising extractant for phenol in SIRs, yielding ΔH = -14.5 and -9.8 kcal/mol, with phenol and thiophenol respectively (MP2/CBS), without dimer formation that would hamper the phenol complexation. In ITC measurements, ΔH^0 of this complex was most negative in the non-coordinating solvent cyclohexane, and slightly less so in $\pi\pi$ interacting solvents such as benzene. The strongest binding was found for the dimethylphosphate – phenol complex (-15.1 kcal/mol (MP2/CBS)), due to the formation of two H-bonds (P=O•••H–O– and P–O–H•••–O–H) however, dimer formation of these phosphates competes with complexation of phenol, and would thus hamper use in industrial extractions. CBS-Q calculations display erroneous trends for sulfur compounds, and were found to be unsuitable to use. Computationally relatively cheap SCS-MP2 and M06-2X calculations did accurately agree with the much more elaborate MP2/CBS method, with an average deviation of less than 1 kcal/mol.

Introduction

Solvent-impregnated resins[1] (SIRs, Figure 1) are used as three-phase separation systems. A solute is present in an aqueous phase; the SIR contains the stationary solvent phase, an organic liquid impregnated in the pores of the inert resin particle. When brought into contact with a SIR, the solute will diffuse from the aqueous phase into the solvent phase, with an extraction constant K_{phys}. Ion-exchange SIRs are already widely used to exchange heavy metal ions in aqueous phases with protons in a fast and simple way.[2-6] These large-scale applications make use of the solubility of the solute in the liquid organic phase.

The usefulness of SIRs hinges on the simplification of the separation process in comparison to extraction – which requires dispersion – and on the flexibility in comparison to ion-exchange resins with chemically bound extractants. In addition SIRs can be reused for different separation tasks by simply rinsing one extractant out and re-impregnating them with another one, thereby saving the cost of expensive resin design and production. Only recently, other applications have been investigated, including the bench-scale or pilot-scale recovery of polar organics like phenols,[7,8] and the separation of organic acids,[9, 10] amino acids[11] and flavonoids.[12] However, large-scale applications for the separation of polar solutes like ethers and phenols from e.g. phenol production line waste water, which is the system under consideration for this project, do not yet exist, largely because the factors that would drive such an extraction process have not been studied in a quantitative manner. Clarification of these factors by quantum chemical calculations is the first aim of this chapter.
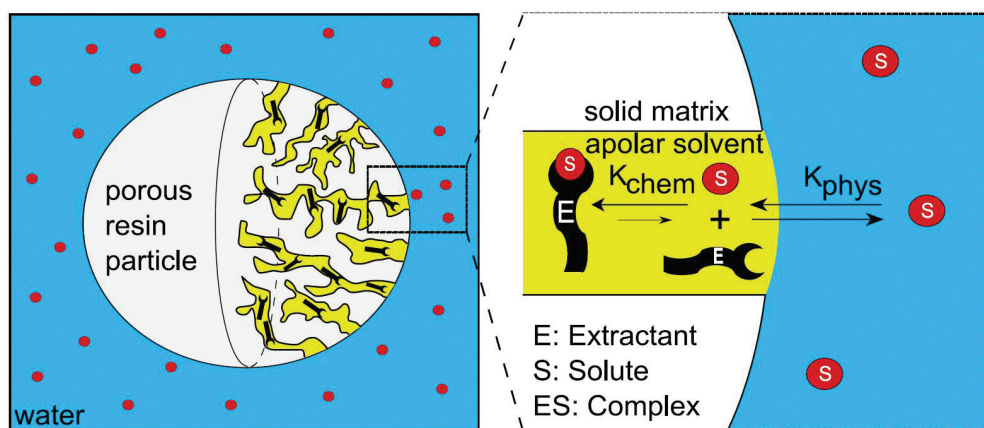

Figure 1. Operational principle of solvent-impregnated resins with an active extracting agent in the pores.

In order to enhance the extraction capacity and selectivity of SIRs, complex-forming extractants can be added to the solvent. We have shown in a previous paper[7] and in Chapter 2 that the equilibrium solute concentration in the solvent phase can be increased dramatically by means of complex formation with an extractant. Optimization of the complex-forming ability of the extractant using molecular modeling can thus be used to improve the performance of the SIR. The most important hydrogen-bond (H-bond) characteristics to be explored in this chapter are the H-bond strength and the geometry of the resulting complexes. From literature, neutral O−H•••O H-bonds are expected to have a strength of ca. 4-15 kcal/mol,[13, 14] covering a range of H-bond lengths and O−H•••O angles,[15, 16] as these parameters depend strongly on the molecular geometry of the system at hand. H-bonds with charged donor or acceptor atoms are usually found to be significantly stronger, with typical values of 15-40 kcal/mol.[13, 14]

Considering the application aspects of SIRs, the optimum binding strength is not necessarily the highest binding strength. After formation of the complex in the extraction process, regeneration at elevated temperatures with concomitant release of the bound phenol is required. This latter step would be problematic in case of formation of very stable complexes. Therefore, the optimum binding enthalpy should be ca. 10-15 kcal/mol.[7]

In this chapter we investigate a set of phosphoryl extractants for the extraction of phenol and thiophenol to establish in detail the molecular basis for a future industrial set-up. To obtain the desired complex stability of ca. 10-15 kcal/mol, formation of strong H-bonds is necessary, which prompted us to use phosphine oxides and phosphates as candidate compounds that can form H-bonding complexes with phenols (Table 1).[7],[13] Trialkylphosphine oxides and phosphates combine a low solubility in water with a partial negative charge on the oxygen atom, making them attractive candidates for this purpose. The interaction between phenols and the extractants has been investigated in detail, yielding detailed information about H-bonding of phenols with phosphine oxides and phosphates. [7],[13],[17-22] Those studies show that the interaction between phenols and phosphate and phosphine oxide molecules consists of H-bonding and that the interaction with phenols is larger for phosphine oxides than for phosphates. The H-bonding parameters were determined from IR experiments, and all measurements were done in CCl_4. Solvent effects were never taken into account. All thermodynamic parameters, if present at all, were estimated based on these IR measurements. Direct measurements of ΔH^0, ΔG^0 or $T\Delta S^0$ have not been published (except in reference [7]), and no theoretical calculations are available to account for the differences between phosphate and

phosphine oxide – phenol interactions whatsoever. Effectively, the detailed molecular interaction between mono-, di- and tri-substituted phosphine oxides and phosphates with phenols has not been systematically studied up to now. For the development of a SIR extraction set-up for the removal of phenols from an aqueous system, these molecular-scale interactions are of vital importance. The present chapter discusses these factors, yielding an optimal candidate by application of isothermal titration calorimetry (ITC) measurements in four different solvents (cyclohexane, mesitylene, toluene and benzene) and a broad set of theoretical methods. On a B3LYP/6-311G(d,p)-optimized geometry four different single-point energies were computed (B3LYP/6-311+G(d,p), MP2/6-311+G(d,p), spin component-scaled (SCS) MP2/6-311+G(d,p) and a complete basis set extrapolation at the MP2 level (MP2/CBS)). Since analysis of a small data set of hydrogen-bonded complexes suggested that the M06 set of density functionals might perform somewhat better in describing hydrogen-bonding interactions,[23] M06-2X/6-311+G(d,p)//M06-2X/6-311G(d,p)[24, 25] calculations were also performed. Finally, the composite CBS-Q method, a complete basis set method of Petersson and coworkers to obtain very accurate energies,[26] was used to obtain an absolute benchmark for the energy values. These different methods were chosen to diminish the chance of finding highly method-dependent results. In recent papers, SCS-MP2 methods, which use the default scaling factors of 6/5 for anti-parallel spins and 1/3 for parallel spins, showed a dramatic increase in accuracy over normal MP2 energies, providing a more balanced description of many systems,[27-30] and sometimes even reaching QCISD or QCISD(T) quality data.[31] As the application of SCS-MP2 on the stability of H-bonding is relatively unexplored, its performance is therefore described in detail. At several of these levels, the effect of the solvent was computationally addressed for the solvents cyclohexane, mesitylene, toluene and benzene using the PCM model, although quantitative correctness is likely not achieved with this solvation model.[32]

Table 1. Compounds under investigation and geometric parameters describing H-bond geometry in phosphine oxides and phosphates. Dihedral angle ϕ (not shown) between carbon atoms C_2, C_1, and r_1.[a]

Compound	Molecular formula	Complex
Phosphine oxides	$O=P(CH_2-CH_3)_nH_{3-n}$ (n = 1-3)	
Phosphine sulfides	$S=P(CH_2-CH_3)_nH_{3-n}$ (n = 1-3)	
Phosphates	$O=P(O-CH_3)_nOH_{3-n}$ (n = 1-3)	
Thiophosphates	$S=P(O-CH_3)_nOH_{3-n}$ (n = 1-3)	

[a] Definitions analogous for thiophenol (Ph-SH).

The theoretical predictions and the experimentally obtained results have been combined in order to provide a detailed molecular picture, and to obtain insight into the complexing behavior of phenols towards several phosphates and phosphine oxides.

Experimental Section

The following materials were used as received without further purification: tri-n-octyl-phosphine oxide (TOPO) (≥ 99%, Sigma Aldrich), phenol (> 99%, Merck), cyclohexane (> 99%, Acros), mesitylene (>99%, Fluka), toluene (99.8%, Sigma Aldrich), benzene (≥99.5 %, Fluka). All ITC measurements were performed with one of the solvents dried on molecular sieves (3 Å).

Computational data of the compounds depicted in Table 1 were all obtained using the Gaussian03 (rev D1)[48] and Gaussian 09 (Rev A2)[49] suite of programs. In this work, the geome-tries of the monomers and complexes have all been optimized at the B3LYP/6-311G(d,p) level of theory, which generally describes the geometries of these systems well.[50, 51] All B3LYP/6-311G(d,p)-optimized stationary points were confirmed as true minima via vibrational frequency calculations. When not indicated otherwise, the 6-311+G(d,p) basis set was used for energy calculations. With such basis sets both B3LYP and MP2 typically provide accurate (within 2 kcal/mol) interaction energies for O/N–H..O/N H-bonding, while MP2 calculations with bigger basis sets are typically even more accurate[52-54], although it is known to systematically overestimate the correlation contribution to complexation slightly. An extrapolation to the complete basis set (CBS) energy limit was obtained using the keyword 'cbsextrapolate'.[55] The option "NMin=10" was specified to account for a minimum of 10 pair natural orbitals for extrapolation to the CBS limit. Counterpoise (CP) correction[56, 57] was applied for all MP2 and SCS-MP2 calculations to correct for over-stabilization due to the supermolecule approach. Obviously, no CP-correction was applied to the MP2/CBS energies. Since MP2 optimization was unpractical for all complexes due to computational limitations, the B3LYP-derived geometries were compared with geometries at the MP2/6-311+G(d,p)//MP2/6-311G(d,p) level for the MEPO complexes under study, and found to agree well: similar geometrical features, and H-bond strengths within 0.2 kcal/mol from MP2/6-311+G(d,p)//B3LYP/6-311G(d,p) data. The B3LYP-derived geometries were taken as input structures for the CBS-Q method, which is known to provide very accurate energy data. The CBS-Q method consists of several different steps, described elsewhere.[26] All CBS-Q structures were confirmed to be true minima in the vibrational frequency analysis that is part of the composite method. The CBS-Q energy at 0 K was used for the presented results.

B3LYP calculations were also combined with an SCRF approach to mimic apolar solvent effects on energy data. For these calculations 'cyclohexane', 'mesitylene', 'toluene' or 'benzene' was specified in the input section, to be able to compare the findings with experiments, which were conducted using these solvents.

Finally, since electrostatic interactions are crucial in determining the strength of H-bonds[13],[58-61] natural population analysis (NPA)[62, 63] was performed as part of calculations. As the latter analysis exhibits a relatively small method dependence and basis set dependence, it has proven to be reliable charge indicators for related theoretical studies of H-bonds.[64-66] In addition, atom-atom overlap-weighted natural atomic orbital (NAO) bond orders were obtained.

ITC was performed using a MicroCal VP-ITC microcalorimeter; the setup is described elsewhere.[67] Results were processed using Origin® 7SR2 V7.0383 (B383) by Origin Lab Corporation. The measuring cell (1.46 mL) was flushed and filled with a freshly prepared and degassed solution of the phenol in one of the carefully dried solvents cyclohexane, mesitylene, or benzene (usually concentrations of 1-10 mM were used). The 280 μL automatic syringe was flushed and filled with a freshly prepared and degassed solution of the complexing agent TOPO in the same dry solvent at a concentration of roughly 10 times the molarity of the cell solution. Depending on the concentration of the compounds in solution and the magnitude of the heat effect per second, the number of injections and the injected volume per injection were chosen. Between subsequent injections a sufficient amount of time, usually 180 to 300 seconds, was chosen to allow for the cell feedback to return to the baseline. The stirring speed for all ITC measurements was 502 rpm (default value). A reference measurement was performed using the same procedure by having only solvent in the measuring cell. By subtracting the data of the reference measurement from that of the actual measurement, the net results were obtained and they were fitted using the one-set-of-sites model implemented in the Origin software.

Results and Discussion

First, the results of the phosphine oxide and phosphine sulfide complexes with phenol and thiophenol will be discussed in detail. Following this, the results on the phosphate and thio-phosphate complexes with phenol and thiophenol will be treated based on the given depictions of the optimized structures, and the results will be compared.

Phosphine oxides and phosphine sulfides. Complexes that were investigated each consisted of a phenol or thiophenol, and one of the phosphates/phosphine oxides (Table 1). The model compounds resemble compounds used in SIR extraction experiments[7] (See Chapter 2) but for computational speed the long alkyl tails that render insolubility in water were replaced by methyl or ethyl groups. In Table 1 the different relevant geometrical parameters are defined for H-bonds in the investigated complexes.

A   **B**   **C**
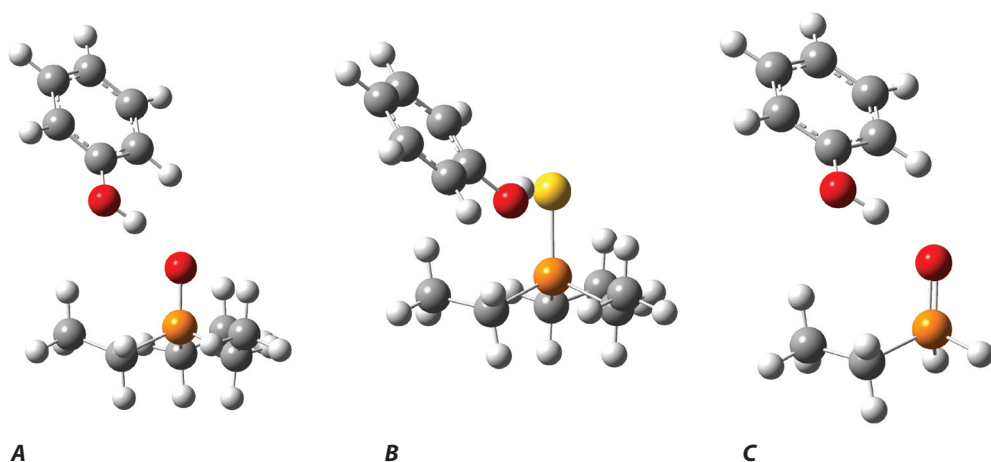
*Figure 2. Optimized structures (B3LYP/6-311G(d,p) (vacuum)) of representative phosphine oxide – phenol complexes. Orange: phosphorus; red: oxygen; yellow: sulfur; black: carbon; white: hydrogen. A: triethylphosphineoxide – phenol (**C1**); B: triethylphosphinesulfide – phenol (**C3**); C: monoethylphosphineoxide – phenol (**C9**).*

As can be seen from the B3LYP-optimized geometries of the selected phosphine oxide – phenol complexes (Figure 2 and Supporting Information, Figure S-1), phenols form a H-bond to the P=O moiety, showing a geometry with a near-ideal linear H-bond. (In general, M06-optimized geometries display the same trends as B3LYP-optimized geometries.) In the triethylphosphine oxide – phenol complex (complex **C1**, Figure 2A), the H-bond length d_1 is short (1.72 Å, Table 2), and the H-bond angle α_1 shows an almost perfectly linear H-bond geometry (α_1 = 171°). In addition, the O–H bond is slightly lengthened upon H-bonding (Δr = 0.021 Å), while the dihedral angle of the phenol, the angle between the O–H bond $r1$ and the bond between two neighboring carbon atoms of the phenyl ring, is close to zero degrees (ϕ = -2.2°).

As can be seen from Table 2, the shortest H-bond lengths are found for the oxide – phenol complexes (d_1 = 1.72 – 1.76 Å). Much longer H-bonds are found for oxide – thiophenol interactions (d_1 = 1.99 – 2.04 Å), for sulfide – phenol interactions (d_1 = 2.35 – 2.41 Å, Figure 2B), and for sulfide – thiophenol interactions (d_1 = 2.63 – 2.76 Å). Phosphine oxide complexes (**C1**, **C2**, **C5**, **C6**, **C9**, **C10**, Figure 2A and 2C) approach the ideal linearity and show an average H-bond angle $<\alpha_1>$ of 170.2 ± 1.4°, while for phosphine sulfide complexes (**C3**, **C4**, **C7**, **C8**, **C11**, **C12**, Figure 2B) $<\alpha_1>$ equals 158.8 ± 5.2°. The lower charge on the sulfur atoms and therefore the lower electrostatic attraction forces are the reason for the longer H-bonds, as well as the longer Van der Waals radius of sulfur. These longer bonds will allow for less rigid linear geometry, hence the angles are slightly more deviating from 180°. In fact, an inverse dependence of α on d has been found earlier and is very common.[33]

An O–H/S–H bond lengthening (Δr_1) of 0.017 – 0.021 Å was observed for the oxide – phenol complexes, and to a lesser extent for the oxide - thiophenol complexes (0.009 – 0.012 Å). A larger donor bond lengthening is indicative for stronger H-bonding, as optimization of the electrostatic interactions between the H-atom and the H-bonded electron-rich element leads to a reduced electron density between the covalently bound O/S and H atoms, and a concomitantly larger O/S–H bond.[34, 35] Significantly smaller O–H/S–H bond lengthening was observed in sulfide – phenol and sulfide – thiophenol H-bonds (0.012 – 0.015 Å for phenols and 0.007 – 0.010 Å for thiophenols), indicative for weaker H-bonding in the case of a thio-compound.[36]

Dihedral angles ϕ of the phenols inside the complexes deviate only slightly from the ideal angle of 0°, with average values of -0.6 ± 1.3° for phenol and -9.5 ± 3.8° for thiophenol. The difference between phenol and thiophenol can be understood by the more shallow potential energy surface for the latter, enabling easier deviation from the ideal geometry (cf. Supp. Info Table S-1).

H-bonding energies in vacuum for the phosphine oxide and phosphine sulfide complexes are summarized in Table 3. The enthalpy of complexation ΔH of complex **C1** is found to be -14.5 kcal/mol for calculations in vacuum at the MP2/CBS level of theory, which has been reported as an excellent method and for us was the highest non-composite method uniformly applicable for medium-sized complexes like the ones under study.[37] The B3LYP value provides a reasonable estimation (-12.0 kcal/mol), while the M06-2X value seems to be slightly too negative (-16.8 kcal/mol). While for B3LYP computations of H-bonded complexes the basis set superposition error (BSSE) is typically small,[38, 39] for M06-type functionals relatively little is yet known about the need for counterpoise (CP) corrections;[37] in fact, a recent study even suggests for (H_2O)$_n$ complexes that

Table 2. Geometric parameters of phosphine oxide and phosphine sulfide complexes in vacuum (B3LYP/6-311G(d,p)-optimized geometries; distances in Å, angles in degrees).

#	Complex	geometric parameters			
		d_1	α_1	$\Delta r_1^{(a)}$	ϕ
C1	$(C_2H_5)_3P=O$ - HO-Ph	1.72	171	0.021	-2.2
C2	$(C_2H_5)_3P=O$ - HS-Ph	1.99	172	0.012	-4.6
C3	$(C_2H_5)_3P=S$ - HO-Ph	2.35	162	0.015	+1.8
C4	$(C_2H_5)_3P=S$ - HS-Ph	2.63	170	0.010	-9.4
C5	$(C_2H_5)_2HP=O$ - HO-Ph	1.74	171	0.019	-1.1
C6	$(C_2H_5)_2HP=O$ - HS-Ph	2.02	171	0.010	-5.4
C7	$(C_2H_5)_2HP=S$ - HO-Ph	2.40	157	0.012	-1.3
C8	$(C_2H_5)_2HP=S$ - HS-Ph	2.68	158	0.009	-15.8
C9	$(C_2H_5)H_2P=O$ - HO-Ph	1.76	168	0.017	-1.7
C10	$(C_2H_5)H_2P=O$ - HS-Ph	2.04	168	0.009	-7.1
C11	$(C_2H_5)H_2P=S$ - HO-Ph	2.41	154	0.012	+0.8
C12	$(C_2H_5)H_2P=S$ - HS-Ph	2.76	152	0.007	-14.7

$^{(a)}\Delta r_1 = d(O\text{-}H)_{complex} - d(O\text{-}H)_{phenol}$ or $d(S\text{-}H)_{complex} - d(S\text{-}H)_{thiophenol}$, respectively. ($d(O\text{-}H)_{phenol} = 0.963$ Å; $d(S\text{-}H)_{thiophenol} = 1.347$ Å).

BSSE corrections worsen the agreement with experiment. Therefore the BSSE was explored for the M06-2X calculations, and were found to range in this set typically between 1-2 kcal/mol (1.4 kcal/mol for TEPO-PhOH and TEPO-PhSH; 1.3 kcal/mol for TEPS-PhOH and 1.2 kcal/mol for TEPS-PhSH). Deviations from the MP2/CBS value therefore seem to become promisingly small (< 1.0 kcal/mol) for BSSE-corrected M06-2X/6-311+G(d,p) calculations, which would warrant further investigations in this area involving second-row elements. The CP-uncorrected MP2 calculations overestimate the binding enthalpy, due to the BSSE. CP correction takes care of this overcompensation, but the then resulting data deviate more from the MP2/CBS value than B3LYP. Interestingly, the MP2/CBS value was approximated to a high degree by the CP-uncorrected SCS-MP2/6-311+G(d,p) calculations: $\Delta H = -14.1$ kcal/mol, which stimulated us to study in more detail the possibility that the SCS-MP2 method may diminish the need for a CP-correction (*vide infra*).

To substantiate such a claim, benchmark calculations were attempted next to the MP2/CBS calculations, namely the CBS-Q model chemistry, which was included in this study given its

reported high accuracy for other hydrogen-bonded complexes.[40] The CBS-Q value found for complex **C1** (ΔH = -15.7 kcal/mol, cf. Supp. Info., Table S-2) is close to the MP2/CBS value of -14.5 kcal/mol. However, the CBS-Q results display an unexpected, systematic error, as CBS-Q predicts the thiophenol complexes to be more stable than the corresponding phenol ones. For example, **C6** and **C5** have ΔH(CBS-Q) values of -13.5 and -10.2 kcal/mol, respectively, while experimental data[7] clearly show that phenol forms significantly stronger H-bonds than thiophenol (binding affinity K is higher for phenol by typically by 1-2 orders of magnitude). Those experimental observations are in line with generally observed differences in binding enthalpies for O•••H–O and O•••H–S H-bonds.[33] This erroneous prediction by CBS-Q can have two possible causes: a) use of correct energy calculations on incorrect geometries, or b) use of incorrect energy calculations on correct geometries. Close inspection of the MP2(FC)/6-31G(d') geometries resulting from the CBS-Q calculations shows only minor differences to the geometries found in the B3LYP optimization, and single-point recalculation of the resulting CBS-Q geometries with MP2/6-311+G(d,p) yielded in all cases enthalpies within 1 kcal/mol of what was obtained in the MP2 calculations on the B3LYP-optimized geometries. The differences between the phenol and thiophenol complexing energies can thus not be accounted for by possible errors in the geometries. Since also no systematic errors have been reported for the computations of oxygen-containing H-bonds using model chemistries like CBS-Q, this indicates that the CBS-Q derived energy values for sulfur compounds contain a systematic error. As a result, and to our surprise, CBS-Q is not useful as a benchmark method in this case.

Analysis of the binding energies of the various phenol and thiophenol complexes yields interesting insights into the differences in H-bond formation between phenol and thiophenol. In line with the indications provided by the geometric parameters given in Table 2, the energy data indeed show that thiophenols form weaker H-bonds than phenols. For phenol, substitution of an oxide for a sulfide yields a much lower binding energy (compare e.g. complexes **C1** and **C3**, with binding energies of -14.5 and -11.7 kcal/mol (MP2/CBS), respectively). However, the same substitution yields only little change in the thiophenol complexes (compare complexes **C2** and **C4**, with binding energies of -9.8 and -8.6 kcal/mol (MP2/CBS), respectively). This is in line with findings that for thiols primarily the proton donor capacity, and not the nature of the proton acceptor, influences the H-bond energy.[41]

Table 3. Calculated binding energies (kcal/mol) of phosphine oxide and phosphine sulfide complexes with phenol and thiophenol (all with 6-311+G(d,p) basis set, except MP2/CBS) in vacuum.

#	Complex	ΔH						
		B3LYP	M06-2X	MP2		SCS-MP2		MP2/CBS
		-cp	-cp	-cp	+cp	-cp	+cp	-cp
C1	$(C_2H_5)_3P=O$ - HO-Ph	-12.0[a]	-16.8	-15.4	-11.7	-14.1	-10.5	-14.5
C2	$(C_2H_5)_3P=O$ - HS-Ph	-6.5[a]	-11.9	-10.4	-7.3	-9.2	-6.2	-9.8
C3	$(C_2H_5)_3P=S$ - HO-Ph	-6.3[a]	-12.8	-12.7	-8.3	-11.3	-7.2	-11.7
C4	$(C_2H_5)_3P=S$ - HS-Ph	-3.7[a]	-10.2	-9.6	-5.6	-8.2	-4.4	-8.6
C5	$(C_2H_5)_2HP=O$ - HO-Ph	-11.5	-15.7	-14.4	-10.8	-13.2	-9.8	-13.4
C6	$(C_2H_5)_2HP=O$ - HS-Ph	-6.2	-11.2	-9.4	-6.7	-8.3	-5.7	-8.8
C7	$(C_2H_5)_2HP=S$ - HO-Ph	-6.7	-11.6	-11.9	-7.4	-10.6	-6.3	-10.8
C8	$(C_2H_5)_2HP=S$ - HS-Ph	-3.9	-10.7	-10.5	-5.9	-9.0	-4.7	-9.1
C9	$(C_2H_5)H_2P=O$ - HO-Ph	-10.7	-15.2	-13.4	-10.0	-12.3	-9.0	-12.4
C10	$(C_2H_5)H_2P=O$ - HS-Ph	-5.7	-10.0	-9.3	-6.4	-8.1	-5.0	-8.6
C11	$(C_2H_5)H_2P=S$ - HO-Ph	-6.5	-11.7	-10.5	-6.7	-9.4	-5.8	-9.5
C12	$(C_2H_5)H_2P=S$ - HS-Ph	-3.7	-10.9	-10.0	-5.7	-8.6	-4.5	-8.7

[a] from ref 7.

Going from the tri- via the di- to the mono-substituted phosphine oxides and sulfides, binding enthalpy decreases for the equivalent species (e.g. complexes **C1**, **C5** and **C9**, with ΔH(MP2/CBS) values of -14.5, -13.4 and -12.4 kcal/mol, respectively; Table 3). This phenomenon can be explained by the electron-donating effect of the alkyl tails in the phosphine oxides and sulfides, resulting in an increased binding affinity for the more highly substituted compounds.

As could be expected on the basis of Van der Waals radii and relative electronegativities,[42] the shortest H-bond lengths are found for the strongest complexes. The H-bond length in complexes with phenol (OH•••O/S) is roughly 0.3 Å shorter than with thiophenol (SH•••O/S), which we attribute to the lower tendency of thiophenol to form H-bonds.[36] The difference in H-bond lengths between analogous oxide (OH/SH•••O) and sulfide (OH/SH•••S) complexes is roughly 0.66 Å, which is due to the combination of the difference in Van der Waals-radii of oxygen and sulfur (0.28 Å), and the lower charge on the sulfide sulfur atom (S=).

The weakening in H-bond energy found upon substitution of oxygen by sulfur (here: 1 – 5 kcal/mol) is similar to what is reported in literature.[33, 42] The increase in H-bond length ($\Delta d_{H\cdots O/S}$) found here for sulfides compared to oxides is somewhat higher than previously reported for a similar substitution: an increase in H-bond length of ~0.5 Å was found for HF - thioether and HF - thiocarbonyl complexes with respect to the analogous H-bonds to oxygen,[42] whereas we find an increase of 0.66 Å for a H-bond to S=P with respect to a H-bond to O=P. This is likely largely due to the fact that HF is a stronger acid than both phenol and thiophenol, and is thus more prone to partial proton transfer, which would increase the H-bond length to a lesser extent, as indeed seen here.

These results are generally produced by all methods under current investigation. Typically the B3LYP data underestimate the stability of the hydrogen-bonded complex (by 2 – 5 kcal/mol, with respect to MP2/CBS) in line with reported trends,[43] while M06-2X performs very well: values are typically within 1 kcal/mol of the MP2/CBS data, after BSSE correction. As shown in the table, the differences between MP2/6-311+G(d,p) and SCS-MP2/6-311+G(d,p) data are small (0.9 - 1.5 kcal/mol). However, there are two remarkable features here: a) SCS-MP2 binding enthalpies are less negative in all cases, and b) the CP-uncorrected SCS-MP2/6-311+G(d,p) values are in all cases in excellent agreement with the computationally much more demanding and highly accurate MP2/CBS computations. On average SCS-MP2/6-311+G(d,p) values are 0.3 kcal/mol less negative than the MP2/CBS values, while the maximum deviation of any of the CP-uncorrected SCS-MP2/6-311+G(d,p) values with respect to the MP2/CBS values is only 0.6 kcal/mol. Interestingly, CP-correction on the SCS-MP2 calculations makes this agreement significantly worse. The much cheaper SCS-MP2/6-311+G(d,p) method therefore appears to provide high-accuracy data and at significantly reduced computational costs.

Since SIRs involve the use of apolar solvents, the next part involved the study of the solvent effects on complex formation. To this aim, the effects of cyclohexane, mesitylene, toluene, and benzene – model solvents for the apolar phase in SIRs – were studied both experimentally and using B3LYP and M06-2X calculations (Table 4). To mimic the solvent effects in the computations, the IEF-PCM model was used,[44] and the resulting computational data are compared to the experimental data, obtained by ITC.

Table 4. ITC results listing all thermodynamic parameters (in kcal/mol) for TOPO-phenol complexes in various solvents, and calculated B3LYP and M06-2X ΔH values for TEPO-phenol complexes.

Parameter	dry cyclohexane	dry mesitylene	dry toluene[a]	dry benzene
N (-)	1.00 ± 0.04	1.00 ± 0.01	0.95 ± 0.01	0.96 ± 0.05
K (M^{-1})	$(6.4 \pm 0.2) \cdot 10^3$	$(1.3 \pm 0.1) \cdot 10^3$	$(1.0 \pm 0.1) \cdot 10^3$	$(9.8 \pm 0.7) \cdot 10^2$
TΔS^0	-1.2 ± 0.3	-3.0 ± 0.1	-2.6 ± 0.1	-3.6 ± 0.8
ΔG^0	-5.3 ± 0.0	-4.3 ± 0.0	-4.2 ± 0.1	-4.2 ± 0.1
ΔH$^0_{exp}$	-6.5 ± 0.3	-7.3 ± 0.1	-6.8 ± 0.2	-7.8 ± 0.5
ΔH$_{B3LYP}$	-9.0	-9.1	-9.0	-9.2
ΔH$_{M06}$	-15.1	-14.8	-14.8	-14.8

[a] Experimental data from ref. 7 and Chapter 2.

ITC experiments yielded a value of ΔH^0 from -6.5 kcal/mol (cyclohexane) to -7.8 kcal/mol (benzene). The B3LYP-calculated ΔH for complex formation in these solvents is -9.1 ± 0.1 kcal/mol, i.e. complex formation in these apolar solvents is predicted to be less stable than *in vacuo* (ΔH$_{calc}$ = -12.0 kcal/mol). This solvent-induced weakening of the complex was also found with other methods. For the three phosphine sulfide – thiophenol complexes even slightly positive ΔH values were found using B3LYP, indicating a solvent-induced resistance to complex formation in these cases, in line with ITC experiments that give no indication of H-bond formation. (See for the full B3LYP data set for **C1** - **C12** in all these solvents the Supp. Info Table S-10.) The entropy factor TΔS^0 displays a significant variation between these solvents, yielding variations in K among these solvents of almost one order of magnitude: in benzene, toluene and mesitylene K-values of $9.8 \cdot 10^2$, $1.0 \cdot 10^3$ and $1.3 \cdot 10^3$ M^{-1}, respectively, were observed, while in the non-aromatic solvent cyclohexane the highest binding affinity was found (K = $6.4 \cdot 10^3$ M^{-1}). Apparently $\pi\pi$ interactions lead to less favorable complex formation, which can be tentatively attributed to stabilization of phenol (without H-bond) by the solvent, as we do not observe any significant changes in e.g. charge indicators within the complex between the various solvents.

This large solvent effect is not borne out by PCM calculations that predict nearly identical thermodynamics for e.g. cyclohexane and benzene. This was confirmed by MP2-SCRF calculations on the MEPO-phenol complex on MP2-optimized structures, which yielded a solvent-induced weakening of the H-bond by 1.5 – 1.8 kcal/mol, with little variation between the different solvents. (MEPO was chosen for reasons of computational efficiency.) Since B3LYP, M06 and MP2

yield qualitatively similar data, the predominant factor is not likely to be the method (DFT or *ab initio*), but the solvent treatment. Four factors seem to contribute to this difference with experiment. First, the incomplete description of the solvent effects by the PCM model can cause a major deviation in the calculated values, as e.g. the orientation-dependent $\pi\pi$ interactions between phenol or thiophenol and the solvent are not accounted for and the partial charges are relatively large to be treated with this implicit solvent model.[45] Second, less-than-optimal geometries in the experimental situation, caused by the dynamic nature of H-bond formation, will also contribute, and will cause the experimental driving force to be less negative than the calculated one, which is solely based on the optimal, minimum-energy geometry. Third, solvent reorganization around the complex, including entropic effects, are not properly modeled, while our experiments show them to be important. Finally, mutually H-bonded phenol molecules (dimers) will have to be separated to form a complex to the phosphoryl moiety. Since the fraction of dimers of phenol in solution is only very low even at high concentrations, this is, however, probably only a relatively small factor (see calculations and IR results in Supp. Info.).

The conclusion from the solvent studies of this combined theoretical and experimental approach therefore has to halt at a somewhat preliminary stage: solvents, also apolar ones, weaken the H-bond formation in the complexes under study, and both enthalpic and entropic contributions play a role in this. The underestimation of gas-phase H-bond strengths by B3LYP actually brings these in an SCRF treatment relatively close to the experimental data (closer than the likely more accurate MP2 and M06-2X data), which we attribute to the incomplete account of solvent effects by the SCRF method. More advanced solvent-solute studies, beyond the scope of the current investigation, that take explicit account of dynamics and entropic effects are required to refine this.

The charge distribution, investigated with the NPA charges of the relevant H-bonding atoms (cf. table S-4 in the Supp. Info.) indeed points to a strong electrostatic contribution to H-bonding, especially in phenol – oxide combinations. In both B3LYP, M06-2X and MP2 calculations, similar values for the charges on the relevant atoms were obtained, supporting the method independence of NPA-derived charges.

In the oxide – phenol complex **C1**, the atom-atom overlap-weighted NAO bond order (BO) between the hydrogen and oxygen that make up the H-bond was found to be 0.076 (BO

O–H•••O=P), indicative of the partly covalent nature[46] of the formed H-bond, while the bond order in the phenol O–H bond was found to be 0.600, i.e. 0.061 smaller than that in the isolated phenol molecule (cf. Supp Info, Table S-4). Interestingly, the bond orders found for the phosphine sulfide complexes with phenol do not differ much from those obtained with thiophenol, which confirms that the reduced electrostatic interactions in the sulfur-containing compounds are the main cause for yielding complexes with a lower H-bond strength.

The shallow energy well for sulfur-containing compounds can also be observed from another geometric parameter. Previous investigations[33, 42] suggest that whereas H-bonds to oxygen (O=) are typically linear, sterically unconstrained H-bonds to sulfur atoms (S=) are linear in some cases[47] while they are strictly non-linear in others (e.g. α = 151 - 158°).[33] In the current cases the H-bond angle α « 180° for compounds involving a S= hydrogen-bond acceptor ($<\alpha_1>$ = 158.8 ± 5.2°), whereas $\alpha \approx$ 180° for O= as H-bond acceptor. Since no discernable trends in e.g. orbital occupation were observed, this is primarily attributable to the shallowness of the potential energy well in combination with optimization of other electrostatic and steric effects within the complex.

For SIR applications, the best extractant from the phosphine oxides and phosphine sulfides studied here would be the trialkylphosphine oxide, as this compound shows the highest interaction with both the phenol and the thiophenol (ΔH (MP2/CBS) = -14.5 kcal/mol for phenol and -9.8 kcal/mol for thiophenol). A strong H-bonded complex is formed; strong enough to bind phenol from an aqueous environment, and weak enough to be disrupted by e.g. steam stripping for reuse of the SIR.

Phosphates and thiophosphates. As can be seen from the optimized geometries of the selected phosphate – phenol complexes (Figure 3A, 3B and 3C and Supp. Info., Figure S-1), phenols also form a H-bond to the P=O moiety in the case of phosphates and thiophosphates, showing a geometry with a near-ideal linear H-bond if only one H-bond is formed. However, the geometry in the mono- and di-substituted phosphates differs markedly from the geometry in the tri-substituted phosphate complexes. The trimethylphosphate - phenol complex (**C13**, Figure 3A) only shows formation of one linear H-bond (much like what was found for the phosphine oxide - phenol complexes, *vide supra*), whereas phenol forms two H-bonds to monomethylphosphate (**C21**, Figure 3C). One non-linear H-bond is formed between the phenol hydrogen and the phosphoryl, while a free phosphate hydroxyl group forms a second H-bond with the phenol

oxygen. This system is very much limited in its geometrical freedom, wherein only a pivotal movement of the phenol benzene ring will be possible. The same happens for a di-substituted phosphate molecule. This clear difference between the mono- and di-substituted phosphates and the tri-substituted phosphates is manifested in both phosphate and thiophosphate complexes with both phenols and thiophenols. The distances and angles d_1, α_1, d_2, α_2, Δr_1, Δr_2, and ϕ that define the complex geometry are defined in the text and in Table 1 and summarized in the Supporting Information. A general description of the features of the phosphate and thiophosphate complexes (based on B3LYP data - M06 geometries typically similar) and their differences with the phosphine oxide and sulfide complexes is given here.

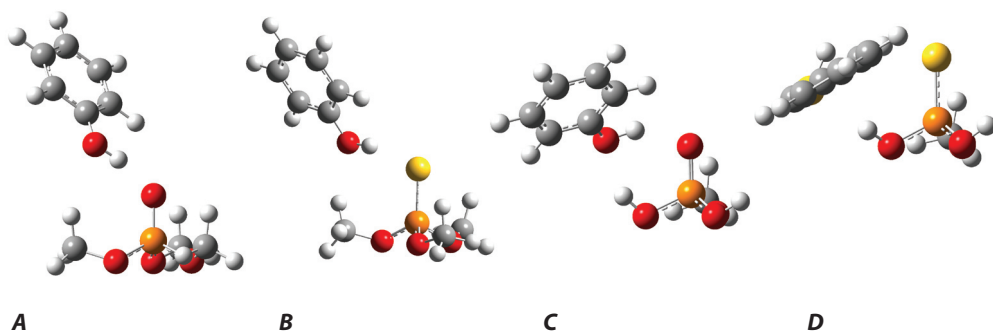**A**   **B**   **C**   **D**

Figure 3. Optimized structures (B3LYP/6-311G(d,p) (vacuum)) of representative phosphate – phenol complexes. Orange: phosphorus; red: oxygen; yellow: sulfur; black: carbon; white: hydrogen.
*A: trimethylphosphate – phenol (**C13**); B: trimethylthiophosphate – phenol (**C15**); C: monomethyl-phosphate – phenol (**C21**); D: monomethylthiophosphate – thiophenol (**C24**; SH moiety at the backside of the phenyl ring, with the protic H atom slightly above the Ph plane).*

Trialkyl(thio)phosphate complexes **C13** – **C16** show an average H-bond angle $<\alpha_1>$ of 168.8 ± 1.2°, i.e. nearly linear as in the case of the phosphine oxides and phosphine sulfides (complexes **C13** and **C15** in Figure 3A and 3B, respectively). However, due to the formation of the additional H-bond in complexes **C17** – **C24** the H-bond is highly bent, and $<\alpha_1>$ only equals 135.6 ± 8.6° (complexes **C21** and **C24** in Figures 3C and 3D, respectively). The additional H-bond angles $<\alpha_2>$ amount to 153.3 ± 4.3° for phosphate complexes (**C17**, **C18**, **C21**, **C22**) and to 166.8 ± 7.1° for thiophosphate complexes (**C19**, **C20**, **C23**, **C24**). The fact that the thiophosphate complexes show an average second H-bond

angle $<\alpha_2>$ closer to 180° again shows the more shallow energy surface of the P=S H-bonds, enabling deviating geometries more readily. H-bond lengths d_1 do not differ much from the corresponding bond lengths found for the phosphine oxide and phosphine sulfide complexes.

The H-bonding energies for the phosphate and thiophosphate complexes are summarized in Table 5. Also in this case the CBS-Q energy values show a different trend than the energy values calculated with the other methods. In this case as well, the discrepancy is believed to be caused by systematic errors in the CBS-Q calculations dealing with sulfur compounds, and not by errors in the other methods, for reasons discussed above (see Supp. Info, Table S-3).

The tri-substituted phosphates show H-bond energies that are generally slightly less negative (weaker complex) than those observed for the phosphine oxides. These small differences in energy can be partly explained by small differences in charge (phosphates have a slightly less negative charge on oxygen than phosphine oxides), and by a reduction of the H-bond bond orders in the phosphates compared to the phosphine oxides. Although the phosphates generally show a lower binding energy than the respective phosphine oxides, the presence of an additional P–OH moiety in the mono- and di-substituted (thio)phosphates yields much stronger complexes than their phosphine oxide and sulfide counterparts. Apart from this, the same trends can be observed in all calculations: phenols bind tighter than thiophenols (e.g. compare complexes **C21** and **C22** with ΔH(MP2/CBS) values of -14.7 and -10.6 kcal/mol, respectively), and phosphates bind slightly tighter than thiophosphates (e.g. compare complexes **C21** and **C23** with ΔH(MP2/CBS) values of -14.7 and -13.2 kcal/mol, respectively).

As with the phosphine oxide complexes, B3LYP interaction energy results are only in qualitative agreement with the MP2/CBS data, while M06-2X data agree reasonably well (0 – 4 kcal/mol before, and 0 – 3 kcal/mol after counterpoise correction). MP2 results lead to equal or slightly more negative values for the complexation enthalpies, which has also been found in literature with these kinds of basis sets.[41] SCS-MP2 results again show slightly less negative enthalpy values (by on average 1.3 kcal/mol) than the corresponding MP2 results.

By examining the changes in the length of the covalent O/S–H bond Δr_1 and Δr_2 (see Table 1 and Supp. Info) the nature of the complexes can be more clearly understood. As the formation of H-bonds to S=P is much weaker than to O=P, the covalent O/S–H bond lengthening Δr_1 is higher in O=P complexes (0.016 - 0.019 Å for phenols and 0.005 - 0.008 Å for thiophenols) than in S=P complexes (0.010 - 0.013 Å for phenols and 0.002 - 0.004 Å for thiophenols). In accordance

with this, the phosphate O–H bond lengthening Δr_2 is largest for the weakest primary H-bonds, i.e. for the ones to S=P, as those complexes can gain most from this second H-bond. These results show the weaker nature of the H-bond to the thiophosphate and the large influence of the second hydrogen bond on the geometry and binding energy of the complex.

Table 5. Calculated binding energies, ΔH (kcal/mol), of phosphate and thiophosphate complexes with phenol and thiophenol (all 6-311+G(d,p) basis set except MP2/CBS) in vacuum.

#	Complex	ΔH						
		B3LYP	M06-2X	MP2		SCS-MP2		MP2/CBS
		-cp	-cp	-cp	+cp	-cp	+cp	-cp
C13	$(CH_3O)_3P=O$ - HO-Ph	-9.8[a]	-13.8	-12.8	-9.3	-11.7	-8.3	-12.2
C14	$(CH_3O)_3P=O$ - HS-Ph	-5.0[a]	-10.7	-9.1	-5.9	-8.0	-4.9	-8.5
C15	$(CH_3O)_3P=S$ - HO-Ph	-4.8[a]	-11.2	-8.1	-5.1	-7.2	-4.3	-7.7
C16	$(CH_3O)_3P=S$ - HS-Ph	-2.4[a]	-8.8	-5.8	-3.3	-5.0	-2.6	-5.6
C17	$(CH_3O)_2(OH)P=O$ - HO-Ph	-12.1	-15.3	-15.0	-10.8	-13.6	-9.6	-15.1
C18	$(CH_3O)_2(OH)P=O$ - HS-Ph	-6.9	-12.6	-10.9	-6.9	-9.4	-5.6	-10.8
C19	$(CH_3O)_2(OH)P=S$ - HO-Ph	-10.0	-13.9	-13.8	-9.0	-12.4	-7.8	-13.3
C20	$(CH_3O)_2(OH)P=S$ - HS-Ph	-5.7	-12.3	-10.3	-6.6	-9.0	-5.5	-9.5
C21	$(CH_3O)(OH)_2P=O$ - HO-Ph	-11.9	-16.9	-14.6	-10.6	-13.2	-9.4	-14.7
C22	$(CH_3O)(OH)_2P=O$ - HS-Ph	-6.8	-14.3	-10.6	-6.7	-9.1	-5.5	-10.6
C23	$(CH_3O)(OH)_2P=S$ - HO-Ph	-10.1	-15.2	-13.7	-8.9	-12.3	-7.7	-13.2
C24	$(CH_3O)(OH)_2P=S$ - HS-Ph	-5.9	-13.6	-10.3	-6.7	-9.0	-5.6	-9.5

[a] from ref 7.

Again, SCS-MP2/6-311+G(d,p) values calculated without CP-correction agree with the MP2/CBS values to a high degree, being on average less negative by 0.9 kcal/mol. The minimum and maximum deviation of the CP-uncorrected SCS-MP2/6-311+G(d,p) values with respect to the MP2/CBS values are 0.5 and 1.5 kcal/mol, respectively. As concluded before, the quickly obtainable CP-uncorrected SCS-MP2/6-311+G(d,p) values can therefore be used as a relatively cheap approach to high-quality data near the basis set limit, without the need for a time-consuming CP-correction.

In comparing the DFT calculations both in vacuum and for the solvents cyclohexane, toluene, and benzene (Table S-10, Supp. Info), similar trends can be observed for the phosphate complexes

as were noted for the phosphine oxides: markedly lower absolute values are obtained for the complexes in the various solvents, and for the trimethylthiophosphate – thiophenol complexes even positive ΔH values were found. For the two other thiophosphates, still slightly negative ΔH values were obtained due to the formation of the second H-bond. Previous experimental studies[7] (See Chapter 2) show that the tributylphosphate (TBP) – phenol complex shows binding enthalpies ΔH^0 of -5.8 kcal/mol, which is in good agreement with theory, although again somewhat less negative than the calculated values for the trimethylphosphate – phenol (**C13**, $\Delta H(\text{B3LYP}_{\text{toluene}})$ = -6.7 kcal/mol).

The charges on the relevant atoms (cf. table S-5 in the Supporting Information) again are much lower in absolute numbers for sulfur-containing compounds than those for their oxygen counterparts, while they are equal to the ones of the phosphine oxides and sulfides, and like in the case of the phosphine oxides/sulfides, the presence of a sulfur atom in the thiophosphate or in the thiophenol or in both lowers the bond orders markedly.

For complexes **C20** and **C24** (Figure 3D) the thiol H-bond to the P=S moiety is very long and thus likely rather weak, making the presence of a H-bond to the P=S moiety in fact debatable. The H-bond lengths $d1$ in **C20** and **C24** amount to 3.26 Å and 3.48 Å, respectively, while the S–H bond lengthening Δr_1 is only 0.002 for both, and the H•••O bond orders of **C20** and **C24** are only 0.002 and 0.001, respectively, i.e. only one-tenth that of a strong H-bond. In these two cases, the O–H•••S H-bond is almost exclusively responsible for both the complex geometry and the H-bond energy.

Additional H-bonds of a phosphate O–H group to the phenol or thiophenol molecule significantly influence the complex geometry and increase its stability by 2.5 – 3 kcal/mol for the mono- and di-substituted phosphates compared to the equivalent tri-substituted phosphates. For example, complexes **C17** and **C21** (with two H-bonds) are more stable than the corresponding complex **C13** with one H-bond by ≥ 2.5 kcal/mol: their corresponding ΔH(MP2/CBS) enthalpies are -15.1, -14.7 and -12.2 kcal/mol, respectively. An even larger stabilization by the formation of the second H-bond can clearly be observed in the case of thiophosphate – thiophenol interactions. In complexes **C20** and **C24** – in which two H-bonds are formed – ΔH(MP2/CBS) enthalpies of complexation are -9.5 kcal/mol, whereas in complex **C16** with only a single H-bond, an enthalpy of complexation of only -5.6 kcal/mol was found. From Table 5 it is also clear that, although involving a thiophosphate moiety, complexes **C19** and **C23** also show much higher binding

enthalpies than could be expected from just a single H-bond: ΔH(MP2/CBS) values are -13.3 and -13.2 kcal/mol, respectively, while in the singly bound complex **C15** this is only -7.7 kcal/mol.
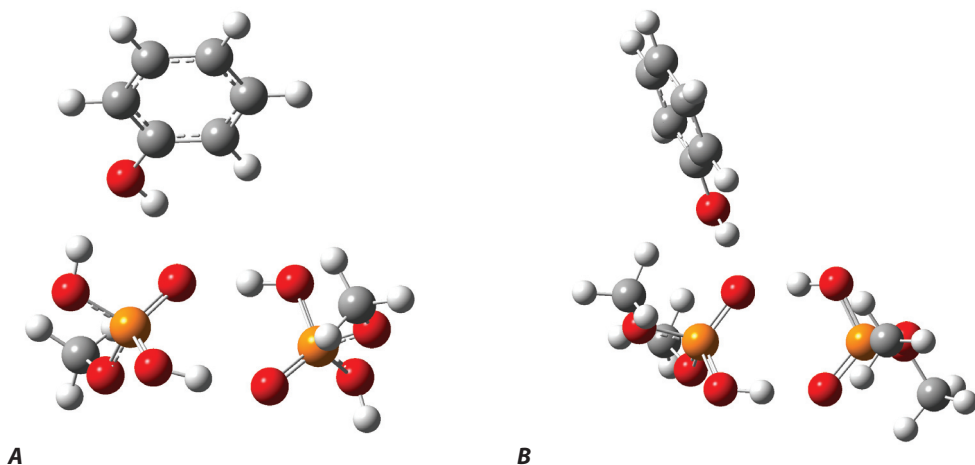

Figure 4. Optimized structures (B3LYP/6-311G(d,p) (vacuum)) of methylphosphate dimer – phenol complex (A) and dimethylphosphate dimer – phenol complex (B). Orange: phosphorus; red: oxygen; black: carbon; white: hydrogen

Based on the calculated enthalpies of complex formation, we suggest that the most suitable extractant to use in SIR applications for both phenol and thiophenol extraction in the phosphate series would be dimethylphosphate, as it yields the highest absolute ΔH upon complex formation in vacuum. However, the formation of dimers of dimethylphosphate, which is also well known for e.g. carboxylic acids, will severely diminish its phenol-binding capacity. Additional results (SCS-MP2/6-311+G(d,p)//B3LYP/6-311G(d,p), no cp-correction; MP2/CBS was prohibitively expensive for these systems) yield dimerization energies for monomethylphosphate and dimethylphosphate of -24.3 and-24.8 kcal/mol, respectively, implying that these compounds will dimerize under the experimental conditions of interest. Complexation of (thio)phenol to the dimer can still take place, and the monomethylphosphate dimer - phenol complex and dimethylphosphate dimer - phenol complex are depicted in Figure 4. The dimethylphosphate dimer shows indeed a markedly lower binding affinity than the monomer: for phenol by 2.2 kcal/mol (from -11.9 to -9.7 kcal/mol) and for thiophenol by 2.0 kcal/mol. In contrast, for the dimer of monomethylphosphate – which displays 2×2 available -OH sites apart from the two P=O sites – this H-bond formation even proceeds with a slightly more negative binding affinity of 0.4 and 0.3 kcal/mol, respectively, for phenol and

thiophenol, compared to the complexation to monomethylphosphate monomer. Unfortunately for SIRs applications, this material with two protic moieties per molecule will be too water soluble and/or surface active to function as useful extractant, even with a long alkyl tail. In addition, at the higher concentrations relevant for SIRs higher aggregates of methylphosphate will be formed involving the second -OH group, which thus limits the extracting capacity (number of H-bonds with phenol or thiophenol that can form per phosphate molecule).

Excluding therefore the compounds that are capable of formation of dimers, the obtained results for phenol extraction with trialkyl phosphine oxides look promising and will probably yield the best results for SIR applications, as binding enthalpies towards both phenol and thiophenol are found to be highest for this compound, and approaching the experimentally desired value of ~15 kcal/mol.

Conclusions

The presented high-level *ab initio* study provides the first detailed view of the H-bonded complexes of phenols and thiophenols with phosphine oxides and phosphates and their thio-analogs, as relevant for solvent-impregnated resin (SIR)-based separations. Using H-bond geometry information (e.g. bond length and bond angle) and electronic properties of the complexes (charges and bond orders), the formation of strong H-bonds was characterized. The highest enthalpy of complexation was found for the dimethylphosphate – phenol complex, ΔH = 15.1 kcal/mol (at the MP2/CBS level of theory). The highest binding enthalpy in a compound that does not form homodimers, and that can thus be used in SIR applications, was found for the tri-ethylphosphine oxide – phenol complex, ΔH = -14.5 kcal/mol (MP2/CBS). The choice for the optimum extractant is crucial for future large-scale SIR applications. The detailed modeling experiments show that phosphine oxides are good candidates for the extraction of phenols and likely better than alkyl phosphates. In combination with industrially relevant properties such as a low melting point (removes the need for an additional solvent) and a high boiling point (for regeneration of the SIR at high temperatures), water-insoluble triethylphosphine oxide analogs are on the basis of these calculations thus expected to combine most of these desired characteristics. The weaker H-bonds found for thio-compounds in comparison to analogous oxygen-containing compounds are largely due to lower charges on the H-bond donor and acceptor atoms, which yield smaller electrostatic interactions. In phosphates, a second H-bond of phenol and thiophenol can be formed to mono- and di-substituted phosphates. This second H-bond stabilizes especially thiophosphates, which show relatively weak primary H-bonds. However, aggregate formation

of these phosphates will strongly hamper the efficient complexation of phenol and thiophenol molecules in SIRs.

In ITC measurements, binding affinities of the trioctyl-phosphine oxide – phenol complex were found to be highest in the non-interacting solvent cyclohexane, and were markedly lower in $\pi\pi$ interacting solvents such as mesitylene, toluene and benzene. While PCM modeling provides qualitative correctness for the solvent-induced weakening, more advanced solvent treatments that also take $\pi\pi$ interactions and entropic effects into account are clearly required for further improvement.

This study also yielded two methodological conclusions: a) for the H-bonded systems at hand it was found that enthalpies computed at the computationally relatively cheap SCS-MP2/6-311+G(d,p) level without counterpoise correction approach the values of the highly accurate and much more elaborate MP2/CBS method, with average deviations of only 0.3 kcal/mol (phosphine oxides and sulfides) and 0.9 kcal/mol (phosphate and thiophosphate complexes). In addition, M06-2X/6-311+G(d,p) calculations with counterpoise corrections also yield data typically within 0 – 2 kcal/mol deviating from MP2/CBS data. These findings open up the accurate study of larger H-bonded complexes. b) The CBS-Q model chemistry was consistently yielding erroneously high stability complexes for sulfur-containing compounds in comparison to those of analogous oxygen-containing complexes. Since the usefulness of CBS-Q for oxygen-based H-bonded complexes is well established, a systematic error for sulfur-containing compounds is therefore suspected.

Acknowledgements

References

(1)   J. L. Cortina, A. Warshawsky, in *Ion Exch. Solvent Extr., Vol. 13* (Eds.: J. A. Marinsky, Y. Marcus), Dekker, New York, 1997, pp. 195.

(2)   M. T. Draa, T. Belaid, M. Benamor, *Sep. Purif. Technol.* **2004**, *40*, 77.

(3)   S. D. Alexandratos, S. D. Smith, *Solvent Extr. Ion Exch.* **2004**, 22, 713.

(4)   B. B. Gupta, Z. B. Ismail, *Comp. Interf.* **2006**, 13, 487.

(5)   S. S. El-Dessouky, E. H. Borai, *J. Radioanal. Nucl. Chem*. **2006**, *268*, 247.

(6)   J. S. Liu, H. Chen, Z. L. Guo, Y. C. Hu, *J. Appl. Pol. Science* **2006**, *100*, 253.

(7)   R. Cuypers, B. Burghoff, A. T. M. Marcelis, E. J. R. Sudhölter, A. B. de Haan, H. Zuilhof, *J. Phys*. *Chem*. *A* **2008**, *112*, 11714.

(8)   B. Burghoff, E. L. V. Goetheer, A. B. de Haan, *React. & Funct. Pol*. **2008**, *68*, 1314.

(9)   R.-S. Juang, H.-L. Chang, *Ind. Eng. Chem. Res*. **1995**, *34*, 1294.

(10)   M. Traving, H.-J. Bart, *Chem. Eng. Technol*. **2002**, *25*, 997.

(11)   A. Kostova, H.-J. Bart, *Chemie Ingenieur Technik* **2004**, *76*, 1743.

(12)   H. Kitazaki, M. Ishimaru, K. Inone, K. Yoshida, S. Nakamura, in *Proceedings of the International Solvent Extraction Conference,* ISEC'96 ed., Melbourne, Australia, 1996, pp. 1667.

(13)   G. A. Jeffrey, *An Introduction to Hydrogen Bonding,* Oxford University Press, New York, Oxford, 1997.

(14)   G. R. Desiraju, T. Steiner, *The Weak Hydrogen Bond,* 1 ed., Oxford University Press, New York, 1999.

(15)   J. P. M. Lommerse, S. L. Price, R. Taylor, *J. Comp. Chem*. **1997**, *18*, 757.

(16)   S. K. Panigrahi, G. R. Desiraju, *Proteins: Structure, Function, and Bioinformatics* **2007**, *67*, 128.

(17)   M. H. Abraham, P. L. Grellier, D. V. Prior, P. P. Duce, J. J. Morris, P. J. Taylor, *J. Chem. Soc., Perkin Trans*. *2* **1989**, 1989, 699.

(18)   M. H. Abraham, P. L. Grellier, D. V. Prior, J. J. Morris, P. J. Taylor, *J. Chem. Soc. Perkin Trans.*. *2* **1990**, 521.

(19)   G. Aksnes, P. Albriktsen, *Acta Chem. Scand*. **1968**, 22, 1866.

(20)   R. M. Badger, S. H. Bauer, *J. Chem. Phys*. **1937**, *5*, 839.

(21)   T. Gramstad, *Acta Chem. Scand*. **1961**, *15*, 1337.

(22)   M. D. Joesten, L. J. Schaad, *Hydrogen Bonding*, Marcel Dekker Inc, 1974.

(23)   Y. Zhao, D. G. Truhlar, *J. Chem. Theory Comput*. **2007**, *3*, 289.

(24)   Y. Zhao, D. G. Truhlar, *Acc. Chem. Res*. **2008**, *41*, 157.

(25)   Y. Zhao, D. G. Truhlar, *Theor. Chem. Acc*. **2008**, *120*, 215.

(26)   J. W. Ochterski, G. A. Petersson, J. A. Montgomery, *J. Chem. Phys*. **1996**, *104*, 2598.

(27)   S. Grimme, *J. Chem. Phys*. **2003**, *118*, 9095.

(28)   T. Schwabe, S. Grimme, *Acc. Chem. Res*. **2008**, *41*, 569.

(29)   J. Antony, S. Grimme, *J. Phys*. *Chem. A* **2007**, *111*, 4862.

(30)   R. A. Bachorz, F. A. Bischoff, S. Hofener, W. Klopper, P. Ottiger, R. Leist, J. A. Frey, S. Leutwyler, *Phys. Chem. Chem. Phys*. **2008**, *10*, 2758.

(31)   S. G. Manuel Piacenza, *ChemPhysChem* **2005**, *6*, 1554.

(32)   C. J. Cramer, D. G. Truhlar, *Acc. Chem. Res*. **2009**, *42*, 493.

(33)   F. Wennmohs, V. Staemmler, M. Schindler, *J. Chem. Phys*. **2003**, *119*, 3208.

(34)   M. Ichikawa, *Acta Crystallographica Section B-Structural Science* **1978**, *34*, 2074.

(35)   S. J. Grabowski, *Tetrahedron* **1998**, *54*, 10153.

(36)   M. G. Govender, T. A. Ford, *J. Mol. Struct.: THEOCHEM* **2003**, *630*, 11.

(37)   V. S. Bryantsev, M. S. Diallo, A. C. T. van Duin, W. A. Goddard, *J. Chem. Theor. Comp*. **2009**, *5*, 1016.

(38)   J. T. Su, X. Xu, W. A. Goddard, *J. Phys. Chem. A* **2004**, *108*, 10518.

3

(39) Y. Zhao, D. G. Truhlar, *J. Chem. Theor. Comp.* **2005**, *1*, 415.

(40) P. R. Rablen, J. W. Lockman, W. L. Jorgensen, *J. Phys. Chem.A* **1998**, *102*, 3782.

(41) V. Barvinchenko, V. Pogorelyi, *Theor.Exp. Chem.* **1982**, *17*, 662.

(42) J. A. Platts, S. T. Howard, B. R. F. Bracke, *J. Am. Chem. Soc.* **1996**, *118*, 2726.

(43) A. J. Bienko, Z. Latajka, *Chem. Phys. Let*t. **2003**, *374*, 577.

(44) M. Cossi, G. Scalmani, N. Rega, V. Barone, *J. Chem. Phys.* **2002**, *117*, 43.

(45) C. P. Kelly, C. J. Cramer, D. G. Truhlar, *J. Phys. Chem.A* **2006**, *110*, 2493.

(46) T. W. Martin, Z. S. Derewenda, *Nat. Struct. Mol. Biol.* **1999**, *6*, 403.

(47) M. Wierzejewska, M. Saldyka, *Chem. Phys. Lett.* **2004**, *391*, 143.

(48) M. J. Frisch, G. W. Trucks, H. B. Schlegel, G. E. Scuseria, M. A. Robb, J. R. Cheeseman, J. A. M. Jr., T. Vreven, K. N. Kudin, J. C. Burant, J. M. Millam, S. S. Iyengar, J. Tomasi, V. Barone, B. Mennucci, M. Cossi, G. Scalmani, N. Rega, G. A. Petersson, H. Nakatsuji, M. Hada, M. Ehara, K. Toyota, R. Fukuda, J. Hasegawa, M. Ishida, T.Nakajima, Y. Honda, O. Kitao, H. Nakai, M. Klene, X. Li, J. E. Knox, H. P. Hratchian, J. B. Cross, C. Adamo, J. Jaramillo, R. Gomperts, R. E. Stratmann, O. Yazyev, A. J. Austin, R. Cammi, C. Pomelli, J. W. Ochterski, P. Y. Ayala, K. Morokuma, G. A. Voth, P. Salvador, J. J. Dannenberg, V. G. Zakrzewski, S. Dapprich, A. D. Daniels, M. C. Strain, O. Farkas, D. K. Malick, A. D. Rabuck, K. Raghavachari, J. B. Foresman, J. V. Ortiz, Q. Cui, A. G. Baboul, S. Clifford, J. Cioslowski, B. B. Stefanov, G. Liu, A. Liashenko, P. Piskorz, I. Komaromi, R. L. Martin, D. J. Fox, T. Keith, M. A. Al-Laham, C. Y. Peng, A. Nanayakkara, M. Challacombe, P. M. W. Gill, B. Johnson, W. Chen, M. W. Wong, C. Gonzalez, J. A. Pople, Gaussian, Inc., Wallingford CT, 2004.

(49) M. J. Frisch, G. W. Trucks, H. B. Schlegel, G. E. Scuseria, M. A. Robb, J. R. Cheeseman, G. Scalmani, V. Barone, B. Mennucci, G. A. Petersson, H. Nakatsuji, M. Caricato, X. Li, H. P. Hratchian, A. F. Izmaylov, J. Bloino, G. Zheng, J. L. Sonnenberg, M. Hada, M. Ehara, K. Toyota, R. Fukuda, J. Hasegawa, M. Ishida, T. Nakajima, Y. Honda, O. Kitao, H. Nakai, T. Vreven, J. Montgomery, J. A., J. E. Peralta, F. Ogliaro, M. Bearpark, J. J. Heyd, E. Brothers, K. N. Kudin, V. N. Staroverov, R. Kobayashi, J. Normand, K. Raghavachari, A. Rendell, J. C. Burant, S. S. Iyengar, J. Tomasi, M. Cossi, N. J. Rega Millam, M. Klene, J. E. Knox, J. B. Cross, V. Bakken, C. Adamo, J. Jaramillo, R. E. Gomperts, O. Stratmann, A. J. Yazyev, R. Austin, C. Cammi, J. W. Pomelli, R. Ochterski, R. L. Martin, K. Morokuma, V. G. Zakrzewski, G. A. Voth, P. Salvador, J. J. Dannenberg, S. Dapprich, A. D. Daniels, O. Farkas, J. B. Foresman, J. V. Ortiz, J. Cioslowski, D. J. Fox, Gaussian, Inc., Wallingford CT, 2009.

(50) G. B. W. L. Ligthart, D. Guo, A. L. Spek, H. Kooijman, H. Zuilhof, R. P. Sijbesma, *J. Org. Chem.* **2008**, *73*, 111.

(51) S. Raub, C. M. Marian, *J. Comp. Chem.* **2007,** *28*, 1503.

(52) C. J. Cramer, *Essentials Of Computational Chemistry: Theories And Models*, 2nd ed., John Wiley & Sons,Ltd, 2004.

(53) P. Jurečka, J. Šponer, J. Černy, P. Hobza, *Phys. Chem. Chem. Phys.* **2006**, *8*, 1985.

(54) M. Kone, B. Illien, J. Graton, C. Laurence, *J. Phys. Chem.* A **2005**, *109*, 11907.

(55) M. R. Nyden, G. A. Petersson, *J. Chem. Phys.***1981**, *75*, 1843.

(56) S. F. Boys, F. Bernardi, *Molecular Physics* **1970**, *19*, 553.

(57) F. B. van Duijneveldt, J. G. C. M. van Duijneveldt - van de Rijdt, J. H. van Lenthe, *Chem. Rev.* **1994**, *94*, 1873.

(58) D. Hadži, *Theoretical treatments of hydrogen bonding*, Wiley, New York, 1997.

(59) H. Umeyama, K. Morokuma, *J. Am. Chem. Soc.* **1977**, *99*, 1316.

(60) S. Cybulski, S. Scheiner, *J. Phys. Chem.* **1990**, *94*, 6106.

(61) G. Alagona, *Int. J. Quant. Chem.* **1987**, *32*, 227.

(62) A. E. Reed, R. B. Weinstock, F. Weinhold, *J. Chem. Phys.* **1985**, *83*, 735.

(63) E. D. Glendening, A. E. Reed, J. E. Carpenter, F. Weinhold., NBO Version 3.1.

(64) X. G. Bao, J. Wang, J. D. Gu, J. Leszczynski, *Proc. Nat. Ac. Sc.* **2006,** *103*, 5658.

(65) M. Peschke, A. T. Blades, P. Kebarle, *J. Am. Chem. Soc.* **2000**, *122*, 10440.

(66) N. Diaz, D. Suarez, K. M. Merz, *Chem. Phys. Lett.* **2000**, *326*, 288.

(67) M. Chellani, *Am. Biotechnol. Lab.* **1999,** *october*, 14.

3

Supporting information
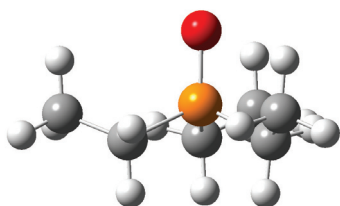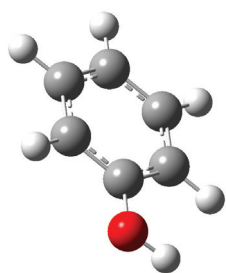
(C₂H₅)₃P=O   - HO-Ph (**C1**)
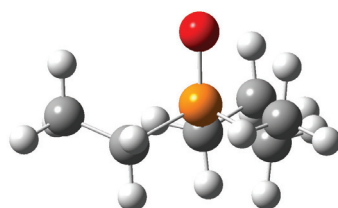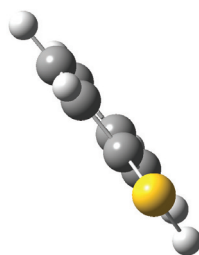
(C₂H₅)₃P=O   - HS-Ph (**C2**)
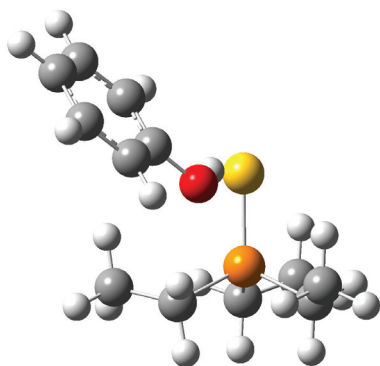
(C₂H₅)₃P=S   - HO-Ph (**C3**)
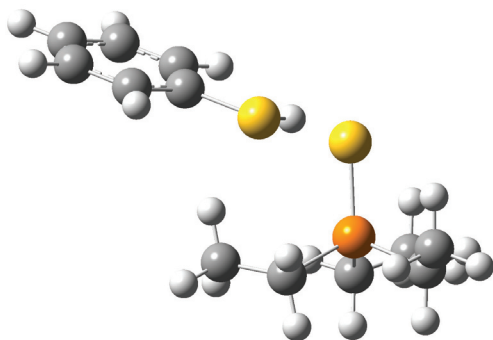
(C₂H₅)₃P=S   - HS-Ph (**C4**)

Figure S-1. Geometry of calculated phosphoryl - phenol complexes.
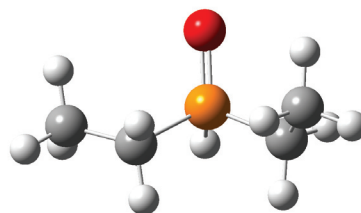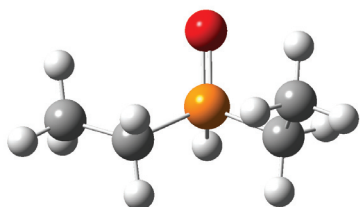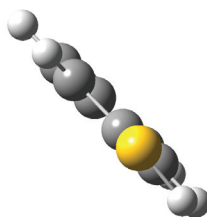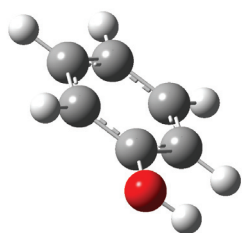
(C$_2$H$_5$)$_2$HP=O - HO-Ph (**C5**)

(C$_2$H$_5$)$_2$HP=O - HS-Ph (**C6**)
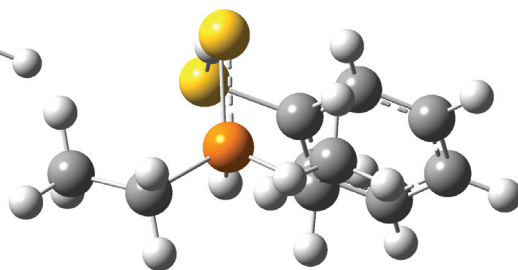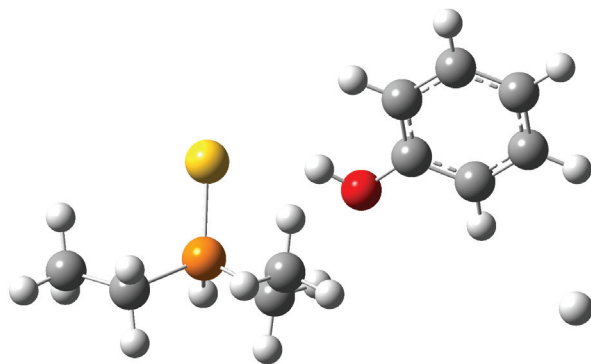
(C$_2$H$_5$)$_2$HP=S - HO-Ph (**C7**)

(C$_2$H$_5$)$_2$HP=S - HS-Ph (**C8**)

Figure S-1 (continued). Geometry of calculated phosphoryl - phenol complexes.
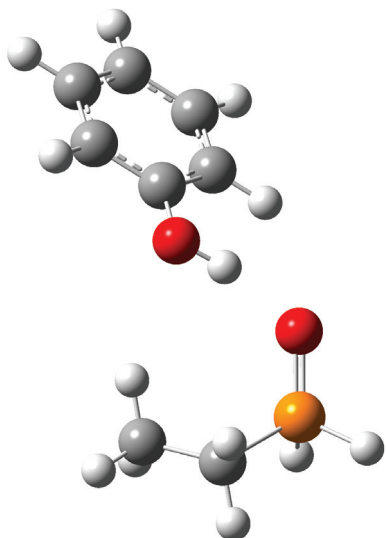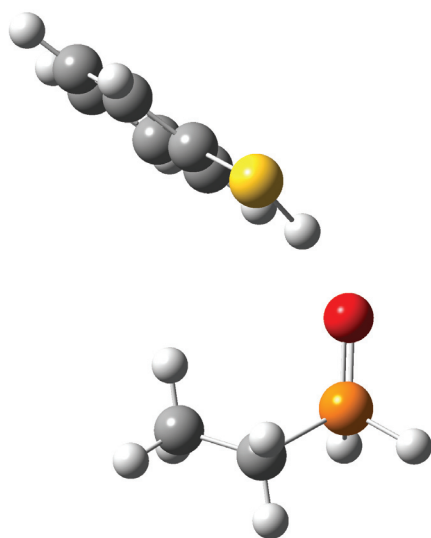
(C$_2$H$_5$)H$_2$P=O - HO-Ph (**C9**)

(C$_2$H$_5$)H$_2$P=O - HS-Ph (**C10**)
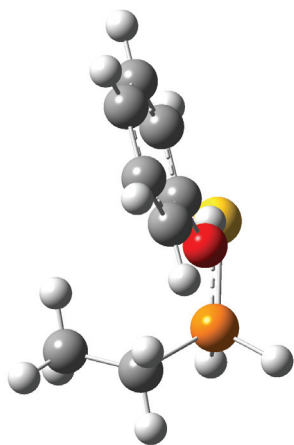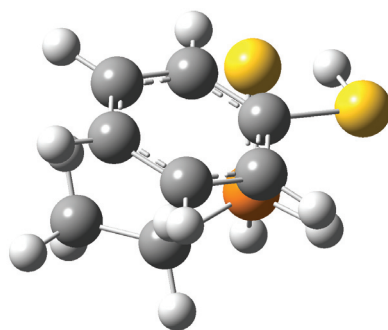
(C$_2$H$_5$)H$_2$P=S - HO-Ph (**C11**)

(C$_2$H$_5$)H$_2$P=S - HS-Ph (**C12**)

Figure S-1 (continued). Geometry of calculated phosphoryl - phenol complexes.
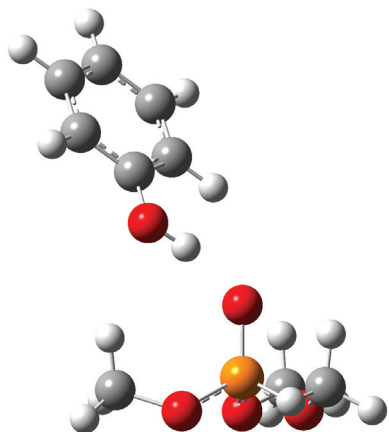
(CH$_3$O)$_3$P=O - HO-Ph (**C13**)
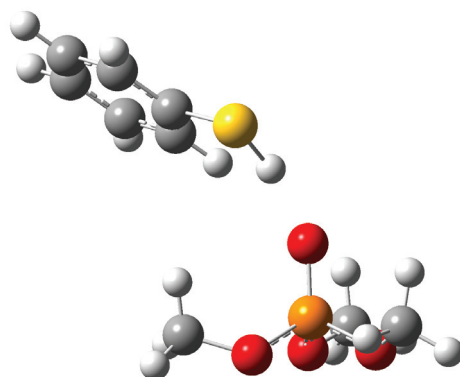
(CH$_3$O)$_3$P=O - HS-Ph (**C14**)
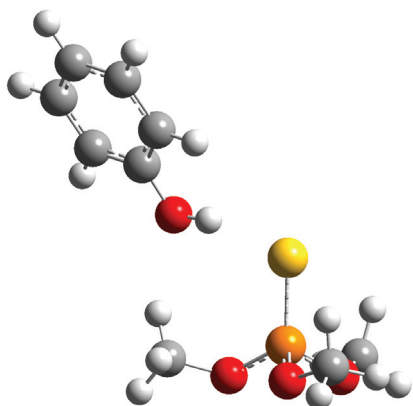
(CH$_3$O)$_3$P=S - HO-Ph (**C15**)
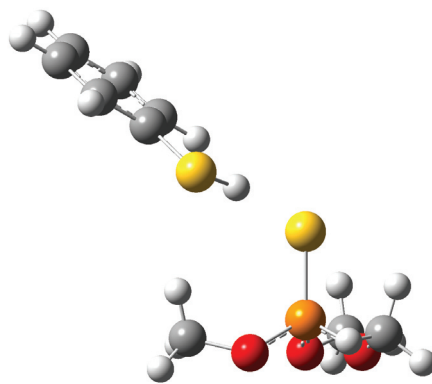
(CH$_3$O)$_3$P=S - HS-Ph (**C16**)

Figure S-1 (continued). Geometry of calculated phosphoryl - phenol complexes.
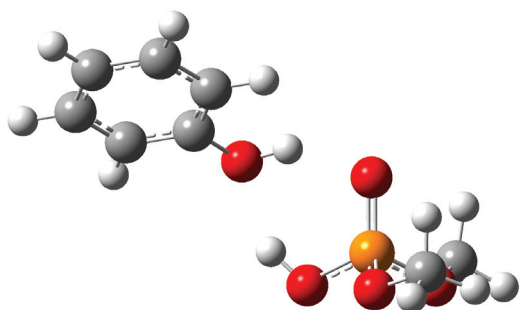
$(CH_3O)_2(OH)P=O$ - HO-Ph (**C17**)
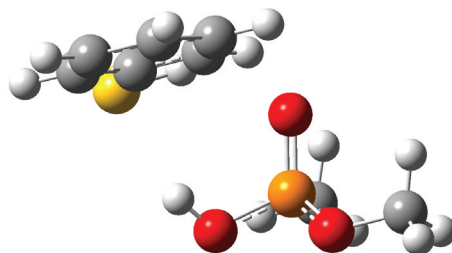
$(CH_3O)_2(OH)P=O$ - HS-Ph (**C18**)
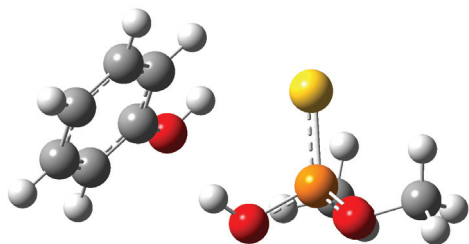
$(CH_3O)_2(OH)P=S$ - HO-Ph (**C19**)

$(CH_3O)_2(OH)P=S$ - HS-Ph (**C20**)

Figure S-1 (continued). Geometry of calculated phosphoryl - phenol complexes.
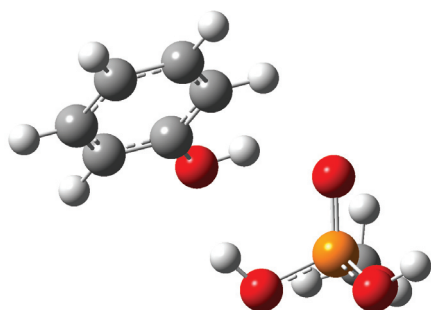
(CH$_3$O)(OH)$_2$P=O - HO-Ph (**C21**)
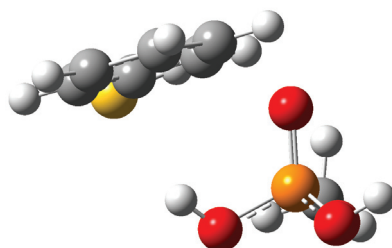
(CH$_3$O)(OH)$_2$P=O - HS-Ph (**C22**)
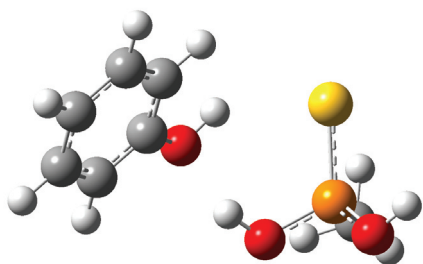
(CH$_3$O)(OH)$_2$P=S - HO-Ph (**C23**)
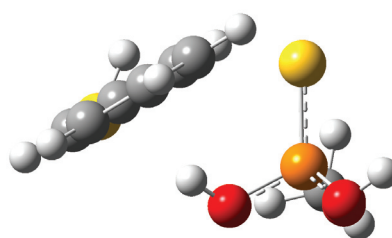
(CH$_3$O)(OH)$_2$P=S - HS-Ph (**C24**)

Figure S-1 (continued). Geometry of calculated phosphoryl - phenol complexes.

Table S-1. Energy barrier of rotation around the C–O/S bond ($E_{O/S-H\ at\ 90°}$ - $E_{O/S-H\ at\ 0°}$, angle with respect to the plane of the benzene ring) of alcohol and thiol group in phenol and thiophenol, respectively. Both methods used a B3LYP/6-311G(d,p) optimized geometry.

	Energy barrier (kcal/mol)	
	B3LYP/6-311+G(d,p)	MP2/6-311+G(d,p)
PhOH	3.5	3.0
PhSH	0.7	0.4

Table S-2. CBS-Q results of phosphine oxide and sulfide complexes.

#	Complex	CBS-Q [kcal/mol]
C1	$(C_2H_5)_3P{=}O$ - HO-Ph	-15.7
C2	$(C_2H_5)_3P{=}O$ - HS-Ph	-14.5
C3	$(C_2H_5)_3P{=}S$ - HO-Ph	-11.1
C4	$(C_2H_5)_3P{=}S$ - HS-Ph	-21.9
C5	$(C_2H_5)_2HP{=}O$ - HO-Ph	-10.2
C6	$(C_2H_5)_2HP{=}O$ - HS-Ph	-13.5
C7	$(C_2H_5)_2HP{=}S$ - HO-Ph	-9.5
C8	$(C_2H_5)_2HP{=}S$ - HS-Ph	-13.8
C9	$(C_2H_5)H_2P{=}O$ - HO-Ph	-8.6
C10	$(C_2H_5)H_2P{=}O$ - HS-Ph	-11.1
C11	$(C_2H_5)H_2P{=}S$ - HO-Ph	-7.3
C12	$(C_2H_5)H_2P{=}S$ - HS-Ph	-13.5

Table S-3. CBS-Q results of phosphate and thiophosphate complexes.

#	Complex	CBS-Q [kcal/mol]
C13	$(CH_3O)_3P=O$ - HO-Ph	-10.8
C14	$(CH_3O)_3P=O$ - HS-Ph	-15.7
C15	$(CH_3O)_3P=S$ - HO-Ph	-7.6
C16	$(CH_3O)_3P=S$ - HS-Ph	-15.3
C17	$(CH_3O)_2(OH)P=O$ - HO-Ph	-11.4
C18	$(CH_3O)_2(OH)P=O$ - HS-Ph	-15.7
C19	$(CH_3O)_2(OH)P=S$ - HO-Ph	-9.4
C20	$(CH_3O)_2(OH)P=S$ - HS-Ph	-13.0
C21	$(CH_3O)(OH)_2P=O$ - HO-Ph	-10.8
C22	$(CH_3O)(OH)_2P=O$ - HS-Ph	-16.0
C23	$(CH_3O)(OH)_2P=S$ - HO-Ph	-8.9
C24	$(CH_3O)(OH)_2P=S$ - HS-Ph	-11.9

Table S-4. Charges and bond orders of phosphine oxide and sulfide complexes

#	Complex	Charge			BO		
		PhOH/PhSH H	PhOH/PhSH O/S	P=O/P=S O/S	H···O/S	PhOH/PhSH O/S-H	ΔBO (O/S-H)
C1	$(C_2H_5)_3P=O$ - HO-Ph	0.51	-0.72	-1.13	0.076	0.600	-0.061
C2	$(C_2H_5)_3P=O$ - HS-Ph	0.19	-0.02	-1.12	0.038	0.708	-0.016
C3	$(C_2H_5)_3P=S$ - HO-Ph	0.49	-0.73	-0.64	0.047	0.611	-0.050
C4	$(C_2H_5)_3P=S$ - HS-Ph	0.16	0	-0.63	0.045	0.708	-0.016
C5	$(C_2H_5)_2HP=O$ - HO-Ph	0.51	-0.72	-1.11	0.070	0.605	-0.056
C6	$(C_2H_5)_2HP=O$ - HS-Ph	0.19	-0.02	-1.10	0.034	0.709	-0.015
C7	$(C_2H_5)_2HP=S$ - HO-Ph	0.49	-0.72	-0.62	0.035	0.617	-0.044
C8	$(C_2H_5)_2HP=S$ - HS-Ph	0.16	0.01	-0.61	0.037	0.708	-0.016
C9	$(C_2H_5)H_2P=O$ - HO-Ph	0.51	-0.72	-1.09	0.065	0.609	-0.052
C10	$(C_2H_5)H_2P=O$ - HS-Ph	0.18	-0.01	-1.08	0.035	0.710	-0.014
C11	$(C_2H_5)H_2P=S$ - HO-Ph	0.49	-0.72	-0.59	0.032	0.618	-0.043
C12	$(C_2H_5)H_2P=S$ - HS-Ph	0.15	0.01	-0.59	0.032	0.709	-0.015

Table S-5. Charges and bond orders of phosphate and thiophosphate complexes.

#	Complex	Charge					BO			
		PhO/SH H	PhO/SH O/S	P=O/S O/S	P-O-H O	P-O-H H	PhO/S-H	H···O	H···O-H	P-O-H
C13	$(CH_3O)_3P=O$ - HO-Ph	0.51	-0.72	-1.12	-[(a)]	-[(a)]	0.611	0.063	-[(a)]	-[(a)]
C14	$(CH_3O)_3P=O$ - HS-Ph	0.18	-0.01	-1.1	-[(a)]	-[(a)]	0.712	0.034	-[(a)]	-[(a)]
C15	$(CH_3O)_3P=S$ - HO-Ph	0.49	-0.71	-0.64	-[(a)]	-[(a)]	0.629	0.032	-[(a)]	-[(a)]
C16	$(CH_3O)_3P=S$ - HS-Ph	0.15	0.02	-0.63	-[(a)]	-[(a)]	0.711	0.021	-[(a)]	-[(a)]
C17	$(CH_3O)_2(OH)P=O$ - HO-Ph	0.52	-0.74	-1.11	-0.98	0.53	0.608	0.058	0.038	0.614
C18	$(CH_3O)_2(OH)P=O$ - HS-Ph	0.18	-0.01	-1.1	-0.99	0.51	0.707	0.015	0.03	0.617
C19	$(CH_3O)_2(OH)P=S$ - HO-Ph	0.5	-0.74	-0.66	-0.99	0.53	0.617	0.031	0.062	0.597
C20	$(CH_3O)_2(OH)P=S$ - HS-Ph	0.16	0.01	-0.64	-0.99	0.51	0.714	0.002	0.05	0.597
C21	$(CH_3O)(OH)_2P=O$ - HO-Ph	0.52	-0.74	-1.11	-0.98	0.53	0.61	0.057	0.039	0.612
C22	$(CH_3O)(OH)_2P=O$ - HS-Ph	0.18	-0.01	-1.1	-0.99	0.51	0.708	0.013	0.031	0.614
C23	$(CH_3O)(OH)_2P=S$ - HO-Ph	0.5	-0.74	-0.65	-0.99	0.53	0.619	0.028	0.06	0.597
C24	$(CH_3O)(OH)_2P=S$ - HS-Ph	0.15	0.01	-0.63	-0.99	0.51	0.715	0.001	0.051	0.596

[(a)] parameter not present in this complex.

Table S-6. Geometric parameters of phosphate and thiophosphate complexes in vacuum.

#	Complex	geometric parameters						
		$d1$ Å	$\alpha1$ °	$d2$ Å	$\alpha2$ °	$\Delta r1^{(b)}$ Å	$\Delta r2^{(c)}$ Å	ϕ °
C13	$(CH_3O)_3P=O$ - HO-Ph	1.76	168	–[a]	–[a]	0.016	–[a]	-1.4
C14	$(CH_3O)_3P=O$ - HS-Ph	2.06	169	–[a]	–[a]	0.008	–[a]	-7.3
C15	$(CH_3O)_3P=S$ - HO-Ph	2.43	167	–[a]	–[a]	0.010	–[a]	4.5
C16	$(CH_3O)_3P=S$ - HS-Ph	2.76	171	–[a]	–[a]	0.004	–[a]	2.1
C17	$(CH_3O)_2(OH)P=O$ - HO-Ph	1.81	147	1.87	150	0.019	0.017	-1.2
C18	$(CH_3O)_2(OH)P=O$ - HS-Ph	2.23	140	2.38	157	0.006	0.015	-10.1
C19	$(CH_3O)_2(OH)P=S$ - HO-Ph	2.43	141	1.76	161	0.013	0.020	2.3
C20	$(CH_3O)_2(OH)P=S$ - HS-Ph	3.26	120	2.30	173	0.002	0.016	-34.3
C21	$(CH_3O)(OH)_2P=O$ - HO-Ph	1.83	146	1.87	149	0.018	0.018	0.0
C22	$(CH_3O)(OH)_2P=O$ - HS-Ph	2.27	138	2.37	157	0.005	0.015	-10.8
C23	$(CH_3O)(OH)_2P=S$ - HO-Ph	2.45	140	1.76	160	0.012	0.021	1.0
C24	$(CH_3O)(OH)_2P=S$ - HS-Ph	3.48	113	2.29	173	0.002	0.017	-35.2

[a] *parameter not present in this complex.*

[b]$\Delta r_1 = d(O\text{-}H)_{complex} - d(O\text{-}H)_{phenol}$ *or* $d(S\text{-}H)_{complex} - d(S\text{-}H)_{thiophenol}$, *respectively.* $[d(O\text{-}H)_{phenol} = 0.963$ Å; $d(S\text{-}H)_{thiophenol} = 1.347$ Å$]$.

[c]$\Delta r_2 = d(O\text{-}H)_{complex} - d(O\text{-}H)_{phosphate}$ $[d(O\text{-}H) = 0.964$ Å *in methylphosphate, methylthiophosphate and dimethylphosphate.* $d(O\text{-}H) = 0.965$ Å *in dimethylthiophosphate].*
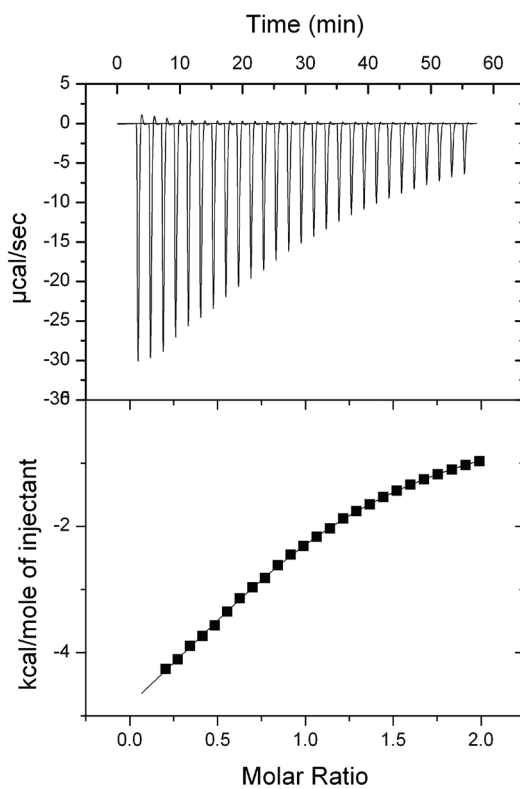
Figure S-2. ITC measurement of TOPO - PhOH in dry mesitylene (30°C).

Table S-7. Phosphate and thiophosphate complexes; charges and bond orders (B3LYP/6-311+G(d,p) in vacuum).

#	Complex	charges			bond orders			
		H	$P=O$ / $P=S$	$O-H$ H	$BO1$ $H\cdots O=P$	ΔBO $O-H$	$BO2$ $H\cdots O-H$	ΔBO $P-O-H$
C13	$(CH_3O)_3P=O$ - HO-Ph	0.51	-1.12	-[a]	0.063	-0.050	-[a]	-[a]
C14	$(CH_3O)_3P=O$ - HS-Ph	0.18	-1.10	-[a]	0.034	-0.012	-[a]	-[a]
C15	$(CH_3O)_3P=S$ - HO-Ph	0.49	-0.64	-[a]	0.032	-0.032	-[a]	-[a]
C16	$(CH_3O)_3P=S$ - HS-Ph	0.15	-0.63	-[a]	0.021	-0.013	-[a]	-[a]
C17	$(CH_3O)_2(OH)P=O$ - HO-Ph	0.52	-1.11	0.53	0.058	-0.053	0.038	-0.036
C18	$(CH_3O)_2(OH)P=O$ - HS-Ph	0.18	-1.10	0.51	0.015	-0.017	0.030	-0.033
C19	$(CH_3O)_2(OH)P=S$ - HO-Ph	0.50	-0.66	0.53	0.031	-0.044	0.062	-0.047
C20	$(CH_3O)_2(OH)P=S$ - HS-Ph	0.16	-0.64	0.51	0.002	-0.010	0.050	-0.047
C21	$(CH_3O)(OH)_2P=O$ - HO-Ph	0.52	-1.11	0.53	0.057	-0.051	0.039	-0.037
C22	$(CH_3O)(OH)_2P=O$ - HS-Ph	0.18	-1.10	0.51	0.013	-0.016	0.031	-0.035
C23	$(CH_3O)(OH)_2P=S$ - HO-Ph	0.50	-0.65	0.53	0.028	-0.042	0.060	-0.047
C24	$(CH_3O)(OH)_2P=S$ - HS-Ph	0.15	-0.63	0.51	0.001	-0.009	0.051	-0.048

[a] parameter not present in this complex.

Table S-8. ITC results of TOPO – PhOH measurements in dry mesitylene at 30 °C.

parameter	value
N	1.00 ± 0.01 [-]
K	1319 ± 50 [M^{-1}]
ΔH⁰	-7.27 ± 0.12 [kcal/mol]
ΔG⁰	-4.33 ± 0.02 [kcal/mol]
ΔS⁰	-9.72 ± 0.46 [cal/mol.K]
TΔS⁰	-2.95 ± 0.14 [kcal/mol]
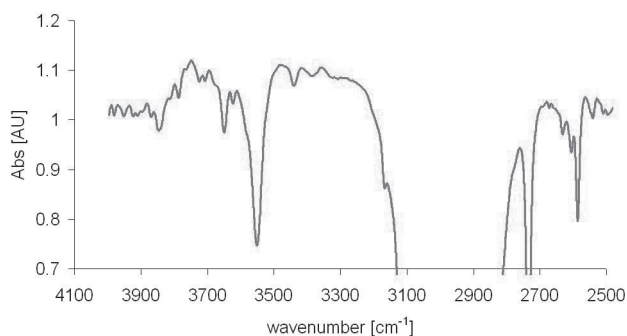
Figure S-3. IR result of 50 mM phenol in dry toluene. The presence of a narrow peak around 3550 cm^{-1} and the absence of a broad peak around 3000-3400 cm^{-1} indicate the absence of H-bonds. The broad peak from 2800-3150 cm^{-1} originates from toluene.

Table S-9. MMP and DMP dimer calculations

	B3LYP	MP2 -cp	MP2 +cp	SCS-MP2 -cp	SCS-MP2 +cp
MMP dimer	-23.95	-26.26	-19.91	-24.29	-18.09
MMP dimer - PhOH	-10.70	-15.18	-10.32	-13.59	-8.95
MMP dimer - 2PhOH	-21.61	-29.23	-19.87	-26.34	-17.43
MMP dimer - PhSH	-5.63	-11.02	-6.39	-9.40	-5.03
MMP dimer - 2PhSH	-11.99	-22.17	-13.61	-19.24	-11.11
DMP dimer	-24.18	-26.80	-20.30	-24.76	-18.42
DMP dimer - PhOH	-7.72	-12.69	-8.12	-11.37	-7.01
DMP dimer - 2PhOH	-15.39	-25.00	-16.19	-22.48	-14.07
DMP dimer - PhSH	-3.85	-8.56	-4.93	-7.42	-3.94
DMP dimer - 2PhSH	-7.18	-19.91	-11.14	-17.28	-8.92

Table S-10. Binding energies (kcal/mol) of phosphine oxide and phosphine sulfide complexes with phenol and thiophenol in various solvents (B3LYP/6-311+G(d,p)).

#	Complex	Cyclohexane	Toluene	Benzene
C1	$(C_2H_5)_3P{=}O$ - HO-Ph	-9.0	-9.0	-9.2
C2	$(C_2H_5)_3P{=}O$ - HS-Ph	-2.6	-2.6	-2.8
C3	$(C_2H_5)_3P{=}S$ - HO-Ph	-3.3	-3.2	-3.4
C4	$(C_2H_5)_3P{=}S$ - HS-Ph	+0.3	+0.4	+0.2
C5	$(C_2H_5)_2HP{=}O$ - HO-Ph	-8.9	-8.8	-9.0
C6	$(C_2H_5)_2HP{=}O$ - HS-Ph	-2.6	-2.6	-2.8
C7	$(C_2H_5)_2HP{=}S$ - HO-Ph	-3.1	-3.0	-3.3
C8	$(C_2H_5)_2HP{=}S$ - HS-Ph	+0.4	+0.4	+0.2
C9	$(C_2H_5)H_2P{=}O$ - HO-Ph	-8.3	-8.3	-8.5
C10	$(C_2H_5)H_2P{=}O$ - HS-Ph	-2.4	-2.4	-2.5
C11	$(C_2H_5)H_2P{=}S$ - HO-Ph	-2.7	-2.4	-2.6
C12	$(C_2H_5)H_2P{=}S$ - HS-Ph	+0.3	+0.3	+0.1
C13	$(CH_3O)_3P{=}O$ - HO-Ph	-6.8	-6.7	-6.9
C14	$(CH_3O)_3P{=}O$ - HS-Ph	-1.5	-1.3	-1.6
C15	$(CH_3O)_3P{=}S$ - HO-Ph	-1.7	-1.7	-1.9
C16	$(CH_3O)_3P{=}S$ - HS-Ph	+1.7	+1.4	+1.2
C17	$(CH_3O)_2(OH)P{=}O$ - HO-Ph	-8.1	-7.9	-8.1
C18	$(CH_3O)_2(OH)P{=}O$ - HS-Ph	-2.6	-2.5	-2.8
C19	$(CH_3O)_2(OH)P{=}S$ - HO-Ph	-6.2	-6.0	-6.2
C20	$(CH_3O)_2(OH)P{=}S$ - HS-Ph	-1.2	-1.1	-1.3
C21	$(CH_3O)(OH)_2P{=}O$ - HO-Ph	-8.1	-7.9	-8.1
C22	$(CH_3O)(OH)_2P{=}O$ - HS-Ph	-2.8	-2.7	-2.9
C23	$(CH_3O)(OH)_2P{=}S$ - HO-Ph	-6.4	-6.3	-6.5
C24	$(CH_3O)(OH)_2P{=}S$ - HS-Ph	-1.6	-1.6	-1.8

CHAPTER 4

Complexation of Phenol by Amine-N-oxides.
Isothermal Titration Calorimetry and *Ab Initio* Calculations.

Abstract

To develop a new solvent-impregnated resin (SIR) system for removal of phenols from water, the complex formation of dimethyldodecylamine-N-oxide (DMDAO), trioctylamine-N-oxide (TOAO) and tris-(2-ethylhexyl)amine-N-oxide (TEHAO) with phenol (PhOH) and thiophenol (PhSH) was studied. To this aim we used isothermal titration calorimetry (ITC) and quantum chemical modeling (on B3LYP/6-311G(d,p)-optimized geometries: B3LYP/6-311+G(d,p), B3LYP/6-311++G(2d,2p), MP2/6-311+G(d,p) and spin-component scaled (SCS) MP2/6-311+G(d,p); M06-2X/6-311+G(d,p)//M06-2X/6-311G(d,p), MP2 with an extrapolation to the complete basis set limit (MP2/CBS), as well as CBS-Q). The complexes were analyzed in terms of structural (e.g. bond lengths) and electronic elements (e.g. charges). Furthermore, complexation and solvent effects (in benzene, toluene and mesitylene) were investigated by ITC measurements, yielding binding constant (K), enthalpy (ΔH^0), Gibbs energy (ΔG^0) and entropy (ΔS^0) of complex formation, and stoichiometry (N). ITC measurements revealed strong 1 : 1 complex formation between both DMDAO – PhOH and TOAO – PhOH. The binding constants (K = 1.7 – 5.7$\cdot$10^4 M^{-1}) weakened markedly when water-saturated toluene was used (K = 5.8$\cdot$10^3 M^{-1}). $\pi\pi$-interaction with the solvent was shown to be relevant. QM modeling confirms formation of stable 1 : 1 complexes, yielding geometries with linear H-bonds that weaken upon attachment of electron-withdrawing groups to the amine-N-oxide moiety. Modeling also showed that complexes with PhSH are much weaker than with PhOH, and in fact too weak for ITC determination. CBS-Q incorrectly predicts equal or even higher binding enthalpies for PhSH than for PhOH, which invalidates it as a benchmark for other calculations. Data from the straightforward SCS-MP2 method without counterpoise correction show a very good agreement with the MP2/CBS values.

Introduction

Solvent-impregnated resins[1] (SIRs, Figure 1) are used as three-phase separation systems to isolate or concentrate dilute solutes from an aqueous phase. The SIR is a porous inert resin particle that contains a stationary organic liquid, impregnated in its pores. When a solute in an aqueous phase is brought into contact with a SIR, the solute will diffuse from the aqueous phase to the solvent phase. Ion-exchange SIRs are already widely used[2-5] to separate heavy metal ions from aqueous phases in a fast and simple way, making use of the solubility of the solute in the liquid organic phase, in exchange for protons. Only recently, investigations on other applications have been performed, e.g. the recovery of apolar organics.[6, 7] Bench-scale or pilot-scale recovery of polar organics like organic acids,[8, 9] amino acids[10] and flavonoids have also been realized.[11] In order to enhance extraction, complex-forming extractants can be added to the organic phase. Complex formation inside the organic solvent increases the overall equilibrium concentration of solute in the SIR, which significantly enhances the overall extraction capacity.

In principle, molecular recognition and complexation of the solute inside the SIR particles, as indicated in Figure 1, can provide a new and fast way to separate even rather polar organic solutes from aqueous streams on a kiloton/yr scale. For the effective removal of polar organic solutes, such as ethers and phenols in water-cleaning processes, the additional complexation step of the solute in the organic solvent phase turns out to be crucial for large-scale application, due to the relatively high solute solubility in water. A rational way of optimizing an extractant for these applications is by using molecular design. For this a thorough understanding of the complexation at the molecular level is required. Molecular modeling can facilitate this understanding by providing useful data about the complex formation that can be compared with those of experiments. In this paper we investigate a set of amine-N-oxide extractants for the extraction of phenol from an aqueous environment, to establish a basis for future industrial design. For the extraction of phenols, strong hydrogen bonds are desired for SIR-based processes. It was shown that complex-forming compounds containing a phosphoryl moiety are suitable extractants.[7, 12] However, Torgov et al.[13-15] indicated that amine-N-oxides would likely be even better for phenol recovery, which prompted this study with amine-N-oxides as potential candidates that can form hydrogen-bonding complexes. For example, an investigation[15] of the removal of low concentrations of phenol (10 – 100 mg/L) from sodium sulfate solutions (0.25 – 0.4 M) with trioctylamine-N-oxide (TOAO) dissolved in toluene (0.25 – 0.4 M), yielded distribution coefficients K_D ([Phenol]$_{org}$/ [Phenol]$_{water}$) of 1100 to 3300.
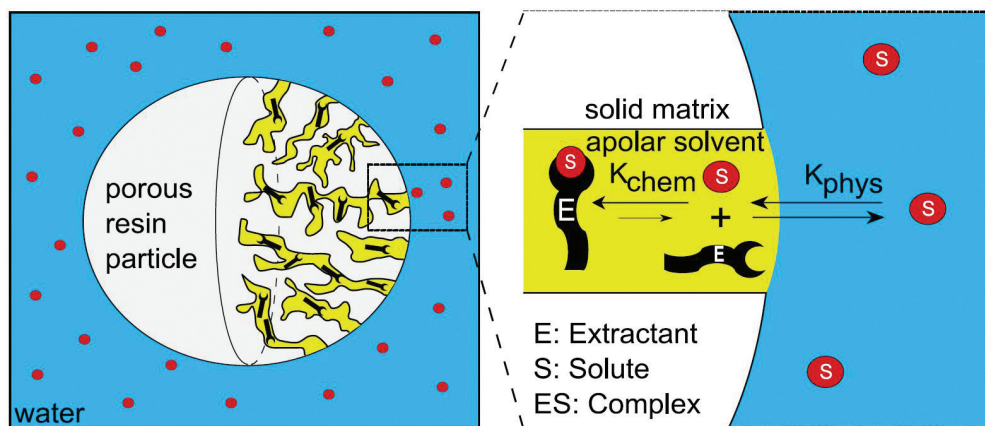
Figure 1. Principle of solute extraction with a Solvent-Impregnated Resin (SIR) with an active extractant in the pores.

Alkylated amine-N-oxides nicely combine a low solubility in water with a high negative charge on the oxygen atom, which is favorable for a hydrogen bond acceptor. The most important hydrogen bond characteristics to be explored in the current study are the hydrogen bond strength and the geometry of the resulting complexes. From literature, neutral O–H•••O hydrogen bonds are expected to have a strength of 4 - 15 kcal/mol,[16, 17] covering a range of H-bond lengths and O–H•••O angles,[18, 19] as these parameters depend strongly on the molecular geometry of the system at hand. Hydrogen bonds between charged donor or acceptor atoms are usually significantly stronger, with typical ΔH^0 values of about -15 - -40 kcal/mol.[16, 17] For amine-N-oxide H-bonds a binding strength in the range of 10 - 15 kcal/mol is expected. Recent computational studies show that accurate geometric information is required to make meaningful predictions.[20]

In this paper, the interaction between the phenols and the extractants is experimentally investigated in detail by isothermal titration calorimetry (ITC) binding experiments. Although some information about hydrogen bonding of phenols to amine-N-oxides is already available,[6, 13-15] this information was obtained indirectly from IR measurements and from liquid-liquid extraction experiments. The current paper presents the measured binding affinities, full thermodynamic description (stoichiometry, K, ΔH^0, ΔG^0, ΔS^0) and a preliminary investigation of solvent effects. This is complemented by the theoretical investigations *in vacuo*. In addition, we report for the first time intrinsic complexation constants, which are obtained in water-free and water-saturated organic solvents, in order to quantify the expected inhibiting effect of an aqueous environment as this is relevant for industrial purposes.

ITC[21-25] measurements can be used to directly obtain the equilibrium constant (K), stoichiometry (N) and enthalpy of complex formation (ΔH^0) in complexation reactions, and the change in entropy (ΔS^0) and free energy (ΔG^0) can be calculated from those values. Although ITC measurements are usually carried out in aqueous solutions,[26, 27] its use is also unproblematic with co-solvents like methanol or DMSO,[28] or with organic solvents like chloroform,[29, 30] toluene[7, 29, 31, 32] and others.[33] Benzene, toluene and mesitylene were used as apolar model solvents. For toluene, a relatively small influence on hydrogen bonding interactions has been reported.[29, 34, 35]

Table 1. Model amine-N-oxide compounds used in the quantum chemical calculations and geometric parameters describing the H-bond geometry.[a]

Compound	Molecular formula	Structure
trimethylamine-N-oxide	$(CH_3)_3N^+\text{-}O^-$	
dimethylethylamine-N-oxide	$(CH_3)_2(C_2H_5)N^+\text{-}O^-$	
triethylamine-N-oxide	$(C_2H_5)_3N^+\text{-}O^-$	
tri(trifluoromethyl)amine-N-oxide	$(CF_3)_3N^+\text{-}O^-$	
pyridine-N-oxide	$C_5H_5N^+\text{-}O^-$	

[a] Definitions analogous for thiophenol (PhSH).

For the development of a SIR extraction set-up for the removal of phenols from aqueous systems, these hydrogen-bonding interactions are of vital importance. The present paper discusses these factors, yielding an optimal candidate by using ITC measurements in combination with quantum chemical theoretical methods. A range of different methods (B3LYP/6-311+G(d,p)// B3LYP/6-311G(d,p), M06-2X/6-311+G(d,p)//M06-2X/6-311G(d,p), MP2/6-311+G(d,p)//B3LYP/6-311G(d,p), MP2/6-311++G(2d,2p)//B3LYP/6-311G(d,p), spin component-scaled (SCS) MP2 using the same basis sets, with and without counterpoise (CP) corrections, and a complete basis set extrapolation (MP2/CBS) method) were applied to the model compounds depicted in Table 1. Since analysis of a small data set of hydrogen-bonded complexes suggested that the M06 set of density functionals might perform somewhat better in describing hydrogen-bonding interactions,[36] M06-2X/6-311+G(d,p)//M06-2X/6-311G(d,p)[37, 38] calculations were also performed. Finally, the composite CBS-Q method, a complete basis set method of Petersson and coworkers to obtain very accurate energies,[39] was used to obtain an absolute benchmark for the energy values. The different methods were chosen to diminish the chance of finding highly method-

dependent results. In recent papers, SCS-MP2 methods, which use the default scaling factors of 6/5 for anti-parallel spins and 1/3 for parallel spins, showed a dramatic increase in accuracy over normal MP2 energies, providing a more balanced description of many systems,[40-43] and sometimes even reaching QCISD or QCISD(T) quality data.[44] Since the application of SCS-MP2 on the stability of H-bonding is relatively unexplored, its performance is therefore described in detail here. The results from the latter method are compared to those of benchmark MP2/CBS method.

Experimental Section

General. The following materials were used as received without further purification: toluene (Riedel de Haan, puriss.), trioctylamine (Aldrich, 98%), hydrogen peroxide (Chemlab, 35% w/w), acetic acid (Fisher, p.a.), phenol (Merck, p.a.), thiophenol (Janssen Chimica, 97%), dimethyl-dodecylamine-N-oxide (Fluka, 98%), tris-2-ethylhexylamine (Fluka, 97%), ethyl acetate (Baker, >99.5%), methanol (Fisher, p.a.), mesitylene (Aldrich, p.a.), cyclohexane (Acros, >99%), benzene (Fluka, ≥99.5 %). Molecular sieves (3 Å, Aldrich) were used as received.

Synthesis of trioctylamine-N-oxide (TOAO). Trioctylamine-N-oxide was synthesized by N-oxidation of trioctylamine according to a modification of the methods of Ejaz and Davis.[53, 54] Oxidation was accomplished with hydrogen peroxide using the following procedure: 8.46 g 35% hydrogen peroxide (87.0 mmol) was added to a solution of 8.2 g of trioctylamine (23.1 mmol) in 50 mL acetic acid. The mixture was stirred at 25 °C for approximately 120 h. Ice-cold water (100 mL) was then added, followed by the addition of chilled NaOH solution until near neutralization of the acetic acid. The white solid that separated after addition of the NaOH solution was filtered on a Büchner funnel, washed repeatedly with ice-cold water and ice-cold hexane, and then recrystallized from hexane. Yield: 7.54 g (20.4 mmol, 88%). The absence of traces of trioctylamine in the final product was checked by thin-layer chromatography (Al_2O_3) with EtOAc : MeOH 19 : 1. TOAO was stored in a vacuo desiccator over NaOH.

^{1}H-NMR (400 MHz): δ ($CDCl_3$): 0.84-0.89 (t, 9H); 1.20-1.35 (m, 30 H); 1.70-1.80 (m, 6H); 3.04-3.09 (m, 6H) ppm. ^{13}C-NMR (100,6 MHz): δ ($CDCl_3$): 65.1; 31.7; 29.2; 29.0; 26.6; 22.9; 22.6; 14.0 ppm.

Synthesis of tris-(2-ethylhexyl)amine-N-oxide (TEHAO). A similar procedure was used as for the synthesis of TOAO, but column chromatography (neutral silica column; EtOAc/MeOH 39 : 1) was used rather than recrystallization. Yield: >80%; liquid. The absence of traces of tris-(2-ethylhexyl)-

amine in the final product was checked by thin-layer chromatography (Al_2O_3) with EtOAc/MeOH 19 : 1.

^{1}H-NMR (400 MHz): δ (CDCl$_3$): 0.80-0.95 (m, 18H); 1.15-1.40 (m, 24 H); 1.40-1.60 (m, 3H); 2.49 (d, 6H) ppm. ^{13}C-NMR (100,6 MHz): δ (CDCl$_3$): 52.9; 38.5; 31.3; 28.9; 24,1; 23.3; 14.1; 10.2 ppm.

Isothermal Titration Calorimetry (ITC). Isothermal Titration Calorimetry (ITC) was performed using a MicroCal VP-ITC microcalorimeter, and the setup was described elsewhere.[55] The results were analyzed using Origin 7SR2 V7.0383 (B383) software (Origin Lab Corporation). The measuring cell (1.46 mL) was flushed and filled with a freshly prepared and degassed solution of phenol or thiophenol in one of the solvents mesitylene, toluene or benzene. The 280 μL automatic syringe was flushed and filled with a freshly prepared and degassed solution of the complexing agent (amine oxide) in the same solvent, at a concentration of roughly 10 times the molarity of the cell solution. The number of injections and the injected volume per injection were optimized depending on the concentration of the solutions and the magnitude of the heat effect per second. Between subsequent injections a sufficient amount of time (usually 180 to 300 seconds) was chosen to allow for the cell feedback to return to the baseline. The stirring speed for all ITC measurements was 502 rpm (default value). A reference measurement was performed using the same procedure by taking only the solvent, not the solute, in the measuring cell. By subtracting the data of the reference measurement from those of the actual measurement the net results were obtained and they were fitted using the one-set-of-sites model implemented in the Origin software.

Molecular Modeling. Computational data of the compounds depicted in Table 1 were obtained using Gaussian03, Revision C.2,[56] and Gaussian09, Revision A.1.[57] The geometries of the monomers and complexes are optimized at the B3LYP/6-311G(d,p) and M062X/6-311G(d,p) level of theory, which generally describes the geometries of these systems well.[18, 20, 37, 38, 58] All B3LYP/6-311G(d,p)-optimized stationary points were confirmed as true minima via vibrational frequency calculations. The B3LYP/6-311+G(d,p) method and the MP2 and SCS-MP2 methods both with the small (6-311+G(d,p)) basis set were chosen to ensure that the conclusions are not influenced by significant method-dependent phenomena. With such basis sets both B3LYP and MP2 typically provide accurate (within 2 kcal/mol) interaction energies for H-bonding, while MP2 calculations with bigger basis sets are typically even more accurate.[58-61] An extrapolation to the complete basis set (CBS) energy limit was obtained using the keyword 'cbsextrapolate'.[62] The option "NMin=10"

was specified to account for a minimum of 10 pair natural orbitals for extrapolation to the CBS limit. Counterpoise (CP) correction[63, 64] was applied for all MP2 and SCS-MP2 calculations to correct for over-stabilization due to the supermolecule approach. Given the large size of an extrapolation to the complete basis set, no CP-correction was applied to the MP2/CBS energies. The B3LYP-derived geometries were taken as input structures for the CBS-Q method, which is known to provide very accurate energy data. The CBS-Q method consists of several different steps, described elsewhere.[39] All CBS-Q structures were confirmed to be true minima in the vibrational frequency analysis that is part of the composite method. The CBS-Q energy at 0 K was used for the presented results. Total energies are given in Table S-4.

Although analysis of a small data set of hydrogen-bonded complexes suggests that other density functionals might perform somewhat better in describing hydrogen-bonding interactions[36] no detailed analysis has been presented in literature that includes a series of amine-N-oxides, and therefore the M06 functional was also used along with the widely used B3LYP functional to compare the results.

Finally, since electrostatic interactions are crucial in determining the strength of H-bonds,[17, 65-68] natural population analysis (NPA)[69, 70] was performed as part of the calculations. As the latter analysis exhibits a relatively small method dependence and basis set dependence, it has been proven to be a reliable charge indicator for related theoretical studies of H-bonds. In addition, atom-atom overlap-weighted natural atomic orbital (NAO) bond orders were obtained.

The model compounds (Table 1) resemble the compounds used in ITC (dimethyldodecylamine-N-oxide (DMDAO), trioctylamine-N-oxide (TOAO) and tris-(2-ethylhexyl)amine-N-oxide (TEHAO)). However, in the latter compounds, the long alkyl tails were replaced by methyl or ethyl groups in order to reduce the computational time as the primary interaction between the complex fragments was not affected by doing so. To get some insight into the influence of electron-withdrawing groups on the complex formation of amine-N-oxides with phenol and thiophenol the complexation behavior was also investigated using tri(trifluoromethyl)amine-N-oxide and pyridine-N-oxide. In Table 1 the different relevant geometrical parameters for hydrogen bonds in the investigated complexes are defined.

Results and Discussion

Isothermal titration calorimetry. An example of a calorimetric titration of phenol with dimethyldodecylamine-N-oxide (DMDAO) in dry toluene at 30 °C is given in Figure 2. The isotherm shows a clear sigmoid curve, indicating a strong binding. By integrating the binding isotherm (top panel), the binding curve is obtained (bottom panel). Fitting yields the stoichiometry (N), binding enthalpy (ΔH^0) and the binding affinity (K) (see Table 2). The binding of DMDAO with phenol is exothermic, with $\Delta H^0 = -7.3$ kcal/mol and $K = 2.8 \cdot 10^4$ M^{-1}. The molar ratio of DMDAO/ phenol was 1.04 at the equivalence point, indicating the formation of a 1 : 1 H-bonded complex without other effects that interfere with direct binding of phenol to DMDAO (Figure 3 A). Similar 1 : 1 stoichiometry was observed for the other complexes under study. The entropy factor $T\Delta S^0$ is negative, indicating an overall increased order upon binding, and showing an enthalpy-driven hydrogen bond complex formation.[22]

In the calorimetric titration of phenol with DMDAO in water-saturated toluene the binding enthalpy ($\Delta H^0 = -7.1$ kcal/mol) is marginally less negative than in dry toluene ($\Delta H^0 = -7.3$ kcal/ mol), but the binding affinity is markedly lower ($K = 5.8 \cdot 10^3$ M^{-1} vs. $K = 2.8 \cdot 10^4$ M^{-1} in dry toluene). This influence of water on the complex-forming behavior is likely caused by entropic complex-ordering effects of water molecules, as can be seen from the different change in entropy. These water molecules (at 30 °C [H_2O] in water-saturated toluene = 28 mM;[7] [amine-oxide] is typically 10-20 mM) will preferably be present near the most polar positions in the molecules, i.e. near the N^+-O^- moiety in amine-N-oxides and near the O–H/S–H moieties in phenol and thiophenol, respectively.
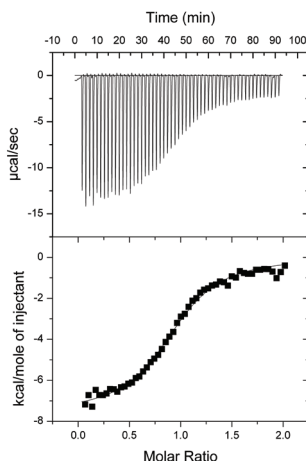

Figure 2. Calorimetric titration of phenol with DMDAO in dry toluene at 30 °C. Top panel: raw data; bottom panel: peak integration data and fitted curve.

Table 2. Thermodynamic parameters derived from the ITC experiments at 30 °C.

Complex	N	K	ΔH⁰	ΔG⁰	TΔS⁰
	(-)	(M⁻¹)	(kcal/mol)	(kcal/mol)	(kcal/mol)
DMDAO-PhOH[a]	1.04 ± 0.07	(2.8 ± 0.5)·10⁴	-7.3 ± 0.4	-6.2 ± 0.1	-1.1 ± 0.4
DMDAO-PhOH[b]	0.98 ± 0.06	(5.8 ± 2.3)·10³	-7.1 ± 1.2	-5.4 ± 0.3	-2.4 ± 1.4
TOAO-PhOH[a]	1.14 ± 0.12	(2.3 ± 1.1)·10⁴	-4.7 ± 1.4	-6.0 ± 0.3	1.3 ± 1.2
TOAO-PhOH[b]	1.19 ± 0.15	(5.8 ± 2.6)·10³	-2.9 ± 1.0	-5.1 ± 0.4	2.2 ± 0.4

[a] In dry toluene. [b] In water-saturated toluene.

Multiple water molecules[45] will be replaced upon phenol binding, and this water, which is freed from every amine-N-oxide and phenol molecule, will form larger water clusters in the apolar solvent and will on average become more structured, even if it remains weakly attached to the amine-N-oxide – phenol complex as a H-bonded large cluster (Figure 3 C). This will likely cause a more negative entropic effect. In accordance with that, upon phenol binding the $T\Delta S^0$ value in the presence of water is more negative than without the presence of water and the ΔH^0 value is nearly the same with or without the presence of water.

In the calorimetric titration of phenol with trioctylamine-N-oxide (TOAO, Figure 3B) in dry toluene again 1 : 1 complexation is observed, with a binding affinity slightly lower than for DMDAO (K = 2.3·10⁴ M⁻¹ *vs.* 2.8·10⁴ M⁻¹ for DMDAO). In addition, ΔH^0 is markedly less negative (ΔH^0 = -4.7 kcal/mol vs -7.3 kcal/mol for DMDAO). This effect could be explained by a slight dimerization of the TOAO molecules, much like is the case for phosphine oxide molecules.[46] Via B3LYP-based calculations, it was shown that indeed dimers of amine-N-oxides can be formed, both for head-to-head and for head-to-tail dimers (head-to-head dimers tend to be more stable than head-to-tail dimers, see Supp. Info, Figure S-1). The presence of three alkyl tails per molecule yields favorable Van der Waals interactions between two TOAO molecules when they are near one another. A micelle-like dimer of two TOAO molecules can be formed, and the breaking up of the apparent dimer and the subsequent binding of a phenol molecule to both TOAO molecules will lead to an overall lower binding enthalpy than what was found for the DMDAO – phenol complex, where these mutual Van der Waals interactions will be weaker because only one long alkyl tail is present. Moreover, we find an entropic effect that is positive ($T\Delta S^0$ = +1.3 kcal/mol), indicating an overall higher degree of freedom after phenol binding, that can be partly attributed to increased disorder in the alkyl chains.

The TOAO – phenol complex in water-saturated toluene (Figure 3D) shows a markedly lower binding affinity (K = $5.8 \cdot 10^3$ M^{-1} vs. $2.3 \cdot 10^4$ M^{-1} in water-free toluene) and less negative ΔH^0 (ΔH^0 = -2.9 kcal/mol vs -4.7 kcal/mol in water-free toluene). This effect is much larger than for the DMDAO – phenol complex. Due to the apparent dimer formation of TOAO and the presence of water near the N$^+$-O$^-$ moiety the replacement of water by phenol is more difficult. In TOAO – phenol complexation in water-saturated toluene, TΔS^0 is positive (+2.2 kcal/mol), and more positive than for water-free toluene, indicating a less ordered situation upon phenol binding. In line with Figure 3B dimer formation of TOAO yields rather structured H$_2$O clusters. If the dimer is broken by addition of phenol, then TOAO-phenol-water complexes are formed, in which the water is bound with more conformational freedom, implying a $\Delta S > 0$. Hydrophobic interactions could further play a stabilizing role here.[47]
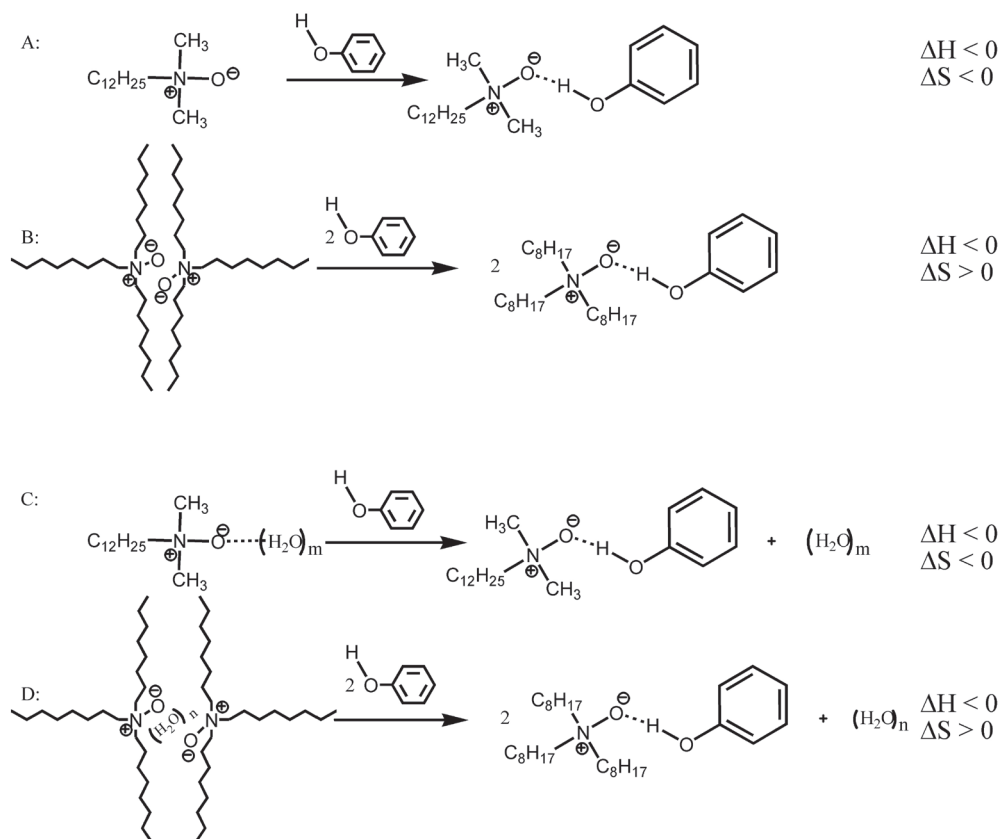

Figure 3. Representation of the proposed complex formation in dry toluene (A and B), and water-saturated toluene (C and D).

The aggregation number of water will depend on the concentration, the chemical environment, and the temperature. Unfortunately, the interaction of water with amine-N-oxides or the mutual interaction of the amine-N-oxides could not be quantified separately by ITC due to the very low heat effect. ITC measurements of the interactions between the extractants and thiophenol also gave only very weak heat effects, making it impossible to accurately quantify any of the thermodynamic parameters.

The ITC titration of phenol with tris-(2-ethylhexyl)amine-N-oxide (TEHAO) in dry toluene (cf. Supp Info, Figure S-2) shows a binding isotherm which is markedly different from that observed for the other amine-N-oxide – phenol interactions. It shows a binding behavior characterized by a low exothermic heat effect (ΔH^0 = -0.5 – -1 kcal/mol), a low binding affinity (absence of a sigmoid curve; K ≈ 300 – 600 M^{-1}) and a large scatter, implying that little phenol binding takes place with TEHAO, likely due to the steric hindrance posed by the three ethyl chains at the 2-position of the hexyl tails.

Modeling. As can be seen from the structures of the complexes (Figure 4 and the Supp Info, Figure S-3), optimized by molecular modeling, the H-bonds of phenol or thiophenol to the N$^+$-O$^-$ moiety are all formed approximately along the O–H / S–H bond, thus forming nearly linear H-bond geometries. In the dimethylethylamine-N-oxide (DMEAO) – phenol complex (a model complex for the experimentally used dimethyl-dodecylamine-N-oxide comples, see complex **C1**, Figure 4A) the H-bond length is short (d = 1.62 Å, cf. Supp Info, Table S-1) and the bond angle is almost linear (α = 169°). In addition, the bond lengthening of the hydrogen bond donor and acceptor are quite substantial (Δr_1 = 0.022 Å; Δr_2 = 0.043 Å) and the dihedral angle of the phenol is close to zero (ϕ = -1.2°), which are all indicative parameters for strong hydrogen bonds.[7]
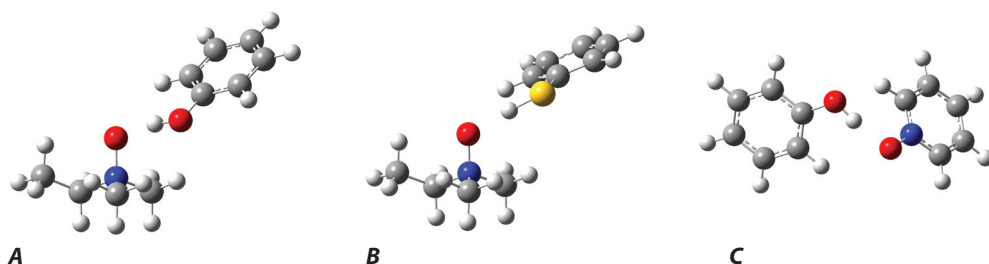

A   B   C

Figure 4: Optimized structures (B3LYP/6-311G(d,p)) of some selected amine-N-oxide – phenol complexes A) DMEAO – phenol, B) DMEAO – thiophenol and C) PNO – phenol.

Enthalpies of complexation for some selected amine-N-oxide complexes are summarized in Table 3 (for ΔH of all investigated amine-N-oxides, see Table S-2 in the Supp. Info). The enthalpy of complex formation ΔH (*in vacuo*) in complex **C1** is found to be -18.4 kcal/mol at the elaborate MP2/CBS level that is considered to be accurate. The CP-corrected MP2/6-311++G(2d,2p) method provides a reasonable estimate (ΔH =-16.3 kcal/mol), whereas B3LYP (*vacuo*) shows only a qualitative agreement (ΔH = -14.7 kcal/mol).

The CP-uncorrected MP2 values all show more negative values than the MP2/CBS value, due to the basis set superposition error (BSSE). SCS-MP2 values are all less negative than the MP2/CBS value, but typically agree with the MP2/CBS value to within one kcal/mol, an observation also made for phosphine oxide – phenol and phosphate – phenol complexes and their thio-analogs.[48] With counterpoise correction, the agreement of both methods with the MP2/CBS method becomes worse. Interestingly, all CP-corrected MP2 values deviate more from MP2/CBS than the CP-uncorrected MP2 values, suggesting that counterpoise correction overcorrects the BSSE. The binding affinities and geometric and electronic parameters of the complexes of phenol and thiophenol with the two other alkylamine-N-oxides (trimethylamine-N-oxide (TMAO) and tri-ethylamine-N-oxide (TEAO)), that were investigated for the direct comparison to experiment that makes use of amine-N-oxides with longer alkyl tails, were found to be almost equal to the ones found for DMEAO complexes, and are therefore only given in the Supporting Information (Tables S-1 and S-2). The binding enthalpies ΔH are found to be a little more negative (all within ~1 kcal/mol) for the more highly substituted complexes, which have a slightly higher electron donor capacity.

Table 3. Enthalpy of complexation ΔH (kcal/mol) of the amine-N-oxide complexes with phenol and thio-phenol (B3LYP/6-311G(d,p)-optimized geometries) in vacuo.

		ΔH											
		B3LYP[a]	MP2				SCS-MP2				MP2/CBS	M06-2X[e]	CBS-Q
			Small[b]		Large[c]		Small[b]		Large[c]				
#	Complex	-CP[d]	-CP	+CP	-CP	+CP	-CP	+CP	-CP	+CP		-CP	
C1	$(C_2H_5)(CH_3)_2N^+-O^-$ - HO-Ph	-14.7	-18.9	-15.1	-19.0	-16.3	-17.4	-13.8	-17.3	-14.6	-18.4	-19.3	-13.7
C2	$(C_2H_5)(CH_3)_2N^+-O^-$ - HS-Ph	-8.2	-12.7	-9.1	-12.6	-10.2	-11.1	-7.6	-10.8	-8.4	-12.4	-13.4	-13.6
C3	$C_5H_5N^+-O^-$ - HO-Ph	-9.8	-12.1	-9.0	-12.4	-10.2	-11.2	-8.2	-11.4	-9.1	-11.8	-13.5	-10.7
C4	$C_5H_5N^+-O^-$ - HS-Ph	-5.1	-9.3	-5.8	-9.0	-6.8	-8.1	-4.8	-7.7	-5.6	-8.8	-9.6	-12.1
C5	$(CF_3)_3N^+-O^-$ - HO-Ph	-6.4	-12.0	-7.5	-11.8	-8.5	-10.9	-6.6	-10.8	-7.4	-11.4	-10.5	-9.5
C6	$(CF_3)_3N^+-O^-$ - HS-Ph	-3.3	-8.8	-4.7	-8.2	-5.4	-7.7	-3.9	-7.2	-4.4	-8.0	-7.6	-11.8

[a] B3LYP/6-311+G(d,p). [b] 6-311+G(d,p). [c] 6-311++G(2d,2p). [d] CP = a posteriori counterpoise correction. [e] M06-2X/6-311+G(d,p)//M06-2X/6-311G(d,p).

The B3LYP-derived natural population analysis (NPA) charges on the oxygen of the amine-N-oxides and the hydrogen of the phenol O–H moiety were found to be -0.7 and +0.5, respectively, and these values did not change significantly from one method (B3LYP, M06-2X, …) to the other. These charges indicate a strong electrostatic tendency to form H-bonds (Supp. Info, Table S-1).[7, 17, 48] Next to the dominant electrostatics, some covalent character is also present, as can be deduced from the atom-atom overlap-weighted NAO bond orders (cf. Supp. Info Table S-3). For example, the bond order between the DMEAO oxygen and the phenol hydrogen amounts to 0.13 in the optimized geometry. The O–H bond order is 0.57, i.e. 0.09 lower than in uncomplexed phenol. These data point to strong complex formation, even stronger than was seen before in phosphine oxide – phenol H-bonds, in which a H-bond order of maximum 0.08 and an O–H bond order decrease of only 0.06 were found.[7, 48]

Thiophenol complexes differ in several aspects from phenol complexes as also seen in the ITC measurements. Binding enthalpies of thiophenol complexes are much less negative than of phenol complexes. For thiophenol complexes, ΔH is on average ca. 6 kcal/mol (MP2/CBS) less negative than of phenol complexes; H-bond lengths d are found to be longer for thiophenol complexes than for phenol complexes ($d = 1.8$ Å vs. $d = 1.6$ Å for phenol complexes, cf. Supporting Information, Table S-2), and donor and acceptor bond length increases Δr_1 and Δr_2 are both markedly smaller than for phenol complexes. Also, the dihedral angle ϕ of the thiophenols with respect to the benzene ring was found to deviate from the optimal angle of 0°, whereas ϕ of the phenols was always found to be close to 0°. This can be understood from the energy barriers of rotation around the C–O/C–S bond. For phenol, the energy barriers ($E_{O-H \text{ at } 90°}$ - $E_{O-H \text{ at } 0°}$ angle with respect to the plane of the benzene ring) are calculated to be 3.5 and 3.0 kcal/mol (B3LYP/6-311+G(d,p) and MP2/6-311+G(d,p), respectively). For thiophenol, the corresponding calculated values are 0.7 and 0.4 kcal/mol, respectively, meaning that the rotation in a thio-phenol complex is nearly free. Therefore, large dihedral angles are more often observed if this is otherwise attractive in the complex, which apparently is the case here. The charge on the thio-phenol hydrogen atom is +0.2, which is significantly less than of the phenol hydrogen atom (+0.5). For thiophenol, the bond order of the H-bond is lower than for the phenol complexes (0.10 for DMEAO – thiophenol vs. 0.13 for DMEAO – phenol, *vide supra*). Clearly, all these data agree with the much lower binding energies found for the thiophenol complexes.

The theoretical findings show that a strong 1 : 1 hydrogen-bonded complex is formed between amine-N-oxides and phenol, in line with the ITC results (high K, highly negative ΔH^0 and ΔG^0 values, and N = 1) obtained in toluene as a solvent. To study the influence of the solvent in slightly more detail, we also performed preliminary investigations of the solvent effects on the complex formation, using mesitylene, toluene, and benzene as model solvents for the apolar phase in SIRs (Table 4).

ITC experiments for the DMDAO – phenol complex yield a value of ΔH^0 = -7.8 kcal/mol in benzene, and slight less negative values in toluene en mesitylene (-7.3 and -5.6 kcal/mol, respectively, Table 4). As can be seen, this trend is opposite to the trend followed by the measured K-values: in benzene, toluene and mesitylene K-values of $1.7 \cdot 10^4$ M^{-1}, $2.8 \cdot 10^4$ M^{-1} and $5.7 \cdot 10^4$ M^{-1} were observed, respectively. This disparity upon increasing methyl substitution of the aromatic solvent points to significant entropic effects, in line with the discussion mentioned above. While a full discussion based on additional experiments and computations involving solvents fall outside the scope of this study and will be published elsewhere, a factor of importance is likely the $\pi\pi$ interaction between phenol and the solvent.

Table 4. All thermodynamic parameters (in kcal/mol) for DMDAO -phenol complexes in various solvents, obtained by ITC.[a]

Parameter	Mesitylene	Toluene	Benzene
N (-)	0.85 ± 0.03	1.04 ± 0.07	0.87 ± 0.02
K (M^{-1})	(5.7 ± 1.8)$\cdot 10^4$	(2.8 ± 0.5)$\cdot 10^4$	(1.7 ± 0.2)$\cdot 10^4$
ΔH^0	-5.6 ± 0.5	-7.3 ± 0.4	-7.8 ± 0.3
$T\Delta S^0$	-1.0 ± 0.6	1.1 ± 0.4	2.0 ± 0.3
ΔG^0	-6.6 ± 0.2	-6.2 ± 0.1	-5.9 ± 0.1

[a] All solvents were dried before use.

The CBS-Q results, initially added for the sake of having highly accurate values for comparison of the other methods used here, are found to be in disagreement with the results obtained by these other calculation methods at all. In the CBS-Q calculations some of the amine-N-oxide – thiophenol complexes show nearly equal or more negative binding enthalpies than the corresponding amine-N-oxide – phenol complexes (compare TEAO - phenol and TEAO - thiophenol

with ΔH values of -15.7 and -16.5 kcal/mol, respectively (see also Table S-2 Supp. Info.). However, experimental data from this and previous work[7] clearly show that phenol uniformly yields stronger H-bonds than thiophenol (binding constant K is higher for phenol by typically 1 - 2 orders of magnitude). These experimental observations are in line with generally observed differences in binding enthalpies for O•••H–O and O•••H– S H-bonds.[49] This erroneous prediction by CBS-Q can have two possible causes: a) use of correct energy calculations on incorrect geometries, or b) use of incorrect energy calculations on correct geometries. Close inspection of the MP2(FC)/6-31G(d') geometries resulting from the CBS-calculations showed only minor differences with the geometries found in the B3LYP optimization, and single-point energy recalculation of the resulting CBS-Q geometries with MP2/6-311++G(2d,2p) yielded energies within 1 kcal/mol of what was obtained on the B3LYP-optimized geometries. Therefore, option b) (incorrect energy calculation on correct geometries) is most likely. Since no systematic errors have been reported for the computations of oxygen-containing H-bonds using model chemistries like CBS-Q, this indicates that the CBS-Q values for sulphur compounds contain a systematic error as was also found previously on H-bonds between phenol/thiophenol and another class of compounds.[48] A closer investigation of the energy values obtained by the CBS-Q series of results revealed that the first steps (up to the MP4SDQ contributions) were in accordance with expected binding energies, while the erroneous output of the CBS-Q method is in fact produced in the last modeling step (CBS extrapolation within the CBS-Q method), which may be related to the size the of the basis sets from which is extrapolated to infinity. As a result, and to our surprise, CBS-Q is not useful as a benchmark method in this case.

The effects of electron-withdrawing groups (EWG) on the complex forming ability of amine-N-oxides were investigated in order to possibly fine-tune the complexation behavior in future applications. Both pyridine-N-oxide (PNO; complexes **C3** and **C4**) and tri(trifluoromethyl)amine-N-oxide (TTFMAO; complexes **C5** and **C6**) show lower phenol binding enthalpy values than the alkylamine-N-oxides for all levels of theory (Table 3). In accordance with this, the H-bond lengths are found to be longer than for the alkylamine-N-oxide complexes (Supp. Info., Table S-1). This can be explained by a reduction of the negative charge on the amine-N-oxide oxygen atoms on both PNO and TTFMAO (-0.6 vs. -0.7 in alkylamine-N-oxide), and by the much lower H•••O bond order (0.05 for TTFMAO and 0.07 for PNO vs. 0.13 for the alkylamine-N-oxide – phenol complexes; see for more extensive data sets the Supp. Info, Tables S-1 through S-3).

An interesting linear correlation can be observed when the binding enthalpy -ΔH (*in vacuo*, MP2/CBS) of the ten investigated complexes (TMAO, EDMAO, TEAO, PNO and TTFMAO with both phenol and thiophenol) is plotted against the N–O bond lengthening (Δr_1) (Figure 5A). The linear correlation parameters are indicated in the plot and show good correlation for both the alkyl-substituted and the EWG-substituted amine-N-oxides. A much higher slope was found for alkyl-amine-N-oxides than for the EWG-amine-N-oxide molecules, indicating a much more rigid N–O bond for the former amine-N-oxides. A plot of the binding enthalpy -ΔH of these ten complexes against the O–H/S–H bond lengthening in the phenol or thiophenol (Δr_2) (Figure 5B) is also linear, and confirms that, while complexes are much weaker for thiophenol than for phenol, S–H bond lengthening is more easily accomplished than O–H bond lengthening.

A   **B**
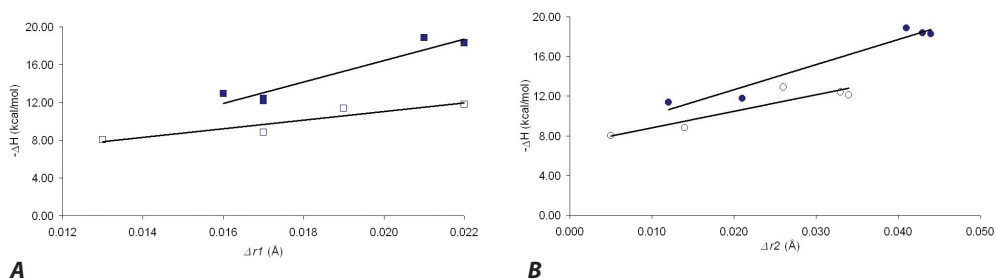
Figure 5. Dependence of the binding enthalpy -ΔH on N–O bond lengthening Δr_1 for alkyl-substituted and electron-withdrawing group-substituted amine-N-oxides (A) and on O–H / S–H bond lengthening Δr_2 for complexes with phenol and with thiophenol (B). Depicted are data obtained with MP2(CBS)// B3LYP/6-311G(d,p) for all ten AO-(thio)phenol complexes.

(a)■ : Alkyl-amine-N-oxide – (thio)phenol (-ΔH = 1140•Δr_1 - 6.35; R^2 = 0.92); □: EWG-amine-N-oxide – (thio)phenol (-ΔH = 458•Δr_1+ 1.87; R^2 = 0.86).

(b)● : Amine-N-oxide – phenol (-ΔH = 251•Δr_2 + 7.65; R^2 = 0.95);○ : Amine-N-oxide – thiophenol (-ΔH = 166• Δr_2 + 7.14; R^2 = 0.85).

The enthalpy of complexation –ΔH of the ten vacuo complexes is plotted against the H-bond distance d(H•••O) (see Figure 6). The H-bond enthalpy is calculated to be approximately proportional to the inverse fifth power of the H-bonding distance: ΔH ~ $d(H•••O)^{-5.04}$. In recent papers[50-52] a calculated H-bond enthalpy proportional to the inverse fifth power of the H-bond distance was also found, in line with a previously made claim[52] that such data should generally fit an inverse power relation –ΔH ≈ $f(r^a)$ with a >3.

Figure 6. Dependence of -ΔH on H-bond distance d for phenol – amine oxide H-bond complexes.
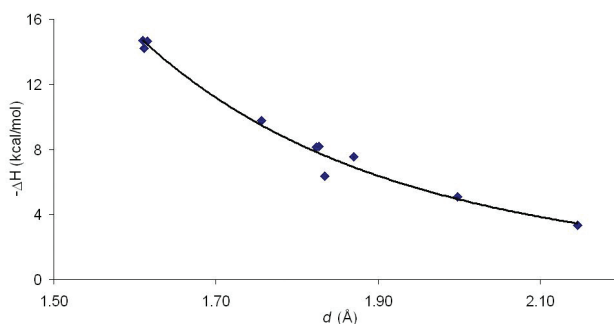
In recent papers[7, 48] we discussed the phenol binding capacity of a number of phosphine oxides and phosphates, and concluded that for phenol recovery from an aqueous environment the liquid phosphine oxide blend Cyanex 923 would be an optimum extractant for SIR applications. This phosphine oxide blend combined a high binding affinity for phenols with industrially relevant properties such as a low melting point (removes the need for a solvent) and a high boiling point (beneficial for regeneration of the SIR). The present study shows that amine-N-oxides are a second, highly interesting class of electronically and sterically tunable materials to extract phenols on a large scale in SIRs-based extractions.

Conclusions

Isothermal titration calorimetry combined with ab initio molecular modeling indicates the enthalpy-driven formation of a strong H-bonded 1 : 1 complex between phenol and amine-N-oxides, which is highly attractive for solvent-impregnated resin (SIR)-based large-scale separations. This complex has a high binding affinity (K = 1.7 – 5.7•10^4 M^{-1}) in dry solvents benzene, toluene and mesitylene, which is reduced significantly in water-saturated solvents (K = 5.8•10^3 M^{-1} in water-saturated toluene). The binding affinity, if found to be too strong for adequate regeneration, can be reduced by using amine N-oxides carrying electron-withdrawing groups, which may be beneficial for large-scale SIR extraction. The complex between amine-N-oxides and thiophenol is calculated to be much weaker, and experimentally the heat effect of the complexation was shown to be too weak to be observed in ITC. The weaker H-bonds found for thiophenols are largely due to lower charges on the H-bond donor atom, which yield smaller electrostatic interactions. CBS-Q modeling consistently predicts an equally strong or even a stronger H-bond for thiophenols than for phenols, in contrast with both experimental and the other modeling results. As a result, CBS-Q cannot be

used as a benchmark in case of complexes of sulphur compounds. The results from relatively cheap SCS-MP2 and M06-2X calculations without counterpoise correction agree well with those of the MP2/CBS method, and are in all cases clearly better than counterpoise corrected calculations.

The choice of an optimal extractant is crucial for future SIR applications. The combination of ITC and modeling experiments shows that liquid amine-N-oxides would be very good candidates for phenol extraction from aqueous media.

Acknowledgments

References

(1)   J. L. Cortina, A. Warshawsky, *in Ion Exch. Solvent Extr., Vol. 13* (Eds.: J. A. Marinsky, Y. Marcus), Dekker, New York, 1997, pp. 195.

(2)   S. S. El-Dessouky, E. H. Borai, *J. Radioanal. Nucl. Chem.* **2006**, *268*, 247.

(3)   B. B. Gupta, Z. B. Ismail, *Comp. Interf.* **2006**, *13*, 487.

(4)   J. S. Liu, H. Chen, Z. L. Guo, Y. C. Hu, *J. Appl. Pol. Sc.* **2006**, *100*, 253.

(5)   K. Ohnaka, A. Yuchi, *Chem. Lett.* **2005**, *34*, 868.

(6)   B. Burghoff, R. Cuypers, M. van Ettinger, E. J. R. Sudhölter, H. Zuilhof, A. B. de Haan, *Sep. Purif. Techn.* **2009,** *67*, 117.

(7)   R. Cuypers, B. Burghoff, A. T. M. Marcelis, E. J. R. Sudhölter, A. B. de Haan, H. Zuilhof, *J. Phys. Chem. A* **2008**, *112*, 11714.

(8)   R.-S. Juang, H.-L. Chang, *Ind. Eng. Chem. Res*. **1995**, *34*, 1294.

(9)   M. Traving, H.-J. Bart, *Chem. Eng. Technol.* **2002**, *25*, 997.

(10) A. Kostova, H.-J. Bart, *Chemie Ingenieur Technik* **2004**, *76*, 1743.

(11) H. Kitazaki, M. Ishimaru, K. Inone, K. Yoshida, S. Nakamura, in *Proceedings of the International Solvent Extraction Conference,* ISEC'96 ed., Melbourne, Australia, 1996, pp. 1667.

(12) B. Burghoff, E. L. V. Goetheer, A. B. de Haan, *React. Funct. Pol.* **2008**, *68*, 1314.

(13) M. K. Drozdova, I. V. Nikolaeva, V. G. Torgov, *Zhurnal Fizicheskoi Khimii* **1997**, *71*, 573.

(14) Y. I. Korenman, S. I. Niftaliev, V. G. Torgov, M. K. Drozdova, *Russ. J. Appl. Chem.* **1993**, *66*, 141.

(15) V. G. Torgov, Y. I. Korenman, M. K. Drozdova, V. V. Rebristaya, R. P. Lisitskaya, *Russ. J. Appl. Chem.* **1993**, *66*, 182.

(16) G. R. Desiraju, T. Steiner, *The Weak Hydrogen Bond*, 1 ed., Oxford University Press, New York, 1999.

(17) G. A. Jeffrey, *An Introduction to Hydrogen Bonding*, Oxford University Press, New York, Oxford, 1997.

(18)   J. P. M. Lommerse, S. L. Price, R. Taylor, *J. Comp. Chem.* **1997**, *18*, 757.

(19)   S. K. Panigrahi, G. R. Desiraju, *Proteins: Structure, Function, and Bioinformatics* **2007**, *67*, 128.

(20)   G. B. W. L. Ligthart, D. Guo, A. L. Spek, H. Kooijman, H. Zuilhof, R. P. Sijbesma, *J. Org. Chem.* **2008**, *73*, 111.

(21)   J. E. Ladbury, *Biotechniques* **2004**, *37*, 885.

(22)   J. E. Ladbury, M. L. Doyle, *Biocalorimetry 2*, John Wiley & Sons, Ltd, New York, 2004.

(23)   S. Leavitt, E. Freire, *Curr. Op. Struct. Biol.* **2001,** *11*, 560.

(24)   P. C. Weber, F. R. Salemme, *Curr. Op. Struct. Biol.* **2003**, *13*, 115.

(25)   T. Wiseman, S. Williston, J. F. Brandts, L.-N. Lin, *Anal. Biochem.* **1989**, *179*, 131.

(26)   T. J. M. de Bruin, A. T. M. Marcelis, H. Zuilhof, L. M. Rodenburg, H. A. G. Niederlander, A. Koudijs, P. E. M. Overdevest, A. Van Der Padt, E. J. R. Sudholter, *Chirality* **2000**, *12*, 627.

(27)   T. J. M. de Bruin, A. T. M. Marcelis, H. Zuilhof, E. J. R. Sudhölter, *Langmuir* **2000**, *16*, 8270.

(28)   H. J. Wiggers, J. Cheleski, A. Zottis, G. Oliva, A. D. Andricopulo, C. A. Montanari, *Anal. Biochem.* **2007**, *370*, 107.

(29)   A. Arnaud, L. Bouteiller, *Langmuir* **2004**, *20*, 6858.

(30)   P. Ballester, M. Capo, A. Costa, P. M. Deya, R. Gomila, A. Decken, G. Deslongchamps, *J. Org. Chem.* **2002**, *67*, 8832.

(31)   D. Merino-Garcia, S. I. Andersen, *Pet. Sc. Technol.* **2003**, *21*, 507

(32)   D. Merino-Garcia, S. I. Andersen, *Langmuir* **2004**, *20*, 4559.

(33)   J. L. Sessler, D. E. Gross, W. S. Cho, V. M. Lynch, F. P. Schmidtchen, G. W. Bates, M. E. Light, P. A. Gale, *J. Am. Chem. Soc.* **2006**, *128*, 12281.

(34)   T. Mizutani, H. Takagi, Y. Ueno, T. Horiguchi, K. Yamamura, H. Ogoshi, *J. Phys. Org. Chem.* **1998**, *11*, 737.

(35)   M. Xiang, M. Jiang, Y. Zhang, C. Wu, L. Feng, *Macromol.* **1997**, *30*, 2313.

(36)   L. F. Molnar, X. He, B. Wang, K. M. Merz, *J. Chem. Phys.* **2009**, *131*.

(37)   Y. Zhao, D. G. Truhlar, *Acc. Chem. Res.* **2008**, *41*, 157.

(38)   Y. Zhao, D. G. Truhlar, *Theor. Chem. Acc.* **2008**, *120*, 215.

(39)   J. W. Ochterski, G. A. Petersson, J. A. Montgomery, *J. Chem. Phys.* **1996**, *104*, 2598.

(40)   J. Antony, S. Grimme, *J. Phys. Chem. A* **2007**, *111,* 4862.

(41)   R. A. Bachorz, F. A. Bischoff, S. Hofener, W. Klopper, P. Ottiger, R. Leist, J. A. Frey, S. Leutwyler, *Phys. Chem. Chem. Phys.* **2008**, *10*, 2758.

(42)   S. Grimme, J. *Chem. Phys.* **2003**, *118*, 9095.

(43)   T. Schwabe, S. Grimme, *Acc. Chem. Res.* **2008**, *41*, 569.

(44)   M. Piacenza, S. Grimme, *ChemPhysChem* **2005**, *6*, 1554.

(45)   V. Kocherbitov, V. Veryazov, O. Soderman, *J. Mol. Struct. - Theochem* **2007**, *80*8, 111.

(46)   T. Malaspina, L. T. Costa, E. E. Fileti, *Int. J. Quant. Chem.* **2009**, *109,* 250.

(47)   A detailed analysis of these further factors falls outside the scope of this paper.

(48)   R. Cuypers, E. J. R. Sudhölter, H. Zuilhof, *ChemPhysChem* **2010**, *11*, 2230.

(49)   F. Wennmohs, V. Staemmler, M. Schindler, *J. Chem. Phys.* **2003**, *119*, 3208.

(50)   J. Chen, M. A. McAllister, J. K. Lee, K. N. Houk, *J. Org. Chem.* **1998**, *63*, 4611.

(51)   E. Espinosa, E. Molins, C. Lecomte, *Chem. Phys. Lett.* **1998**, *285*, 170.

(52)   M. Rozenberg, A. Loewenschuss, Y. Marcus, *Phys. Chem. Chem. Phys.* **2000**, *2*, 2699.

(53)   M. M. Davis, H. B. Hetzer, *J. Am. Chem. Soc.* **1954**, *76*, 4247.

(54)   M. Ejaz, *Anal. Chim. Acta* **1974**, *71*, 383.

(55)   M. Chellani, *Am. Biotechnol. Lab.* **1999**, *17*, 14.

(56)   M. J. Frisch, G. W. Trucks, H. B. Schlegel, G. E. Scuseria, M. A. Robb, J. R. Cheeseman, J. A. M. Jr., T. Vreven,
       K. N. Kudin, J. C. Burant, J. M. Millam, S. S. Iyengar, J. Tomasi, V. Barone, B. Mennucci, M. Cossi,
       G. Scalmani, N. Rega, G. A. Petersson, H. Nakatsuji, M. Hada, M. Ehara, K. Toyota, R. Fukuda, J. Hasegawa,
       M. Ishida, T. Nakajima, Y. Honda, O. Kitao, H. Nakai, M. Klene, X. Li, J. E. Knox, H. P. Hratchian, J. B. Cross,
       C. Adamo, J. Jaramillo, R. Gomperts, R. E. Stratmann, O. Yazyev, A. J. Austin, R. Cammi, C. Pomelli,
       J. W. Ochterski, P. Y. Ayala, K. Morokuma, G. A. Voth, P. Salvador, J. J. Dannenberg, V. G. Zakrzewski,
       S. Dapprich, A. D. Daniels, M. C. Strain, O. Farkas, D. K. Malick, A. D. Rabuck, K. Raghavachari,
       J. B. Foresman, J. V. Ortiz, Q. Cui, A. G. Baboul, S. Clifford, J. Cioslowski, B. B. Stefanov, G. Liu,
       A. Liashenko, P. Piskorz, I. Komaromi, R. L. Martin, D. J. Fox, T. Keith, M. A. Al-Laham, C. Y. Peng,
       A. Nanayakkara, M. Challacombe, P. M. W. Gill, B. Johnson, W. Chen, M. W. Wong, C. Gonzalez,
       J. A. Pople, Gaussian, Inc., Wallingford CT, 2004.

(57)   M. J. Frisch, G. W. Trucks, H. B. Schlegel, G. E. Scuseria, M. A. Robb, J. R. Cheeseman, G. Scalmani,
       V. Barone, B. Mennucci, G. A. Petersson, H. Nakatsuji, M. Caricato, X. Li, H. P. Hratchian, A. F. Izmaylov,
       J. Bloino, G. Zheng, J. L. Sonnenberg, M. Hada, M. Ehara, K. Toyota, R. Fukuda, J. Hasegawa, M. Ishida,
       T. Nakajima, Y. Honda, O. Kitao, H. Nakai, T. Vreven, J. Montgomery, J., A., J. E. Peralta, F. Ogliaro,
       M. Bearpark, J. J. Heyd, E. Brothers, K. N. Kudin, V. N. Staroverov, R. Kobayashi, J. Normand,
       K. Raghavachari, A. Rendell, J. C. Burant, S. S. Iyengar, J. Tomasi, M. Cossi, N. J. Rega Millam, M. Klene,
       J. E. Knox, J. B. Cross, V. Bakken, C. Adamo, J. Jaramillo, R. E. Gomperts, O. Stratmann, A. J. Yazyev,
       R. Austin, C. Cammi, J. W. Pomelli, R. Ochterski, R. L. Martin, K. Morokuma, V. G. Zakrzewski, G. A. Voth,
       P. Salvador, J. J. Dannenberg, S. Dapprich, A. D. Daniels, O. Farkas, J. B. Foresman, J. V. Ortiz, J. Cioslowski,
       D. J. Fox, Gaussian, Inc., Wallingford CT, 2009.

(58)   S. Raub, C. M. Marian, *J. Comput. Chem.* **2007**, *28*, 1503.

(59)   C. J. Cramer, *Essentials Of Computational Chemistry: Theories And Models*, 2nd ed.,
       John Wiley & Sons,Ltd, 2004.

(60)   P. Jurečka, J. Šponer, J. Černy, P. Hobza, *Phys. Chem. Chem. Phys.* **2006**, *8*, 1985.

(61)   M. Kone, B. Illien, J. Graton, C. Laurence, *J. Phys. Chem. A* **2005**, *109*, 11907.

(62)   M. R. Nyden, G. A. Petersson, *J. Chem. Phys.* **1981**, *75*, 1843.

(63)   S. F. Boys, F. Bernardi, *Mol. Phys.* **1970**, *19*, 553.

(64)   F. B. van Duijneveldt, J. G. C. M. van Duijneveldt - van de Rijdt, J. H. van Lenthe, *Chem. Rev.* **1994**,
       94, 1873.

(65)   G. Alagona, *Int. J. Quant. Chem.* **1987**, *32*, 227.

(66)   S. Cybulski, S. Scheiner, *J. Phys. Chem.* **1990**, *94*, 6106.

(67)   D. Hadži, *Theoretical treatments of hydrogen bonding*, Wiley, New York, 1997.

(68) H. Umeyama, K. Morokuma, *J. Am. Chem. Soc*. **1977**, *99,* 1316.

(69) E. D. Glendening, A. E. Reed, J. E. Carpenter, F. Weinhold., NBO Version 3.1.

(70) A. E. Reed, R. B. Weinstock, F. Weinhold, *J. Chem. Phys.* **1985**, *83*, 735.
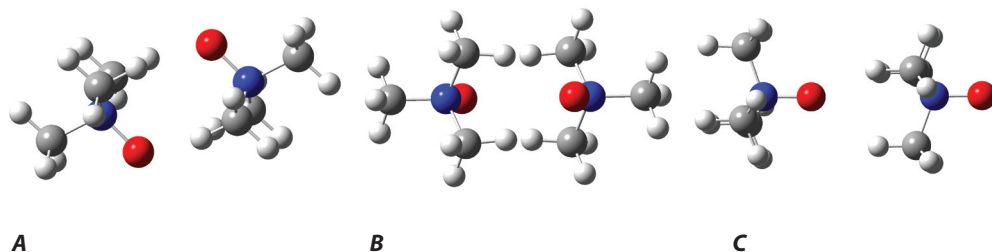
Figure S-1. Optimized geometries (B3LYP/6-31G(d) in vacuo) of calculated trimethylamine-N-oxide dimers; (A: head-to-head dimer (side) and B: head-to-head dimer (top, ΔH = -17 kcal/mol); and C: head-to-tail dimer (ΔH = -9 kcal/mol)).
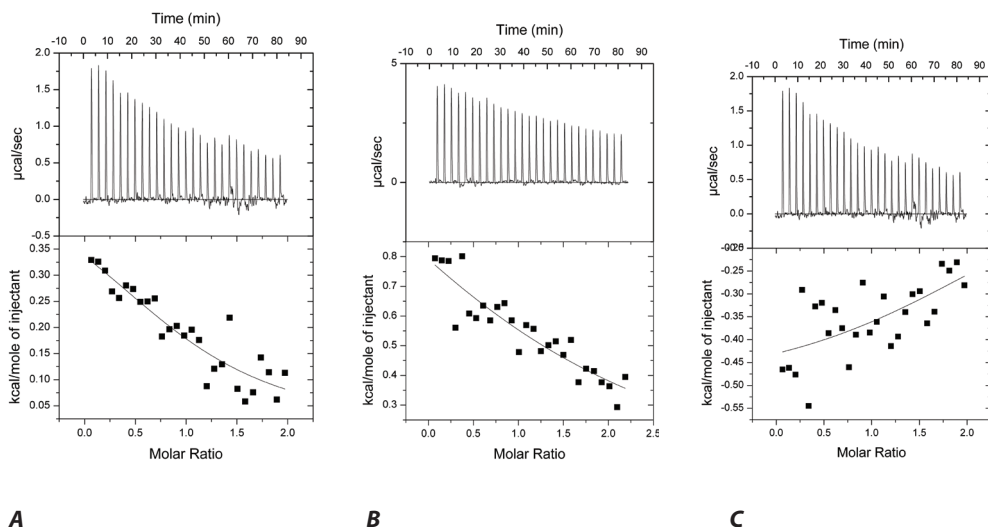
Figure S-2: Calorimetric titration of phenol in dry toluene with TEHAO in dry toluene at 30 °C ((A) raw data & (C) after subtraction of blank); (B): blank measurement, addition of TEHAO in dry toluene to dry toluene at 30 °C. Top panes: measured heat effects; bottom panes: processed data.
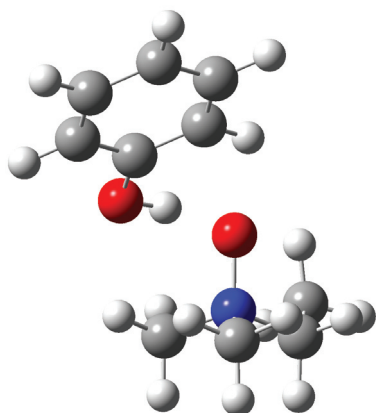
(C$_2$H$_5$)(CH$_3$)$_2$N$^+$-O$^-$ - HO-Ph **(C1)**
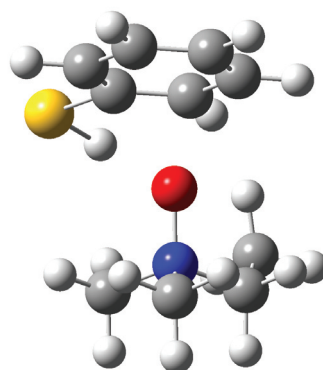
(C$_2$H$_5$)(CH$_3$)$_2$N$^+$-O$^-$ - HS-Ph (**C2**)
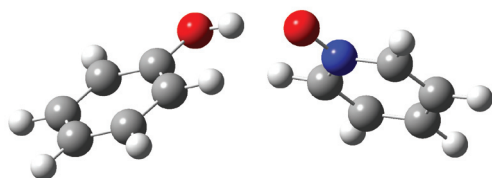
C$_5$H$_5$N$^+$-O$^-$ - HO-Ph (**C3**)
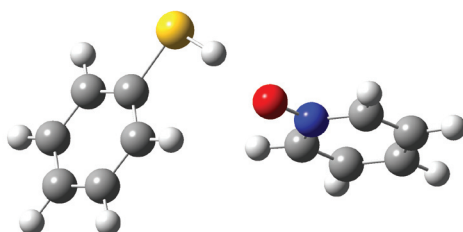
C$_5$H$_5$N$^+$-O$^-$ - HS-Ph (**C4**)

Figure S-3. Optimized geometry (B3LYP/6-311G(d,p)) of calculated Amine-N-oxide – (thio)phenol complexes.
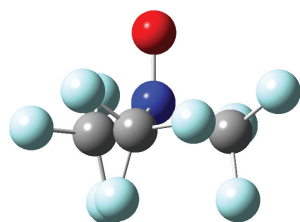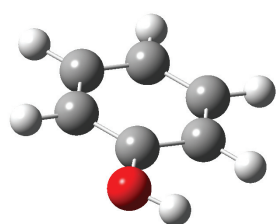
(CF$_3$)$_3$N$^+$-O$^-$ - HO-Ph (**C5**)
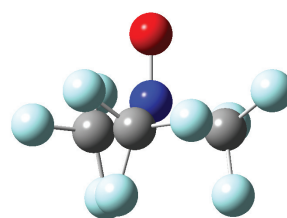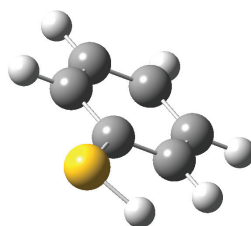
(CF$_3$)$_3$N$^+$-O$^-$ - HS-Ph (**C6**)
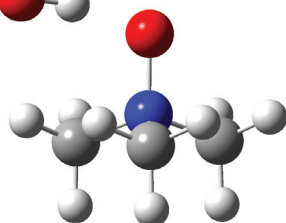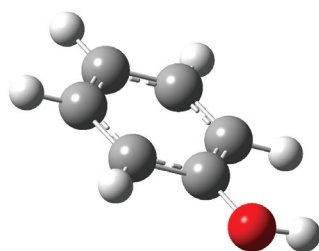
(CH$_3$)$_3$N$^+$-O$^-$ - HO-Ph (**C7**)
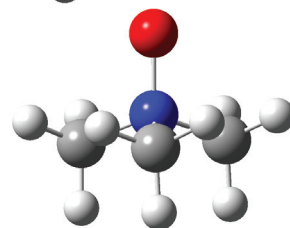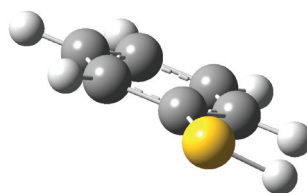
(CH$_3$)$_3$N$^+$-O$^-$ - HS-Ph (**C8**)

Figure S-3. Optimized geometry (B3LYP/6-311G(d,p)) of calculated Amine-N-oxide – (thio)phenol complexes (continued).
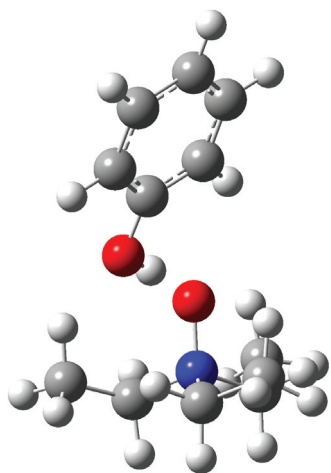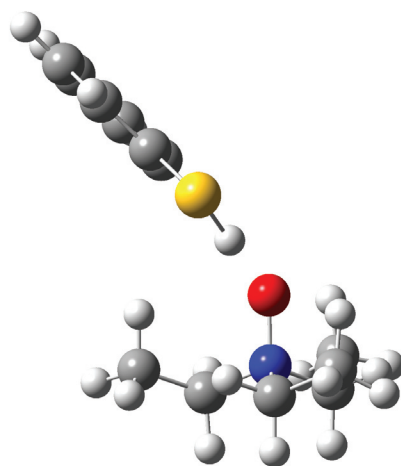
(C$_2$H$_5$)$_3$N$^+$-O$^-$ - HO-Ph (**C9**)   (C$_2$H$_5$)$_3$N$^+$-O$^-$ - HS-Ph (**C10**)

Figure S-3. Optimized geometry (B3LYP/6-311G(d,p)) of calculated Amine-N-oxide – (thio)phenol complexes (continued).

Table S-1: Selected geometric parameters and charges on hydrogen bond forming atoms of the amine-N-oxide complexes with phenol and thiophenol.[a]

#	Complex	geometric parameters					NPA charge (B3LYP)	
		d	α	$\Delta r1$[b]	$\Delta r2$[b]	ϕ	oxide O	phenol H
C1	$(C_2H_5)(CH_3)_2N^+\text{-}O^-$ - HO-Ph	1.62	169	0.022	0.043	-1.2	-0.73	+0.50
C2	$(C_2H_5)(CH_3)_2N^+\text{-}O^-$ - HS-Ph	1.83	173	0.017	0.033	9.9	-0.74	+0.20
C3	$C_5H_5N^+\text{-}O^-$ - HO-Ph	1.76	167	0.022	0.021	-0.3	-0.58	+0.50
C4	$C_5H_5N^+\text{-}O^-$ - HS-Ph	2.00	168	0.017	0.014	10.7	-0.57	+0.17
C5	$(CF_3)_3N^+\text{-}O^-$ - HO-Ph	1.83	170	0.019	0.012	-0.3	-0.64	+0.49
C6	$(CF_3)_3N^+\text{-}O^-$ - HS-Ph	2.15	171	0.013	0.005	-2.5	-0.62	+0.16
C7	$(CH_3)_3N^+\text{-}O^-$ - HO-Ph	1.61	169	0.022	0.044	1.1	-0.73	+0.50
C8	$(CH_3)_3N^+\text{-}O^-$ - HS-Ph	1.82	173	0.017	0.034	-9.1	-0.76	+0.20
C9	$(C_2H_5)_3N^+\text{-}O^-$ - HO-Ph	1.61	175	0.021	0.041	1.0	-0.75	+0.50
C10	$(C_2H_5)_3N^+\text{-}O^-$ - HS-Ph	1.87	173	0.016	0.026	-9.1	-0.75	+0.19

[a] d, α, $\Delta r1$, $\Delta r2$ and ϕ, as shown in Table 1. [b] $\Delta r = r_{complex} - r_{non\text{-}complexed\ molecule}$; $(r_1((CH_3)_3N^+\text{-}O^-) =$ 1.359 Å; $r_1((C_2H_5)_3N^+\text{-}O^-) = 1.353$ Å; $r_1((C_2H_5)(CH_3)_2N^+\text{-}O^-) = 1.358$ Å; $r_1((CF_3)_3N^+\text{-}O^-) = 1.292$ Å; $r_1(C_5H_5N^+\text{-}O^-) = 1.269$ Å; $r2_{phenol} = 0.963$ Å; $r2_{thiophenol} = 1.347$ Å).

Table S-2: Enthalpy of complexation ΔH (kcal/mol) of the amine-N-oxide complexes with phenol and thiophenol (B3LYP/6-311G(d,p)-optimized geometries).

|		ΔH											
		B3LYP[a]	MP2				SCS-MP2				MP2/CBS	M06-2X[e]	CBS-Q
			Small[b]		Large[c]		Small[b]		Large[c]				
#	Complex	-CP[d]	-CP	+CP	-CP	+CP	-CP	+CP	-CP	+CP	-CP	-CP	-CP
C1	$(C_2H_5)(CH_3)_2N^+\text{-}O^-$ - HO-Ph	-14.7	-13.0	-18.9	-15.1	-19.0	-16.3	-17.4	-13.8	-17.3	-14.6	-18.4	-13.7
C2	$(C_2H_5)(CH_3)_2N^+\text{-}O^-$ - HS-Ph	-8.2	-7.0	-12.7	-9.1	-12.6	-10.2	-11.1	-7.6	-10.8	-8.4	-12.4	-13.6
C3	$C_5H_5N^+\text{-}O^-$ - HO-Ph	-9.8	-8.5	-12.1	-9.0	-12.4	-10.2	-11.2	-8.2	-11.4	-9.1	-11.8	-10.7
C4	$C_5H_5N^+\text{-}O^-$ - HS-Ph	-5.1	-4.1	-9.3	-5.8	-9.0	-6.8	-8.1	-4.8	-7.7	-5.6	-8.8	-12.1
C5	$(CF_3)_3N^+\text{-}O^-$ - HO-Ph	-6.4	-5.5	-12.0	-7.5	-11.8	-8.5	-10.9	-6.6	-10.8	-7.4	-11.4	-9.5
C6	$(CF_3)_3N^+\text{-}O^-$ - HS-Ph	-3.3	-2.8	-8.8	-4.7	-8.2	-5.4	-7.7	-3.9	-7.2	-4.4	-8.0	-11.8
C7	$(CH_3)_3N^+\text{-}O^-$ - HO-Ph	-14.7	-12.9	-18.7	-15.0	-18.9	-16.2	-17.2	-13.7	-17.2	-14.5	-18.3	-13.0
C8	$(CH_3)_3N^+\text{-}O^-$ - HS-Ph	-8.1	-6.9	-12.3	-8.8	-12.3	-10.0	-10.6	-7.4	-10.5	-8.2	-12.1	-12.8
C9	$(C_2H_5)_3N^+\text{-}O^-$ - HO-Ph	-14.2	-13.1	-20.1	-15.6	-19.7	-16.6	-18.6	-14.3	-18.1	-14.9	-18.9	-15.7
C10	$(C_2H_5)_3N^+\text{-}O^-$ - HS-Ph	-7.5	-6.9	-13.7	-9.6	-13.2	-10.5	-12.1	-8.1	-11.4	-8.7	-12.9	-16.5

[a] 6-311+G(d,p). [b] 6-311+G(d,p). [c] 6-311++G(2d,2p). [d] CP = a posteriori counterpoise correction.

Table S-3: NPA overlap-weighted bond orders of monomers and complexes C1-C10.

#	Compounds	NPA Overlap Weighted Bond Order		
		N-O	H•••O	O/S-H
-	PhOH	-	-	0.661
-	PhSH	-	-	0.724
-	$(C_2H_5)(CH_3)_2N^+$-O^-	0.825	-	-
-	$C_5H_5N^+$-O^-	0.982	-	-
-	$(CF_3)_3N^+$-O^-	0.925	-	-
-	$(CH_3)_3N^+$-O^-	0.822	-	-
-	$(C_2H_5)_3N^+$-O^-	0.843	-	-
C1	$(C_2H_5)(CH_3)_2N^+$-O^- - HO-Ph	0.788	0.133	0.569
C2	$(C_2H_5)(CH_3)_2N^+$-O^- - HS-Ph	0.797	0.101	0.687
C3	$C_5H_5N^+$-O^- - HO-Ph	0.928	0.072	0.600
C4	$C_5H_5N^+$-O^- - HS-Ph	0.940	0.049	0.703
C5	$(CF_3)_3N^+$-O^- - HO-Ph	0.891	0.048	0.620
C6	$(CF_3)_3N^+$-O^- - HS-Ph	0.891	0.027	0.712
C7	$(CH_3)_3N^+$-O^- - HO-Ph	0.782	0.138	0.566
C8	$(CH_3)_3N^+$-O^- - HS-Ph	0.793	0.102	0.686
C9	$(C_2H_5)_3N^+$-O^-- HO-Ph	0.790	0.133	0.565
C10	$(C_2H_5)_3N^+$-O^-- HS-Ph	0.802	0.086	0.694

4

Table S-4. *Total vacuo energies (in Hartrees) of reference compounds and complexes (B3LYP/6-311+G(d,p)//B3LYP/6-311G(d,p), MP2/6-311+G(d,p)//B3LYP/6-311G(d,p) and MP2/6-311++G(2d,2p)//B3LYP/6-311G(d,p), SCS-MP2/6-311+G(d,p)//B3LYP/6-311G(d,p) and SCS-MP2/6-311++G(2d,2p)//B3LYP/6-311G(d,p), MP2/CBS and CBS-Q).*

| species | B3LYP | MP2 | | SCS-MP2 | | MP2/CBS | CBS-Q |
		small	large	small	large		
PhOH	-307.5586085	-306.6655587	-306.7386514	-306.6345714	-306.7072123	-306.8760241	-306.945315
PhSH	-630.5252559	-629.2513847	-629.3233473	-629.2252481	-629.2963385	-629.4599453	-629.54273
$(C_2H_5)(CH_3)_2N^+-O^-$	-289.027304	-288.1735905	-288.2497208	-288.1652349	-288.2410754	-288.3834648	-288.408438
$C_5H_5N^+-O^-$	-323.5400245	-322.6254047	-322.7028133	-322.5891087	-322.6656771	-322.8476444	-322.918336
$(CF_3)_3N^+-O^-$	-1143.104437	-1140.695928	-1140.961832	-1140.583639	-1140.839648	-1141.388483	-1141.70231
$(CH_3)_3N^+-O^-$	-249.7012736	-248.9755879	-249.0412704	-248.9682301	-249.0335697	-249.1559048	-249.180925
$(C_2H_5)_3N^+-O^-$	-367.6768711	-366.5673264	-366.6644081	-366.5568459	-366.6537377	-366.8364316	-366.863239
$(C_2H_5)(CH_3)_2N^+-O^-$ - HO-Ph	-596.6092827	-594.8693127	-595.0185934	-594.8275519	-594.9758748	-595.2887313	-595.375638
$(C_2H_5)(CH_3)_2N^+-O^-$ - HS-Ph	-919.5655976	-917.4452745	-917.5931204	-917.4080945	-917.5546014	-917.8632129	-917.972774
$C_5H_5N^+-O^-$ - HO-Ph	-631.1141723	-629.310207	-629.4612213	-629.2414781	-629.3909964	-629.7424497	-629.880736
$C_5H_5N^+-O^-$ - HS-Ph	-954.0733996	-951.8915989	-952.0404669	-951.8271918	-951.9742582	-952.3216267	-952.480408
$(CF_3)_3N^+-O^-$ - HO-Ph	-1450.673197	-1447.38063	-1447.71936	-1447.235614	-1447.564	-1448.282668	-1448.662687
$(CF_3)_3N^+-O^-$ - HS-Ph	-1773.635013	-1769.96126	-1770.298264	-1769.821163	-1770.147449	-1770.861223	-1771.263797
$(CH_3)_3N^+-O^-$ - HO-Ph	-557.2832703	-555.6709176	-555.8100427	-555.6301328	-555.7682139	-556.0610432	-556.146946
$CH_3)_3N^+-O^-$ - HS-Ph	-880.2394698	-878.2465162	-878.384298	-878.2103639	-878.3467106	-878.6351889	-878.744059
$(C_2H_5)_3N^+-O^-$ - HO-Ph	-675.2581153	-673.2649715	-673.4344342	-673.2210388	-673.3897595	-673.7425469	-673.833629
$(C_2H_5)_3N^+-O^-$ - HS-Ph	-998.2141441	-995.8406113	-996.008731	-995.8013236	-995.9683125	-996.3169597	-996.432295

4

CHAPTER 5

Complexation of MTBE by Phenols. *Ab Initio* Computations and Isothermal Titration Calorimetry.

Abstract

To develop a new solvent-impregnated resin (SIR) system for the removal of methyl-*t*-butyl ether (MTBE) from dilute aqueous solutions, the complex formation of phenols to MTBE was studied by a combined theoretical and experimental approach: isothermal titration calorimetry (ITC) and quantum chemical modeling (B3LYP, M06-2X, MP2, SCS-MP2 and CBS-Q, with basis sets from 6-311G(d,p) to extrapolations to the complete basis set (CBS)).These complexes were analyzed in terms of structural (e.g. bond lengths) and electronic elements (e.g. charges), both *in vacuo* and using the PCM and SMD solvent models to simulate apolar solvents. Higher binding energies were found for phenols substituted with more and stronger electron-withdrawing groups, in line with their pK_a values, except for pentachlorophenol and pentafluorophenol, in which competing electronic and steric effects play a role. CBS-Q predicts inconsistent binding enthalpies for the investigated phenols, and can thus not be used as a bench-mark method. Both SCS-MP2/6-311+G(d,p) and M06-2X/6-311+G(d,p) values without counterpoise correction show a very good agreement with the MP2/CBS values. On the basis of these results, four new, water-insoluble alkyl-substituted cyanophenols with low melting points were designed and synthesized. Their complex formation with MTBE was investigated experimentally by ITC, where 1 : 1 complex formation was found. For 3-alkyl-4-cyanophenol, MTBE binding affinities ranged from K = 12 – 23 M^{-1}, yielding overall distribution coefficients of ~$4 \cdot 10^2$, which would be ample for industrial applications. This combination of modeling and subsequent experimentation showed that these new liquid extractants have the desired properties (low melting point, low water solubility, binding affinity for MTBE) for implementation in SIR-based separation processes for removal of MTBE from dilute aqueous solutions.

Introduction

Methyl-*t*-butyl ether (MTBE) is mainly known as a tetra ethyl lead-replacing fuel oxygenate, which is added to petrol as an octane enhancer to minimize engine 'knocking' through an increased oxygen content.[1]   MTBE has a high water solubility (42 g/L)[2] compared to other fuel constituents, such as benzene (1.79 g/L).[3] Combined with the low soil adsorption coefficient of MTBE this causes immediate groundwater contamination from leakages of storage facilities.[4] In the United States, more than 80 % of 1000 tested groundwater sites were shown to be contaminated with MTBE and concentrations as high as 23 mg/L have been measured.[5] Since MTBE has a very low taste and smell threshold in water of 40 μg/L and 15 μg/L,[6] respectively, it needs to be removed during the production of high-quality potable water from groundwater. Currently, in western societies MTBE is slowly being replaced in gasoline fuels by the analog ethyl-*t*-butyl ether (ETBE), which is more easy to remove because of its lower water solubility. The high current concentrations of MTBE in the environment and its continued large-scale use in many developing economies, however, do still require efficient methods to diminish a long-term problem in water purification.

Conventional processes for MTBE removal are air stripping and granular activated carbon (GAC) adsorption,[6] amongst others. High process costs, high amounts of adsorbent, or a competitive adsorption of other organic compounds in ground water result in an unsatisfactory performance for these techniques. In some investigations, the development of supported polymeric liquid membranes for MTBE recovery is discussed.[7] Distribution coefficients K_D between 9 and 18 were
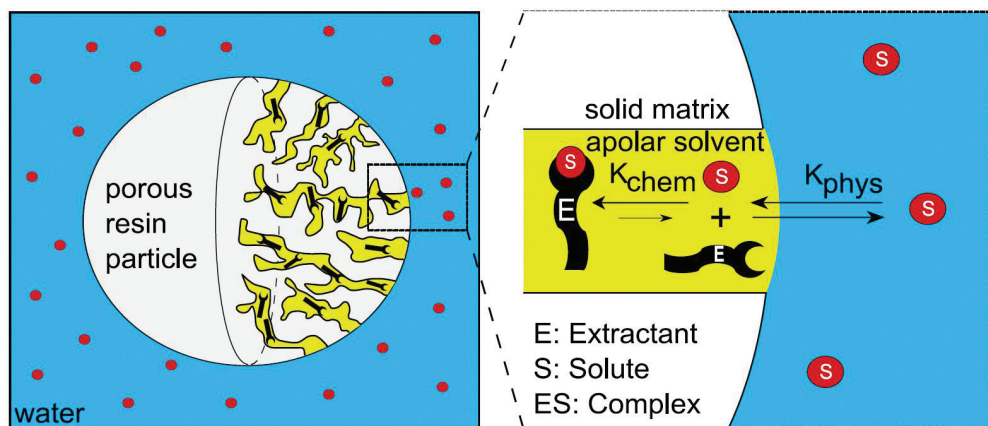
Figure 1. Working principle of Solvent-Impregnated Resins (SIR) with an active extractant in the pores.

found for MTBE,[7, 8] but for an effective removal from contaminated aqueous streams with a high capacity extractant such a K_D is too low.

Solvent-impregnated resins[9] (SIRs, Figure 1) are used as three-phase separation systems. A solute is present in an aqueous phase; the SIR contains the stationary, solvent phase, an organic liquid impregnated in the pores of the inert resin particle. When brought into contact with a SIR, the solute will diffuse from the aqueous phase into the solvent phase. Ion-exchange SIRs are already widely used[10-13] to separate heavy metal ions from aqueous phases in a fast and simple way, making use of the solubility of the solute in the liquid organic phase, in exchange for protons. Only recently, other applications have been investigated, e.g. the recovery of slightly polar organics[14-17] and bench-scale or pilot-scale recovery of polar organics like organic acids,[18, 19] amino acids[20] and flavonoids.[21] In order to enhance MTBE extraction from an aqueous environment, complex-forming extractants can be added to the solvent. By means of complex formation inside the organic solvent, the overall equilibrium concentration of solute in the SIR can be increased,[14-17] in which case the overall extraction will be significantly enhanced.

In principle, molecular recognition and complexation of the solute inside the SIR particles, as indicated in Figure 1, can provide a new and fast way to separate more polar organic solutes from aqueous streams on a kiloton/yr scale. For the effective removal of more polar organic solutes like MTBE the additional complexation step of the solute in the solvent phase turns out to be crucial for large-scale application,[14-17, 22] due to the relatively high solute solubility in water. This is the incentive for the performed screening of extractants to achieve a high MTBE capacity. A rational way of optimizing an extractant for these applications is by using molecular design. For this a thorough understanding of the complexation at the molecular level is required.
Molecular modeling can facilitate this by providing useful data about the complex formation that can be compared with those of experiments.

Table 1. Compounds under investigation and geometric parameters describing H-bond geometry in phenol – MTBE complexes; d (Å), α (°), r (Å), φ (°).

Compound	Molecular formula	Compound	Molecular formula
Phenol	C_6H_5OH	3-chlorophenol	$3\text{-}Cl\text{-}C_6H_4OH$
4-nitrophenol	$4\text{-}NO_2\text{-}C_6H_4OH$	3,5-dichlorophenol	$3,5\text{-}Cl_2\text{-}C_6H_3OH$
3-cyanophenol	$3\text{-}CN\text{-}C_6H_4OH$	Pentachlorophenol	C_6Cl_5OH
4-cyanophenol	$4\text{-}CN\text{-}C_6H_4OH$	3-fluorophenol	$3\text{-}F\text{-}C_6H_4OH$
3-methyl-4-cyanophenol	$3\text{-}Me\text{-}4\text{-}CN\text{-}C_6H_3OH$	3,5-difluorophenol	$3,5\text{-}F_2\text{-}C_6H_3OH$
2-methyl-4-cyanophenol	$2\text{-}Me\text{-}4\text{-}CN\text{-}C_6H_3OH$	pentafluorophenol	C_6F_5OH
3,5-dichloro-4-methylphenol	$3,5\text{-}Cl_2\text{-}4\text{-}CH_3\text{-}C_6H_2OH$		

Complex:
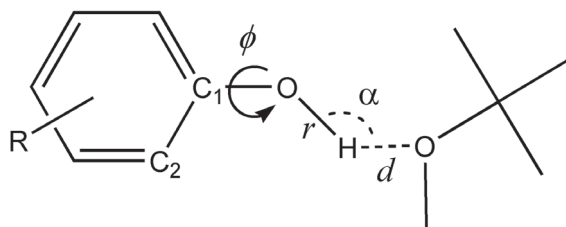
In this chapter we investigate a set of phenol extractants for the extraction of MTBE from an aqueous environment, to establish the basis for a future industrial design. Hydrogen bonds of a well-tuned strength (~ 10 - 15 kcal/mol) are desired for SIR-based processes. Since such process requires repetitive complexation and decomplexation/SIR regeneration, the optimum binding strength is not necessarily the highest binding strength. This regeneration would be problematic in case of formation of very stable complexes, which makes the optimum binding strength ca. 10 to 15 kcal/mol.[15] The search for such suitable extractants prompted this study with substituted phenols. Phenols can form hydrogen-bonding complexes, and they do not suffer from the problem of loss of their binding ability after dimer formation, that was previously shown to disturb any advantageous effect with another class of complexing agents[16] (see Chapter 3).

Alkylated phenols with electron-withdrawing groups (EWG) can combine a low solubility in water with a partial positive charge on the hydrogen atom, favorable for a hydrogen bond donor. The most important hydrogen bond characteristics to be explored in this chapter are the hydrogen

bond strength, its decomposition in enthalpic and entropic factors, and the geometry of the resulting complexes. From literature, neutral O–H•••O hydrogen bonds are expected to have a ΔH^0 for complex formation of ca. -4 to -15 kcal/mol,[23, 24] covering a range of H-bond lengths and O–H•••O angles[25, 26] as these parameters depend strongly on the molecular geometry of the system at hand. Hydrogen bonds between charged donor or acceptor atoms are usually significantly stronger, with typical ΔH^0 of complex formation between -15 and -40 kcal/mol.[24] H-bonds of phenols with electron-withdrawing groups are expected to yield ΔH^0 between -5 and -14 kcal/mol, but recent computational studies show that accurate geometric information is required to make meaningful predictions.[27]

The interaction between MTBE and the extractants is investigated experimentally with isothermal titration calorimetry (ITC) binding experiments. Although some information about hydrogen bonding of phenols to ethers is available,[28] this information was obtained indirectly from IR and UV measurements. The current chapter presents the first directly measured binding affinity and thermodynamic description (stoichiometry, K, ΔH^0, ΔG^0, ΔS^0). This is complemented by the first theoretical investigations on these complexes, to properly assess the assumptions made in these literature overviews.

ITC[29-33] can be used to directly measure the binding affinity (equilibrium constant, K) and thermodynamic parameters (ΔH^0, and the stoichiometry N) in complexation reactions, and the values of ΔS^0 and ΔG^0, can be derived directly from this. Although most of the reported ITC measurements are carried out in aqueous solutions,[34, 35] its use is also unproblematic with co-solvents like methanol or DMSO,[36] or with organic solvents like chloroform,[37, 38] toluene[15-17, 37, 39, 40] and others.[41] Toluene was therefore used as apolar model solvent, with a relatively small influence on hydrogen bonding interactions.[37, 42, 43]

For the development of a SIR extraction set-up for the removal of MTBE from an aqueous system, these molecular-scale interactions are of vital importance. The present chapter discusses these factors, yielding an optimal candidate by application of ITC measurements and theoretical methods. A range of different methods (B3LYP/6-311+G(d,p)//B3LYP/6-311G(d,p) in vacuum and in the solvents cyclohexane, mesitylene, toluene and benzene, MP2/6-311+G(d,p)//B3LYP/6-311G(d,p) and MP2/6-311++G(2d,2p)//B3LYP/6-311G(d,p), spin component-scaled (SCS) MP2 calculations with the same basis sets, and a complete basis set extrapolation (MP2/CBS)) were applied to the model compounds depicted in Table 1. Since analysis of a small data set of hydrogen-bonded complexes suggested that the M06 set of density functionals might perform somewhat better in describing hydrogen-bonding interactions,[44] M06-2X/6-311+G(d,p)//M06-2X/6-311G(d,p) calculations[45, 46]

were also performed. Finally, the composite CBS-Q method, a complete basis set method to obtain very accurate energies,[47] was used to obtain an absolute benchmark for the energy values. The different methods were chosen to diminish the chance of finding highly method-dependent results. In recent papers,[48-51] SCS-MP2 methods, which use the default scaling factors of 6/5 for anti-parallel spins and 1/3 for parallel spins, showed a dramatic increase in accuracy over normal MP2 energies, providing a more balanced description of many systems, and sometimes even reaching QCISD or QCISD(T) quality data.[52] Since the application of SCS-MP2 on the stability of H-bonding is relatively unexplored, its performance is therefore described in detail here. The results from the latter method are compared to those of benchmark MP2/CBS method.

Experimental Section

General. The following materials were used as received without further purification: toluene (Riedel de Haan, puriss.), phenol (Merck, p.a.), methyl-*t*-butyl ether (Acros, 99%). Molecular sieves (3 Å, Aldrich) were used as received.

Isothermal Titration Calorimetry (ITC). was performed on a MicroCal VP-ITC microcalorimeter; the setup is described elsewhere.[65] Results were processed using Origin 7SR2 V7.0383 (B383) software by Origin Lab Corporation. The measuring cell (1.46 mL) was flushed and filled with a freshly prepared and degassed solution (usually concentrations between 1 and 10 mM were used) of MTBE in toluene. The 280 μL automatic syringe was flushed and filled with a freshly prepared and degassed solution of the complexing agent (the phenol) in the same solvent, at a concentration of roughly 10 times the molarity of the cell solution. The number of injections and the injected volume per injection were optimized depending on the concentration of the compounds and the heat effect per second. Between subsequent injections a sufficient amount of time was chosen to allow the cell feedback to return to the baseline, usually 150 to 300 seconds. Stirring speed for all ITC measurements was 502 rpm (default value). A reference measurement was performed using the same procedure, with only solvent in the measuring cell. By subtracting the reference measurement from the actual measurement the net results were obtained and they were fitted using the one-set-of-sites model present in the Origin software.

Modeling. Computational data of the compounds depicted in Table 1 were all obtained using Gaussian 09.[66] A range of different methods (B3LYP/6-311+G(d,p)//B3LYP/6-311G(d,p), M06-2X/6-311+G(d,p)//M06-2X/6-311G(d,p)[44-46], MP2/6-311+G(d,p)//B3LYP/6-311G(d,p), MP2/6-311++G(2d,2p)/

/B3LYP/6-311G(d,p), spin component-scaled (SCS) MP2[48-51] using the same basis sets, a complete basis set extrapolation (MP2/CBS) and the composite CBS-Q[47] method) were applied to the model compounds depicted in Table 1. With such basis sets both B3LYP and MP2 typically provide interaction energies for H-bonding within a few kcal/mol from experimental data, while MP2 calculations with bigger basis sets are typically even more accurate,[67-69] although it is known to slightly overestimate the correlation contribution to a complexation. An extrapolation to the complete basis set (CBS) energy limit was obtained using the keyword 'cbsextrapolate'.[70] The option "NMin=10" was specified to account for a minimum of 10 pair natural orbitals for extrapolation to the CBS limit. Counterpoise (CP) correction[71, 72] was applied for all MP2 and SCS-MP2 calculations to correct for over-stabilization due to the supermolecule approach. Obviously, no CP-correction was applied to the MP2/CBS energies. The B3LYP-derived geometries were taken as input structures for the CBS-Q method, which is known to provide very accurate energy data. The CBS-Q method consists of several different steps, described elsewhere.[47] All CBS-Q structures were confirmed to be true minima in the vibrational frequency analysis that is part of the composite method. The CBS-Q energy at 0 K was used for the presented results.

B3LYP and M06-2X calculations were not only used to provide data *in vacuo*, but were also combined with a self-consistent reaction field (SCRF) approach to mimic apolar solvent effects on energy data. For these calculations the solvent 'cyclohexane', 'mesitylene', 'toluene' or 'benzene' was specified in the Gaussian input section with both the IEF-PCM[60] and SMD[61] solvent model, to be able to relate the findings to experiments, which were conducted using toluene.

Finally, since electrostatic interactions are crucial for the strength of H-bonds[24, 73-76] natural population analysis (NPA)[77, 78] charges were obtained, as these display a relatively small method dependence and basis set dependence, and have proven to be reliable charge indicators for related theoretical studies of H-bonds.[27, 79] In addition, atom-atom overlap-weighted natural atomic orbital (NAO) bond orders were obtained.

The model compounds resemble the compounds used in ITC, but for computational speed the long alkyl tails were replaced by a methyl group. In Table 1 the different relevant geometrical parameters are defined for hydrogen bonds in the investigated complexes.

Synthesis. The synthesis of cyanophenols proceeds via two consecutive steps: First, *p*-benzoquinone is substituted with the appropriate alkyl tail by reaction with the corresponding alkanoic acid. Second, the resulting alkyl-substituted benzoquinone is reduced to the respective cyanophenol. The detailed reaction descriptions are given below.

Alkylquinones. In a typical procedure,[80] *p*-benzoquinone was dissolved with 1.5 molar equivalents of the alkanoic acid in a sufficient amount of 1 : 1 v/v water : acetonitrile. To this solution a small amount of $AgNO_3$ (0.12 molar equivalents) was added as a catalyst and the solution was refluxed. Over a period of more than 2 h a solution of 1.5 molar equivalents of $(NH_4)_2S_2O_8$ in water was added dropwise to the refluxing solution. After full addition, the solution was refluxed for another 30 min. The progress of the reaction was followed by TLC. After the reaction had finished, the mixture was extracted three times with petroleum-ether 40/60. The combined organic layers were washed three times with a 10% $NaHCO_3$-solution in water. The organic layer was subsequently dried and filtrated and the solvent was removed *in vacuo*. A further purification step with silica-based column chromatography (eluens: CH_2Cl_2) was sometimes necessary.

2-Undecyl-1,4-benzoquinone: The general reaction was performed with 1.55 g (14.3 mmol, 1 eq.) 1,4-benzoquinone, 4.33 g (21.6 mmol, 1.5 eq.) dodecanoic acid, 0.53 g (3.12 mmol, 0.2 eq.) $AgNO_3$ and 4.89 g (21.4 mmol, 1.5 eq.) $(NH_4)_2S_2O_8$. Yield: 1.88 g (7.17 mmol, 50.1 %). ^{1}H NMR ($CDCl_3$, 300 MHz): δ = 6.77 (m; 1 H), 6.72 (m; 1 H), 6.57 (m; 1 H), 2.43 (m; 2 H), 1.51 (m; 2 H), 1.27 (m; 16 H), 0.89 ppm (t; 3 H).

2-(1-n-Hexylnonyl)-1,4-benzoquinone: The general reaction was performed with 2.61 g (24.1 mmol, 1 eq.) 1,4-benzoquinone, 9.32 g (36.4 mmol, 1.5 eq) 2-n-hexyldecanoic acid, 0.75 g (4.41 mmol, 0.18 eq.) $AgNO_3$ and 8.30 g (36.4 mmol, 1.5 eq.) $(NH_4)_2S_2O_8$. Yield after column chromatography: 2.33 g (7.32 mmol, 30.3 %). ^{1}H NMR ($CDCl_3$, 300 MHz): δ = 6.7 (m; 2 H), 6.5 (m; 1 H), 2.81 (m; 1 H), 1.48 (m; 2 H), 1.21 (m; 20 H), 0.85 ppm (m; 6 H).

Cyanophenols. The general procedure[81-83] for transformation of quinones to cyanophenols consists of two parts. The first part, the quinone cyanosilylation, involves the addition of a catalytic amount (0.01 - 0.02 eq.) of potassium cyanide - 18-crown-6 complex to a stirred mixture of quinone (1 eq.) and trimethylsilyl cyanide (TMSCN, 1.1 eq.) in CH_2Cl_2 under a N_2-atmosphere. After stirring (R.T., 30 min) the solvent was removed *in vacuo* and the compounds were dissolved in THF. For the second part, the reduction, this mixture was added very slowly to 2 eq. 0.1 M SmI_2 in THF at room temperature. After total addition, the mixture was stirred for another 2 h. Subsequently, it was added to saturated aqueous NH_4Cl solution and extracted thrice with diethyl ether. The ether was dried, filtrated and removed *in vacuo*.

2-Undecyl-4-cyanophenol and 3-Undecyl-4-cyanophenol: The general procedure was followed with 1.30 g (4.95 mmol, 1 eq.) 2-undecyl-1,4-benzoquinone, 0.64 g (6.45 mmol, 1.2 eq.) TMSCN and 0.012 eq. potassium cyanide - 18-crown-6 complex. For the second step, 1.12 g (3.5 mmol, 1 eq.) unpurified product was added to 80 mL 0.1 M SmI_2 solution in THF. After purification, two products were obtained.

2-Undecyl-4-cyanophenol: Yield: 60 mg (0.22 mmol, 7.7 %). ^{1}H NMR (CDCl$_3$, 300 MHz): δ = 7.44 (m; 1 H), 7.40 (m; 1 H), 6.86 (m; 1 H), 6.13 (s; 1 H), 2.62 (t; 2 H), 1.64 (m; 2 H), 1.32 (m; 16 H), 0.90 ppm (m; 3 H).

3-Undecyl-4-cyanophenol: Yield: 70 mg (0.26 mmol, 9.1 %). ^{1}H NMR (CDCl$_3$, 300 MHz): δ = 7.50 (m; 1 H), 6.77 (m; 1 H), 6.74 (m; 1 H), 5.86 (s; 1 H), 2.78 (t; 2 H), 1.67 (m; 2 H), 1.32 (m; 16 H), 0.90 ppm (m; 3 H).

2-(1-n-Hexylnonyl)-4-cyanophenol and 3-(1-n-Hexylnonyl)-4-cyanophenol: The general procedure was followed with 2.33 g (7.32 mmol, 1 eq.) 2-(1-n-hexylnonyl)-1,4-benzoquinone, 0.90 g (9.07 mmol, 1.2 eq.) TMSCN and 0.013 eq. potassium cyanide - 18-crown-6 complex. For the second step, 3.11 g (7.74 mmol, 1 eq.) unpurified product was added to 200 mL 0.1 M SmI_2 solution in THF. After purification two products were obtained.

2-(1-n-Hexylnonyl)-4-cyanophenol: Yield: 200 mg (0.6 mmol, 8.3 %). ^{1}H NMR (CDCl$_3$, 300 MHz): δ = 7.42 (m; 1 H), 7.38 (m; 1 H), 6.82 (m; 1 H), 5.38 (s; 1 H), 2.92 (m; 1 H), 1.61 (m; 4 H), 1.23 (m; 20 H), 0.88 ppm (m; 6 H).

3-(1-n-Hexylnonyl)-4-cyanophenol: Yield: 120 mg (0.36 mmol, 4.9 %). ^{1}H NMR (CDCl$_3$, 300 MHz): δ = 7.48 (m; 1 H), 7.73 (m; 1 H), 6.71 (m; 1 H), 5.45 (s; 1 H), 2.99 (m; 1 H), 1.60 (m; 4 H), 1.26 (m; 20 H), 0.89 ppm (m; 6 H).

Results and Discussion

Modeling. As can be seen from the optimized structures of the phenol-MTBE complexes as depicted in Figure 2 (see also Supp. Info. Figure S-1), H-bonds from the phenols to the ether moiety are all formed approximately along the O–H axis of the phenol, yielding nearly linear H-bond geometries. Only pentachlorophenol and pentafluorophenol deviate slightly from this

generalized picture. In the phenol – MTBE complex (complex **C1**, Figure 2) the H-bond length is relatively long (d = 1.80 Å, see Table 2 and Table S-1 in the Supp. Info.) while the bond angle is almost linear (α = 175°). For a phenol substituted with an electron-withdrawing group (henceforward EWG-substituted phenol), H-bond lengths are typically shorter. For example, in the 4-nitrophenol – MTBE complex (complex **C2**), the H-bond length d = 1.74 Å, while the shortest H-bond d = 1.71 Å was found for the pentafluorophenol – MTBE complex (**C9**, see Supp. Info. Figure S-1 and Table S-1).

d = 1.799 Å	d = 1.744 Å
A	B

d = 1.753 Å	d = 1.754 Å
C	D
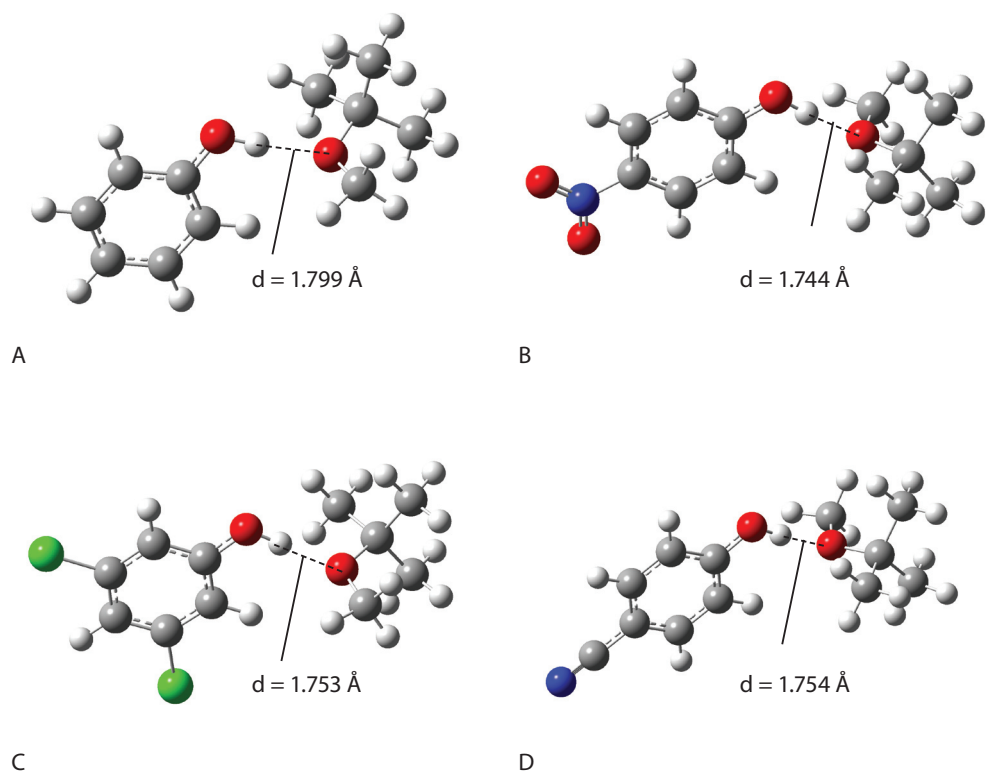
*Figure 2. B3LYP/6-311G(d,p)-optimized structures of four representative phenol – MTBE complexes: Phenol - MTBE (**C1**, A), 4-nitrophenol - MTBE (**C2**, B), 3,5-dichlorophenol - MTBE (**C4**, C) and 4-cyanophenol – MTBE (**C5**, D).*

In that case and in the case of pentachlorophenol, the H-bond angle α was found to be 163.7° and 151.8°, respectively, i.e. deviating markedly from the ideal 180°. The dihedral angle of these phenols was slightly larger than for the other phenols, and the formed H-bond was found to be tilted away

from the phenol ring. Steric effects are thus likely the cause for this deviating behavior. The bond lengthening (Table 2) of the hydrogen bond donor (phenolic O–H bond; r) upon complexation are found to be quite substantial (Δr = 0.015 Å for phenol and Δr = 0.020 Å for 4-nitrophenol; the highest Δr was found for pentafluorophenol – MTBE, Δr = 0.025 Å) and the dihedral angle of the phenols (C_2-C_1-O-H; ϕ) is close to zero (ϕ = -4.5 – +1.6°). This was also found recently for phenol – phosphine oxide complexes, while for example thiophenol – phosphine oxide complexes display a wide range of H-bond dihedral angles[15, 16] (see Chapters 2 and 3).

Table 2. Geometric parameters of selected B3LYP/6-311G(d,p)-optimized phenol – MTBE complexes; d (Å), α (°), Δr (Å), ϕ (°).

#	Complex	geometric parameters			
		d	α	Δr	ϕ
C1	Phenol – MTBE	1.799	175.1	0.015	-1.8
C2	4-nitrophenol – MTBE	1.744	176.2	0.020	1.4
C3	3-chlorophenol – MTBE	1.771	177.1	0.017	-1.3
C4	3,5-dichlorophenol – MTBE	1.753	177.0	0.019	-1.3
C5	4-cyanophenol – MTBE	1.754	176.3	0.019	1.3
C6	3-methyl-4-cyanophenol – MTBE	1.759	175.9	0.018	1.6

Enthalpies of complexation for selected phenol – MTBE complexes are summarized in Table 3 (a more extensive data set can be found in the Supp. Info. Tables S-2 through S-5). The enthalpy of complex formation ΔH (*in vacuo*) in complex **C1** is found to be -11.3 kcal/mol at the elaborate MP2/CBS level that is considered to be highly accurate.[16, 17] The counterpoise (CP) corrected MP2/6-311++G(2d,2p) method provides a reasonable estimate (ΔH = -9.1 kcal/mol), while CP-uncorrected B3LYP (*vacuo*) shows only a qualitative agreement (ΔH = -7.6 kcal/mol). The CP-uncorrected MP2 values all show more negative values than the MP2/CBS value due to the basis set superposition error (BSSE). Especially the ones with the smaller 6-311+G(d,p) basis set show an overestimation of the H-bonding energy (see Table 3 and Supp. Info, Tables S-2 and S-3). SCS-MP2 energy values are all less negative than the MP2/CBS value, but typically agree the MP2/CBS value on average to within 1.5 kcal/mol, an observation also made for phosphine oxide – phenol complexes and amine-N-oxide – phenol complexes (See Chapters 2-4).[16, 17] With CP-correction, the agreement of both methods with the MP2/CBS method becomes worse, suggesting that CP-

correction seriously overestimates the BSSE. M06-2X values calculated on the 6-311+G(d,p) level without CP-correction are on average only 0.1 kcal/mol off from the MP2/CBS energy values with a maximum deviation of only 0.39 kcal/mol, which is better than both the MP2 and the SCS-MP2 method. This fast and simple method therefore indeed seems to provide excellent energy predictions for the investigated complexes.

Table 3. Selected CP-uncorrected phenol – MTBE H-bond complex enthalpies (kcal/mol) in vacuo and in 'toluene' (mimicked by PCM (B3LYP) and SMD (M06-2X); in parentheses).

#	Complex	CBSQ	B3LYP	M06-2X	MP2	MP2	MP2	SCS-MP2	SCS-MP2
			A	A	CBS	A	B	A	B
C1	Phenol – MTBE	-7.24	-7.63 (-6.05)	-11.08 (-10.41)	-11.26	-11.69	-11.38	-10.40	-10.03
C2	4-nitrophenol –MTBE	-22.93	-9.81 (-8.08)	-13.10 (-12.35)	-13.16	-13.63	-13.26	-12.23	-11.79
C3	3-chlorophenol – MTBE	-2.32	-8.62 (-6.66)	-12.37 (-11.51)	-12.51	-13.11	-12.56	-11.72	-11.12
C4	3,5-dichlorophenol – MTBE	-22.87	-9.30 (-7.25)	-12.96 (-12.47)	-13.35	-13.85	-13.35	-12.43	-11.87
C5	4-cyanophenol – MTBE	-5.54	-9.36 (-7.68)	-12.67 (-11.87)	-12.88	-13.36	-12.97	-11.97	-11.52
C6	3-methyl-4 -cyanophenol – MTBE	-22.42	-9.10 (-7.46)	-13.05 (-12.36)	-12.69	-13.10	-12.76	-11.73	-11.34

A: 6-311+G(d,p)
B: 6-311++G(2d,p)

The CBS-Q energy results, initially added for the sake of having highly accurate values for comparison of the other methods used here, are found to be in disagreement with the results obtained by the other calculation methods. In the CBS-Q calculations, some of the EWG-phenol – MTBE complexes are found to show less negative binding enthalpies than the phenol – MTBE complex (compare 3-chlorophenol – MTBE (**C3**, Supp. Info. Figure S-1 and Table S-2) and phenol – MTBE (**C1**) with ΔH_{CBS-Q} values of -2.3 and -7.2 kcal/mol, respectively). Other EWG-phenol – MTBE interactions are found to show non-systematic behavior (cf. phenol (**C1**), 3-fluorophenol (**C7**), 3,5-difluorophenol (**C8**) and pentafluorophenol (**C9**) with ΔH_{CBS-Q} values of -7.2, -1.3, -17.2 and -13.2 kcal/mol, respectively). The erroneous behavior of the CBS-Q method cannot be explained as yet. Recently, similar behavior of the CBS-Q method was found for computations of H-bonds with oxygen-containing and sulphur-containing compounds[16, 17] where it was experimentally shown

that the CBS-Q results were not valid (see Chapters 2 through 4). These erroneous predictions by CBS-Q can have two possible causes: a) use of correct energy calculations on incorrect geometries, or b) use of incorrect energy calculations on correct geometries. Close inspection of the MP2(FC)/6-31G(d') geometries resulting from the CBS-Q calculations showed but a minor difference to the geometries found in the B3LYP optimization, and single-point energy recalculation of the resulting CBS-Q geometries with MP2/6-311++G(2d,2p) yielded energies within 1 kcal/mol of what was obtained on the B3LYP-optimized geometries. Therefore option b) is most likely. As a result, CBS-Q is also not useful as a benchmark method in these cases.

The B3LYP-derived natural population analysis (NPA) charges on the oxygen of the ether and the hydrogen of the phenol O–H moiety in the various complexes were found to be -0.65 ± 0.01 and +0.51 ± 0.01, respectively, and these values did not change significantly from one method to another. These charges indicate a clear electrostatic tendency to form H-bonds[24] (Table S-4 in the Supp. Info.). Some covalent character is also present, as can be deduced from the atom-atom overlap-weighted NAO bond orders (cf. Supp. Info. Table S-4). For example, the bond order between the phenol hydrogen and the MTBE oxygen amounts to 0.049 in the optimized geometry for the phenol – MTBE complex (**C1**), whereas the H-bond order is 0.063 for the 4-nitro-phenol – MTBE complex (**C2**). The highest H•••O bond order was found for the pentafluorophenol – MTBE complex (**C9**) and amounts to 0.073. The O–H bond order in the bound complex was found to be 0.62 for phenol and 0.60 for 4-nitrophenol, i.e. respectively 0.045 and 0.055 lower than in the unbound phenol. These data clearly suggest a partially covalent nature of the H-bond, but by far not as strong as was found in other H-bonds, e.g. amine-N-oxide – phenol H-bonds, where a maximum H-bond order of 0.13 and an O–H bond order decrease of 0.09 were found[16] (Chapter 4). Those H-bonds were formed involving a formally negatively charged oxygen atom, while in MTBE, of course, only a small negative charge is found on the oxygen atom (*vide supra*), forming a weaker H-bond.

In recent papers[16, 53, 54] a calculated H-bond enthalpy proportional to the inverse fifth power of the H-bond distance was found, in line with a claim[55] that such data should generally fit an inverse power relation $-\Delta H \approx f(d^{-a})$ with a >3. It can be seen from Figure 3, that the enthalpy of H-bonding $-\Delta H$ (MP2/CBS) in the current study is calculated to be proportional to the H-bond length $d_{H\cdot\cdot O}$ to the power -5.6 (i.e. $d_{H\cdots O}^{-5.6}$, $d_{H\cdots O}$ = H-bond distance). The proportionality to the inverse 5.6th power is rather steep, and in fact, steeper than what was found in the mentioned papers, but it still

implies that the present data also fit this claim, even though the current data concern much weaker H-bonds than those investigated in the mentioned papers.

The geometric and electronic parameters and binding affinities of the MTBE-complexes of other phenols are comparable to the ones mentioned in Tables 2 and 3, and are therefore only given in the Supp. Info. Tables S-1 through S-5.

In the modeling experiments as described here, the binding enthalpies ΔH are found to be more negative for the more highly EWG-substituted phenols. The phenol – MTBE complex (**C1**) shows the weakest H-bond (-11.3 kcal/mol at the MP2/CBS level), and H-bonds are stronger with more acidic phenols (cf.: 3-chlorophenol – MTBE (**C3**) and 3,5-dichlorophenol – MTBE (**C4**) with binding strengths of -12.5 and -13.4 kcal/mol (MP2/CBS), respectively). Other well-performing phenols for MTBE binding are 4-nitrophenol, 3-cyanophenol and 4-cyanophenol with ΔH values of -13.2, -13.2 and -12.9 kcal/mol (MP2/CBS), respectively. Considering the pKa values of phenol (9.98),[56] 3-chlorophenol (9.02),[56] 3,5-dichlorophenol (8.04)[57] and 4-cyanophenol (7.95),[56] this can be attributed to their higher electron-accepting ability (i.e., a more acidic proton yields a stronger H-bond). However, much stronger H-bonds would then be expected for the pentachlorophenol and pentafluorophenol, with pKa values of 4.74[58] and 5.53,[58] respectively, though this is not the case. Comparative B3LYP and M06-2X-calculations (both with the 6-311+G(d,p) basis set) on 2,6-difluorophenol (pKa = 7.51[58]; see Supp. Info table S-6) showed a weaker complex formation than for 3-fluorophenol (pKa = 9.28)[56] and 3,5-difluorophenol (pKa = 8.66),[58] where on the basis of its pKa a stronger complex was expected. Although for 2,6-difluorophenol – MTBE the H•••O H-bond order was found to be higher and the O-H bond order (in the phenol) was found to be lower than for 3-fluorophenol and 3,5-difluorophenol, i.e. pointing to stronger electronic inter-actions, the overall H-bonding strength is apparently lower because the H-bond angle of the complex is deviating more from the ideal angle of 180°, resulting in a less-than-optimal H-bond geometry, and thus yielding lower bond energies. The favorable electronic features are thus dominated by unfavorable steric features that apparently hamper the formation of a strong H-bond, as has been shown in a similar fashion for surface adsorption of substituted phenols.[59] Nonetheless, these high ΔH values indicate that the more acidic phenols might be good candidates for MTBE binding for use in SIRs, as ΔH approximates the -15 kcal/mol value that would combine efficient binding with efficient regeneration at higher temperatures. Of course, this is critically dependent on the H-bonding interactions of e.g. phenol with itself *(vide infra)*.
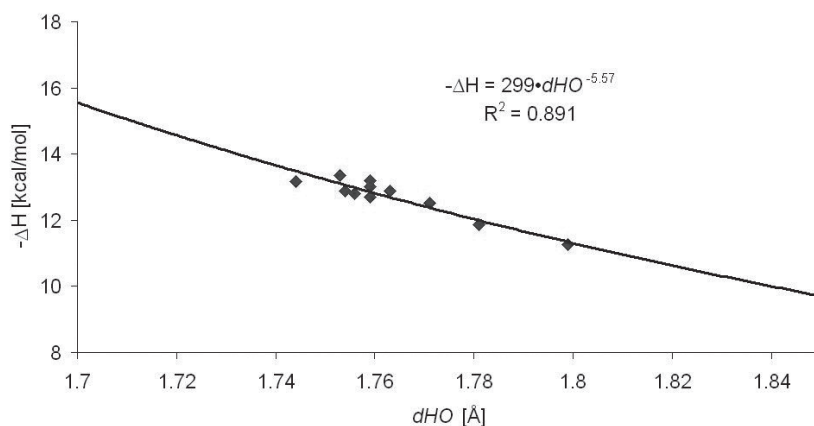
$-\Delta H = 299 \cdot dHO^{-5.57}$
$R^2 = 0.891$

Figure 3. Relation between −ΔH (MP2/CBS) and H-bond distance $d_{H\cdots O}$ for phenol – MTBE H-bond complexes.[84]

The modeling results predict the formation of a 1 : 1 H-bonded complex between phenol and MTBE, but the data *in vacuo* cannot provide an accurate account of the experimental ΔH^0 values in solution, as they neglect the effect of e.g. any breaking up of phenol dimers/oligomers upon complex formation, and the effect of solvents (*vide infra*). The effect of the solvent polarity on the H-bond binding energy in cyclohexane, mesitylene, toluene, and benzene was studied in more detail via solvent continuum models. These solvents are model solvents for the apolar phase in SIRs. B3LYP and M06-2X calculations (Table 3, values for toluene are in parentheses; a more extensive data set can be found in the Supp. Info Table S-5) were used to this aim. To mimic the solvent effects in the computations, the IEF-PCM[60] and SMD[61] models were used.

The calculated ΔH for complex formation for model complex **C1** in toluene was -6.1 kcal/mol (B3LYP/PCM, Table 3 and Supp. Info. Table S-5), i.e. markedly less stable than *in vacuo* (ΔH^{vac}_{B3LYP} = -7.6 kcal/mol). Weaker complex formation was also found for the other apolar solvents. Also for the M06-2X/SMD calculations, the solvent complexes showed less negative binding enthalpies (compare e.g. complex **C1** with ΔH^{tol}_{M06-2X} = -10.4 kcal/mol vs. ΔH^{vac}_{M06-2X} = - 11.1 kcal/mol). For M06-2X/SMD, solvent-induced weakening of the complex is found to be most pronounced in cyclohexane (dielectric permittivity ε = 2.202), less in mesitylene (ε = 2.265) and toluene (ε = 2.379), and least in benzene (ε = 2.247) in all cases. For B3LYP/PCM, this systematic behavior was not observed (See for the full data set in all these solvents the Supp. Info. Table S-5).

For actual physical application of phenols for MTBE binding in solution, the halogen-containing phenols and 4-nitrophenol are problematic, because their solubility in apolar organic solvents is limited and their water solubility is high. Of the compounds under current study the only phenols that are soluble to a certain extent are phenol and cyanophenol. To increase solubility in hydrophobic solvents and, with the application in mind, to decrease water solubility, an aliphatic tail must be introduced. As the synthesis of alkylated halogen-containing phenols is elaborate and therefore likely not cost-effective, only alkyl-substituted 4-cyanophenols were synthesized. The calculated alkyl-substituted cyanophenol (model compound 3-methyl-4-cyanophenol, complex **C6**) performed almost as well as the unsubstituted 4-cyanophenol. The binding enthalpy (MP2/CBS) was found to be -12.7 kcal/mol, vs. -12.9 kcal/mol for the 4-cyanophenol and thus significantly more negative than phenol itself (-11.3 kcal/mol), displaying the potential of such materials.

Isothermal Titration Calorimetry. In ITC measurements the synthesized alkyl-substituted cyano-phenols were tested for their MTBE-binding ability. An example of a calorimetric titration of MTBE with 3-undecyl-4-cyanophenol in toluene at 30 °C is given in Figure 4. From integrating the binding isotherm (top pane), the binding curve can be fitted (integrated heat effect per injection; bottom pane), which yields the stoichiometry N, binding enthalpy ΔH^0, and the binding affinity K (see Table 4).

The binding of MTBE by 3-undecyl-4-cyanophenol is characterized by a binding affinity K of 12 ± 6 M^{-1} and a ΔH^0 of $+9 \pm 5$ kcal/mol. The H-bonding process is therefore entropy-driven. Because of the relatively low binding affinity and therefore shallow binding isotherm, the equivalence point is not clear and could not be determined precisely, but the data unequivocally point to a 1 : 1 complex for all phenols involved. The fitted 1 : 1 binding ratio suggests that binding of phenol to MTBE, however weak, is not accompanied by any other binding event. Because of the relatively low binding affinity K (compare for example the H-bond of alkylamine-N-oxides with phenol in toluene with K ~ 10^4 M^{-1} in Chapter 4),[17] these values show a relatively large uncertainty (see Table 4). Interestingly, the overall enthalpy change is positive in all cases, whereas an overall negative ΔH^0 was expected for H-bonding.[30] Evidently, breaking up of the H-bonds between (clusters of) the phenols and of the Van der Waals interactions and $\pi\pi$ interactions between the phenol and the solvent in the surrounding solvent system (all relatively weak), can contribute to the unfavorable ΔH upon complex formation. Although more extensive studies would be required to accurately model specifically the changes involving the solvents, some indications for this discrepancy can

be provided. In ITC measurements, dimer formation of the phenols could not be demonstrated: no dilution-induced breaking of phenol dimers could be measured, probably due to low concentrations and a low heat effect.
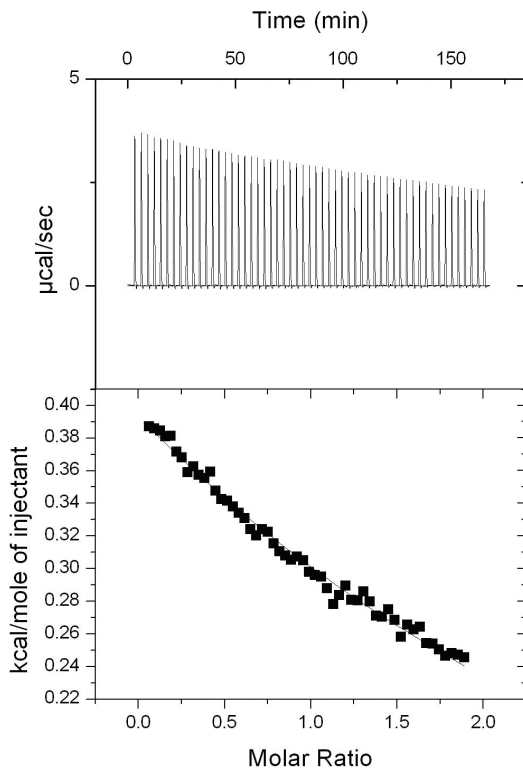
Figure 4. Calorimetric titration of MTBE with 3-undecyl-4-cyanophenol in toluene at 30 °C. Top pane: raw data; bottom pane: integrated data.

Therefore additional calculations of dimers of phenol, 3-fluorophenol, 3,5-difluorophenol, 4-cyanophenol and 3-methyl-4-cyanophenol *in vacuo* (M06-2X/6-311+G(d,p)//M06-2X/6-311G(d,p)) and in solvents (M06-2X/SMD) were performed, which revealed that ΔH of dimerization is around -8 kcal/mol *in vacuo* and around -6 to -8 kcal/mol in the various solvents (see Supp. Info Table S-7). This is close to the experimentally observed value of -5.75 kcal/mol for phenol dimers in CCl_4.[62] If phenols are primarily present as dimers in toluene at the used concentrations, this would thus cost half of the 6 – 8 kcal/mol per H-bond – if phenol is predominantly present within larger clusters, this could cost up to 8 kcal/mol per H-bond. In addition, $\pi\pi$ interactions might have lead to less favorable complex formation to MTBE, caused by stabilization of the phenol (without H-bond) by

the solvent, with a ΔH^0 of approximately -1.85 kcal/mol in benzene.[63] Phenol – solvent complexes in toluene (the solvent used in the present studies) are likely similar in strength. Such considerations would predict an overall enthalpy change of close to zero or a slightly positive value. Although then these values do as yet not add up to predict quantitative agreement with our ITC data, it is clear that such inter-phenolic H-bonds, $\pi\pi$ interactions, and, for the alkane-substituted phenols, as yet unaccounted for entropic effects (*vide infra*) do play a role. For further studies therefore both more extensive solvent models and more accurate experimental thermodynamic data are needed.

Table 4. Results of ITC experiments for complexation of phenols with MTBE at 30 °C in toluene.

Phenol	K [M^{-1}]	ΔH^0 [kcal/mol]	ΔG^0 [kcal/mol]	$T\Delta S^0$ [kcal/mol]
3-C$_{11}$-4-CN-PhOH	12 ± 6	9 ± 5	-2 ± 1	11 ± 2
2-C$_{11}$-4-CN-PhOH	3 ± 1	22 ± 9	-1 ± 1	23 ± 6
3-C$_6$C$_9$-4-CN-PhOH	23 ± 19	3 ± 4	-2 ± 1	5 ± 2
2-C$_6$C$_9$-4-CN-PhOH	6 ± 2	17 ± 9	-1 ± 1	18 ± 6

In the calorimetric titration of MTBE with 2-undecyl-4-cyanophenol in toluene the binding affinity is markedly lower than for 3-undecyl-4-cyanophenol (K = 3 and 12 M^{-1}, respectively). The calculated stability of MTBE complexes of 2-methyl-4-cyanophenol and 3-methyl-4-cyanophenol (complexes **C6** and **C13**, model complexes for the ones investigated by ITC) did not yield large differences (up to 0.2 kcal/mol; MP2/CBS) with that obtained with 4-cyanophenol (complex **C5**). Because the difference in binding affinity that was found in the ITC measurements can thus not be assigned to electronic effects, this lower binding affinity can only be due to the different position of the alkyl chain on the phenolic ring. Therefore, it is likely that the alkyl chain on the 2-position hinders the H-bonding with the MTBE molecule sterically, and thereby weakens the H-bond and lowers K. The same effect can be seen with the 1-n-hexylnonyl-substituted cyanophenols, where the 2-alkyl compound shows a markedly lower binding strength than the 3-alkyl cyanophenol (K = 6 and 23 M^{-1}, respectively). Moreover, the fact that the binding of MTBE is accompanied with such a large change of entropy might be explained by dimerization of the alkyl-substituted phenols prior to H-bonding. The alkyl-chains cannot move around freely in a phenolic dimer, as they are mutually sterically hindered. On MTBE binding, these chains regain their full entropic freedom and thus cause the binding of MTBE to be energetically favorable. A non-optimized

space-filling 3D depiction of 2-(1-n-hexyl-nonyl)-4-cyanophenol (Figure 5) shows that the O-H group is almost buried under the alkyl tail, which thus can really hamper H-bonding given the rotational freedom of the C–C bonds in the alkyl moiety.
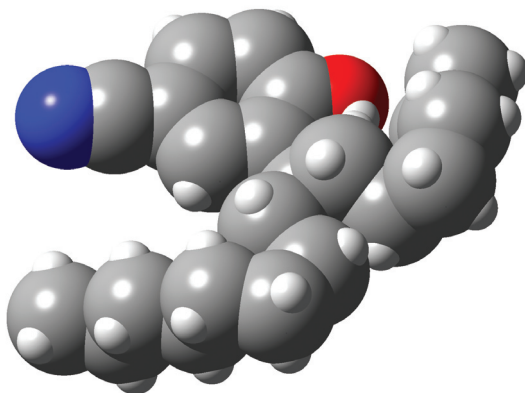

Figure 5. A space-filling 3D depiction of 2-(1-n-hexylnonyl)-4-cyanophenol, showing that the O–H moiety (top-midst) can be almost buried under the alkyl chains.

The investigated phenols show a moderate binding affinity for MTBE. However, for applications such as SIRs the moderate binding behavior might just be sufficient. Previously found distribution coefficients of MTBE are as low as 9 with a liquid silicone polymer,[7] but around 18 for toluene.[8] With a presently found value for the binding affinity of over 23 M^{-1} with alkyl-substituted cyano-phenols in toluene, combined with a reasonable physical distribution coefficient of 18 for the used solvent, the overall water-organic solvent distribution coefficients will be significantly enhanced to ~ $4 \cdot 10^2$. This value is even higher than current industrially used distribution coefficients of 36 to 172 (for the extraction of phenol),[64] and thus shows that alkylated cyanophenols are, in principle, viable compounds. The branched alkyl-substituted cyanophenols have industrially relevant properties such as a low melting point (removes the need for a solvent) and a high boiling point (beneficial for regeneration of the SIR). They have a good solubility in organic solvents and they are virtually insoluble in water. The present study shows that these alkyl-substituted cyanophenols are a class of electronically tunable materials, and they might just provide the edge that is needed to enhance the SIR extraction process, so that it can be carried out more adequately in the near future.

Conclusion

Isothermal titration calorimetry combined with quantum chemical molecular modeling shows that formation of a H-bonded 1 : 1 complex between phenols and MTBE occurs in apolar solvents. This is highly attractive for large-scale solvent-impregnated resin (SIR)-based separations. Isothermal titration calorimetric measurements of these phenol – MTBE complexes yield a binding affinity of up to $K = 23$ M^{-1} in toluene, especially for phenols with electron-withdrawing groups (EWGs) attached to the phenyl ring. This H-bond equilibrium is entropically driven, and results from an enthalpically favorable H-bond between phenols and MTBE (-10 to -13 kcal/mol) (M06-2X/SMD values), in combination with enthalpically unfavorable breaking of H-bonds between phenols and phenol-solvent interactions. Alkyl tails were attached to the EWG-substituted phenols to obtain the industrially important characteristics of a low melting point (removes, in principle, the need for a solvent), a high solubility in organic solvents and a really low solubility in water. The combination of experiments and calculations thus yielded 3-alkyl-4-cyanophenols as materials for which an overall distribution coefficient of $\sim 4 \cdot 10^2$ can be reached, making this an industrially interesting class of compounds for the environmentally highly relevant problem of MTBE removal in water purification.

CBS-Q modeling was found to predict inconsistent results and as a result, it can not be used as a benchmark in these H-bond complexes. Relatively cheap SCS-MP2/6-311+G(d,p) and M06-2X/6-311+G(d,p) calculations without counterpoise correction agree very well with the MP2/CBS values, and in all cases clearly agree better than counterpoise corrected calculations.

Acknowledgments

References

(1)   http://www.epa.gov/mtbe/gas.htm, **2010**.

(2)   European Fuel Oxygenates Association, **2010**.

(3)   W. E. May, S. P. Wasik, M. M. Miller, Y. B. Tewari, J. M. Brownthomas, R. N. Goldberg, *J. Chem. Eng. Data* **1983**, *28*, 197.

(4)   A. A. M. Langenhoff, Netherlands Centre for Soil Quality Management and Knowledge Transfer (SKB SV-018), **2000**.

(5)   A. A. Keller, *Health and Environment Assessment of MTBE, Report to Legislature of the State of California, Volume III,* 1998.

(6)   U. Peters, F. Nierlich, E. Schulte-Körne, M. Sakuth, R. Deeb, M. Laugier, M. Suominen, M. Kavanaugh, in *Encyclopedia of Industrial Chemistry, Methyl-tert-Butyl Ether*, 7 ed., John Wiley & Sons, 2003.

(7)   J. Martinez, A. A. Keller, *Development of Supported Polymeric Liquid Membrane Technology for Aqueous MTBE Mitigation,* Electric Power Research Institute, 2002.

(8)   B. Burghoff, J. Schiferli, J. S. Marques, A. B. de Haan, *Chem. Eng. Sci.* **2009**, *64*, 2887.

(9)   J. L. Cortina, A. Warshawsky, in *Ion Exch. Solvent Extr., Vol. 13* (Eds.: J. A. Marinsky, Y. Marcus), Dekker, New York, 1997, pp. 195.

(10)   S. S. El-Dessouky, E. H. Borai, *J. Radioanal. Nucl. Chem.* **2006**, *268*, 247.

(11)   B. B. Gupta, Z. B. Ismail, *Comp. Interf.* **2006**, *13*, 487.

(12)   J. S. Liu, H. Chen, Z. L. Guo, Y. C. Hu, *J. Appl. Pol. Sc.* **2006**, *100*, 253.

(13)   K. Ohnaka, A. Yuchi, *Chem. Lett.* **2005**, *34*, 868.

(14)   B. Burghoff, R. Cuypers, M. van Ettinger, E. J. R. Sudhölter, H. Zuilhof, A. B. de Haan, *Sep. Purif. Techn.* **2009**, *67*, 117.

(15)   R. Cuypers, B. Burghoff, A. T. M. Marcelis, E. J. R. Sudhölter, A. B. de Haan, H. Zuilhof, *J. Phys. Chem. A* **2008**, *112*, 11714.

(16)   R. Cuypers, E. J. R. Sudhölter, H. Zuilhof, *ChemPhysChem*, **2010**, *11*, 2230.

(17)   R. Cuypers, S. Murali, A. T. M. Marcelis, E. J. R. Sudhölter, H. Zuilhof, *ChemPhysChem,* accepted.

(18)   R.-S. Juang, H.-L. Chang, *Ind. Eng. Chem. Res.* **1995**, *34*, 1294.

(19)   M. Traving, H.-J. Bart, *Chem. Eng. Technol.* **2002**, *25*, 997.

(20)   A. Kostova, H.-J. Bart, *Chemie Ingenieur Technik* **2004**, *76*, 1743.

(21)   H. Kitazaki, M. Ishimaru, K. Inone, K. Yoshida, S. Nakamura, in *Proceedings of the International Solvent Extraction Conference*, ISEC'96 ed., Melbourne, Australia, 1996, pp. 1667.

(22)   B. Burghoff, E. L. V. Goetheer, A. B. de Haan, *React. Funct. Pol.* **2008**, *68*, 1314.

(23)   G. R. Desiraju, T. Steiner, *The Weak Hydrogen Bond*, 1 ed., Oxford University Press, New York, 1999.

(24)   G. A. Jeffrey, *An Introduction to Hydrogen Bonding*, Oxford University Press, New York, Oxford, 1997.

(25)   J. P. M. Lommerse, S. L. Price, R. Taylor, *J. Comp. Chem.* **1997**, 18, 757.

(26)   S. K. Panigrahi, G. R. Desiraju, *Proteins: Structure, Function, and Bioinformatics* **2007**, *67,* 128.

(27)   G. B. W. L. Ligthart, D. Guo, A. L. Spek, H. Kooijman, H. Zuilhof, R. P. Sijbesma, *J. Org. Chem.* **2008**, *73*, 111.

(28)   A. S. N. Murthy, C. N. R. Rao, *Appl. Spectr. Rev.* **1968**, *2,* 69.

(29)   J. E. Ladbury, *Biotechniques* **2004**, *37*, 885.

(30)   J. E. Ladbury, M. L. Doyle, *Biocalorimetry 2*, John Wiley & Sons, Ltd, New York, 2004.

(31)   S. Leavitt, E. Freire, *Curr. Op. Struct. Biol.* **2001**, *11*, 560.

(32)   P. C. Weber, F. R. Salemme, *Curr. Op. Struct. Biol.* **2003**, *13*, 115.

(33)   T. Wiseman, S. Williston, J. F. Brandts, L.-N. Lin, *Anal. Biochem.* **1989**, *179*, 131.

(34)   T. J. M. de Bruin, A. T. M. Marcelis, H. Zuilhof, L. M. Rodenburg, H. A. G. Niederländer, A. Koudijs, P. E. M. Overdevest, A. van der Padt, E. J. R. Sudhölter, *Chirality* **2000**, *12*, 627.

(35)   T. J. M. de Bruin, A. T. M. Marcelis, H. Zuilhof, E. J. R. Sudholter, *Langmuir* **2000**, *16*, 8270.

(36)   H. J. Wiggers, J. Cheleski, A. Zottis, G. Oliva, A. D. Andricopulo, C. A. Montanari, *Anal. Biochem.* **2007,** *370*, 107.

(37)   A. Arnaud, L. Bouteiller, *Langmuir* **2004**, *20*, 6858.

(38)   P. Ballester, M. Capo, A. Costa, P. M. Deya, R. Gomila, A. Decken, G. Deslongchamps, *J. Org. Chem.* **2002**, *67*, 8832.

(39)   D. Merino-Garcia, S. I. Andersen, *Pet. Sc. Technol.* **2003**, *21,* 507

(40)   D. Merino-Garcia, S. I. Andersen, *Langmuir* **2004**, *20*, 4559.

(41)   J. L. Sessler, D. E. Gross, W. S. Cho, V. M. Lynch, F. P. Schmidtchen, G. W. Bates, M. E. Light, P. A. Gale, *J. Am. Chem. Soc.* **2006**, *128*, 12281.

(42)   T. Mizutani, H. Takagi, Y. Ueno, T. Horiguchi, K. Yamamura, H. Ogoshi, *J. Phys. Org. Chem.* **1998**, *11*, 737.

(43)   M. Xiang, M. Jiang, Y. Zhang, C. Wu, L. Feng, *Macromol.* **1997**, *30*, 2313.

(44)   Y. Zhao, D. G. Truhlar, *J. Chem. Theor. Comp.* **2007**, *3,* 289.

(45)   Y. Zhao, D. G. Truhlar, *Acc. Chem. Res.* **2008**, *41*, 157.

(46)   Y. Zhao, D. G. Truhlar, *Theor. Chem. Acc.* **2008**, *120*, 215.

(47)   J. W. Ochterski, G. A. Petersson, J. A. Montgomery, *J. Chem. Phys.* **1996**, *104,* 2598.

(48)   J. Antony, S. Grimme, *J. Phys. Chem. A* **2007**, *111*, 4862.

(49)   R. A. Bachorz, F. A. Bischoff, S. Hofener, W. Klopper, P. Ottiger, R. Leist, J. A. Frey, S. Leutwyler, *Phys. Chem. Chem. Phys.* **2008**, *10*, 2758.

(50)   S. Grimme, *J. Chem. Phys.* **2003**, *118*, 9095.

(51)   T. Schwabe, S. Grimme, *Acc. Chem. Res.* **2008**, *41*, 569.

(52)   M. Piacenza, S. Grimme, *ChemPhysChem* **2005**, *6*, 1554.

(53)   J. Chen, M. A. McAllister, J. K. Lee, K. N. Houk, *J. Org. Chem.* **1998**, *63*, 4611.

(54)   E. Espinosa, E. Molins, C. Lecomte, *Chem. Phys. Lett.* **1998**, *285*, 170.

(55)   M. Rozenberg, A. Loewenschuss, Y. Marcus, *Phys. Chem. Chem. Phys.* **2000**, *2*, 2699.

(56)   K. C. Gross, *Int. J. Quant. Chem.* **2001**, *85,* 569.

(57)   V. Pino, F. Conde, J. Ayala, V. González, A. Afonso, *Chromatographia* **2006**, *63*, 167.

(58)   K. Liao, B. W. Pack, N. P. Toltl, *J. Pharm. Biom. Anal.* **2007**, *44*, 118.

(59)   S. R. Holmes-Farley, *Langmuir* **1988**, *4*, 766.

(60)   M. Cossi, G. Scalmani, N. Rega, V. Barone, *J. Chem. Phys.* **2002**, *117*, 43.

(61)   A. V. Marenich, C. J. Cramer, D. G. Truhlar, *J. Phys. Chem. B* **2009**, *113*, 6378.

(62)   P. Hobza, C. Riehn, A. Weichert, B. Brutschy, *Chem. Phys.* **2002**, *283*, 331.

(63)   M. O. Sinnokrot, C. D. Sherrill, *J. Phys. Chem. A* **2003**, *107*, 8377.

(64)   C. F. Yang, Q. A. Yu, L. J. Zhang, J. Z. Feng, *Chem. Eng. J.* **2006**, *117*, 179.

(65)   M. Chellani, *Am. Biotechnol. Lab.* **1999**, *17*, 14.

(66)   M. J. Frisch, G. W. Trucks, H. B. Schlegel, G. E. Scuseria, M. A. Robb, J. R. Cheeseman, G. Scalmani, V. Barone, B. Mennucci, G. A. Petersson, H. Nakatsuji, M. Caricato, X. Li, H. P. Hratchian, A. F. Izmaylov, J. Bloino, G. Zheng, J. L. Sonnenberg, M. Hada, M. Ehara, K. Toyota, R. Fukuda, J. Hasegawa, M. Ishida,

T. Nakajima, Y. Honda, O. Kitao, H. Nakai, T. Vreven, J. A. Montgomery, Jr., J. E. Peralta, F. Ogliaro, M. Bearpark, J. J. Heyd, E. Brothers, K. N. Kudin, V. N. Staroverov, R. Kobayashi, J. Normand, K. Raghavachari, A. Rendell, J. C. Burant, S. S. Iyengar, J. Tomasi, M. Cossi, N. J. Rega Millam, M. Klene, J. E. Knox, J. B. Cross, V. Bakken, C. Adamo, J. Jaramillo, R. E. Gomperts, O. Stratmann, A. J. Yazyev, R. Austin, C. Cammi, J. W. Pomelli, R. Ochterski, R. L. Martin, K. Morokuma, V. G. Zakrzewski, G. A. Voth, P. Salvador, J. J. Dannenberg, S. Dapprich, A. D. Daniels, O. Farkas, J. B. Foresman, J. V. Ortiz, J. Cioslowski, D. J. Fox, Gaussian, Inc., Wallingford CT, **2009**.

(67) C. J. Cramer, *Essentials Of Computational Chemistry: Theories And Models*, 2nd ed., John Wiley & Sons, Ltd, 2004.

(68) P. Jurečka, J. Šponer, J. Černy, P. Hobza, *Phys. Chem. Chem. Phys*. **2006**, *8*, 1985.

(69) S. Raub, C. M. Marian, *J. Comput. Chem*. **2007**, *28*, 1503.

(70) M. R. Nyden, G. A. Petersson, *J. Chem. Phys*. **1981**, *75*, 1843.

(71) S. F. Boys, F. Bernardi, *Mol. Phys*. **1970**, *19*, 553.

(72) F. B. van Duijneveldt, J. G. C. M. van Duijneveldt - van de Rijdt, J. H. van Lenthe, *Chem. Rev*. **1994**, *94*, 1873.

(73) G. Alagona, *Int. J. Quant. Chem*. **1987**, *32*, 227.

(74) S. Cybulski, S. Scheiner, *J. Phys. Chem*. **1990**, *94*, 6106.

(75) H. Umeyama, K. Morokuma, *J. Am. Chem. Soc*. **1977**, *99*, 1316.

(76) D. Hadži, *Theoretical treatments of hydrogen bonding*, Wiley, New York, 1997.

(77) E. D. Glendening, A. E. Reed, J. E. Carpenter, F. Weinhold., NBO Version 3.1.

(78) A. E. Reed, R. B. Weinstock, F. Weinhold, *J. Chem. Phys*. **1985**, *83*, 735.

(79) D. W. Guo, R. P. Sijbesma, H. Zuilhof, *Org. Lett*. **2004**, *6*, 3667.

(80) R. Jockers, R. D. Schmid, H. Rieger, K. Krohn, *Liebigs Ann. Chem*. **1991**, *4*, 315.

(81) D. A. Evans, J. M. Hoffman, L. K. Truesdale, *J. Am. Chem. Soc*. **1973**, *95*, 5822.

(82) S. H. Olson, S. J. Danishefsky, *Tetrahedron Lett*. **1994**, *35*, 7901.

(83) R. Yoneda, S. Harusawa, T. Kurihara, *J. Org. Chem*. **1991**, *56*, 1827.

(84) The pentafluorophenol and pentachlorophenol complexes were left out of this analysis because in those two complexes steric effects also influence the binding enthalpies (*vide supra*).
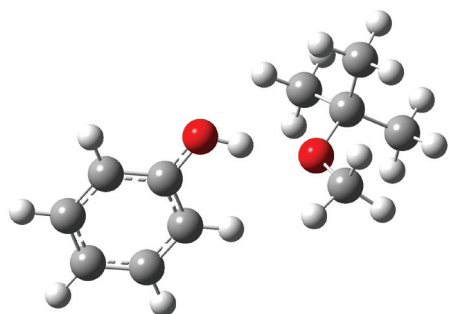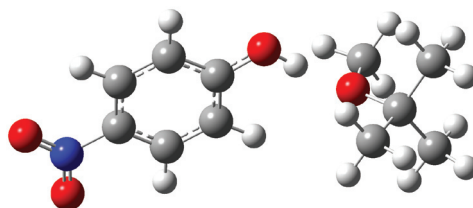
Phenol – MTBE (**C1**)

4-nitrophenol – MTBE (**C2**)
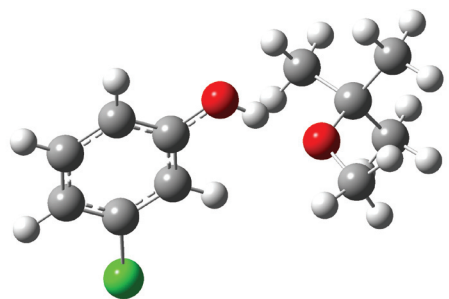
3-chlorophenol – MTBE (**C3**)
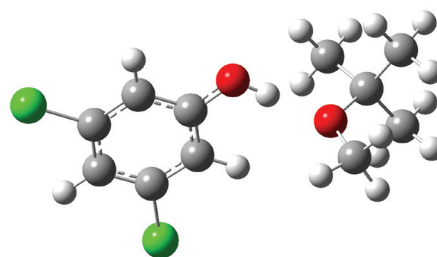
3,5-dichlorophenol – MTBE (**C4**)

Figure S-1. B3LYP/6-311G(d,p)-optimized structures of all phenol – MTBE complexes.
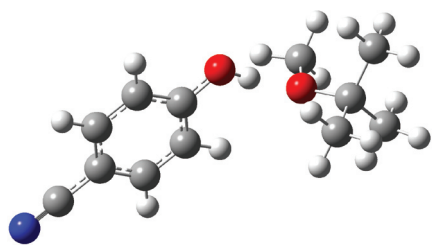
4-cyanophenol – MTBE (**C5**)
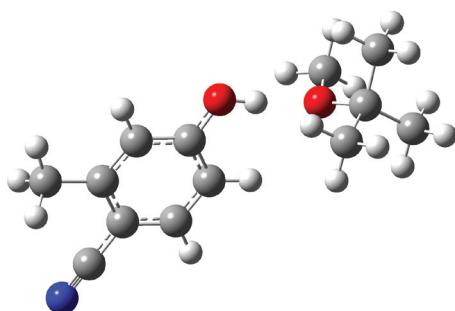
3-methyl-4-cyanophenol – MTBE (**C6**)
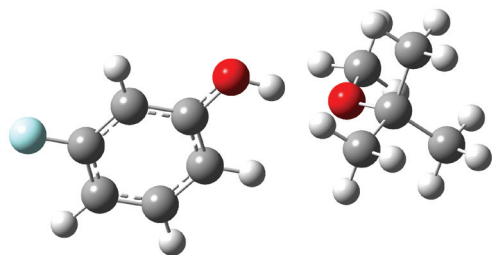
3-fluorophenol – MTBE (**C7**)
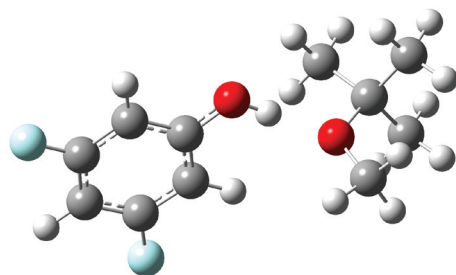
3,5-difluorophenol – MTBE (**C8**)

Figure S-1. B3LYP/6-311G(d,p)-optimized structures of all phenol – MTBE complexes (continued).
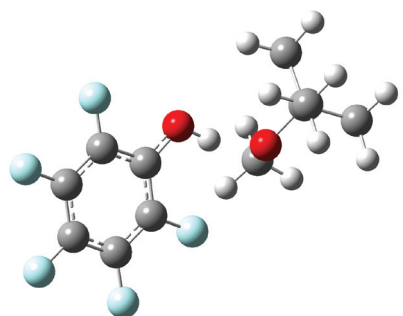
pentafluorophenol – MTBE (**C9**)
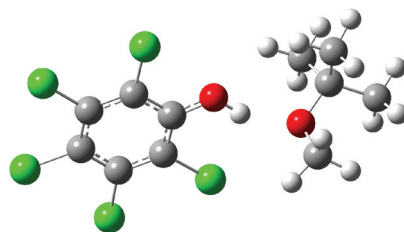
pentachlorophenol – MTBE (**C10**)
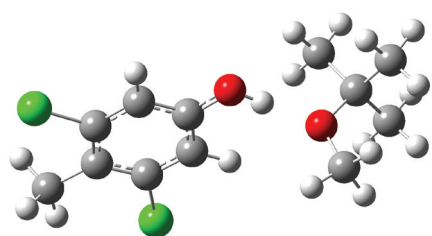
3,5-dichloro-4-methylphenol – MTBE (**C11**)
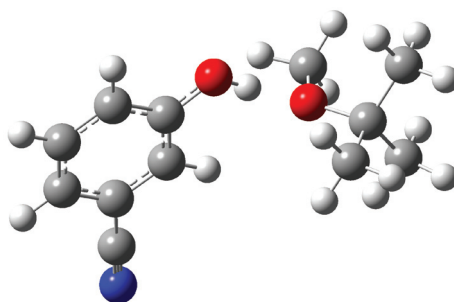
3-cyanophenol – MTBE (**C12**)

Figure S-1. B3LYP/6-311G(d,p)-optimized structures of all phenol – MTBE complexes (continued).
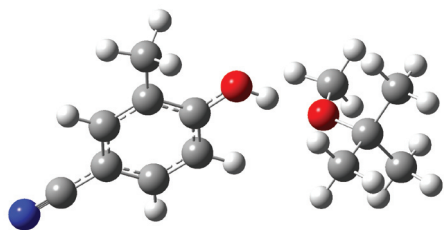
2-methyl-4-cyanophenol – MTBE (**C13**)

Figure S-1. B3LYP/6-311G(d,p)-optimized structures of all phenol – MTBE complexes (continued).

Table S-1. Geometric parameters of B3LYP/6-311G(d,p)-optimized phenol – MTBE complexes in vacuo; d (Å), α (°), Δr (Å) and ϕ (°).

#	Complexant	geometric parameters			
		d	*α*	*Δr*	*ϕ*
C1	PhOH	1.799	175.1	0.015	-1.8
C2	4-NO$_2$-PhOH	1.744	176.2	0.020	1.4
C3	3-Cl-PhOH	1.771	177.1	0.017	-1.3
C4	3,5-Cl$_2$-PhOH	1.753	177.0	0.019	-1.3
C5	4-CN-PhOH	1.754	176.3	0.019	1.3
C6	3-Me-4-CN-PhOH	1.759	175.9	0.018	1.6
C7	3-F-PhOH	1.781	175.5	0.016	1.6
C8	3,5-F$_2$-PhOH	1.763	176.9	0.018	-1.2
C9	F$_5$-PhOH	1.712	163.7	0.025	-4.5
C10	Cl$_5$-PhOH	1.794	151.8	0.019	-2.3
C11	3,5-Cl$_2$-4-Me-PhOH	1.759	177.1	0.018	-1.6
C12	3-CN-PhOH	1.759	177.6	0.018	1.1
C13	2-Me-4-CN-PhOH	1.756	176.2	0.019	1.4

Table S-2. CP-corrected phenol – MTBE H-bond complex enthalpies in vacuo (kcal/mol).

#	Complexant	CBSQ	MP2	MP2	MP2	SCS-MP2	SCS-MP2
			CBS	A	B	A	B
C1	PhOH	-7.24	-11.26	-8.45	-9.09	-7.30	-7.72
C2	4-NO$_2$-PhOH	-22.93	-13.16	-10.10	-10.76	-8.84	-9.25
C3	3-Cl-PhOH	-2.32	-12.51	-9.34	-10.02	-8.12	-8.55
C4	3,5-Cl$_2$-PhOH	-22.87	-13.35	-9.94	-10.71	-8.70	-9.21
C5	4-CN-PhOH	-5.54	-12.88	-9.93	-10.58	-8.69	-9.10
C6	3-Me-4-CN-PhOH	-22.42	-12.69	-9.71	-10.33	-8.49	-8.88
C7	3-F-PhOH	-1.28	-11.86	-9.03	-9.61	-7.87	-8.22
C8	3,5-F$_2$-PhOH	-17.15	-12.89	-9.84	-10.39	-8.65	-8.97
C9	F$_5$-PhOH	-13.18	-12.54	-9.08	-9.71	-7.82	-8.18
C10	Cl$_5$-PhOH	-21.90	-11.69	-7.58	-8.43	-6.34	-6.87
C11	3,5-Cl$_2$-4-Me-PhOH	-19.87	-13.01	-9.69	-10.38	-8.45	-8.90
C12	3-CN-PhOH	-11.53	-13.20	-10.19	-10.82	-8.91	-9.30
C13	2-Me-4-CN-PhOH	-18.98	-12.82	-9.85	-10.49	-8.59	-9.00

A: 6-311+G(d,p)
B: 6-311++G(2d,2p)

Table S-3. CP-uncorrected phenol – MTBE H-bond complex enthalpies in vacuo (kcal/mol).

#	Complexant	CBSQ	MP2	B3LYP	MP2	MP2	SCS-MP2	SCS-MP2	M06-2X
			CBS	A	A	B	A	B	A
C1	PhOH	-7.24	-11.26	-7.63	-11.69	-11.38	-10.40	-10.03	-11.08
C2	4-NO$_2$-PhOH	-22.93	-13.16	-9.81	-13.63	-13.26	-12.23	-11.79	-13.10
C3	3-Cl-PhOH	-2.32	-12.51	-8.62	-13.11	-12.56	-11.72	-11.12	-12.37
C4	3,5-Cl$_2$-PhOH	-22.87	-13.35	-9.30	-13.85	-13.35	-12.43	-11.87	-12.96
C5	4-CN-PhOH	-5.54	-12.88	-9.36	-13.36	-12.97	-11.97	-11.52	-12.67
C6	3-Me-4-CN-PhOH	-22.42	-12.69	-9.10	-13.10	-12.76	-11.73	-11.34	-13.05
C7	3-F-PhOH	-1.28	-11.86	-8.32	-12.31	-11.94	-11.02	-10.57	-11.70
C8	3,5-F$_2$-PhOH	-17.15	-12.89	-9.15	-13.30	-12.83	-11.97	-11.43	-12.64
C9	F$_5$-PhOH	-13.18	-12.54	-9.05	-13.03	-12.72	-11.62	-11.21	-13.16
C10	Cl$_5$-PhOH	-21.90	-11.69	-6.74	-12.90	-11.72	-11.39	-10.17	-11.85
C11	3,5-Cl$_2$-4-Me-PhOH	-19.87	-13.01	-8.97	-13.35	-12.99	-11.95	-11.53	-12.70
C12	3-CN-PhOH	-11.53	-13.20	-9.36	-13.78	-13.25	-12.34	-11.76	-12.83
C13	2-Me-4-CN-PhOH	-18.98	-12.82	-9.10	-13.20	-12.89	-11.79	-11.43	-13.59

A: 6-311+G(d,p)
B: 6-311++G(2d,2p)

Table S-4. NPA Charges and atom-atom overlap weighted NAO Bond Orders of phenol – MTBE H-bond complexes.

#	Complexant	Bond Order			Charge		
		O–H	C–O	H•••O	O_{PhOH}	H_{PhOH}	O_{MTBE}
C1	PhOH	0.6156	0.8719	0.0485	-0.71	0.50	-0.65
C2	4-NO$_2$-PhOH	0.6030	0.8959	0.0630	-0.69	0.50	-0.66
C3	3-Cl-PhOH	0.6101	0.8801	0.0548	-0.70	0.50	-0.66
C4	3,5-Cl$_2$-PhOH	0.6058	0.8871	0.0594	-0.70	0.50	-0.66
C5	4-CN-PhOH	0.6055	0.8906	0.0602	-0.70	0.50	-0.66
C6	3-Me-4-CN-PhOH	0.6064	0.8889	0.0583	-0.70	0.50	-0.66
C7	3-F-PhOH	0.6114	0.8791	0.0525	-0.71	0.50	-0.65
C8	3,5-F$_2$-PhOH	0.6076	0.8855	0.0569	-0.70	0.50	-0.66
C9	F$_5$-PhOH	0.5937	0.9026	0.0732	-0.68	0.51	-0.65
C10	Cl$_5$-PhOH	0.5925	0.9227	0.0512	-0.69	0.52	-0.65
C11	3,5-Cl$_2$-4-Me-PhOH	0.6077	0.8824	0.0578	-0.70	0.50	-0.66
C12	3-CN-PhOH	0.6071	0.8841	0.0585	-0.70	0.50	-0.66
C13	2-Me-4-CN-PhOH	0.6057	0.8868	0.0594	-0.70	0.50	-0.66

5

Table S-5. MTBE binding energies (kcal/mol) of the B3LYP/6-311+G(d,p)/IEF-PCM and M06-2X/6-311+G(d,p)/SMD calculations in cyclohexane, mesitylene, toluene and benzene.

#	Complexant	Cyclohexane		Mesitylene		Toluene		Benzene	
		B3LYP	M06-2X	B3LYP	M06-2X	B3LYP	M06-2X	B3LYP	M06-2X
C1	PhOH	-5.06	-10.57	-5.77	-10.44	-6.05	-10.41	-4.08	-10.37
C2	4-NO$_2$-PhOH	-8.04	-12.55	-8.22	-12.39	-8.08	-12.35	-8.25	-12.33
C3	3-Cl-PhOH	-6.58	-11.70	-6.30	-11.55	-6.66	-11.51	-6.83	-11.47
C4	3,5-Cl$_2$-PhOH	-7.20	-12.63	-7.32	-12.50	-7.25	-12.47	-7.44	-12.43
C5	4-CN-PhOH	-7.63	-12.07	-7.83	-11.90	-7.68	-11.87	-7.85	-11.84
C6	3-Me-4-CN-PhOH	-7.37	-12.54	-7.89	-12.39	-7.46	-12.36	-7.62	-12.32
C7	3-F-PhOH	-6.66	-11.13	-6.60	-10.98	-6.75	-10.95	-6.92	-10.92
C8	3,5-F$_2$-PhOH	-7.31	-12.20	-7.38	-12.05	-7.38	-12.02	-7.55	-11.99
C9	F$_5$-PhOH	-7.66	-13.04	-6.88	-12.93	-7.70	-12.90	-7.89	-12.85
C10	Cl$_5$-PhOH	-4.77	-11.55	-4.49	-11.45	-4.92	-11.42	-5.10	-11.36
C11	3,5-Cl$_2$-4-Me-PhOH	-6.85	-12.10	-6.71	-11.95	-6.92	-11.91	-7.09	-11.88
C12	3-CN-PhOH	-7.13	-12.05	-7.58	-11.86	-7.14	-11.82	-7.35	-11.80
C13	2-Me-4-CN-PhOH	-7.05	-13.13	-8.67	-12.99	-7.09	-12.96	-7.26	-12.92

Table S-6. Binding energies (kcal/mol), H-bond length d (Å), angle α (°), and bond order (-) of additional calculations on 2,6-difluorophenol – MTBE interactions.

Parameter	B3LYP/6-311+G(d,p)	M06-2X/6-311+G(d,p)
ΔH	-7.12	-11.23
d	1.745	1.705
α	164.1	168.8
BO H•••O	0.0594	0.0662

Table S-7. Binding energies (kcal/mol) of selected dimers of phenols (M06-2X/6-311+G(d,p)) in vacuo and in several solvents (M06-2X/SMD).

	Vacuum	**Cyclohexane**	**Mesitylene**	**Toluene**	**Benzene**
(PhOH)$_2$	-8.12	-7.19	-7.02	-6.98	-6.96
(3-F-PhOH)$_2$	-7.72	-6.73	-6.56	-6.51	-6.50
(3,5-F$_2$-PhOH)$_2$	-7.59	-6.58	-6.39	-6.35	-6.33
(4-CN-PhOH)$_2$	-7.44	-6.38	-6.21	-6.16	-6.14
(3-Me-4-CN-PhOH)$_2$	-8.81	-7.89	-7.71	-7.68	-7.66

5

CHAPTER 6

Conclusions and Discussion.

Abstract

In this chapter, conclusions about the performed research described in the previous chapters and a brief outlook on the future scientific challenges are given. Furthermore, some personal views and ideas about the future of separation technology using solvent-impregnated resins (SIRs), and further applications and recommendations are also described.

6

Conclusions

The extraction of phenols or MTBE from aqueous media can be strongly improved via the use of SIRs that contain complex-forming agents. In this thesis, investigations are described that outline in detail some of the chemistry-based factors that need to be controlled to achieve this improvement. Potentially interesting compounds were investigated by quantum chemical modeling methods and subsequent synthesis and physical characterization using highly accurate calorimetric measurements. This allowed a balanced evaluation of hydrogen-bond formation as the driving force behind complex formation with phenol/MTBE. Such insights will be critical for optimizing both the extractant and the operating conditions of any SIR-based process that will make use of such interactions.

In Chapter 2, the binding of phenol and thiophenol by phosphine oxides, phosphates, and their thio-analogs was investigated using modeling experiments, ITC measurements, and liquid-liquid extraction experiments. In particular, the binding behavior of one of the phosphine oxides (tri-n-octylphosphine oxide, TOPO) towards phenol and a series of electron-withdrawing group-substituted phenols was studied, both in the presence and absence of water in the system.

High phenol binding affinities were obtained for the investigated phosphine oxides, but the presence of water in the system – as can be expected in industrial applications – causes lower phenol binding affinities by as much as 60 %, compared to experiments in water-free solvent, but the binding stoichiometry remained specific and 1 : 1 complexes were still found. Furthermore, even higher binding affinities were obtained for phenols having electron-withdrawing groups (EWG). Thio-compounds showed markedly lower binding affinities. In order to gain insight into the factors responsible for the observed binding behavior, these investigations were extended to the modeling of the full homologous series of mono-, di- and tri-substituted phosphine oxides and phosphates and their thio-analogs, as described in Chapter 3. Although, in principle, di- and mono-alkyl phosphates were shown to exhibit high binding affinities for the investigated phenols, phosphate dimer formation diminishes this completely.

In addition, in Chapter 4, the complexation of phenols by another group of even stronger H-bond acceptors, amine-N-oxides, was investigated. The binding properties for phenol and thiophenol with three different amine-N-oxides yielded binding affinities up to 30 times higher than for the phosphine oxide compounds. In order to further fine-tune the H-bond interaction, EWG-amine-N-oxides were investigated and they were shown to markedly lower binding affinities towards phenols. Steric interactions prevented a liquid amine-N-oxide extractant to exhibit the desired

binding affinity for phenols. The results in Chapters 2 through 4 show that phosphates, phosphine oxides, and amine-N-oxides could all be used in future SIR extraction systems, and the choice between these classes of compounds can be made based on more detailed considerations.

The MTBE-binding properties of EWG-phenols were investigated and described in Chapter 5. A detailed modeling study of a number of different EWG-substituted phenols for MTBE binding was carried out, pinpointing the interesting compounds for actual MTBE complexation and identifying the various factors effecting successful binding. Different quantum chemical methods were used to study the structural and electronic properties of the investigated complexes and the influence of solvents on the binding behavior. The investigated complexing agents were found to show moderate binding affinities to MTBE. Furthermore, steric and entropic effects are found to be important to yield successful binding of MTBE. In combination with the existing MTBE distribution coefficient for apolar phases, these moderate binding affinities were found to be able to enhance extraction, in principle, up to the point where it becomes industrially relevant to use such extractants in SIR-based extractions. Moreover, with future molecular improvements, e.g. liquid extraction agents that can be used neatly and still retain their MTBE binding affinity, these binding affinities can likely be further improved.

Comparison of experimental and theoretical binding results in different solvents shows that solvent effects are important. However, while molecular modeling in vacuum is really accurate, the solvent is still a very difficult medium to properly take into account in calculations. Despite claims to the contrary in studies that develop novel solvent models, it can only be hoped that 10 years from now these models have become appreciably more accurate, as difference between theory and experiment are rather frequently caused by improper calculation of all solvent effects.

Modeling and ITC experiments showed that even solvents that were previously thought to be inert (like toluene) clearly influence the complex formation. Solvents in which $\pi\pi$ interactions are possible yielded lower phenol binding affinities for the investigated extractants than solvents in which $\pi\pi$ interactions are severely hindered or absent. Also water was shown to have a large influence on complex formation, as in water-saturated solvents, the binding strength of the investigated complexes was markedly lowered compared to the water-free system. Even the extractants were in several cases shown to be able to form complexes with themselves, thereby diminishing their potential binding affinity for the desired compound. Future use of SIR extraction systems should therefore keep in mind the restrictions and possibilities that have been given in the present investigations, as the molecular system at hand may demand very specific solutions.

Future outlook for separation of phenols and ethers by solvent-impregnated resins

As has been shown in this thesis, complexation of phenols is possible with high binding affinities (Chapters 2-4), and complexation of MTBE can be achieved with moderate binding affinities (Chapter 5).

Phenol binding by extractant molecules has shown to be possible with a large range of binding affinities (~ 10 – 30000 M^{-1}). This should be sufficient for application of the proposed method in large-scale separations. As phenol binding by the extractants that were investigated is specific, and as the obtained binding affinities in combination with known phenol physical distribution coefficients can yield high overall distribution coefficients, enhanced performance can be expected for improved SIR-based processes in comparison to both adsorption and extraction. The proper choice of extractant obviously remains important for the objective at hand. On the one hand, opting for the desired binding behavior to facilitate a good extraction is necessary, while on the other hand, ease of regeneration can be equally important.

Extraction of MTBE by SIRs might remain more difficult because of the moderate binding affinities found in the present study, even for EWG-substituted phenols. Only with the combination of a strong yet specific binding to MTBE will the liquid complexation of MTBE or the ethyl analog ETBE be feasible. Phenols are likely useful as archetypical compounds for this purpose, but may turn out to be not the final solution for this problem. While higher binding efficiencies may be achievable, several boundary conditions of SIRs may limit this to a rather select subset of suitable candidates. Two of these do, in my opinion, stick out, namely strong surface-bound extractants and metal-based extractants. Extractants such as phosphoric acid are calculated to bind ethers like MTBE with high affinity (K values of an order of magnitude better than obtained with phenols). The dimer formation that was reported in Chapter 2 does, however, prevent their use in solution. Linking such extractants to the wall of the SIR will minimize dimer formation, and can thus allow the use of these moieties for SIR-based extractions. The drawback of this approach is that any surface-linked agent will only be available in a small amount, i.e., this limits the capacity of SIRs significantly. This may be improved by increasing the internal area of SIRs, and thus allow the attachment of more extractants. Another option is linking these extractants via polymeric chains to the wall, in the setting of dendrimer-coated polymers, and thus increase the number of extractant moieties per internal surface area. The second approach centers around metal-based extractants. Such extractants have as an advantage that the positively charged metal ion will have a really strong interaction with the partly negatively charged oxygen atom of the ether moiety. The problem is: how to get the metal into the highly apolar, water-immiscible solvent? Most likely, the solubility of

metal ions in such solvents will be too low, even when contained in an appropriate crown ether and in the presence of highly water-insoluble counter ions like PF_6^- or $B(Ph)_4^-$. Preliminary experiments in this area were performed, but not described in this thesis due to lack of time and success. Alternatively, embedding the metal in an organic framework may be tried (e.g. as the central metal ion in a porphyrin unit), but this comes, of course, at the price of decreased interactions with the solute. As a result, several options are still open, which is nice as progress is surely still desired to increase the chances that would make SIR-based extractions of ethers a viable route.

Future outlook for water purification based on complex formation

In the future, the use of SIRs for the extraction of polar organics from water will have to prove its value. A versatile method like the one presented in this thesis surely has some great advantages. A tailor-made method to complex a broad range of polar organics is now within reach, for it will not only be possible to remove phenols and ethers from an aqueous medium using this method, but also other relatively polar organic compounds like amines, imines, ketones, and aldehydes and possibly several kinds of acids including amino acids and proteins. Moreover, in the fast-growing industry of metal recovery from waste materials, the principles of the solvent-impregnated resin extraction described in this thesis might be of significant use, if applied reversibly to the crown-ether system mentioned briefly. Possibly, even CO_2 or H_2 might be bound to SIR-like systems in the future, to provide a solution for the global societal problem of growing CO_2 concentrations in the environment or a versatile method for H_2 storage, respectively. The combined theoretical and experimental approach presented in this thesis will likely be highly useful to find many new applications, besides the ones mentioned here.

Although the present results suggest an easy and quick implementation in present and future separations, possibly SIR separation will only be viable for very specific cases. Due to some clear drawbacks, like inevitable solvent losses, possible low binding strength, or the fact that no appropriate 'strong and specific' binding agent is available for the task at hand, other methods might be competitive both physically and economically. Ionic liquids, now widely investigated and used, will definitely be able to perform some of the tasks now performed by extractants in SIR extraction. Their charged nature (either positive for electron donor complexing or negative for electron acceptor complexing) will likely bind the compounds at hand more strongly than the presently investigated extractant molecules, thereby facilitating more effective extraction. Moreover, new water-immiscible ionic liquids become commercially available at a high rate. Using ionic liquids, extraction of slightly polar organics might be possible routinely in the future, and

much more elaborate method of SIR extraction might not be the method of choice in these cases.

Future perspectives of this scientific approach (modeling/synthesis/measurements)

The approach used to investigate the properties of the various complexes at hand was threefold. Modeling experiments were used to screen the spectrum of different kinds of molecules and molecular groups for their expected ability to form stable H-bonded complexes with the desired molecules. If such a molecule or moiety was found with the right binding properties, the designed molecules were synthesized to combine these binding properties with good solubility and/or melting properties. Once synthesized in reasonable amounts (or commercially purchased), ITC measurements were performed to assess the binding behavior under real physical conditions.

This methodology adds valuable information and gives rise to a manifold of options from the start. Present modeling methods are reasonably accurate, and provide a geometrically accurate life-like physical view inside the small world of the molecules, and valuable information about energies and electronic properties of the system. This evidently yields leads for the next step in the research. In the future, this scientific approach, the combination of modeling experiments with synthesis and physical property determinations, will show to be a *sine qua non* for many complex problems. Furthermore, modeling will surely take a leap in formulating better models, employing new and faster calculation methods and computers, and this way gaining in accuracy and applicability for ever larger systems.

Scientific challenges

The results described in the experimental Chapters 2-5 provide a reasonable understanding of the binding event taking place in complexing agent – pollutant interactions. H-bond formation, the intrinsic process directing the observed binding, has been elaborately described both in theory and in experiment. Influences on complex strength of electronic effects, solvent interaction, entropic and steric effects are described as well. Still, apart from the already mentioned ones, many scientific challenges still remain.

Solvent effects, although qualitatively mostly correctly described by the PCM and SMD models, cannot be quantitatively predicted yet. For example, $\pi\pi$ stacking (of the solvent, the solute and the extractant, and their mutual $\pi\pi$ interactions) is presently not taken into account properly. More accurate modeling of the solvent would predict these effects more clearly and less ambiguously. Better solvation models should therefore be used in future modeling of these systems.

For the modeling of the binding interactions in general, faster methods would, of course, make

an appreciable difference in speeding up the research. This is the reason that part of the research described in this thesis deals with finding sufficiently accurate alternative methods, finishing in much shorter periods of time without compromising the accuracy of the calculations. Both improved DFT methods and spin-scaled MP2 methods are highly promising in this case, but both involve an as yet empirical basis for their improvement. A sound theoretical underpinning of the causes behind this improvement is required, so that any further progress can be made in a more systematic way.

Another challenge involves measuring the binding affinity of future binding agents. Should these future binding agents be bound to the solid wall of the SIR particle, direct binding can likely not be observed in the present ITC setup, because of practical limitations. It would therefore become necessary to change the setup of this method as to fit the desired system.

The research described in this thesis is meant to be and claims to be 'science with impact' in the worlds of physical chemistry, computational chemistry, process engineering and waste water purification. However, for many topics within these disciplines the tools that are currently available do not provide us with enough answers to solve the pollution problems at hand once and for all. Therefore, I do need to conclude with perhaps the most famous words in academic research projects: to tackle this complex challenge, more research is needed! In fact, given the current global societal developments we do not have the luxury not to do this…

SUMMARY

The purification of waste water is very important, for clean potable water is a common good and a necessity. Surface water purification is nowadays carried out on a massive industrial scale, and clean water is at our disposal virtually everywhere and always. However, cleaning industrial waste water can be a difficult task. Although apolar and slightly polar compounds can be removed from water relatively easily e.g. by extraction to an apolar phase, more polar pollutants like phenol and methyl-*tert*-butyl ether (MTBE), the two main compounds that this thesis deals with, cannot be removed as easily. A more effective method is therefore needed to clean water that is contaminated with either phenol or MTBE.

Solvent-Impregnated Resins (SIRs) are porous polymer beads containing apolar organic extractant liquids. They are used as three-phase separation systems. When brought into contact with a SIR, a solute will preferentially partition from the aqueous phase into the impregnated solvent phase. A drawback to the use of solely the organic extraction liquid in SIRs is the limited solubility of more polar compounds like phenols and ethers in such a medium. In order to enhance extraction, complex-forming extractants can be added to the organic solvent. By means of complex formation inside the organic solvent, the overall equilibrium distribution can be shifted towards the SIR, with a concomitant enhancement of the extraction efficiency. A tight binding of the pollutant molecules to the extractant will eventually ensure high distribution coefficients. However, a moderate binding strength would enable a relatively easy regeneration of the complexing agent after a binding event, enabling multiple uses of the same compound.

In this thesis hydrogen-bond (H-bond) complexation, a specific and strong yet reversible way of binding is investigated for phenol recovery and MTBE recovery from aqueous environments, involving the use of organic complexing agents that can be used inside the SIR to enhance the extraction. Potentially interesting compounds were investigated on a molecular scale by quantum chemical modeling methods and subsequent synthesis and physical characterization by primarily calorimetric means. H-bond complex formation has been evaluated and the important parameters determining the binding process have been described.

After a general introduction in Chapter 1, Chapters 2 through 4 describe phenol complexation by several different classes of complexing agents. In Chapter 2, the binding of phenol and thio-phenol by phosphine oxides, phosphates, and their thio-analogs was investigated. Modeling experiments, isothermal titration calorimetry (ITC) measurements, and liquid-liquid extraction experiments showed that, in principle, the binding affinity of the oxide compounds for phenol is

high, whereas the sulfide compounds show only low affinity. In particular, the binding behavior of tri-n-octylphosphine oxide towards phenol and a series of electron-withdrawing group (EWG)-substituted phenols was studied, both in the presence and absence of water in the system. It was found that the presence of water in the system – as can be expected in industrial applications – yields lower binding affinities by as much as 60 %, but the binding stoichiometry remained specific and 1 : 1 complexes were still found. Electronic and steric effects were shown to play an important role in phenol binding in the investigated environment.

In Chapter 3, these investigations were extended to the modeling of the full homologous series of mono-, di- and tri-substituted phosphine oxides and phosphates and their thio-analogs. Different modeling methods were used to investigate both structural and electronic elements. Dimethylphosphate was found to form the strongest complexes to the investigated phenols, but because this compound forms very strong homo-dimers in solution it cannot be used as an effective extractant. The SCS-MP2 method, that was relatively unexplored for H-bonding until now, was found to yield very accurate energy predictions, whereas the CBS-Q method was found to predict false binding affinities. Solvent effects are shown to immensely influence the binding behavior.

Another, even stronger group of H-bond acceptors, amine-N-oxides, was investigated as described in Chapter 4. The binding properties for phenol and thiophenol with three different amine-N-oxides yielded very high binding affinities (up to 30 times higher than for the phosphine oxide compounds). Introduction of EWGs in the amine-N-oxides was shown to yield markedly lower binding affinities towards phenols, providing a handle to fine-tune the interaction and facilitating easier regeneration of the complexing agent in future SIR applications. Solvent effects and the influence of water in the system were investigated, and it was shown that they both influence the phenol binding strength. The results in Chapters 2 through 4 show that phosphates, phosphine oxides, and amine-N-oxides could all be used in future SIR extraction systems, and the choice between these classes of compounds can be made based on more detailed considerations.

MTBE binding by several complexing agents was described in Chapter 5. A detailed modeling study of a number of different substituted phenols for MTBE binding was carried out, and the influence of solvents on the binding behavior was investigated, using a.o. the recently developed M06-2X functional and SMD solvent model. The investigated complexing agents were found to show moderate binding affinities to MTBE with binding strengths being closely linked to the acidity of the extractant. Steric effects and a proper consideration of entropic effects are also found to be important to yield successful binding of MTBE. In combination with the existing MTBE

distribution coefficient for apolar phases, these moderate binding affinities were found to be able to enhance extraction, in principle, up to the point where it becomes industrially relevant to use such extractants in SIR-based extractions.

Finally, in Chapter 6 the performed research is reviewed, and conclusions, recommendations and a wider perspective for future scientific challenges are given.

SAMENVATTING

Waterzuivering is erg belangrijk, want schoon drinkwater is een algemeen goed en een eerste levensbehoefte. De zuivering van oppervlaktewater wordt tegenwoordig op grote schaal uitgevoerd en schoon water is nagenoeg overal en altijd te verkrijgen. Echter, de zuivering van industrieel afvalwater kan een lastige taak zijn. Apolaire en enigszins polaire stoffen kunnen relatief makkelijk uit water worden verwijderd, bijvoorbeeld door extractie naar een apolaire fase. Fenol en Methyl-*tert*-butyl ether (MTBE), de stoffen waar dit proefschrift vooral over gaat, zijn meer polaire stoffen en daardoor veel moeilijker uit water te verwijderen. Een betere methode om water te zuiveren dat vervuild is met een van deze stoffen is daarom hard nodig.

Solvent-Impregnated Resins (SIRs, harsdeeltjes geïmpregneerd met organisch oplosmiddel als extractievloeistof) kunnen gebruikt worden om water te zuiveren. Ze worden gebruikt als scheidingssysteem met drie fasen. Bij contact met SIRs zal een waterverontreiniging preferent oplossen in de extractievloeistof. Een nadeel van uitsluitend het gebruik van de organische extractievloeistof in SIRs is de beperkte oplosbaarheid van de meer polaire stoffen zoals fenolen en ethers in een dergelijk medium. Om de extractie significant te verbeteren kunnen stoffen die een complex vormen met de verontreiniging aan het organisch oplosmiddel worden toegevoegd. Door deze complexvorming in het organisch oplosmiddel kan de evenwichtsconstante van extractie worden verschoven in de richting van de SIRs, waardoor de efficiëntie van die extractie wordt verhoogd. Een sterke binding van de verontreiniging aan de complexvormende stoffen zal uiteindelijk leiden tot hoge evenwichtsconstanten voor extractie. Echter, een matige binding van de verontreiniging aan de complexvormende stoffen zal een relatief eenvoudige regeneratie van de SIRs na een extractie mogelijk maken, waardoor een soort complexvormende stof meerdere keren kan worden gebruikt.

Voor dit proefschrift is waterstofbrugvorming (H-brug vorming), een specifieke en sterke maar reversibele binding, onderzocht, om fenol en MTBE uit water te verwijderen met organische complexvormende stoffen. Mogelijk interessante stoffen zijn op moleculair niveau onderzocht met quantum-chemische modelleringsmethoden. Daaropvolgend zijn interessante stoffen gesynthetiseerd en fysisch gekarakteriseerd, voornamelijk met calorimetrie. Complexvorming door middel van H-bruggen is onderzocht en de belangrijke factoren die het bindingsproces beïnvloeden zijn beschreven.

Na een algemene introductie in Hoofdstuk 1, beschrijven de Hoofdstukken 2 tot en met 4 fenolbinding door verschillende typen van complexvormers. In Hoofdstuk 2 wordt de binding van

fenol en thiofenol aan fosfine oxides, fosfaten, fosfine sulfides en thiofosfaten beschreven. Gebruikmakend van moleculaire modellering, isotherme titratiecalorimetrie-metingen (ITC) en vloeistofvloeistof extractie-experimenten is aangetoond dat de affiniteit van de fosfine oxides voor fenol in principe hoog is, terwijl de sulfides en thiofosfaten slechts een lage affiniteit voor fenol hebben. De bindingseigenschappen van tri-n-octylfosfine oxide voor fenol en een serie van fenolen met elektronenzuigende groepen zijn tot in detail onderzocht, zowel in de aanwezigheid als in de afwezigheid van water in het gebruikte medium. De aanwezigheid van water in het systeem – zoals kan worden verwacht in industriële toepassingen – levert bindingsconstanten op die tot 60 % lager liggen dan bij afwezigheid van water, terwijl de binding nog steeds specifiek is en de bindingsratio 1 : 1 blijft. Elektronische en sterische effecten blijken een belangrijke rol te spelen bij de onderzochte omstandigheden.

In Hoofdstuk 3 worden de bindingseigenschappen van deze stoffen verder onderzocht door modellering van de volledige reeks van mono-, di- en tri-gesubstitueerde fosfine oxides, fosfaten, fosfine sulfides en thiofosfaten. Verschillende modelleringsmethoden zijn gebruikt om zowel structurele als elektronische effecten te onderzoeken. Dimethylfosfaat blijkt de sterkste complexen met de onderzochte fenolen te vormen, maar kan niet worden gebruikt als effectieve complexvormer vanwege vorming van zeer sterke homo-dimeren in oplossing. De SCS-MP2 methode, die nog relatief weinig werd toegepast in het onderzoek naar H-brugvorming, blijkt zeer nauwkeurige energievoorspellingen te geven, terwijl de CBS-Q methode onjuiste bindingsenthalpieën voorspelt. De invloed van het oplosmiddel op het bindingsgedrag blijkt zeer groot.

Het onderzoek naar een andere, sterkere klasse van H-brugvormers, amine-N-oxides, wordt beschreven in Hoofdstuk 4. De bindingssterkte van drie verschillende amine-N-oxides aan fenol en thiofenol is zeer hoog (tot 30 keer hoger dan voor de onderzochte fosfine oxides). De invoering van elektronenzuigende groepen in de amine-N-oxides levert beduidend lagere bindingssterkten op voor fenolen. Dit biedt een handvat om de interactie verder te optimaliseren en om gemakkelijkere regeneratie van de complexvormende stoffen in toekomstige SIR toepassingen te waarborgen. De fenolbinding wordt beïnvloed door de verschillende oplosmiddelen, evenals door het al dan niet aanwezig zijn van water in het systeem. De resultaten in Hoofdstukken 2 tot en met 4 geven aan dat fosfaten, fosfine oxides en amine-N-oxides alle gebruikt kunnen worden in toekomstige SIR extractiesystemen. De keuze tussen de verschillende typen stoffen zal afhangen van meer gedetailleerde overwegingen.

De binding van MTBE door verscheidene complexvormers wordt beschreven in Hoofdstuk 5. Er is een gedetailleerd modelleringsonderzoek naar een aantal verschillende gesubstitueerde

fenolen voor MTBE binding uitgevoerd. Tevens is de invloed van oplosmiddelen op het bindingsgedrag onderzocht met onder andere de recent ontwikkelde M06-2X functionaal en het SMD-oplosmiddelmodel. De onderzochte complexvormers tonen matige affiniteit voor MTBE, en tonen bindingssterkten die nauw verbonden zijn met de zuurgraad van de complexvormer. Het is belangrijk om rekening te houden met sterische effecten en entropische factoren om MTBE succesvol te kunnen binden. In combinatie met de bestaande verdelingscoëfficiënten voor MTBE in apolaire fasen zijn deze matige bindingscoëfficiënten in principe voldoende om extractie te verbeteren tot het punt waarop het industrieel relevant wordt om dergelijke complexvormers te gebruiken in SIR extracties.

Tenslotte wordt in Hoofdstuk 6 het uitgevoerde onderzoek tegen het licht gehouden en worden conclusies, aanbevelingen en een breder perspectief gegeven voor toekomstige wetenschappelijke uitdagingen.

CURRICULUM VITAE

Ruud Cuypers werd geboren op 3 september 1981 te Geldrop. Na het behalen van zijn VWO diploma op het Strabrecht College te Geldrop begon hij in 1999 aan de studie Moleculaire Wetenschappen aan de Wageningen Universiteit. Hij deed afstudeervakken bij de vakgroepen Organische Chemie en Biofysica en een stage bij Philips NatLab in Eindhoven. In november 2004 begon hij aan zijn promotieonderzoek aan de Wageningen Universiteit bij de vakgroep Organische Chemie onder leiding van Prof. dr. H. Zuilhof en Prof. dr. E.J.R. Sudhölter. De belangrijkste resultaten van dit promotieonderzoek staan beschreven in dit proefschrift. Sinds mei 2009 is Ruud werkzaam als wetenschappelijk onderzoeker bij TNO Bouw en Ondergrond te Delft.

Ruud Cuypers was born on September 3, 1981 in Geldrop (The Netherlands). After finishing highschool (VWO) at the Strabrecht College in Geldrop he studied Molecular Sciences at Wageningen University. He did undergraduate research projects in the departments of Organic Chemistry and Biophysics and an internship in Philips NatLab in Eindhoven. He started his PhD research at Wageningen University in the Organic Chemistry department under supervision of Prof. dr. H. Zuilhof and Prof. dr. E.J.R. Sudhölter in November 2004. The most important results of this research are described in this thesis. Ruud is working as a scientific researcher at TNO Built Environment and Geosciences in Delft since May 2009.

LIST OF PUBLICATIONS

"Complexation of MTBE by Phenols. Ab Initio Computations and Isothermal Titration Calorimetry"
R. Cuypers, E. J.R. Sudhölter, H. Zuilhof, *submitted*.

"Complexation of Phenol by Amine-N-oxides. Isothermal Titration Calorimetry and Ab Initio Calculations"
R. Cuypers, S. Murali, A. T. M. Marcelis, E. J. R. Sudhölter, H. Zuilhof, *ChemPhysChem*, **2010**, accepted.

"Hydrogen Bonding in Phosphine Oxide/Phosphate–Phenol Complexes"
R. Cuypers, E. J. R. Sudhölter, H. Zuilhof, *ChemPhysChem*, **2010**, *11*, 2230.

"Evaluation of tri-n-octylamine oxide as phenol extractant in a solvent"
impregnated resin" B. Burghoff, R. Cuypers, M. van Ettinger, E.J.R. Sudhölter, H. Zuilhof, A.B. de Haan,
Separation and Purification Technology, **2009**, *67*, 117.

"Complexation of Phenols and Thiophenol by Phosphine Oxides and Phosphates. Extraction, Isothermal Titration
Calorimetry, and ab Initio Calculations" R. Cuypers, B. Burghoff, A. T. M. Marcelis, E. J. R. Sudhölter, A. B. de Haan,
H. Zuilhof, *Journal of Physical Chemistry A,* **2008**,*112*, 11714.

Other Publications:

"Practical, reliable and inexpensive detection assay of lycopene in tomato products based on the
combined use of light emitting diode (LED) and the optothermal window" D. Bicanic, R. Cuypers,
M. Sporec, S. Luterotti, A. Zoppi, *Acta Chimica Slovenica*, **2008**, *55*, 468.

"Large amplitude light-induced motion in high elastic modulus polymer actuators" K. D. Harris, R. Cuypers,
P. Scheibe, C. L. van Oosten, C. W. M. Bastiaansen, J. Lub, D. J. Broer, *Journal of Materials Chemistry,* **2005**, *15*, 5043.

"Molecular orientation control for thermal and UV-driven polymer MEMS actuators" K. D. Harris, R. Cuypers,
P. Scheibe, G. N. Mol, J. Lub, C. W. M. Bastiaansen, D. J. Broer, *Proceedings of SPIE-The*
International Society for Optical Engineering, **2005**, *5836*, 493.

"Asymmetric banana-shaped liquid crystals with two different terminal alkoxy tails" R. Achten, R. Cuypers,
M. Giesbers, A. Koudijs, A. T. M. Marcelis, E. J. R. Sudhölter, *Liquid Crystals,* **2004,** *31*, 1167.

"Vergelijking van de inhalatie-anesthetica Desfluraan, Enfluraan, Halotaan, Isofluraan en Sevofluraan"
R. Cuypers, K. Boer, Y. H. J. van Helden, N. J. P. Smits, R. M. Stenger, G. M. Visser, R. Remie, *Biotechniek,* **2003,** *42*, 131.

OVERVIEW OF COMPLETED TRAINING ACTIVITIES

Discipline specific activities

Courses

Molecular Modeling, University of Amsterdam, 2005

Advanced Isothermal Titration Calorimetry, Microcal, Milton Keynes, United Kingdom, 2005

Advanced course Bio-Nanotechnology, VLAG, 2005

COSMO-RS, Cosmologic, Leverkusen, Germany, 2006

Molecular Affinity Separations, Eindhoven Technical University, 2008

Meetings

Annual NWO Conference Lunteren, 2005-2008

Wageningen Symposium of Organic Chemistry, Wageningen University, 2006, 2008

Jahrestreffen des ProcessNet-Fachausschuss Extraktion, Clausthal-Zellerfeld, Germany, 2006.

International Solvent Extraction Conference, Tucson AZ, USA, 2008

General courses

Philosophy and Ethics of Food Science and Technology, Wageningen University, 2008

VLAG aio-dagen, VLAG, Bilthoven, 2005

Optionals

Preparation PhD research proposal

Literature meetings, Laboratory of Organic chemistry, Wageningen University, 2007-2008

Group meetings, Laboratory of Organic chemistry, Wageningen University, 2004-2008

Colloquia, Laboratory of Organic chemistry, Wageningen University, 2005-2008

PhD study trip, Organized by Laboratory of Organic chemistry, USA, 2005

PhD study trip, Organized by Laboratory of Organic chemistry, Sweden, 2007

DANKWOORD

Na een leerzame en leuke tijd van onderzoek, revisies aan papers en hoofdstukken, en opmaak-perikelen is het eindelijk af: mijn proefschrift ligt nu voor je neus! Hoewel het kleine witte boekje toch zoiets gewoons lijkt, heeft de totstandkoming ervan toch enige voeten in de aarde gehad. Natuurlijk krijg je zoiets bij lange na niet alleen voor elkaar en daarom wil ik op deze plaats de belangrijkste mensen bedanken die een rol hebben gespeeld in de afgelopen jaren.

Allereerst wil ik Prof. dr. Han Zuilhof bedanken. Han, toen ik bij je langskwam om informatie in te winnen over een interessant projectje wist je me te interesseren voor de modellering en voor de fysisch-chemische aspecten die een scheiding op basis van waterstofbruggen met zich mee-brengt. Deze interesse is uitgegroeid tot het proefschrift dat hier nu voor ons ligt en zonder jouw kundige hulp en scherpe commentaar was dit niet gelukt. Je hebt me geleerd kritisch te zijn op mezelf en op anderen, niet alles wat je leest voor waar aan te nemen. En naast wetenschappelijke zaken heb je me ook wereldlijke zaken doen inzien en begrijpen en dat is veel waard. Hartelijk dank voor het vertrouwen, de vrijheid die je me gaf en je inzet om van dit project een succes te maken.

Ook voor de hulp van Prof. dr. Ernst Sudhölter ben ik zeer erkentelijk. Ernst, hoewel ik je al tijdens mijn afstudeervak intensief heb meegemaakt, heb ik je pas goed leren kennen tijdens de AIO-reis naar Californië. Tijdens meerdere wandelingen en diners hebben we uitgebreid gesproken over de alledaagse dingen des levens, wetenschap, maar ook over meer abstracte en filosofische zaken. Ik kijk met veel plezier terug op deze gesprekken en op onze samenwerking. Dank voor je mate-loze enthousiasme en je vertrouwen en voor je fysisch-chemische inbreng in het project. Ik vond het ook leuk om de laatste tijd af en toe met je in Delft te lunchen, wat mij betreft houden we dat erin!

Dr. Ton Marcelis wil ik ook speciaal noemen op deze plek. Ton, je hebt een grote rol gespeeld in het gereedkomen van mijn proefschrift en zelfs bij het feit dat ik überhaupt bij Organische Chemie een aio-onderzoek ben gaan doen. Tijdens mijn afstudeervak bij het onderzoek van Remko heb ik mogen ruiken (soms letterlijk!) aan het fysisch-chemisch onderzoek. Mede op basis van die leuke en leerzame periode heb ik besloten om ook zelf aan een dergelijk onderzoek te beginnen. Hoewel je niet direct bij mijn project betrokken was, heb je daaraan toch zeer veel aandacht besteed. In het begin, toen ik bij je op de kamer zat, heb je me wegwijs gemaakt in het lab, later heb je me telken-male geholpen met goede commentaren en fysische inzichten in mijn papers. Voor deze inbreng en voor je gezelligheid en interesse wil ik je hartelijk danken!

De leden van mijn thesis-commissie wil ik hartelijk bedanken voor het beoordelen van mijn proef-

schrift, de leden van mijn gebruikerscommissie voor de inbreng tijdens de halfjaarlijkse meetings, en Prof. André de Haan en dr. Bernd Burghoff voor de goede samenwerking tussen mijn onderzoek en dat van hen, eerst in Twente, later bij de TU Eindhoven.

Op het praktische vlak ben ik ook een aantal mensen veel dank verschuldigd. Cindy, jij hebt me de eerste kneepjes van het modelleren *in silico* bijgebracht. André, dankzij de markante namen die je aan de rekencomputers gaf zal ik menig vijfletterig eilandstaatje niet meer vergeten en zonder de Jerry's en Moore's was er van mijn rekenaspiraties niet veel terecht gekomen. Anton, waar mijn kennis van ITC zich voorheen uitstrekte tot een enkel proefje om de CMC van CTAB te meten, kan ik mijzelf dankzij jouw hulp nu een ervaren ITC'er noemen. Ik kijk met genoegen terug op de tijd dat we samen aan deze apparaten hebben gesleuteld! Arie, je hebt me veel kennis van organische synthese bijgebracht. Jacob, vooral tijdens de laatste loodjes was jij steeds slechts een e-mailtje van me verwijderd. Zelfs toen een Moore het op het allerlaatst begaf, kon je me helpen om mijn berekeningen toch nog op tijd af te krijgen. Allen hartelijk bedankt!

Murali, during the last year that I was employed by ORC we shared a room in the basement. Thank you for your successful efforts to enhance my papers; we now share a nice publication. En omdat jij tegenwoordig vloeiend Nederlands spreekt: Bedankt voor de Duitse les, de "potjes" en voor een leuke tijd!

Mijn andere kamergenoten bij ORC zijn legio, mede dankzij 3 (!) interne verhuizingen. Ton, Arie, Tina, Remko, Ioan, Ganesan, dank voor een leuke tijd, en Kim en Feng, naast een leuke periode op één kantoor, ook extra dank voor een fijne samenwerking in "ons" lab.

Jurjen, Michel, Luc en Remco, ook bedankt voor alle "kopjes" en de "rentrées", voor de vissies op donderdag en voor de gezelligheid die dat met zich mee heeft gebracht! Wiebe, dank voor het ping-pongen en Fluxxen! Daarnaast gaat ook voor de normale doch zeer belangrijke algemene gang van zaken op de vakgroep dank uit naar verscheidene mensen; Barend voor de NMR en IR metingen, Marcel voor de scriptjes voor excel, Ronald voor chemicaliënvoorziening en de borrel-cie, Elly en Aleida voor algemene secretariële zaken, Teris, Kishore, TuHa, Bart, Loes en de rest voor de spelletjesavonden. De rest van de vakgroep bedankt voor de gezelligheid en collegialiteit.

Zonder de hulp en steun van mijn vrienden had ik dit project niet tot een goed einde kunnen brengen. Rens en Bram, dank voor jullie steun en voor het nintendoën op momenten dat ik eigenlijk moest studeren. Karin en Peter, Jessica en Wilger, Matthijs en Suzanne, Lidwien en Laurens, Sake en Attje-Rieke en Egbert en Outi, jullie weten wat het is om een promotieonderzoek te doen (of om met iemand samen te zijn die hieraan werkt). Daarom was het voor mij zo fijn om regelmatig

met jullie te eten, te squashen, mijn hart te luchten, spelletjes te doen, een biertje te drinken, of weekendjes weg te gaan. Bij twee van jullie heb ik de kunst van het promoveren al mogen afkijken, bij drie anderen zal ik daar hopelijk snel getuige van kunnen zijn en bij één wellicht nog in de verre toekomst? Dank voor jullie steun en vriendschap, speciaal voor Sake en Egbert omdat jullie mijn paranimfen willen zijn! Karin en Mark, dank voor jullie gezelligheid tijdens etentjes en tijdens het skiën.

Speciale dank gaat uit naar de gehele familie Westerhoff voor jullie steun en interesse; Wim bedankt voor ervaringen uit eerste hand en je daaruit voortkomende adviezen!

Ook mijn familie wil ik bedanken voor de steun, de liefde en het luisterend oor dat ik van hen mocht ontvangen. Papa, mama, hopelijk helpt dit boekje een beetje om mijn uitleg van de afgelopen jaren over waar ik nou helemaal mee bezig was te verduidelijken. Dank voor jullie mentale hulp en steun. Karin, speciale dank voor jouw grote hulp en inzet. Dankzij jou ziet mijn boekje er nu fantastisch uit. Ik vond het heel leuk om zo intensief met je samen te werken in de laatste periode van het schrijven, bedankt voor je deskundigheid en professionaliteit!

En als laatste mijn lieve Isthar. Is, tijdens de hele periode van mijn promotieonderzoek ben je altijd geïnteresseerd geweest en gebleven in mijn bezigheden, vorderingen, tekeningetjes en schemaatjes, problemen en oplossingen en in periodes wanneer ik een schop onder mijn kont nodig had was je er om me die te geven! Bedankt voor je liefde, vrolijkheid en geduld. Ik woon kei leuk met jou en nu mijn project afgerond is kunnen we daar samen nog meer van genieten!

Ruud

September 2010